

Role of CLIC5A in Maintaining Glomerular Filtration Barrier Integrity

by

Mahtab Tavasoli

A thesis submitted in partial fulfillment of the requirements for
the degree of

Doctor of Philosophy

Department of Medicine

University of Alberta

© Mahtab Tavasoli, 2016

Abstract

Renal glomeruli are specialized capillaries that produce a protein-free ultrafiltrate of plasma at an extremely high rate. Glomerular endothelial cells (EC) and podocytes sustain the integrity of filtration barrier, and glomerular mesangial cells provide intravascular support.

Podocytes cover the exterior of renal glomerular capillaries and wrap regularly spaced, actin-based projections, the foot processes, around the capillary loops, giving strength to the capillary in the face of the high glomerular capillary pressure. Filtration slits between foot processes allow passage of water and small molecules, but not larger proteins. The lumen of the capillaries is lined by glomerular EC, which are perforated by fenestrae that make the capillary highly permeable to water and small solutes. A glycocalyx covers the EC surface and extends into the fenestrae, preventing large proteins from being filtered. To adapt to changes in mechanical forces, for instance glomerular capillary hypertension, glomerular cells undergo remodeling. Maladaptive remodeling can lead to proteinuria, and end stage renal disease.

This thesis explores the function of CLIC5A (chloride intracellular channel 5A), which is selectively enriched in glomerular podocytes and EC. CLIC5A function is poorly understood, and it probably is not a chloride channel. CLIC5A co-localizes with ezrin in podocyte foot processes, and moesin in glomerular EC. Ezrin and moesin are ERM (ezrin, radixin, moesin) proteins that connect membrane-spanning proteins to cortical actin. Their activation requires docking on PI[4,5]P2 in lipid bilayers. CLIC5A stimulates clustered PI[4,5]P2 accumulation in the plasma membrane, facilitating ERM docking, unfolding and phosphorylation. Activated ezrin links the transmembrane glycoprotein podocalyxin to actin, controlling the architecture of podocytes.

The molecular interactions between CLIC5A, ERM proteins and PI[4,5]P2 generating

PI[4]P5 kinases had not been worked out. Since it was previously shown that Rac1 stimulates the activity of PI[4]P5 kinases and ERM protein activation, and since Rac1 participates in podocyte actin remodeling, I determined whether CLIC5A-dependent PI[4,5]P2 generation and ERM activation are mediated by Rac1. I also determined whether the podocyte response to DOCA/Salt hypertension is CLIC5A-dependent.

In COS7 cells, null for CLIC5A at baseline, ectopic CLIC5A expression stimulated Rac1 activity and phosphorylation of the Rac1 effector Pak1. CLIC5A-induced PI[4,5]P2 generation, as well as Pak1 and ERM phosphorylation were all Rac1-dependent. In vivo, DOCA/Salt hypertension increased phosphorylated Pak1 in podocytes in CLIC5^{+/+}, but not in CLIC5^{-/-} mice. In DOCA/Salt hypertensive CLIC5^{-/-} mice glomerular capillary microaneurysms and albuminuria were much greater than in hypertensive CLIC5^{+/+} mice. There also was a marked reduction in glomerular EC fenestrae in hypertensive CLIC5^{-/-}, but not in CLIC5^{+/+} mice. Thus, CLIC5A stimulates Rac1-dependent PI[4,5]P2 generation, ERM and Pak1 phosphorylation, and the accumulation of phosphorylated Pak1 in DOCA/Salt hypertension requires CLIC5. My data suggest that augmented hypertension-induced glomerular capillary injury in mice lacking CLIC5 results from abrogation of Rac1-dependent Pak and ERM activation, perhaps reducing the tensile strength of podocytes.

In CLIC5^{-/-} mice, ERM phosphorylation is profoundly reduced in podocytes, but preserved in glomerular EC, even though CLIC5A is expressed in both cell types in wild-type mice. Since glomerular EC also express CLIC4, I reasoned that CLIC4 could potentially compensate for the CLIC5A loss in glomerular EC. In glomeruli of CLIC5^{-/-} mice, CLIC4 expression was up-regulated in glomerular EC, but not in podocytes. In cultured glomerular EC, CLIC4 silencing reduced ERM activation, which was rescued by CLIC4 or CLIC5A. In mice

lacking either CLIC4 or CLIC5, ERM phosphorylation was retained in glomerular EC, but in mice lacking both CLIC4 and CLIC5, glomerular EC ERM phosphorylation was profoundly reduced. Although glomerular EC fenestrae developed normally in dual CLIC4/CLIC5 deficient mice, the density of fenestrae declined substantially by 8 months of age. The dual CLIC4/CLIC5 deficient mice also developed spontaneous proteinuria and mesangial matrix expansion. Thus, CLIC4 stimulates ERM activation, and can compensate for CLIC5A in glomerular EC. My findings suggest that CLIC4/CLIC5A-mediated ERM activation is required for sustained maintenance of the glomerular capillary architecture.

In summary, I found that CLIC5A activates Rac1, and that Rac1 activation is necessary for CLIC5A-dependent PI[4,5]P2 synthesis, as well as ERM and Pak1 activation. This mechanism is induced by DOCA/Salt hypertension in wild-type, but not CLIC5^{-/-} mice. In glomerular EC, CLIC4 and CLIC5A both activate ERM proteins and compensate for each other. My work shows that these CLICs maintain the long-term integrity of glomerular capillaries.

Preface

Author Contributions

Portions of chapter 3 have been published in *Kidney International*, 2016. **Mahtab Tavasoli**, Laiji Li, Abass Al-Momany, Lin-Fu Zhu, Benjamin A. Adam, Zhixiang Wang and Barbara J. Ballermann. , *The chloride intracellular channel 5A stimulates podocyte Rac1, protecting against hypertension-induced glomerular injury*. *Kidney Int*, 2016. 89(4): p. 833-47.

Portions of Chapter 4 have been submitted in a peer-reviewed journal: **Mahtab Tavasoli**, Abass Al-Momany, Xin Wang, M, Laiji Li, John C. Edwards and Barbara J. Ballermann, *Both CLIC4 and CLIC5A activate ERM Proteins in Glomerular Endothelium*. *Am. J. Physiol., Renal Physiology* 2016.

Mahtab Tavasoli designed and performed all the experiments in chapter 3, 4 and 5 and prepared the first drafts of the *Kidney International* and *American Journal of Physiology Renal Physiology* papers for publication (including the figures and the legends).

Laiji Li, PhD., Research Associate in the laboratory, prepared the different cDNA/Vector constructs of CLIC5A (including GFP-CLIC5A and GST-CLIC5A) used in this study, performed mouse genotyping, provided the protocol for GST-Pull down experiments and assisted in glomerular isolation and animal handling.

Dr. Benjamin Adam, pathologist, performed the morphological analysis of PAS stained slides (Figure 3.16).

Dr. Barbara Ballermann did the morphometric analysis (Figure 3.11 a and b) and (Figure 4.9 b and d), blinded to experimental groups.

Dr. David Rayner, pathologist, performed histological analysis on PAS slides (Figure 3.12 b and c), blinded to experimental groups.

Dr. Xin Wang performed CLIC4 silencing in human glomerular ECs (Figure 4.6 a and d).

Zhixiang Wang, Ph.D. provided the plasmids for expression of dominant negative Rac1.

Abass Al-Momany, Ph.D., performed portions of experiments for (Figure 4.5 b and c), (Figure 5.4 a) (Figure 5.5 a).

Dr. Barbara J. Ballermann, the principal investigator, helped with the design of the experiments, supervised the studies overall and prepared the final drafts of the *Kidney International* and *American Journal of Physiology Renal Physiology* manuscripts for submission.

Dedication

I dedicate my dissertation work to my family. Words cannot express how grateful I am to my loving parents, Nahid and Javad Tavasoli who have always loved me unconditionally and whose good examples have taught me to work hard for the things that I aspire to achieve. I will always appreciate all they have done for me. My dear sisters Maryam and Mahsa and my nephew Shervin are very special to me and I'd like to thank them for their constant love and support.

This thesis work is also dedicated to my beloved husband, Vincent, who has been a constant source of support and encouragement during the challenges of graduate school and life. He has been patient with me when I am frustrated, he celebrates with me when even the smallest things go right, and he is there whenever I need him to just listen. I am truly grateful for having you in my life!

Acknowledgements

First and foremost I offer my sincerest gratitude to my supervisor, Professor Barbara J. Ballermann, for accepting me into her group at the critical stage of my Ph.D studies.

During my PhD program, she contributed to a rewarding graduate school experience by giving me intellectual freedom in my work, supporting my attendance at various conferences, engaging me in new ideas, and demanding a high quality of work in all my endeavors. The joy and enthusiasm she has for research was contagious and motivational for me. I would like to thank her for encouraging my research and for allowing me to grow as a research scientist. I could not have imagined having a better advisor and mentor for my Ph.D study.

I would like to extend my deepest gratitude to my supervisory committee: Dr. Todd Alexander and Dr. Sean McMurtry for their insightful comments and encouragement, but also for the hard questions, which incentivized me to widen my research from various perspectives. I also thank Dr. Valerie Luyckx a former Ph.D committee member, who was instrumental to the initiation of this project. I am especially grateful to Dr. McMurtry for his guidance and support as our department graduate coordinator and to Dr. Alexander for giving me access to his research facilities and serving as my Ph.D committee member even when he was in France.

I would like to express my deepest appreciation to our lab manager and research associate Dr. Laiji Li for being the remarkable person he is. He has been actively interested in my work and has always been available to advise me and support my research. I am very grateful for his patience, motivation, enthusiasm, and skills. This work would not have been possible without his guidance, support and encouragement.

I would like to thank my former supervisor Professor Fakhreddin Jamali who believed in me and helped me to start my doctoral research in Canada and supported me even when I transferred to a different faculty.

I am very grateful to Dr Russ Tsuyuki, our former graduate coordinator who facilitated my transfer to Dr Ballermann's lab; who saw the potential in me, and provided a solid anchor at a crucial moment in my PhD when needed most.

I am so grateful to Arlene Oatway for her great technical support with scanning and transmission electron microscopy and for our friendly discussions.

I thank my fellow lab mates Dr. Abass Al-Momany and Dr. Marya Obeidat for their support and the stimulating discussions and my friends outside the lab, Forough, Nazila, Anahita and Maryam for their encouragement and advice and all the joyful moments we had together.

I would like to recognize the department of medicine administrative staff, especially Sonia, Gloria and Maggie who performed their job so competently it appeared effortless.

I gratefully acknowledge the funding received towards my PhD from P.E.O. International Peace Scholarship, Shoppers Drug Mart Scholarships, Dr. Ronald Micetich Memorial Graduate Scholarship and Canadian Federation of University Women scholarship. I would like to thank the research funding agencies Kidney Foundation of Canada, the Canadian Institutes of Health Research and the Division of Nephrology at the University of Alberta for supporting my tuition.

Lastly and most importantly I would like to express the deepest gratitude to my family: my parents and to my sisters for supporting me spiritually throughout writing this thesis and my life in general. I would like to extend my deepest gratitude to my dear husband for his continued and unfailing love, support and understanding underpins my persistence in the graduation career and makes the completion of this thesis possible.

Table of Contents

Chapter 1. Literature Review, Hypothesis and Objectives.....	1
1- Introduction.....	2
1.1 The kidney: In charge of overall body homeostasis.	4
1.1.1 Glomeruli: The filtering units of the kidney.....	6
1.1.1.1 Components of the glomerular filtration barrier and their contribution to glomerular permselectivity	9
1.1.1.1.1 Glomerular endothelial cells.....	9
1.1.1.1.2 Glomerular basement membrane.....	11
1.1.1.1.3 Podocytes.....	14
1.1.1.2. Regulation of glomerular hemodynamics.....	18
1.2. Hypertension, the leading risk factor for premature death worldwide.....	20
1.2.1 Hypertensive nephrosclerosis.....	21
1.2.1.1 Glomerular capillary hypertension and mechanical stress.....	23
1.2.1.1.1 Response of endothelial cells to hypertension.....	25

1.2.1.1.1 Fenestral glycocalyx contributes to the overall hydraulic resistance of the glomerular filtration barrier.....	26
1.2.1.1.2 Response of mesangial cells to hypertension.....	26
1.2.1.1.3 Response of podocyte to hypertension.....	27
1.3. Rho GTPases: The master regulators of cytoskeleton remodeling.....	28
1.3.1 RhoA.....	29
1.3.2 Cdc42.....	30
1.3.3 Rac1.....	31
1.3.3.1 The PAK family of serine/threonine kinases: downstream effectors of Rac1/Cdc42.....	34
1.4. ERM proteins: Bridging the gap between cytoskeleton and plasma membrane.....	34
1.4.1 ERM protein activation requires PI[4,5]P2 binding.....	36
1.4.3 PI[4]P5K activation is regulated by members of Rho GTPases	37
1.5. Chloride Intracellular Channels (CLICs) a perplexing family of proteins.....	38
1.5.1 Functional relationships between CLICs, Rho GTPases and ERM proteins....	40

1.5.1.1 CLIC1.....	40
1.5.1.2 CLIC3.....	41
1. 5.1.3 CLIC4.....	42
1.5.1.4 CLIC5.....	44
1.5.1.4.1 CLIC5, radixin & stereocilia	44
1. 5.1.4.2 CLIC5, Ezrin & integrity of glomerular filtration barrier.....	45
1.5.1.4.3 CLIC5A regulates ERM protein phosphorylation by PIP5K activation.	46
1.6 Hypothesis and Objectives.....	48
Chapter 2. Materials And Methods	51
2.1 Reagents and antibodies.....	52
2.2 Experimental animals	52
2.2.1 Generation of CLIC5 ^{-/-} mice.....	52
2.2.2 Generation of CLIC4 ^{-/-} CLIC5 ^{-/-} mice.....	53
2.3 Cell culture, cell transfection and cell lysis.....	54

2.3.1 COS7 cells	54
2.3.2 Conditionally immortalized mouse podocytes.....	54
2.3.3 Human glomerular endothelial cells (EC)	55
2.3.3.1 CLIC4 and CLIC5A rescue experiments.....	56
2.4 Plasmid and adenoviral constructs	56
2.5 RNA interference	58
2.5.1 CLIC4 silencing.....	58
2.6 GTP-Rac1/Cdc42/Rho pull-down and Rac1 Inhibition.....	59
2.7 Western blot analysis (WB) and quantification.....	59
2.8 Live cell imaging.....	60
2.9 Immunofluorescence studies.....	60
2.10 UNx-DOCA/Salt hypertension in mice.....	61
2.11 Urine protein electrophoresis and serum biochemistry.....	61
2.12 Glomerular isolation.....	62
2.13 Cytoskeleton preparation.....	62

2.14 Perfusion fixation and microscopy.....	63
2.15 Morphometric analysis of PAS stained glomeruli.....	64
2.16 Statistical analysis.....	65
Chapter 3. CLIC5A stimulates Rac1-dependent Pak and ERM protein activation, protecting against hypertension-induced glomerular injury.....	68
3.1 Introduction.....	69
3.2 Results.....	73
3.2.1 Activation of Rac1 and Pak1 phosphorylation in COS7 cells expressing CLIC5A.....	73
3.2.2 CLIC5A-dependent ERM and Pak1,3 phosphorylation require Rac1 activity..	74
3.2.3 Inhibition of Rac1 abolishes CLIC5A-induced clustered PI[4,5]P2 accumulation.	75
3.2.4 Glomerular Pak phosphorylation in UNx-DOCA/Salt Hypertension requires CLIC5.....	75
3.2.5 Glomerular ERM phosphorylation in DOCA/Salt hypertension requires CLIC5.....	78

3.2.6 Both, DOCA/Salt hypertension and CLIC5 deletion lower glomerular podocalyxin levels.....	78
3.2.7 CLIC5 deficiency potentiates glomerular injury in DOCA/Salt hypertensive mice.....	79
3.2.8 CLIC5 deficiency or DOCA/Salt hypertension does not change VEGF protein expression but abrogate VEGFR2 activation in renal glomeruli in mice.....	80
3.2.9 CLIC5 deficiency results in expansion of glomerular capillary lumen in mice.....	81
3.3 Discussion.....	82
3.4 Figures.....	88
Chapter 4. Both CLIC4 and CLIC5A activate ERM Proteins in Glomerular Endothelium.....	105
4.1 Introduction.....	106
4.2 Results.....	112
4.2.1 Increased glomerular endothelial cell CLIC4 abundance in CLIC5 deficient mice.....	112

4.2.2 CLIC4 co-localizes with moesin and ezrin in glomeruli, and CLIC4 deletion results in reduced ERM protein abundance in glomerular capillaries.....	112
4.2.3 CLIC4 co-localizes with moesin and ezrin in proximal tubule brush border, and CLIC4 deletion results in reduced ERM protein association with the renal cortical cytoskeletal fraction.	113
4.2.4 Reduced ERM protein activation in cultured glomerular EC upon CLIC4 silencing.	114
4.2.5 Reduced ERM phosphorylation by CLIC4 silencing is rescued with overexpressed CLIC5A.....	114
4.2.6 Defective ERM protein phosphorylation in dual CLIC4/CLIC5 deficient mice... ..	115
4.2.7 Ultrastructural abnormalities in glomerular endothelial cells of dual CLIC4/CLIC5 deficient mice	116
4.3 Discussion.....	117
4.4 Figures.....	126
Chapter 5. Investigating the interaction between CLIC5A, CLIC4 and small Rho-GTPases.....	139
5.1 Introduction.....	140

5.2 Results.....	144
5.2.1 CLIC5A binds directly/indirectly to Rho GTPase, Rac1.....	144
5.2.2 Activation of Pak1,3 in human glomerular ECs expressing CLIC5A.....	145
5.2.3 CLIC4 silencing down-regulates Rac1 and Cdc42 protein expression in human glomerular ECs.....	146
5.2.4 P21-activated kinase (Pak) phosphorylation and Rac1/Cdc42 protein expression in kidney samples of CLIC4 ^{+/+} and CLIC4 ^{-/-} mice.	146
5.2.5 CLIC4 is required for VEGF mediated ERM activation in cultured human glomerular ECs.....	147
5.2.6 Similar to CLIC5A, EGF dependent ERM protein phosphorylation requires Rac1.....	148
5.3 Discussion.....	149
5.4 Figures.....	156
Chapter 6. General discussion and future directions.....	162
6.1 General discussion.....	163
6.1.1 Rac1 activation by CLIC5A.....	168

6.1.1.1 CLIC5A-induced PI[4,5]P2 cluster formation results in Rac1 activation.....	168
6.1.1.2 CLIC5A-induced formation of Podocalyxin/NHERF2/Ezrin complex regulates Rac1/RhoA activation.	169
6.1.2 Model of CLIC5A/Rac1 action in podocytes.....	169
6.2 Future Directions.....	172
6.2.1 To Explore the nature of molecular and functional interaction between CLIC5A and Rac1.	172
6.2.2 Mechanism(s) regulating the CLIC5A-plasma membrane association.	173
6.2.3 To explore whether CLIC5A/Rac1-dependent cytoskeletal remodeling is spatially restricted both at baseline and during kidney injury.	174
6.2.4 To explore the role of CLIC5A-Rac1-Ezrin and CLIC5A-Rac1-Pak1 pathway in diabetic nephropathy.	176
6.3. Figures.....	178
References.....	181
Appendices.....	229
1. Ethics approval for animal use protocol.....	229

List of tables

Table 2.1 Antibodies.....	66
Table 3.1 Body, heart and kidney weights in UNx and UNx-DOCA/salt CLIC5 ^{+/+} and CLIC5 ^{-/-} mice.....	109
Table 3.2 Serum electrolyte and glucose concentrations in CLIC5 ^{+/+} and CLIC5 ^{-/-} mice before and 20 days after initiation of DOCA/Salt treatment.....	109

Figures

Chapter 1

Figure 1.1 Glomerular capillary loop and glomerular capillary wall.8

Figure 1.2 Podocytes.....13

Figure 1.3 Laplace's law.....24

Chapter 3

Figure 3.1 Increased Rac1 activity but not Rho or Cdc42 in COS7 cells expressing CLIC5A...88

Figure 3.2 Increased Pak1,3 and ERM protein phosphorylation in COS7 cells expressing CLIC5A.....89

Figure 3.3 Increased Pak1,2,3 and ERM protein phosphorylation in undifferentiated podocytes expressing CLIC5A.....90

Figure 3.4 CLIC5A-induced ERM and Pak1,3 protein phosphorylation requires Rac1 activity.....91

Figure 3.5 Abrogation of CLIC5A-dependant apical PI[4,5]P2 cluster formation by NSC23766.....93

Figure 3.6 Systemic Hypertension in UNx-DOCA/Salt treated CLIC5^{+/+} and CLIC5^{-/-} mice.....94

Figure 3.7 Pak Phosphorylation in glomeruli of UNx-DOCA/Salt and UNx control CLIC5 ^{+/+} and CLIC5 ^{-/-} mice.....	95
Figure 3.8 P21-activated kinase (Pak) phosphorylation in glomeruli of UNx-DOCA and UNx-DOCA and UNx control CLIC5 ^{+/+} mice.....	97
Figure 3.9 ERM protein phosphorylation in glomeruli of UNx-DOCA/Salt and UNx control CLIC5 ^{+/+} and CLIC5 ^{-/-} mice.	98
Figure 3.10 Podocalyxin expression in glomeruli of UNx-DOCA/Salt and UNx control CLIC5 ^{+/+} and CLIC5 ^{-/-} mice.....	100
Figure 3.11 Ultrastructure of glomerular capillaries from UNx-DOCA/Salt and UNx control CLIC5 ^{+/+} and CLIC5 ^{-/-} mice.....	102
Figure 3.12 Greater glomerular injury in hypertensive UNx-DOCA/Salt CLIC5 ^{-/-} mice.....	103
Figure 3.13 Development of urine albumin-to-creatinine ratio as a function of time in DOCA/Salt.....	104
Figure 3.14 VEGF signaling in glomeruli of UNx DOCA/salt and UNx control CLIC5 ^{+/+} and CLIC5 ^{-/-} mice.....	105
Figure 3.15 AKT and ERK1/2 phosphorylation in glomeruli of UNx DOCA/salt and UNx control CLIC5 ^{+/+} and CLIC5 ^{-/-} mice	106

Figure 3.16 CLIC5 deficiency leads to expansion of capillary lumen in mice.....107

Figure 3.17 Model of CLIC5A-Rac1 action in podocytes.....108

Chapter 4

Figure 4.1 Increased abundance and endothelial localization of CLIC4 in glomeruli of CLIC5 deficient mice.....131

Figure 4.2 CLIC4 co-localizes with moesin and ezrin in glomeruli, and CLIC4 deletion results in reduced ERM protein abundance in glomerular capillaries.....132

Figure 4.3 Co-localization of CLIC4 with moesin and ezrin in renal cortex, and reduced ERM protein association with the renal cortical cytoskeletal fraction.....134

Figure 4.4 Proximal tubule vacuolization and brush border disorganization in 8-month old CLIC4^{-/-} mice.....135

Figure 4.5 Reduced ERM protein activation in cultured glomerular EC upon CLIC4 silencing.....136

Figure 4.6 Reduced ERM phosphorylation is rescued with overexpressed CLIC4 or CLIC5A.....137

Figure 4.7 Defective ERM protein phosphorylation in dual CLIC4/CLIC5 deficient mice by immunofluorescence (IF) microscopy.....138

Figure 4.8 Defective ERM protein phosphorylation in kidney cortex from dual CLIC4/CLIC5 deficient mice.....	139
Figure 4.9 Ultrastructural abnormalities in glomerular endothelial cells of dual CLIC4/CLIC5 deficient mice.....	140
Figure 4.10 Ultrastructural abnormalities in glomerular endothelial cells of dual CLIC4/CLIC5 deficient mice.	141
Figure 4.11 Glomerular hypercellularity, mesangial matrix deposition and albuminuria in 8-month old dual CLIC4/CLIC5 deficient mice.	142
 Chapter 5	
Figure 5.1 Rac1 binds to GST-CLIC5A in COS7 cells.....	161
Figure 5.2 CLIC5A enhances Pak1,3 phosphorylation in human glomerular ECs	162
Figure 5.3 CLIC4 silencing down-regulates Rac1 and Cdc42 protein expression in human glomerular ECs.....	163
Figure 5.4 P21-activated kinase (Pak) phosphorylation and Rac1/Cdc42 protein expression in kidney samples of CLIC4 ^{+/+} and CLIC4 ^{-/-} mice.....	164
Figure 5.5 CLIC4 is required for VEGF mediated ERM activation in cultured human glomerular ECs.....	165

Figure 5.6 EGF enhances ERM protein phosphorylation via Rac1 in COS7 cells transfected with GFP-Vector and GFP-CLIC5A.....166

Chapter 6

Figure 6.1 Protamine sulfate infusion in mice.....183

Figure 6.2 Schematic model of CLIC5A function in apical plasma membrane of podocytes.....184

Figure 6.3 Schematic model of apical domain of podocyte foot processes in CLIC5 deficient (CLIC5^{-/-}) mice.....185

Abbreviations and Symbols

aa	Amino Acid
BSA	Bovine Serum Albumin
Cal A	Calyculin A
Cdc42	Cell division control protein 42 homolog
cDNA	Complementary DNA
CLIC	Chloride Intracellular Channel
CLIC5A	Chloride Intracellular Channel 5A
DAG	Diacylglycerol
DOCA	Deoxy Corticosterone Acetate
EBP50	ERM Binding Protein 50
EC	Endothelial Cell
EGF	Epidermal Growth Factor
ERK	Extracellular signal–Regulated Kinases
ERM	Ezrin/Radixin/Moesin protein
NHERF2	Sodium-hydrogen exchange regulatory cofactor
ERMAD	ERM Association Domain
FERM	Four-point-one, Ezrin, Radixin, Moesin
FAK	Focal Adhesion Kinase
F-actin	Filamentous Actin
GDP	Guanosine diphosphate
GBM	Glomerular Basement Membrane
GFP	Green Fluorescent Protein

GFB	Glomerular Filtration Barrier
GST	Glutathione-S-Transferase
GTP	Guanosine triphosphate
GPCR	G-protein Coupled Receptor
IAA-94	Indanyloxy Acetic Acid 94
IP3	Inositol 3,4,5 Trisphosphate
IP	Immunoprecipitation
IF	Immunofluorescence
KO	Knock Out
Kras	Kirsten rat sarcoma viral oncogene homolog
LPS	Lipopolysaccharide
Merlin	Moesin, Ezrin, Radixin-like Protein
PA	Phosphatidic Acid
Pak	p21 activated kinases
PBS	Phosphate Buffered Saline
PECAM-1	Platelet Endothelial Cell Adhesion Molecule-1
P-ERM	Phosphorylated ERM (on C-terminal Thr)
PH	Plextrin Homology domain
PI[4]P	Phosphatidylinositol 4, phosphate
PI[4,5]P2	Phosphatidylinositol 4,5 bisphosphate
P[3,4,5]P3	Phosphatidylinositol 3,4,5 trisphosphate
PIP5K	Phosphatidylinositol 4 phosphate 5 kinase
PI5P4K	Phosphatidylinositol 5 phosphate 4 kinase
PLC	Phospholipase C

PKA	Protein kinase A
PKC	Protein Kinase C
PLD	Phospholipase D
PM	Plasma Membrane
PS	Protamine sulfate
Rac1	Ras-related C3 botulinum substrate 1
RFP	Red Fluorescent Protein
Rho GAP	Rho GTPase-activating proteins
Rho GEF	Rho guanine nucleotide exchange factors
Rho GDI	Rho protein GDP dissociation inhibitor
ROCK	Rho Associated Kinase
SAGE	Serial Analysis of Gene Expression
SEM	Scanning Electron Microscopy
siRNA	Small Interfering Ribo-Nucleic Acid
TCA	Trichloroacetic Acid
T-Ezrin	Total Ezrin
TEM	Transmission Electron Microcopy
TGF- β 1	Transforming Growth Factor beta 1
UNx	Uni-nephrectomized
VEGF	Vascular Endothelial Cell Growth Factor
WASP	Wiskott–Aldrich syndrome protein
WAVE	WASP-family verprolin-homologous protein
WT	Wild Type

Prefixes

K	kilo (10^3)
m	milli (10^{-3})
μ	micro (10^{-6})
n	nano (10^{-9})

Units

L	liter
g	gram
kDa	Kilo dalton
$^{\circ}\text{C}$	degree Celsius

Symbols

α	alpha
β	beta
γ	gamma

Chapter 1

Literature Review, Hypothesis and

Objectives

Chapter 1

1. Introduction

Everyday, adult human kidneys produce approximately 180 liters of ultrafiltrate from plasma at capillary pressures that are much higher than other systemic capillaries. Despite this tremendous workload and high capillary pressure the glomerulus remains intact during our lifetime. Filtration occurs in renal glomeruli, a specialized tuft of capillaries that lies between two resistance vessels, the afferent and efferent arterioles, which control the intracapillary pressure. Glomerular capillary cells have evolved to be highly specialized in their structure and function to maintain the integrity of glomerular filtration barrier. Dynamic interactions between plasma membrane proteins with subjacent cortical actin filaments are necessary to regulate the three-dimensional cyto-structure and function of these specialized cells.

The glomerular filtration barrier (GFB) consists of three layers: facing the interior of the capillaries are the glomerular endothelial cells (EC), which are extremely flat with a large fenestrated area. The fenestrae assure a high permeability to water and small solutes (hydraulic conductivity). The glomerular fenestrae are trans-cellular pores lined by plasma membrane, and ringed by cortical actin. A layer of highly glycosylated proteins covers the glomerular EC and contributes to the permselectivity of the glomerular capillary wall. The second layer of the GFB is the basement membrane, which is much thicker than the basement membranes in other vascular beds and is believed to account for much of the resistance to water flow across the glomerular barrier [1]. The exterior surface of renal glomerular capillaries is wrapped by interdigitating podocyte foot processes, which are podocyte projections, with highly specialized actin architecture. The space between foot processes, referred to as filtration slits, creates a large surface area for filtration of water and small sized molecules. The filtration slit diaphragm,

which spans this space, forms a size-selective barrier for protein filtration. The actin-based podocyte primary projections and foot processes also provide capillary wall strength in the face of the high ($\sim 45\text{-}50$ mmHg) glomerular capillary pressure. Increased glomerular capillary pressure results in an increase in wall tension and can further challenge the delicate architecture of glomerular cells [2]. To adapt to changes in the mechanical forces and in response to injury, glomerular cells undergo structural and functional changes known as cell remodeling. Disturbances in the usual structure and function of the glomerular cells may reduce the glomerular filtration rate, lead to proteinuria, and can progress to end stage renal disease. It turns out that hypertension, presumably because of its damaging effect on glomerular capillaries is a major risk factor for the progression of kidney disease to end stage, and the most important treatment of progressive kidney disease is blood pressure reduction. Even so, there really is no treatment that can reliably halt the course of progressive kidney failure. Understanding the signaling pathways that regulate the dynamic changes of actin cytoskeleton, may uncover new therapeutic targets to slow down the progression of kidney diseases.

CLIC5A, an extremely enriched protein in kidney glomeruli [3], stimulates the accumulation of the signaling phospholipid, PI[4,5]P₂ in apical plasma membrane patches, promoting Ezrin docking, phosphorylation and actin coupling, which maintain the unique podocyte architecture [4, 5]. Ezrin connects transmembrane protein podocalyxin to cortical actin and loss of this interaction results in disturbance of specialized architecture and functions of podocyte [3]. Podocalyxin in complex with Ezrin is involved in maintaining foot process architecture via activation of small Rho GTPases [6-8]. The small Rho GTPases are master regulators of cytoskeleton dynamics and similar to CLIC5, enhance PI[4,5]P₂ production via PIP5Kases [9].

This thesis describes a novel role for CLIC5A protein in protecting against hypertension-induced glomerular injury in podocytes by stimulating Rac1-dependent activation of ERM proteins as well as the Rac1 effector PAK. In addition, we show for the first time that there is a functional redundancy between CLIC5A and its homologue CLIC4 in glomerular EC, at least in regards to ERM protein activation.

1.1 The kidney: In charge of overall body homeostasis.

Homeostasis refers to the ability of an organism or environment to maintain stability in spite of environmental changes. With this definition, kidneys are one of our most important organs for body fluid and electrolyte homeostasis. Maintaining homeostasis of a large number of solutes and the composition and volume of the extracellular fluid despite the changes in dietary intake or endogenous production is the main function of the kidney.

The kidney regulates the concentration of numerous electrolytes such as sodium (the main osmole in the extracellular space), potassium (the major intracellular cation), chloride (the major extracellular anion) and minerals such as calcium, phosphorus and magnesium. In mammals, the kidneys maintain nearly constant blood plasma osmolality and pH. The kidneys regulate osmolarity mainly via urine concentrating mechanisms [10]. Precise pH is maintained by the kidney through excretion of hydrogen ions and regulation of the concentration of the major extracellular buffer, bicarbonate (HCO_3^-)[11]. Endogenously produced waste materials such as urea, creatinine and uric acid are all excreted from the body by the kidneys.

The kidney also has a number of endocrine roles and secretes multiple hormones and humoral factors. Kidney releases erythropoietin in response to hypoxia to produce hemoglobin for red blood cells. Moreover kidney is the sole source for renin, the key enzyme that activates

the renin-angiotensin-aldosterone axis (RAAS). It also produces 1-alpha-hydroxylase, enzyme that generates 1,25 dihydroxy vitamin D3. The kidneys are additionally involved in catabolism of small peptide hormones such as insulin and can produce glucose via gluconeogenesis during fasting.

The kidneys produce a number of paracrine substances, such as prostaglandins (PGI2, PGE2) and bradykinin. Nitric oxide is an endothelial factor produced by kidney, which causes vasodilation and natriuresis. Endothelin is the other endothelial factor generated by kidney, which is the most potent vasoconstrictor known.

Among other critical roles of the kidney is the maintenance of normal blood pressure. Kidneys are able to excrete sufficient sodium chloride to maintain normal sodium balance, extracellular fluid volume and blood volume to regulate arterial pressure. Moreover kidney produces some vasodilatory substances and controls RAAS, which is an important hormone system responsible for regulation of blood pressure. In response to reduced renal blood flow, juxtaglomerular (JG) cells surrounding the renal afferent arterioles produce renin from its inactive precursor and secrete it directly into the systemic circulation. Plasma renin converts circulating angiotensinogen, which is released by the liver to angiotensin I. Angiotensin I has mild vasoconstrictor properties and does not cause significant changes in blood pressure but is subsequently converted to Angiotensin II by the enzyme Angiotensin Converting Enzyme (ACE) found in the lungs. ACE is a dipeptidylcarboxypeptidase enzyme and a zinc metalloproteinase in EC that splits off the histidyl-lucine complex from the decapeptide angiotensin I to produce the octapeptide angiotensin II. The majority of ACE enzyme is localized in lung EC. However, one study in 1992 reported that ACE protein is expressed in nearly all blood vessel EC [12]. Angiotensin II is a potent vasoactive peptide, which is able to cause a major increase in blood

pressure. ACE2 is a more recently described member of RAAS system. Compared to ACE1, ACE2 has a more restricted distribution and is expressed mainly in heart and kidney. ACE2 cleaves a single residue from angiotensin I to generate Angiotensin 1-9, and degrades Angiotensin II to the vasodilator Ang 1-7. It is suggested that ACE2 might act as a counter-regulator of ACE1 to maintain the balance between vasoconstrictors and vasodilators in heart and kidney [13, 14].

Angiotensin II also stimulates the secretion of the steroid hormone, aldosterone, from the adrenal cortex. Aldosterone is the primary endogenous member of mineralocorticoids. Aldosterone increases reabsorption of sodium and an associated passive reabsorption of water into the blood. Aldosterone also stimulates excretion of K^+ by the principal cells of the collecting duct along with the active secretion of H^+ by proton ATPase in the luminal membrane of intercalated cells of the collecting duct. This leads to the volume expansion of extracellular fluid in the body, increasing the blood pressure [15, 16]. In conclusion the kidneys are essential for homeostasis of the body's extracellular fluids and the cascade of functional proteins of the RAAS system play a central role in blood pressure regulation.

1.1.1 Glomeruli: The filtering units of the kidney

Glomeruli are highly specialized capillaries situated between two resistance arterioles that produce a nearly protein-free ultra-filtrate from plasma at a very high rate. The pressure inside these capillaries is much higher than other systemic capillaries and unlike other capillary beds that are surrounded by interstitial tissue; glomerular capillaries are situated in Bowman's space, into which the glomerular filtrate passes. Therefore, unique support structures are required to maintain the necessary flow in these capillaries and protect them against the high pressure. The

glomerular capillary wall, which forms the glomerular filtration barrier, consists of three layers; glomerular endothelial cells, basement membrane and podocytes. Mesangial cells, the third specialized glomerular cell type, form a supporting interstitium inside the space delineated by the glomerular basement membrane. So, unlike other interstitial cells, they actually form an intracapillary supporting network of cells that contributes to the integrity of the glomerular capillaries. Mesangial cells often respond to injury and disease by proliferating and producing additional extracellular matrix [17]. Taken together this extremely intricate structure allows the formation of approximately 180 liter of filtrate from plasma everyday under great pressure to maintain overall body homeostasis.

A dysfunction of the highly permselective glomerular filtration barrier results in increased glomerular permeability and excessive leakage of protein into the urine. Nephrotic syndrome (NS) is one of the most common kidney conditions which is characterized by a urinary protein level more than 3.5 g per 1.73 m² body surface area per day in adults, low blood levels of albumin (less than 2.5 g/dl; hypoalbuminemia), elevated levels of lipids (hyperlipidemia) and abnormal accumulation of fluid in the interstitium (edema) that begins in the face [18]. Nephrotic syndrome may be kidney specific and be the result of a glomerular disease, called primary (idiopathic) nephrotic syndrome (primary glomerulonephrosis), or occurs as the result of a systemic condition such as diabetes or hepatitis B etc., which is called secondary nephrotic syndrome. Genetic and environmental factors both can be the underlying causes of the NS [19].

Here I summarize the most important features of each layer of glomerular filtration barrier.

Figure 1.1

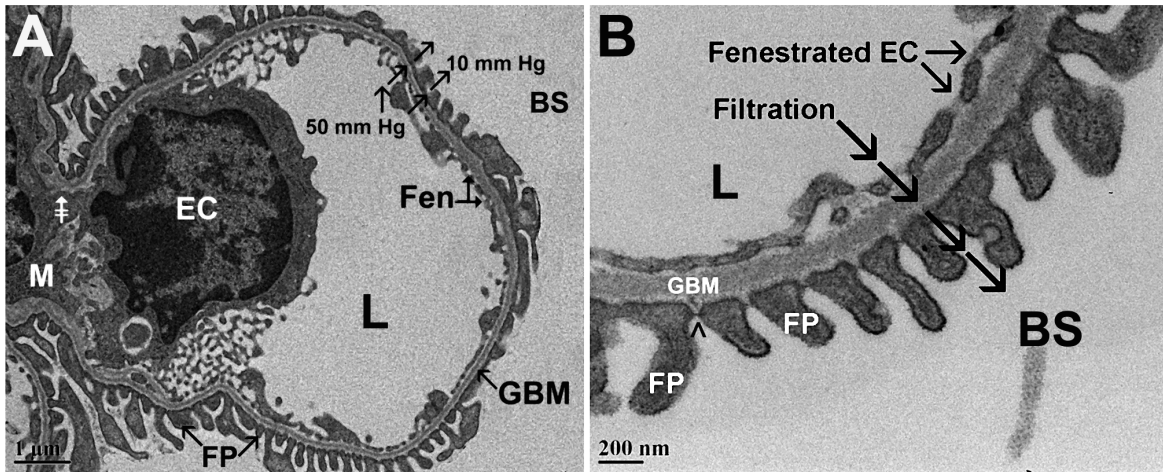


Figure 1.1 | Glomerular Capillary Loop (A) and Glomerular Capillary Wall (B). The images illustrate the anatomical relationships of the specialized cellular and supporting structures of the glomerulus. (A): Transmission electron microscopic (TEM) image of a glomerular capillary loop in cross-section. Endothelial Cell (EC), Fenestrae of glomerular EC (Fen), Mesangial Cell (M), Glomerular basement membrane (GBM), Podocyte Foot Processes (FP), Capillary Lumen (L) and Bowman's Space (BS). The hydraulic pressure gradient from the capillary lumen (~ 50 mmHg) into Bowman's Space (~ 10 mmHg) drives filtration. The GBM does not separate the endothelial cells from the mesangium (\ddagger). (Scale bar = 1 μ m. (B): High-power TEM image of the glomerular capillary wall in cross-section. Endothelial Cell (EC), Glomerular basement membrane (GBM), Foot Processes (FP), Capillary Lumen (L), Bowman's Space (BS). The nearly protein-free ultrafiltrate (multiple arrows) moves from the capillary lumen into Bowman's Space, through glomerular EC fenestrae, through the GBM and then through filtration slits between the foot processes. It is evident that the EC are extremely flat around the circumference of the capillary loop, in the range of 50 nm high. The filtration slit diaphragm can be seen between some of the foot processes (^). Scale bar = 200 nm. These images were taken in our lab, from a 2-month old wild-type mouse as part of the study described in Chapter 4.

1.1.1.1 Components of the glomerular filtration barrier and their contribution to glomerular permselectivity

1.1.1.1.1 Glomerular endothelial cells

The first layer in the glomerular filtration barrier is the glomerular endothelium, which is in direct contact with the blood. Like all other EC, these cells form an anti-coagulant surface that prevents blood coagulation, and they are the first layer of the barrier that prevents blood cells and large proteins from escaping into the urine. The cell body of glomerular EC usually abuts the mesangial cells, without any basement membrane separating them, and the remainder of the cells extends around the inner surface of the capillary loop. Except for the cell body, glomerular ECs are sieve-like cells that are ridiculously flattened and contain thousands of trans-cellular pores measuring 70–100 nm in diameter, called fenestrae.

Fenestrated area constitutes 20-50% of the endothelial surface [20] and allows the high permeability to water and small solutes (hydraulic conductivity). It has been shown that the variation in glomerular endothelial cell fenestrae density and size correlate with variation in GFR. At the ultrastructural level, all fenestrae are ringed with actin [21, 22]. Although the exact mechanisms regulating glomerular endothelial fenestrae formation are not clear, it is widely accepted that podocyte-derived VEGF-A, TGF- β 1 and laminin β 3/ α 3 in the basement membrane are among the key factors required for the formation of glomerular EC fenestrae. Podocyte specific deletion of VEGF-A in mice [23], inhibition of TGF- β 1 in developing rat kidney [24], mutation in laminin β 3 gene in human [25, 26] and deletion of laminin α 3 gene in mice [27], all result in loss of glomerular EC fenestrae formation.

On the luminal side, of the glomerular EC membrane-bound glycoproteins form a glycocalyx layer that coats the glomerular endothelium and extends into the fenestrae. Associated with this protein-polysaccharide coat are more loosely associated proteoglycans which form the endothelial surface layer. The glycoprotein/endothelial surface layer is around 200 nm thick, so much thicker than the EC themselves, and it is negatively charged because of its high sialic acid content. The endothelial surface layer and glycocalyx prevent negatively charged proteins from crossing into the fenestrae and therefore contribute to the perm-selectivity of the glomerular filtration barrier [28]. Therefore, endothelial cell fenestrae are extremely important in maintaining the glomerular hydraulic conductivity and the protein-polysaccharide coat covering the glomerular EC and the fenestrae helps in maintaining the glomerular permselectivity to plasma proteins. A healthy GFR and glomerular permselectivity relies on the integrity of fenestrated glomerular EC [29].

The size of glomerular fenestrae is approximately 60–80 nm [29, 30], which is too large to prevent passage of proteins such as albumin. However, the negatively charged glycocalyx coat covering the fenestrae prevents albumin and large proteins from passing through the fenestrae, and is a key determinant of charge selectivity [31]. The glomerular endothelial glycocalyx layer is sensitive to the hypoxia during tissue fixation but newer fixation and staining methods enabled the researchers to reveal the presence of a thin glycoprotein coat and an associated endothelial surface layer extending more than 200 nm along the glomerular endothelium. It is reported that disruption of the endothelial surface layer in Adriamycin-induced kidney injury [32] or by oxidative stress [33] enhance the permeability of glomerular filtration barrier to proteins and other macromolecules. It has also been suggested that accumulation of the

negatively charged plasma proteins in the endothelial surface layer by filtration itself contribute to the glomerular filtration charge selectivity [34].

A reduction in both size and density of fenestrations and endothelial thickening has been observed in preeclampsia and is associated with a reduction in GFR. A similar change in the endothelial ultrastructure is reported in animal models of kidney injury such as experimental diabetes [35], anti-Thy-1 nephritis [36] and cyclosporine nephropathy [37] as well as in human diseases such as diabetic nephropathy [38] and transplant glomerulopathy [39] suggesting that endothelial injury contributes to the reduced GFR and increased albuminuria.

1.1.1.1.2 Glomerular basement membrane

The glomerular capillary basement membrane (GBM), the second layer of the glomerular filtration barrier, is a specialized extracellular matrix consisting mainly of laminins (mainly laminin11; $\alpha5\beta\gamma1$), type IV collagen (collagen $\alpha3$, $\alpha4$, and $\alpha5$ chains), fibronectins and heparan sulfate proteoglycan [40]. Both, glomerular EC and podocytes produce these proteins, so the GBM is a fusion of the glomerular EC and podocyte basal laminas [41].

Mutations in the genes encoding collagen chains proteins results in pathological conditions such as Alport's syndrome with glomerulonephritis features [42]. The basement membrane also contains negatively charged proteoglycans. Although GBM may contribute to the renal permselectivity [43, 44] but the magnitude of contribution has been debated [45-47]. It is suggested that the basement membrane is mainly responsible for the restriction of fluid flux [47, 48]. Therefore, GBM still plays an important role in the glomerular filtration barrier.

Studies localizing ferritin or high molecular weight dextran (62–125 kDa) by electron microscopy showed that in normal mice these macromolecules do not pass GBM. However, puromycin aminonucleoside results in deeper penetration of the dextran macromolecules into the GBM. This finding was interpreted to indicate that the GBM plays a significant role in glomerular permselectivity [49, 50]. Similarly, GBM abnormalities caused by the absence of laminin β 2 in mice [51] and humans [52] can cause significant albuminuria. However it is noteworthy to mention that in many studies the GBM does not prevent the passage of proteins and macromolecules if there was glomerular endothelial or podocyte detachment. Thus, the appearance of protein in the urine is due to damage or detachment of the glomerular endothelial and/or podocyte layer, while the GBM itself is quite permeable to macromolecules [53-55].

Figure 1.2

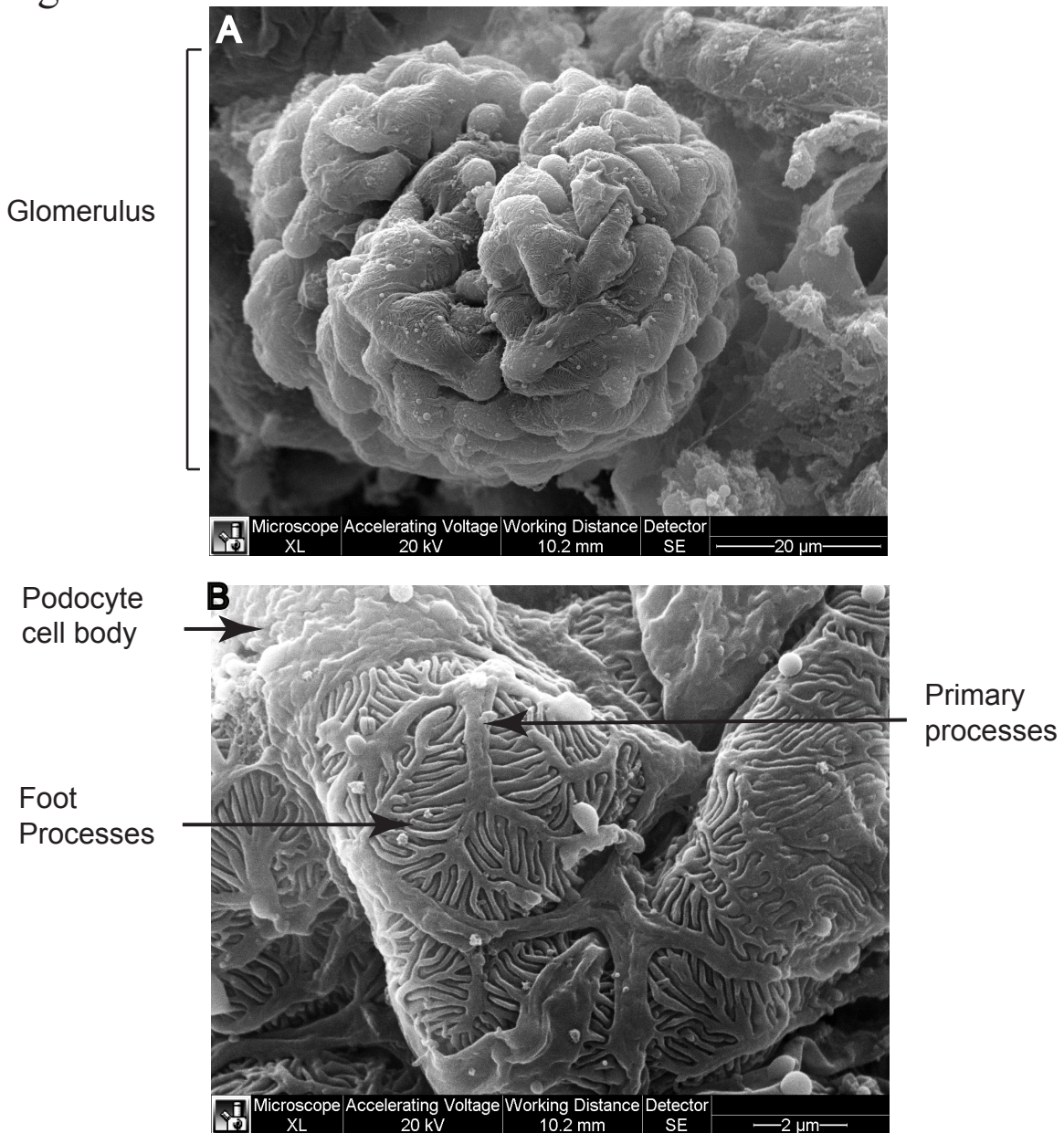


Figure 1.2 | Podocytes. (A) Scanning electron micrograph of an adult mouse glomerulus (a tuft of capillaries located at the beginning of a nephron in the kidney). (B) A higher magnification Scanning electron micrograph of the same glomerulus showing podocyte cell body, primary thick processes that branch to form secondary interdigitating foot processes wrapping around capillary loop. Arrow indicate interdigitating secondary processes of two neighboring podocytes. These images were taken in our lab, from a 2-month old CLIC5 deficient mouse. Podocytes appear relatively normal, although the number of foot processes is reduced, and they are, on average, broader.

1.1.1.1.3 Podocytes

The third layer of the glomerular filtration barrier is composed of specialized visceral epithelial cells, the podocytes. The podocytes cyto-architecture consists of the voluminous cell body, microtubule and intermediate filament-based long primary processes, and interdigitating actin-based foot processes. Podocytes wrap their specialized long inter-digitated foot processes around capillaries of the glomerulus and form filtration slits (40 nm in diameter) between adjacent processes. Just like the fenestrae of glomerular EC, the filtration slits between the podocyte foot processes provides a large surface area through which glomerular filtrate can pass. These filtration slits are bridged by the filtration slit diaphragm, composed of nephrin and associated molecules that link adjacent foot processes to each other. Along with the negatively charged glycocalyx of glomerular ECs and podocytes, the filtration slit diaphragm tightly restricts the passage of macromolecules.

Damage to podocyte causes effacement or simplification of the actin based foot processes into broader structures. Podocyte injury is an early hallmark of many kidney diseases and is clinically accompanied with proteinuria.

The podocyte cytoskeleton is believed to be the key component of podocyte and maintains the shape of podocytes and enables its continuous forming and adapting [56]. Podocytes and their complex cytoskeleton act as a scaffolding system to support the integrity of the capillary loops and counteract the high hydraulic glomerular perfusion pressure. Cytoskeletal actin in foot processes consists of a dense highly ordered parallel contractile actin filament bundles and a cortical actin meshwork just underneath the plasma membrane of the foot processes. The actin cytoskeleton is linked with other actin-binding proteins. Podocyte foot processes themselves are polarized with three domains: The basal domain, the lateral, or slit diaphragm domain, and the

apical domain [57]. All three domains are connected to the foot process actin cytoskeleton and disruption of any of the three domains triggers reorganization of actin filaments which may lead to foot processes effacement and proteinuria. Many of these dynamic changes in actin cytoskeleton are mediated by localized activation of Rho GTPases including Rac1 [57, 58].

The basal domain of podocyte foot processes contains several adhesion proteins that function to anchor them to the underlying GBM. $\alpha 3\beta 1$ integrin and α and β dystroglycans are among the proteins located at the basal domain of the foot processes. α and β dystroglycans bind electrostatically to cationic regions of ECM proteins such as laminin and agrin. Inside the cell, dystroglycans attached to the actin meshwork via utrophin. $\alpha 3\beta 1$ integrin connect to actin cytoskeleton via interaction with talin, paxillin and vinculin, spans the plasma membrane and anchors the foot process by binding to fibronectin, laminins and collagen in the basement membrane. Integrin-linked kinase (ILK), an intracellular serine/threonine kinase in association with β integrins mediates diverse signaling in the basal domain of foot processes [59].

The filtration slit diaphragm is a highly specialized cell junction, connecting the neighboring foot processes to each other. The slit diaphragm contains a multi-protein signaling complex. The proteins that constitute the slit diaphragm function as scaffolding proteins, structural proteins, receptors, and ion channels. Nephrin, the first member of slit diaphragm, was discovered in 1999 [60]. Nephrin is an immunoglobulin like transmembrane protein that acts as a structural and signaling protein. Nephrin binds podocin via its cytoplasmic tail and also interacts with scaffolding protein CD2AP. A complex of nephrin, podocin and CD2AP is believed to be the functional unit for slit diaphragm assembly [57]. Mutation in several other proteins residing in slit diaphragm such as FAT, a member of cadherin superfamily, Neph-1, Neph-2, Neph-3 and scaffolding protein densin resulted in immense proteinuria and provided critical evidence that the

slit diaphragm plays an important role in maintaining normal function of the glomerular filtration barrier. Moreover, protein complexes in slit diaphragm are shown to participate in podocyte signaling events to interact with other podocyte proteins and regulate actin dynamics.

Fyn is a membrane-associated tyrosine kinase that phosphorylates the cytoplasmic tails of nephrin and Neph-1. Phosphorylated nephrin recruits a number of Src homology 2 and 3 adaptor proteins to form a protein complex, which not only mediate cell survival but also regulates the dynamics of actin polymerization. Growth-factor receptor binder 2(Grb2) [61], PLC- γ [62], p85/phosphatidylinositol 3-kinase (PI3K)[63], chicken tumor virus no. 10 regulator of kinase (Crk)1/2 [64] and Non catalytic kinase (Nck)1/2 are among the proteins that are involved in actin signaling in the podocyte slit diaphragm [65]. For instance activation of scaffolding proteins, non catalytic kinase (Nck)1/2, by phospho-nephrin results in relocalization of the actin nucleation protein, neuronal Wiskott–Aldrich syndrome protein (N-WASP), and Pak1/2 activation [66], all together mediating actin polymerization [65]. It has been reported that in motile podocytes Rac1 and Pak1 play a major role during the active remodeling of focal adhesion complexes [66, 67].

The apical membrane domain of podocyte foot processes faces the urinary space and is coated with the CD34 related, negatively charged proteins podocalyxin, podoplanin, and podoendin. The negative charge contributes to the charge repulsion properties of the glomerular filtration barrier inhibiting the passage of anionic proteins and also keeps the neighboring podocytes separated and confers anti-adhesive properties. Another important molecule on the apical domain of podocyte foot processes is glomerular epithelial protein 1 (GLEPP1), which is a podocyte receptor membrane protein tyrosine phosphatase. Deletion of GLEPP1 in mice results in shortening and widening of the foot processes. Reduced filtration surface area in GLEPP1

deficient mice was accompanied by reduced glomerular nephrin and decreased glomerular filtration rate [68]. In another study GLEPP1 protein and mRNA were reduced 5 days after intraperitoneal injection of puromycin aminonucleoside. The reduction in GLEPP1 protein and mRNA was associated with proteinuria and foot process effacement, and GLEPP1 was suggested to be a potential marker for acute podocyte injury [69].

Podocalyxin is a member of CD34 family of transmembrane sialomucins which consist of three members (CD34, Podocalyxin and Endoglycan) [70]. Podocalyxin was initially identified as the major apical sialoglycoprotein of the podocyte and was characterized as a marker of glomerular podocytes [71]. Later studies proved the expression of podocalyxin by other cell types such as hematopoietic progenitors, vascular endothelial cells, and a subset of neurons. By being negatively charged, podocalyxin functions to keep adjacent foot processes separated. Podocalyxin can induce cell microvillus formation accompanied with actin cytoskeleton recruitment to the polarized membrane region. Podocalyxin also independently regulates the size and topology of apical cell domains through its transmembrane and extracellular domains [72]. The NHERF2/Ezrin protein complex connects transmembrane podocalyxin to the actin cytoskeleton and this interaction is disrupted in pathologic conditions associated with effacement of podocyte foot processes. Podocalyxin can also directly bind to Ezrin through a FERM-binding motif [73]. Podocalyxin has an extensively O-glycosylated and sialylated serine, threonine and proline-rich extracellular mucin domain, putative sites of N-glycosylation cysteine-containing globular domain and a juxtamembrane stalk region. It has a single pass transmembrane domain, which is followed by short cytoplasmic tails containing putative phosphorylation sites, FERM-binding motif and C-terminal PDZ-domain docking sites (DTEL or DTHL). Podocalyxin is encoded by eight exons [70, 74]. Intracellular podocalyxin in

complex with Ezrin influences the activities of RhoA [7] Rac1 [8], MAPK and PI3K [75]. Aberrant expression of podocalyxin has also been shown in a wide range of malignancies, such as breast and prostate cancers and although has not proven yet the most probable functional implication of podocalyxin upregulation is increased metastasis [70].

1.1.1.2. Regulation of glomerular hemodynamics

The glomerular filtration rate (GFR) is defined as the volume of fluid filtered by renal glomerular capillaries into Bowman's space per unit time, and averages 125 ml/min in a resting healthy man. The renal plasma flow (RPF) delivers approximately 600 ml/min for filtration and the perfusion pressure, maintained at ~ 45 – 50 mm Hg is the driving force for ultrafiltration. The fraction of plasma is filtered across the glomerular capillary wall is referred to as the filtration fraction $FF = GFR/RPF$ and ranges from 20% under normal conditions up to 35-40% under conditions of volume depletion. The glomerular ultrafiltration coefficient (K_f , ml/min/mmHg) is the product of the filtration surface area and the capillary wall hydraulic conductivity. Assuming plasma flow is not limiting, the net ultrafiltration pressure gradient across the glomerular capillary wall together with the K_f determine the rate of glomerular filtration: $GFR = K_f \times (P_{GC} - P_{BS}) - (\pi_{GC} - \pi_{BS})$. The hydraulic pressure in the glomerular capillaries, P_{GC} , drives filtration. The oncotic pressure (π_{GC}) due to blood proteins in the glomerular capillaries and the hydraulic pressure in Bowman's space (P_{BS}) oppose filtration. In spite of wide variations in systemic blood pressure and extracellular volume status, glomerular blood flow and glomerular capillary hydraulic pressure are tightly regulated under normal conditions [76], keeping the GFR relatively constant. The glomerular capillary flow rate and pressure are regulated by the relative resistances of afferent and efferent arterioles. The fact that

glomerular capillaries empty into a resistance vessel, the efferent arteriole, is a remarkable adaptation that allows glomerular capillaries to be perfused at their relatively high pressure. Any increase in the afferent arteriolar resistance tends to reduce the pressure within the glomerulus, whereas an increase in efferent arteriolar resistance tends to raise glomerular capillary pressure.

Autoregulation tends to keep the glomerular capillary flow rate and GFR constant over a very wide range of systemic blood pressure. Autoregulation results predominantly from increments and decrements in afferent arteriolar resistance. Contraction of efferent arterioles contributes to the regulation of GFR under conditions of renin-angiotensin system (RAS) activation and high angiotensin II levels, for instance volume contraction.

The major mechanisms contributing to the RBF (and GFR) autoregulation are the afferent arteriolar myogenic stretch reflex [77] and tubule-glomerular feedback [78, 79]. The myogenic stretch reflex causes rapid contraction of afferent arteriolar vascular smooth muscle cells due to Ca^{2+} entry in response to intraluminal pressure [77]. Conversely, a decrease in perfusion pressure results in vasodilation of the afferent arteriole decreasing renal vascular resistance (RVR) and increasing the RBF. Tubulo-glomerular feedback is a negative feedback control mechanism that modulates the RBF and ultimately GFR by utilizing information from alterations in tubular reabsorption [78, 79]. Changes in the delivery of Na^+ and Cl^- are sensed by macula densa cells, a group of specialized tubule epithelial cells in the thick ascending loop of Henle, located between afferent and efferent glomerular arterioles. Increased NaCl transport by macula densa cells utilizes ATP and consequently produces adenosine, which in turn acts as a vasoconstrictor on renal afferent arterioles decreasing RBF. In addition, prostaglandins and nitric oxide modulate the resistance of afferent arterioles. By contrast, angiotensin II acting

predominantly on efferent arterioles tends to vasoconstrict them, which can also increase the RVR, increasing P_{GC} .

Microperfusion studies have shown that in certain experimental models of disease in rats, the P_{GC} and the ultrafiltration pressure gradient (ΔP) are significantly increased and contribute to morphologic changes in the glomerulus and progressive loss of renal function [80]. For example, an increase in P_{GC} and ΔP has been observed in several models of systemic hypertension in rats such as desoxycorticosterone/salt (DOCA/Salt) hypertension [81], Goldblatt hypertension [82], experimental diabetes mellitus [83, 84] and in several models of immune-induced glomerular disease [85, 86]. Furthermore reduced renal mass in the 5/6th, or subtotal nephrectomy model results in hemodynamic and molecular responses that lead to glomerular remodeling and hypertrophy [87], and complex changes in the neuro-humoral environment eventually lead to glomerulosclerosis [87]. Interestingly, nephron loss also seems to promote hemodynamic and molecular adaptations in the remaining nephrons that can make the kidney more resilient and precondition them against ischemic injury [88].

1.2. Hypertension: The leading risk factor for premature death worldwide

Elevated blood pressure (hypertension) is the leading risk factor for cardiovascular deaths, causing 7.6 million deaths every year worldwide. Moreover the number of deaths caused by high blood pressure is on the rise [89, 90]. Over 1 billion people worldwide have hypertension, making it one of the most common chronic diseases [91]. According to statistics by the Public Health Agency of Canada, hypertension affects more than one in five Canadians. High blood

pressure significantly increases risk for stroke, ischemic heart disease, peripheral vascular disease and heart failure.

Blood pressure is regulated by integrated actions of multiple control systems including: cardiovascular, renal, neural, endocrine, and local tissue systems. The short-term blood pressure regulation can be explained by the well-known formula “mean arterial pressure = cardiac output x total peripheral resistance”. The short-term mechanisms regulate blood vessel diameter, heart rate and contractility and the long-term mechanisms control blood volume. Short-term control of blood pressure is mediated by the nervous system and chemicals that begin to function within a few seconds. Within a few minutes or hours after a change in blood pressure, other control systems start to react. For example in response to decreased blood pressure, fluid from the interstitial spaces shifts into the blood or vice versa. In addition activation of the renin angiotensin aldosterone system RAAS plays an important role for regulation of blood pressure.

1.2.1 Hypertensive Nephrosclerosis

Hypertension attributed nephropathy is the second leading cause of end-stage renal disease and is particularly importance in the black population [92]. It is well accepted that elevated systemic blood pressure will expedite the progression of underlying chronic kidney disease (CKD). Hypertensive nephrosclerosis is characterized by a series of vascular lesions that can also be detected in different degrees in obesity and aging kidney [93, 94]. There are different factors contributing to hypertensive nephrosclerosis. The first factor is arterial stiffening accompanied by an increased pulse pressure at the afferent arteriole. Arterial thickening and stiffening happens even as a part of the normal aging process and is greater among blacks

compared to whites [95]. Unlike other capillaries in the body, glomerular capillaries are particularly vulnerable to injury by hypertension. To begin with, glomerular capillaries are normally perfused at a very high pressure, which is necessary to drive glomerular filtration. The filtration pressure is controlled by moment-to-moment adjustments of afferent and efferent arteriolar resistances, a phenomenon referred to as autoregulation. Loss of renal autoregulation can lead to glomerular capillary hypertension, which leads to remodeling and eventual replacement of the delicate glomerular capillary tuft by mesangial matrix. Alteration in renal autoregulation has been reported in various models of kidney injury including 5/6 nephrectomy model [96] streptozotocin-induced diabetes [97] and desoxycorticosterone-induced hypertension [98] as well as in human [99, 100]. Stiffened and dilated arterioles lead to glomerular hyperperfusion and hypertrophy, which contribute significantly to nephrosclerosis [92]. Also contributing to hypertensive nephrosclerosis is ischemic glomerulosclerosis which is followed by hypoxia in the tubulointerstitium, leading to tubular atrophy and interstitial fibrosis [101]. Moreover, studies have shown that there are molecular mechanisms that contribute to promote hypertensive kidney injury, such as the RAAS, endothelial dysfunction, oxidative stress, genetic and epigenetic factors [102]. For instance MYH9 and/or APOL1 gene polymorphisms in blacks make them more genetically susceptible to hypertension-induced ESRD and focal segmental glomerular sclerosis [103, 104]. A better understanding of the contributory molecular

mechanisms underlying the promotion of hypertensive nephrosclerosis will assist us to develop better therapeutic strategies toward hypertensive nephropathy

1.2.1.1 Glomerular capillary hypertension and mechanical stress

The trans-capillary hydraulic pressure gradient, ΔP , applies a continuous mechanical stretch to the glomerular wall. According to Laplace's law, [105] the wall tension, T , is directly proportional to the pressure gradient, ΔP , and the capillary radius, R . An increase in ΔP will cause a proportional increase of wall tension and subject the components of the glomerular wall to an increased mechanical stretch [105] similarly, an increase in diameter of the glomerular capillary loop, augments the wall tension (T). Therefore, the association of the glomerular hypertension and glomerular hypertrophy can accelerate glomerular injury [106].

To response to increased intraglomerular capillary hydraulic pressure and to adapt to enhanced mechanical forces, glomerular EC, podocytes, mesangial cells and their surrounding extracellular matrix undergo structural and functional changes known as cellular remodeling. Increased expression of growth factors, integrins and their receptors, adhesion molecules and many enzymes are among the known mechanisms modulating the remodeling process [107, 108]. Within the glomerular cells, the cytoskeletal remodeling response to mechanical forces probably evolved to resist increased perfusion pressures, but in the long run the glomerular capillary hypertension-induced changes may be counterproductive and contribute to glomerular sclerosis.

Figure 1.3

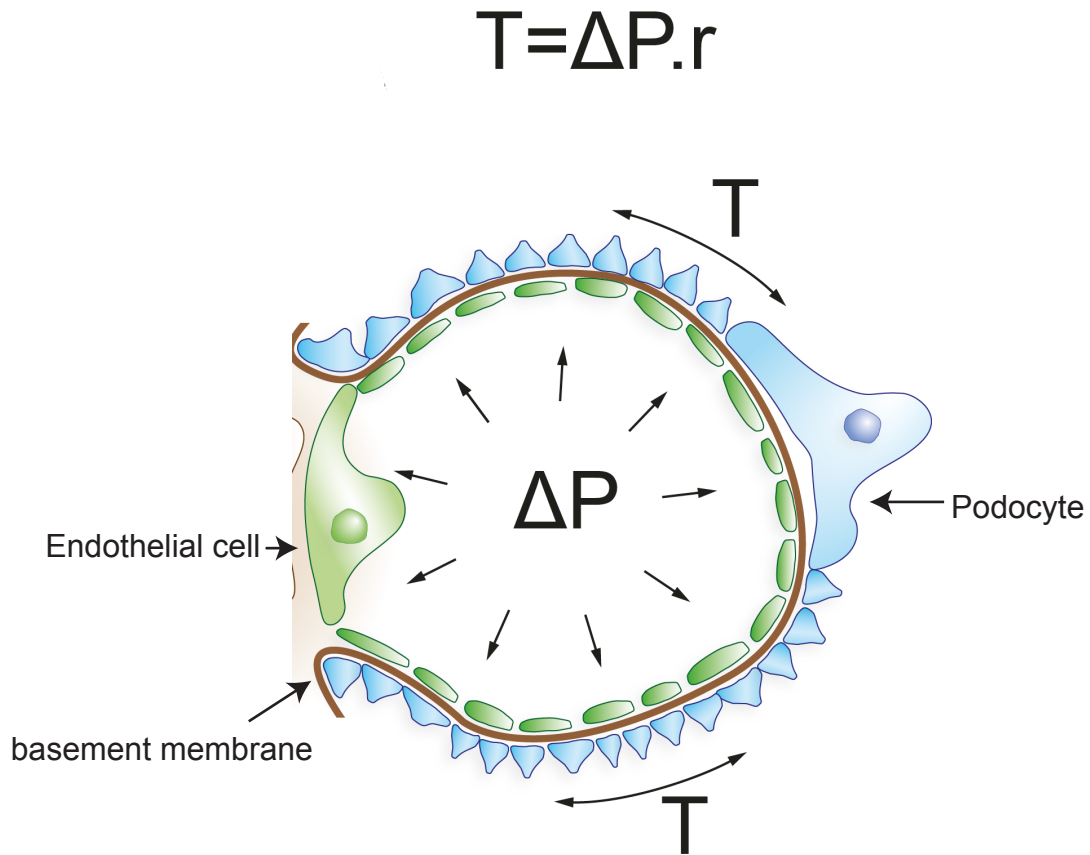


Figure 1.3 | Laplace's law. According to Laplace's law, the wall tension (T) is directly proportional to the pressure gradient (ΔP) and the capillary radius (r). An increase in ΔP will cause a proportional increase of wall tension and subject the components of the glomerular wall to an increased mechanical stretch; similarly, an increase in diameter of the glomerular capillary loop (r), augments the wall tension (T).

1.2.1.1.1 Response of endothelial cells to hypertension

Endothelial cells are sensitive to mechanical strain. Ex vivo studies using perfusion organs show that axial stretch increases the neointimal thickness in EC and enhances their rate of proliferation [109]. In vivo, exposing arteriolar ECs to hypertension can result in hyaline lesions, which are characterized by thickening of the walls of arterioles by the deposits that appear as homogeneous pink hyaline material in routine staining. Hypertension-induced glomerular EC injury was described to cause platelets aggregation, fibrin accumulation, and the formation of intracapillary microthrombi with subsequent progressive glomerular sclerosis [110]. Mechanical stretch induces an inflammatory response in EC, stimulating the exocytosis of Weibel-Palade bodies (WPBs), which contain von Willebrand factor (vWF), interleukin-8 (IL-8) and P-selectin [111-115]. Mechanical stretch also promotes endothelial nitric oxide synthase (eNOS) activation in EC through PKA and Akt signaling pathways [116]. Nitric oxide (NO) in ECs plays a protective role against mechanical stretch, by opposing vasoconstrictors and platelet activation, thus protecting against intravascular thrombosis [116].

Glomerular hypertension in several experimental models resulted in the formation of glomerular microaneurysms evident by ballooning and merging of adjacent EC [81, 117]. The formation of microaneurysms is initiated by mesangial failure lesions and is based on the endothelial dysfunction [118].

1.2.1.1.1 Fenestral glycocalyx contributes to the overall hydraulic resistance of the glomerular filtration barrier

As already described in section 1.1.1.1.1, the luminal surface of vascular endothelium is coated with an endothelial glycocalyx, composed of glycoproteins including proteoglycans and glycosaminoglycans and plasma constituents. The glycocalyx of glomerular capillary EC, which extends into the fenestrae, provides resistance to the transcapillary movement of water and macromolecules [119]. Biophysical models show that the glycocalyx layer in fenestrae strongly contributes (~ 50%) to the overall hydraulic resistance of the glomerular filtration barrier [48, 120]. Therefore, changes in glycocalyx within the fenestrae may damage the glomerular filtration barrier and potentially affect GFR [121]. Podocalyxin is the major constituent of the glomerular EC glycocalyx. It is of note that others and we found that the abundance of podocalyxin protein is reduced in CLIC5^{-/-} mice at baseline [122, 123].

1.2.1.1.2 Response of mesangial cells to hypertension

Accumulating evidence indicates the complex cytoskeleton of mesangial cells can be affected by mechanical stretch caused by glomerular capillary hypertension [124-126]. For example, exposing cultured mesangial cells to physical strain induces phenotypic changes in these cells. Under physical stress mesangial cells produce pro-inflammatory mediators such as cytokines, adhesion molecules, growth factors and cyclooxygenase products. Moreover, mechanical stretch increases mesangial cells proliferative activity and stimulates the production of collagen fibers [127-130]. Mesangial cells are separated from the blood stream only by the fenestrated endothelial layer therefore any increase in intracapillary pressure can irritate the mesangial cells by exposing them to more immunoglobulins and other components of an inflammatory environment [131].

1.2.1.1.3 Response of podocytes to hypertension

Glomerular podocytes are characterized by their complex actin-based architecture. Podocyte foot processes contain a subcortical network of branched actin filaments as well as longitudinal bundled filaments. Numerous studies show that disruption of podocyte cytoskeleton is the underlying reason of many renal diseases. For instance the majority of identified mutations that cause nephrotic syndrome occur in proteins that directly or indirectly regulate podocyte cytoskeleton dynamics and this involves almost always a change in the activity of small GTPases [56]. Recent studies show that podocytes have contractile capabilities, which may help them to withstand the high capillary pressure and adapt to their local environment [56, 132, 133]. Podocytes not only contain stretch activated receptors such as Ca^{2+} activated K^+ channels [134] but also express proteins consistent with differentiated smooth muscle cells including smoothelin, calponin and myocardin [132], and they contract in response to angiotensin II. Time-lapse imaging of human podocytes in vitro clearly shows constant motility and reorganization of cell edges [135]. Such podocyte movements have also been observed in vivo by newly developed 2-photon live imaging technology. In vitro studies show that stretched podocytes contain more activate Rho GTPases, which results in cytoskeleton reorganization and loss of stress fibers [136]. In response to stretch, the synthesis and secretion of various hormones and their receptors in a paracrine and autocrine manner is also increased. Stretch alters the podocyte cell adhesion through changes in integrin expression and activation [2]. In summary, in response to glomerular capillary hypertension podocytes undergo extensive cytoskeletal remodeling to maintain the integrity of the glomerular capillary loops, but in long term these changes may be counter-productive and result in foot processes effacement, albuminuria and sclerosis.

1.3. Rho GTPases the master regulators of cytoskeleton remodeling

The Rho family of GTPases is a family of small signaling G proteins with molecular weight around 20 kDa and is a subfamily of the Ras superfamily. Rho GTPases are precisely regulated molecular switches that control many aspects of cell signaling. The members of this family are known as master regulators of the actin cytoskeleton [137, 138], but they are also involved in cell polarity [139], membrane transport [140] and transcription activities [141]. There are 20 members of this family in humans, of which Rho, Rac and Cdc42 are the best-studied members.

Rho GTPases are called switches because they cycle between the active and the inactive conformational states. In the active state (on switch) they are bound to GTP. They intrinsically hydrolyze GTP to GDP forming the inactive conformational state (Off switch). In the active state they are able to bind to their target proteins and regulate their functions.

There are 3 known classes of Rho GTPase regulators: guanine nucleotide exchange factors (GEFs), which activate Rho proteins by facilitating the exchange of GTP for GDP; GTPase activating proteins (GAPs), which enhance the intrinsic ability of Rho proteins to hydrolyze GTP to GDP, and guanine nucleotide dissociation inhibitors (GDI), which form a large complex with the Rho protein, preventing the exchange of GTP for GDP as well as membrane association [142]. Researchers have identified more than 60 GEFs and more than 70 GAPs in the human genome. There are also other important regulatory mechanism to allow further spatiotemporal control of the members of Rho GTPases such as post-translational regulatory mechanisms for Rho GTPase-encoding mRNAs, phosphorylation, ubiquitination, AMPylation and transglutamination. There are over 60 targets identified for the three best-known members of Rho GTPases (Rho, Rac and Cdc42). Rho GTPases are involved in actin

cytoskeleton remodeling by controlling actin assembly and nucleation through interacting with Diaphanous-related formins (DRFs), WASP-family verprolin-homologous protein (WAVE) / Wiskott–Aldrich syndrome protein (WASP), cofilin and profilin. They are associated with the proteins that couple membranes to F-actin such as ERM, NHERF-1, NHERF-2 and also interact with PIP5K to generate PI[4,5]P₂.

1.3.1 RhoA

Ras homolog gene family member A (RhoA) is the most studied member of Rho GTPases. RhoA is involved in various cellular processes such as transcriptional control and cell cycle maintenance, but its main role is regulating cytoskeleton structures, mostly actin stress fibers formation and actomyosin contractility [143]. Inverted formin 2 (INF2) is a member of a protein family called the formins and is Rho effector [144, 145]. In response to activation of Rho signaling, diaphanous-related formins (mDia) stimulate actin polymerization. This signaling pathway can be antagonized by INF2. Mutations in INF2 genes result in aberrant activation of mDia through RhoA stimulation. Mutations in INF2 genes, result in dysregulation of RhoA signaling pathway and cause different forms of focal segmental glomerulosclerosis (FGSR) [145-147].

One of the most important effectors of RhoA function is Rho associated kinase (ROCK). Hyper-activation of the ROCK signalling pathway inhibits the activity of myosin phosphatase, therefore keeping the myosin regulatory light chain in the active, phosphorylated state. This activity of ROCK causes contraction of vascular smooth muscle cells disturbing the balance of vasodilating and vasoconstricting agents (thrombin, reactive oxygen species, TNF α , Ang II and lysophosphatidic acid) and produces an elevation of the vascular tone, therefore contributing to

hypertension. RhoA/ROCK inhibition is shown to prevent endothelial dysfunction in different models of vascular diseases [148].

RhoA activation is reported in various models of kidney injury such as in 5/6 nephrectomy, Puromycin aminonucleoside nephrosis (PAN) and Streptozocin (STZ) induced diabetes; Furthermore inhibition of RhoA kinase attenuates RhoA induced kidney damage [149-151]. Podocyte specific induction of both constitutively active RhoA [152, 153] or dominant negative RhoA [152] in mice can lead to foot process effacement, proteinuria and FSGS. Therefore, deviation of RhoA toward both hyper- and hypoactivity has deleterious effects in glomerular podocytes. Nonetheless, Scott et al [154] reported that RhoA is not required in the podocyte during development or in adulthood, suggesting either that RhoA is largely responsible for the remodeling response of podocytes, or that other Rho GTPases can substitute for RhoA during development. Further research is required to fully understand the role of RhoA signaling in physiological vs. pathological conditions.

1.3.2. Cdc42

Cell division control protein 42 homolog (Cdc42) is another member of small Rho GTPases. Cdc42 is involved in various cellular functions including cell morphology, endocytosis, migration and cell cycle control. Alternative splicing during gene transcription, as is also the case for Rac1 (see section 1.3.3 below) results in multiple Cdc 42 transcript variants. Cdc42 has a role in actin polymerization by binding directly to Neural Wiskott-Aldrich syndrome protein (N-WASP) and activating Arp2/3. In mice, podocyte-specific deletion of Cdc42 leads to congenital nephrotic syndrome [154, 155].

Interestingly, it is also suggested that Cdc42 activation after induction of synaptopodin deficiency results in proteinuria in mice. Synaptopodin binds to adaptor protein IRSp53 to prevent filopodia formation through inhibition of the Cdc42-IRSp53-Mena complex. Blocking Cdc42 activation via Mena inhibition prevents the podocyte injury and albuminuria in LPS induced kidney injury [156]. Therefore similar to the other members of Rho family, Cdc42 has a divergent role in podocyte health and disease [155].

1.3.3. Rac1

The Ras-related C3 botulinum toxin substrate 1 (Rac1) gene produces different versions of the Rac1 protein through differential splicing. They each appear to have different functions. Like RhoA and Cdc42, Rac1 is regulator of many cellular processes, including the cell cycle, cell-cell adhesion, motility and of epithelial differentiation.

Mutation in genes that encode specific regulators of Rac1 results in heritable nephrotic syndrome. So far three mutations in the ARHGDI α gene, which encodes a Rho GDP dissociation inhibitor α (Rho GDI α) that acts on Rac1, have been reported in patients with congenital nephrotic syndrome [157-159]. In vitro silencing the endogenous RhoGDI α , in cultured podocytes resulted in Rac1 hyper-activation, increased protrusion and retraction of leading edge, impaired actin polymerization and increased cellular projections. Microarray analysis of gene expression in isolated podocytes from developing mouse kidneys show that GDI α mRNA expression in podocytes is increased during kidney development. In contrast only immature podocytes contained active Rac1 indicating that GDI α has a critical role in suppressing Rac1 activity in mature podocytes under physiological condition [159].

Arhgap24, a Rac1 GTPase-activating protein (Rac1-GAP), is another gene for which mutations have been described that produce focal and segmental glomerulosclerosis (FSGS). In vitro and in vivo studies show that Arhgap24, is upregulated in podocytes as they differentiate, resulting in decreased Rac1 activity [160]. Two independent groups have reported generation of podocyte-specific deletion of Rac1 in mice with different outcomes. Babelova et al. [149] reported that Rac1 KO mice display normal podocyte morphology without glomerular dysfunction well into adulthood. In contrast, Ishizaka et al. [161] showed that Rac1 KO mice exhibit an increased foot process effacement and proteinuria. The differences in the observations by these groups may be explained by the environmental factors and genetic heterogeneity of the mutated mice.

Blantner et al. [155] reported that podocyte-specific deletion of Rac1 lead to completely different results in acute or chronic models of podocyte injury, protamine sulfate vs DOCA/Salt hypertension model respectively, with protection against injury after protamine sulfate infusion, but increased chronic injury in the DOCA/Salt model of hypertension. Podocyte-specific deletion of Rac1 also increases the progression of diabetic nephropathy in Streptozocin (STZ) diabetic mice [161]. The authors suggested that Rac1 deletion might impair hypertrophic signaling pathways in podocytes to match glomerular tuft growth. The failure of podocyte hypertrophy might have resulted in proteinuria and glomerulosclerosis in UNX-DOCA hypertension model as well as in STZ-induced diabetic mice. Moreover, a role for Rac1 activation in actin organization in glomerular podocytes during podocyte recovery has been suggested in passive Heymann nephritis (a model of immune renal disease that closely resembles human membranous nephropathy) [162].

In contrast to these positive roles for Rac1, it has been reported that Rac1 activation either by podocyte specific induction of constitutively active Rac1 in mice [163] or by silencing Rho GDI [164] results in foot processes effacement and enhanced albuminuria in mice. Conversely, a protective role for Rac1 inhibitors in different models of kidney injury has also been described [149, 165, 166].

Therefore, excessive Rac1 activation seems to be deleterious, but Rac1 activation is nevertheless necessary for the glomerular podocyte remodeling response to hypertension and diabetes, and perhaps other stresses. Together these experimental results highlight the importance of meticulous regulation of Rac1 signaling in podocytes in maintaining the integrity of glomerular filtration barrier.

Rac1 also has a role in fenestrae formation. In the mouse corneal angiogenesis assay, Rac1 inhibition by cell-permeable Rac1 antagonist (TAT-RacN17) prevented fenestration formation and short-term vascular permeability in new vessels induced by VEGF [167]. Studies in EC cultures showed that VEGF stimulated phosphorylation of VEGF receptor-2 (VEGFR-2), leading to activation of Rac as well as increased phosphorylation of phospholipase C γ (PLC γ), Akt, eNOS, and Erk1/2. In the EC, phosphatidylinositol-3-OH kinase (PI3K) was the upstream stimulator of Rac1 and Akt-eNOS in VEGF/VEGFR-2 signaling [167]. In contrast, others have shown that dominant negative Rac1 and a Rac1 inhibitor decrease the persistent and basal barrier function of monolayer ECs [168-170]. These apparently conflicting results suggest that Rac1 probably regulates basal permeability, persistent leakiness, and acute hyper-permeability by distinct mechanisms.

1.3.3.1 The PAK family of serine/threonine kinases: downstream effectors of Rac1/Cdc42

The activity of Rho GTPases is tightly regulated both spatially and temporally. These regulatory mechanisms are performed by controlling of nucleotide binding and hydrolysis by GEFs and GAPs, subcellular localization as well as protein expression levels [171]. Once activated and translocated to their specific subcellular locations, Rho GTPases interact with downstream effector molecules to regulate specific signaling events. The PAK family of serine/threonine kinases is one of the most well known effectors of Rac1 and Cdc42. The PAK family contains six members. Based on sequence and structural similarities, PAK members are divided into two groups. Group I PAKs, which has been studied in detail and is fairly well characterized, consists of PAK1, PAK2, and PAK3. Group II PAKs contains PAK4, PAK5, and PAK6 and is less well-studied [172]. Although PAK kinases play important roles in a wide range of biological events, including MAP kinase activation and gene regulation, their main action appears to be the regulation of cytoskeletal dynamics in different cells, including podocytes [66]. It has been shown that in podocytes nephrin binds the Nck adaptor proteins, which control actin polymerization through interacting with N-WASP and PAK proteins [56, 66]. Pak1 phosphorylates LIM kinases 1 and 2 (on Thr508/505), which inactivate the actin severing function of Cofilin1/2 through a Ser3 phosphorylation [173].

1.4. ERM proteins: Bridging the gap between cytoskeleton and plasma membrane

The specialized actin-rich cortex of the cells lies directly beneath the plasma membrane. The dynamic interplay between the plasma membrane and the underlying actin cytoskeleton is crucial for maintenance of cell shape, cell adhesion, signaling, migration and division. The majority of the linkage between the actin microfilaments and the cell membrane are mediated by specialized actin binding proteins. Ezrin, radixin and moesin (ERM) proteins are major

regulators of cell surface architecture and link actin filaments to the membrane either directly by binding the cytoplasmic tails of transmembrane proteins or indirectly through linker proteins such as intermediate phosphoprotein 50 (EBP50, also known as NHERF-1) or E3KARP (NHERF-2).

The ERM protein family belongs to the band 4.1 superfamily and are closely related the tumor suppressor merlin, which also has a role in regulating cytoskeletal membrane. ERM proteins are highly conserved throughout evolution and share more than 75% identity (73-81%) in their amino acid sequence [174]. All three ERM members are present in vertebrates, whereas non-vertebrates usually have only one ERM gene; for instance dmoesin is the only ERM protein in *Drosophila* and ERM-1 is the only one in *C. elegans* [175, 176].

ERM proteins have a conserved N-terminal FERM (4.1-ezrin–radixin–moesin) domain, which is able to bind to specific phospholipids and integral plasma membrane proteins or scaffolding proteins. The FERM domain adopts a tri-lobed cloverleaf structure and consists of three subdomains (F1, F2 and F3). The central domain of ERM proteins is an extended alpha helical coiled-coil domain, and the C-terminal domain contains a major F-actin-binding site. In the C terminal there is a conserved threonine amino acid (Human ezrin, T567; radixin, T564, moesin, T558, respectively), which is phosphorylated upon activation. Western blot analysis and immunofluorescence microscopy showed that in most cultured cells all three ERM proteins are co-expressed and co-localized. In mammals, ezrin, radixin and moesin show an organ- and tissue-specific expression pattern with ezrin being expressed mostly by epithelial cells, radixin by lymphoid cells and hepatocytes and moesin by EC. Although most tissue in mice co-expresses all three ERM proteins, ezrin and radixin expression is missing in liver and intestine, respectively [177].

It is suggested that ERM proteins can compensate for each other when individual members are lost, and that they have functional redundancy. This idea is supported by the lack of overt phenotypes in Ezrin, Moesin and Radixin deficient mice [177-179]. Moesin deficient mice do not exhibit distinct phenotype and there is no compensatory up-regulation of other members in different tissues from these mice[177]. Radixin knockout mice are viable and suffer from mild liver defects and deafness. Deafness is a result of stereocilia degeneration in the inner ear hair cells that only express radixin [178]. Ezrin deficient mice are also viable but die within 3 weeks after birth because of defects in intestinal villous formation which exclusively express ezrin [179].

Ezrin was the first member of ERM protein identified in 1983 during the characterization of the components of microvilli by Bretscher et al [180]. Later, other studies showed that ERM proteins are not only associated with the formation and maintenance of actin rich structures such as microvilli, stereocilia, phagosomes and podocyte foot processes [181-183] but are also involved in cell-cell adhesion, cell motility and membrane trafficking. Moreover ERM proteins regulate Rho family signaling pathway by recruiting their regulators. They act both upstream [184, 185] and downstream [176, 186, 187] of Rho GTPases.

1.4.1 ERM Protein activation requires PI[4,5]P₂ binding

ERM proteins exist in either a cytoplasmic dormant, auto-inhibited state, or in the active state. The conformational changes between active and inactive form regulates their activation and function. The FERM domain has an affinity to bind its own F-actin binding domain and this intra-molecular interaction maintains ERM proteins into a dormant, folded form. While inactive, the ERM proteins are uncoupled from actin and are cytosolic. The change from inactive to the

active conformation of the ERM proteins is initiated by binding of the FERM domain to the plasma phospholipid PI[4,5]P2 [188]. This results in a conformational change that unmasks the actin-binding site and N-terminal sites that can bind trans-membrane proteins. Binding of the C-terminal ERM domain to actin can occur without its phosphorylation since T564 phosphorylation of recombinant COOH-terminal half radixin did not affect its ability to bind to actin [160], but binding of ERM protein to cortical actin is further stabilized by phosphorylation of conserved serine and threonine residues by kinases such as Rho-kinase [189, 190], PKC θ [190] and PKC α [191]. Our lab reported that ectopic expression of CLIC5A in COS7 cells, which do not express CLIC5A at baseline, stimulates the accumulation of PI[4,5]P2 in the apical plasma membrane patches or clusters, followed by Ezrin phosphorylation and cytoskeletal association, along with actin polymerization and cell-surface ruffling. PI[4,5]P2 depletion either by PLC activation or PIP5K silencing prevented CLIC5A-stimulated Ezrin phosphorylation [4]. These results suggest that CLIC5A stimulates ERM activation via PI[4,5]P2 cluster formation.

1.4.3 PI[4]P5Ks activation is regulated by members of Rho GTPases

Production of different pools of PI[4,5]P2 are temporally and spatially regulated via precise regulation of the activity of different PIP5K isoforms. PI[4,5]P2 generation is also reported in different intracellular compartments, including the mitochondria, nucleus, lysosomes, autolysosomes, endosomes, autophagic precursor membranes, endoplasmic reticulum and the Golgi complex [192]. PIPKs, PI[4,5]P2 phosphatases and PI[4,5]P2 effectors all together regulate the PI[4,5]P2 signaling at a particular location within the cell. Rho/Rac [193], talin [194], Arf [195], Ajuba, phosphatidic acid [196] and Phospholipase D [194, 197] are among the well-studied regulators of PIP5K activation. For instance Rac1 and Rho can selectively regulate PIP5K, promoting recruitment of the kinase to the membrane to produce PI[4,5]P2. PI[4,5]P2

production in discrete locations of the plasma membrane enhances the binding of the active Rho GTP to the membrane and provide a positive feedback loop [198]. PIP5KI isoforms are selectively recruited and activated at the plasma membrane by Rac1 to generate PI[4,5]P2 in ruffles and lamellipodia, at focal contacts, and in clathrin-coated pits, and Rac1 forms a multi-molecular complex engaging PIP5KI [199]. Moreover, yeast two-hybrid screens suggest that CLIC1 and CLIC4 may interact with the C-terminal region of the type 1 β PIP5K (<http://www.signalinggateway.org>). Our lab recently showed that CLIC5A enhances clustered PI[4,5]P2 accumulation via interaction with PI4P5 kinases at the apical domain of the COS7 cells. The fact that different members of CLIC family are located in diverse subcellular locations, for instance at the base of actin-based microvilli, stereocilia, nuclei, the Golgi apparatus, mitochondria and secretory vesicles [4] and that different pools of PI[4,5]P2 are located and function in different intracellular organelles [192] suggest that some members of the CLICs (including CLIC4) may regulate production of various pools of PI[4,5]P2 in specific intracellular organelles via interaction with different PIP5K isoforms and/or Rho GTPases.

1.5 Chloride Intracellular Channels (CLICs) a perplexing family of proteins

The chloride intracellular channel (CLIC) family is a diverse group of 6 mammalian CLIC proteins (CLIC1-6) that belong to a subgroup of the glutathione-S-transferase (GSTs) superfamily [200]. Although the CLIC proteins have arisen from a single chordate CLIC and share about 60–75% similarity in a 240 amino acid domain, termed “CLIC domain”, they have diversified in functions [201]. Some CLICs such as CLIC1 and CLIC4 exist in a wide range of cells while others such as CLIC5A and CLIC6 appear in very limited cell types [202]. Distinct CLIC family members are able to associate with nucleus [203-205], the Golgi [206],

mitochondria [203] and secretory vesicles [207]. CLIC proteins exist as both soluble globular proteins and integral membrane proteins. The membrane localization is redox-regulated and strongly depends on pH [208, 209]. Under oxidizing conditions *in vitro*, CLICs undergo a conformational change due to stabilization of an intra-molecular disulphide bond. This allows association with lipid bilayers and extension of their N-terminal alpha helical region. Hydrophobic domains at the N and C terminal mediate spontaneous association from the soluble form with lipid bilayers and an associated ion conductance, which has been referred to as chloride ion channel activity [201, 210, 211]. CLICs were named as chloride channels when initially p64 (CLIC5B) was purified with the non-selective Cl⁻ channel inhibitor IAA-94. Some CLICs were also reported to have a role in vacuolar/vesicular acidification in different cells [212, 213]. However, in contrast to their name, CLICs do not fit the patterns of other, more conventional ion channels. Unlike other well-characterized chloride channels that show clear and often multiple trans-membrane domains, CLICs have only one short N-terminal hydrophobic domain. Although it has been suggested that that this domain can spontaneously insert into, and span lipid bilayers, our laboratory believes this to be unlikely, because it would require that a beta-pleated sheet region in the molecule becomes alpha-helical, which does not usually occur. Also, my own studies (see below) show that GFP-CLIC5A (with GFP fused to the N-terminus) can rapidly dissociate from the plasma membrane, which should not be possible for a trans-membrane protein. Whether CLICs function as genuine chloride channels *in vivo*, or whether they modify the activity of other chloride channels is still controversial [200, 213].

It is also suggested that CLICs may function as a molecular scaffold involved in the formation of localized multi-protein complexes [201, 202, 214]. The focus is shifting on a role for CLICs in defining actin based cellular structures [4, 207, 211]; however, the exact

mechanism(s) of CLICs action is/are not completely understood, and they are the subject of investigation in our laboratory.

1.5.1 Functional relationship between CLICs, Rho GTPases and ERM proteins

1.5.1.1 CLIC1:

CLIC1 (also called nuclear chloride channel-27 or NCC27) was first cloned in 1997 from an activated human macrophage cell line. Multiple studies suggest that CLIC1 can form an actin-regulated membrane channel. Purified, recombinant CLIC1 auto-insert into membranes and induces ion conductances. This putative channel activity CLIC1 is strongly inhibited by F-actin, an effect that can be reversed by cytochalasin B, which disrupts polymerized actin [215]. Moreover, a role for CLIC1 in phagosomal acidification has been reported [216]. Macrophages engulf microorganisms or foreign particles via phagocytosis to form phagosomes. Phagosomes undergo gradual maturation by trafficking into a series of increasingly acidic endosomes [217, 218]. It is established that actin cytoskeleton remodeling has an essential role in phagosomal maturation. Actin remodeling during phagosomal maturation is regulated by ERM proteins and Rho GTPases such as Rac2 and RhoA [219]. While in resting macrophages, CLIC1 exist in vesicle-like cytoplasmic structure with dense peri-nuclear distribution, upon ingestion of serum opsonized zymosan particles, CLIC1 translocates to phagosomal membrane where it co-localizes with ezrin, Rac2 and RhoA [216]. These data suggest that the CLIC1 membrane association requires orchestrated actions of Rho GTPases and potentially also ERM proteins. Alternatively, it is also possible that the CLIC1 membrane association is mediated by Rac2 and/or RhoA, resulting in ERM protein activation through the production of PI[4,5]P2 in the cytoplasmic face of the phagosomal lipid membrane.

1.5.1.2 CLIC3

Endosome trafficking is now recognized as a major function for recycling of cell surface receptors and other trans-membrane proteins in many cells. There is an established role for the members of Rho GTPases and ERM proteins in regulating endocytic traffic [220-222]. For example, integrins, which are heterodimeric transmembrane proteins with α and β subunits that link the intracellular actin cytoskeleton to the extracellular matrix (ECM) components undergo endocytosis and endosomal recycling during neoplastic cell migration and invasion. This process is mediated by Rho GTPases [223]. A number of studies suggest that CLIC3 plays an important role in the sorting and recycling of such integrin-containing endosomes.

CLIC3 was initially identified using yeast two-hybrid screen with the COOH-terminal tail of extracellular signal-regulated kinase 7 (ERK7) as bait. CLIC3 was shown to be highly expressed in placenta, lung and heart and to a less extent in skeletal muscle, kidney, and pancreas and was undetectable in brain [204].

Studies in a cancer cell line by Dozynkiewicz et al. [224] show that CLIC3 together with the small Rho GTPase Rab25 directs endocytic trafficking of active β 1-integrin from the late endosome to the plasma membrane causing dissociation from the matrix, enhanced motility and invasion. Later the same group reported that CLIC3, independent of Rab25, is able to facilitate the polarized delivery of pro-invasive matrix metalloprotease (MT1) in 2 breast cancer cell lines [225]. There are similar findings regarding the role of CLIC1 and CLIC3 in endocytic trafficking of integrins in cancer cell lines [226, 227].

1.5.1.3 CLIC4

CLIC4 was originally isolated from a protein complex containing actin, tubulin and 14-3-3 from brain lysate. CLIC4 directly binds to the actin regulators 14-3-3 and dynamin but it does not bind actin directly [228, 229]. The retinal pigment epithelium (RPE) of the eye is a monolayer of pigmented cells sandwiched between the photoreceptors and the choroid capillaries that nourishes retinal visual cells. Retinal Pigment Epithelium cells are characterized by long apical microvilli, which allows close structural interaction to the photoreceptors[230]. CLIC4 is enriched in the actin-based apical microvilli of retinal pigment epithelial cells similar to Ezrin. Knocking out CLIC4 or ezrin induces loss of microvilli structures. Ezrin overexpression rescues impaired microvillus processes but is unable to restore other abnormalities caused by CLIC4 silencing [231].

Stimulation of NIE-115 neuroblastoma cells expressing GFP-CLIC4 with lysophosphatidic acid (LPA), thrombin receptor activating peptide, or sphingosine-1-phosphate, resulted in a drastic movement of CLIC4 to the plasma membrane. CLIC4 translocation to the plasma membrane was dependent on G α 13-mediated RhoA activation, but not ROCK activity, and was accompanied with recruitment of NHERF-2 to the same sites. Mutation of the CLIC4 hydrophobic region prevented its membrane recruitment and NHERF-2 co-localization [232]

Tubulogenesis is the process by which epithelial and endothelial tubes are generated to enable the efficient transport of substances into and out of tissues. Tube formation is essential in organs like the kidney, in the vascular system, in exocrine glands, in the digestive tract and in the lung. Cortical actin, ERM and Rho GTPases are crucial in the process of tubulogenesis [233, 234]. Tube formation can occur through the assembly of adjacent cells that then form polarized

apical and basolateral regions, with the apical region facing a central lumen. Alternatively, in some systems, for example in capillary formation and in the formation of the exocrine duct of *C. elegans*, fusion of large intracellular acidic vacuoles of adjacent cells (similar to the stacking of several doughnuts on top of each other) results in lumen formation [235]. Numerous studies have shown that CLIC4 has a role in intracellular membrane trafficking leading to tubulogenesis of endothelial and epithelial cells [236-238]. It has been postulated that CLICs could provide for Cl^- influx into intracellular organelles during electrogenic vacuolar H^+ -ATPase-mediated acidification [213].

In 3-dimensional MDCK cultures, an *in vitro* model of tubulogenesis, CLIC4 modulates apical vesicular trafficking by negatively regulating the branched actin expression on early endosomes. CLIC4 suppression inhibited merging of the apical vesicles, disrupting central lumen formation. The small Rho GTPases, Rab8 and Cdc42, were able to rescue the effect of CLIC4 silencing in this model system. Furthermore, CLIC4 regulates selective apical localization of Phosphatase and tensin homolog (PTEN) to the newly formed lumen plasma membrane [229]. PTEN dephosphorylates phosphatidylinositol (3,4,5)-trisphosphate (PIP3) at the plasma membrane to form $\text{PI}[4,5]\text{P}_2$, which serves as a docking site for actin binding proteins such as ERM, cofilin and profilin [239]. It therefore seems possible that CLIC4 acts in conjunction with small GTPases to regulate the formation of $\text{PI}[4,5]\text{P}_2$, which in turn leads to ERM activation during the formation of epithelial and endothelial cell tubes. *In vivo*, impaired angiogenesis in CLIC4 deficient mice results in reduced arterial collaterals in skeletal muscle and brain [240] as well as a decreased number of renal glomeruli and peri-tubular capillaries [241].

1.5.1.4 CLIC5

CLIC5 is transcribed from two alternative exons 1 (1A and B). Exon 1A transcription results in production of a ~32 kDa isoform with 251 amino acids called CLIC5A and Exon 1B transcription results in production of a second isoform containing 410 amino acids (~49 kDa) called CLIC5B [206]. CLIC5A was originally discovered in human placental microvilli in an actin-based protein by using ezrin as bait [182]. When CLIC5A was ectopically expressed in JEG-3 placental choriocarcinoma cells it displayed a polarized distribution in apical microvilli along with ezrin and became resistant to the detergent, Triton X-100, extraction. The fact that CLIC5A remained coupled to the cytoskeleton suggesting a role in the assembly and/or maintenance of actin based structures at the cell cortex [242].

1.5.1.4.1 CLIC5, radixin & stereocilia in inner ear hair cells.

Stereocilia are the mechanosensing actin-based membrane extensions of hair cells in inner ear. Stereocilia in the cochlear sensory hair cells are responsible for hearing whereas vestibular stereocilia are in charge of balance. Radixin is the only detectable species of ERM protein in the stereocilia of the cochlear sensory hair cells, whereas in vestibular stereocilia ezrin co-expresses with radixin [243]. Interestingly radixin deficient adult mice are deaf and their cochlear hair cell stereocilia degenerate with time, but they have no obvious vestibular dysfunction. It is thought that in mice lacking radixin, ezrin can compensate in the cells responsible for vestibular function. Since the cochlear hair cell stereocilia are normal early in life, it seems that ezrin can substitute for radixin during the development of cochlear stereocilia, but not later in life [178]. In inner ear, CLIC5A co-localizes with actin at the base of the both cochlear and vestibular hair cell stereocilia, similar to distribution of radixin. A spontaneous mutation of the CLIC5 gene in Jitterbug mice results in the absence of detectable CLIC5 protein

expression[183]. Similar to the observations in mice lacking radixin, in the CLIC5-deficient mice, stereocilia develop normally and subsequently degenerate with age, causing hair cell loss, vestibular dysfunction and deafness by the age 7 month [244]. The existence of both cochlear and vestibular dysfunction in Jitterbug mice suggests that CLIC5 interacts with both radixin and ezrin to maintain the integrity of hair cell stereocilia.

1.5.1.4.2 CLIC5, Ezrin & integrity of glomerular filtration barrier

Our laboratory found for the first time that the CLIC5 mRNA is enriched about 30 fold in glomerular EC compared to non-glomerular EC [3] and about 800 fold in human glomeruli, relative to most other non-glomerular human tissues and cells [3]. The high level of expression of CLIC5 in human glomeruli was confirmed by in situ hybridization and RT-PCR. The glomerular transcript encodes the CLIC5A isoform of CLIC5 [3, 245].

Further our laboratory showed that within glomeruli CLIC5A immunoreactivity is localized to both, glomerular EC and podocytes. By immunogold transmission electron microscopy (TEM) with affinity-purified anti-CLIC5A antibody, CLIC5A labeling was observed in both, glomerular podocytes and glomerular EC. Although immunogold labeling was also detected in fenestrated peritubular capillaries, morphometric quantification of immunogold density showed that labeling was greatest in podocytes and glomerular ECs. In glomerular ECs, CLIC5A was localized in both the fenestrated and non-fenestrated areas. In podocyte foot processes, CLIC5A localized in a polarized fashion at the apical plasma membrane, far from the filtration slit diaphragm, similar to the known localization of trans-membrane protein podocalyxin and ezrin [58, 246, 247]. Dual IF studies showed that CLIC5A co-localized with

podocalyxin and ezrin and podocalyxin co-immunoprecipitated with CLIC5A from mouse glomerular lysates [5].

Morphometric analysis of TEM images from CLIC5 deficient mice showed a very perceptible broadening of podocyte foot processes. Although the thickness and fenestration frequency of glomerular EC was the same in wild type and *jbg/jbg* mutant mice, there was an increase in the number of large vacuoles and the total capillary lumen area in CLIC5 deficient mice compared to the wild type. The renal ultrastructural abnormalities in *jbg/jbg* mutant mice were accompanied by microalbuminuria at baseline and enhanced proteinuria followed by Adriamycin injection. Unchanged nephrin abundance (unpublished) and mild albuminuria in CLIC5 deficient mice, suggested that the slit diaphragm complex is intact [245]. Collectively these results indicate that in podocytes of CLIC5A-deficient mice the link between apical podocalyxin and actin, which requires ezrin, is weakened, which enhances the susceptibility of CLIC5 deficient mice to the Adriamycin-induced kidney injury.

1.5.1.4.3 CLIC5A regulates ERM protein phosphorylation by PIP5K activation.

Using ectopic expression of CLIC5A in COS7 cells, our lab showed that CLIC5A enhances ezrin activation and actin-dependent cell-surface remodeling [4]. Overexpression of CLIC5A in COS7 cells led to an increase in ERM phosphorylation and increased association of the ERM proteins with the actin cytoskeleton. CLIC5A also stimulated actin polymerization and the formation of actin-based cellular extensions at the apical cell surface. The CLIC5A mediated enhancement of ERM phosphorylation was not inhibited by chloride channel inhibitor IAA-94, indicating that this action is not due to CLIC5A-stimulated Cl⁻ channel activity. CLIC5A lead to translocation of the PI[4,5]P₂ reporter RFP-PH-PLC from cytosol to the dorsal plasma

membrane, and a dramatic re-organization of negatively charged phospholipids into discrete clusters. This indicates that CLIC5A results in enhanced formation of PI[4,5]P2 clusters in the apical plasma membrane. CLIC5A co-localized with HA tagged PI[4,5]P2 generating enzyme, PIP5K α at the apical plasma membrane, but CLIC5A was not necessary for the recruitment of the kinase to the membrane. Even so, overexpression of HA-PIP5K α alone did not increase the formation of PI[4,5]P2 clusters or ERM protein activity, which required CLIC5A. Moreover, silencing of PIP5K α eliminated the CLIC5A-induced PI[4,5]P2 production and ERM phosphorylation in COS-7 cells [4]. These findings suggest that if CLIC5A augments PI[4,5]P2 generation in the plasma membrane, it does so not by recruiting the PI[4,5]P2 generating kinase to the membrane, but by activating it, either directly or indirectly. The laboratory also showed that the HA-tagged isoforms of PIP5K(α and β) as well as PIP4K(α and β) were pulled out of cell lysates with immobilized GST-CLIC5A, but not with immobilized GST [4]. This suggests that CLIC5A can interact with several PI[4,5]P2 generating enzymes, but whether the interaction is direct or requires intermediate proteins still needs to be worked out. Consistent with the in vitro data, in CLIC5^{-/-} mice, the association of NHERF2 and ezrin with the cytoskeleton was markedly reduced and the ezrin and podocalyxin levels were lower in CLIC5^{-/-} than in wild-type mice[4]. Therefore, CLIC5A interaction with PI[4,5]P2 generating kinases mediates clustered PI[4,5]P2 accumulation and downstream ezrin phosphorylation. In turn, phosphorylated ezrin links NHERF-2 to actin, which results in actin-dependent cell surface remodeling.

1.6 Hypothesis and Objectives

Rationale

This thesis centers on the potential role of CLIC5A, an ERM-activating protein, in maintaining the specialized architecture of podocytes. I propose that CLIC5A acts upstream of Rac1, and that the Rac1-dependent podocyte response to hypertension, is impaired when CLIC5A is absent.

As I have described, glomerular capillaries are normally perfused under a relatively high hydraulic pressure, which drives glomerular filtration. The high intracapillary pressure creates capillary wall tension which is mitigated, in part, the actin-based primary projections and secondary foot processes of podocytes, which wrap around the exterior of the glomerular capillary wall. In response to physical forces such as shear stress [248] and cyclical strain [249], podocytes undergo cytoskeletal remodeling. Although mature podocyte foot processes are relatively stable under unchallenged conditions, they are mobile and can undergo dramatic cytoskeletal changes, for instance during the recovery from effacement [250]. It is believed that dynamic regulation of the actin cytoskeleton of podocyte is crucial for normal kidney function and that proteins regulating podocyte architecture maintain the integrity of the glomerular filtration barrier[251]. I propose that actin remodeling also has to occur when podocytes are challenged by hypertension.

The Rho family of GTPases is widely accepted to be among the major regulators of podocytes actin dynamics [164, 250], and Rac1 activation in vivo and in vitro increases cell motility and active remodeling of focal adhesions as well as cell-cell junctions. Rac1 stimulates ERM activity by increasing the levels of PI[4,5]P2 in the plasma membrane through its activating effect on PI4P5 kinases. Rac1 also stimulates actin polymerization, in part through its

effect on the effector Pak1, which inhibits the actin-severing protein cofilin. RhoA-stimulated ROCK can also directly phosphorylate the ERM C-terminus.

Our laboratory began to focus on CLIC5A because its expression was 800 fold greater in human glomeruli compared to other tissues [3]. CLIC5A localizes specifically to the apical domain of podocyte foot processes in a complex with NHERF-2, podocalyxin and ezrin. In CLIC5A deficient mice the glomerular ezrin abundance is profoundly reduced, and podocyte foot processes are fewer in number, shorter, and broader than those in wild-type mice. The mice have microalbuminuria and are more susceptible to adriamycin-induced injury than wild-type mice.

At the molecular level, our laboratory established that CLIC5A regulates the ERM-associated cytoskeletal architecture through an interaction with PI4P5 kinases that leads to PI[4,5]P2 accumulation in the apical plasma membrane. PI[4,5]P2 in turn is the first step in ezrin activation and facilitates ERM binding to actin [252]. Although our lab showed that CLIC5A interacts with PIP5K to regulate PI[4,5]P2 production the nature of this relationship is still unclear.

Based on this knowledge, I postulate that the Rho GTPases, and in particular Rac1, could well serve as the target of CLIC5A, since both CLIC5A and Rac1 activate PI[4,5]P2 generation, both CLIC5A and Rac1 stimulate PI[4]P5 kinases and both CLIC5A and Rac1 as well as RhoA participate in ERM-mediated actin remodeling. I therefore set out to determine whether CLIC5 regulates Rac1 and/or RhoA activity and whether CLIC5-dependent Rac1 and/or Rho activation participate in the glomerular response to high blood pressure.

Finally, our lab also reported that in glomeruli of CLIC5 deficient mice, ERM phosphorylation was only reduced in podocytes and not in glomerular capillary ECs [5], even

though CLIC5A is expressed by glomerular ECs in wild-type mice and in culture [3, 5]. Since CLIC4, a CLIC5 homologue is also expressed by glomerular EC and is also associated with ERM proteins I considered whether CLIC4 could also activate ERM proteins, and could compensate for lack of CLIC5 in glomerular EC.

HYPOTHESIS

CLIC5A maintains the specialized architecture and function of podocytes by regulating Rac1-dependent ERM activation and the lack of CLIC5A is detrimental under conditions of increased mechanical strain and leads to accentuated kidney damage in mice.

Objectives

Objective 1. Explore whether CLIC5A-stimulated ERM phosphorylation requires Rac1 activation.

Objective 2. Determine whether podocyte injury in a model of hypertension is accentuated in CLIC5A deficient mice, and define the role of the podocalyxin/ezrin/CLIC5A complex in the podocyte response to hypertension.

Objective 3. Explore whether Rac1 activation is a component of the podocyte response to DOCA/Salt hypertension and determine whether the vulnerability of CLIC5A deficient mice to glomerular injury results from altered Rac1-dependent cytoskeletal remodeling.

Objective 4. Determine whether CLIC4, which is highly homologous with CLIC5A and is expressed in EC, compensates for the lack of CLIC5A in glomerular EC in CLIC5 deficient mice.

Chapter 2

Materials and Methods

2.1 Reagents and Antibodies

The Rac1 Activation Assay Kit was obtained from Cytoskeleton Inc. (Denver, CO), the Rho Pull-Down and Detection Kit from Thermo Scientific (Rockford, IL), the Rac1 inhibitor (NSC 23766) from Santa Cruz Biotechnology Inc. (San Diego, CA), and the DOCA slow-release pellets from Innovative Research of America (Sarasota, FL). Antibody sources and dilutions are shown in (table 2.1). Unless specified, all other reagents were purchased from Sigma-Aldrich Canada Co. (Oakville, ON, Canada).

2.2 Experimental Animals: All procedures in mice were approved by the University of Alberta Animal Care and Use Committee (protocol #AUP00000222).

2.2.1 Generation of CLIC5^{-/-} mice

CLIC5 deficient Jitterbug mice (CLIC5^{*jbjbg*}) on the CH3/HeJ background were obtained from Jackson Laboratories (Bar Harbor ME). The CLIC5^{*jbjbg*} mice were discovered in The Jackson Laboratory (Bar Harbor, MN, USA) due to their head bobbing and circling behavior, a characteristic abnormality mainly observed in mice with defects in the vestibular apparatus. This strain of mice, initially on the C3H/HeJ background was therefore given the name “jitterbug”. Through positional cloning they were discovered to have a spontaneous 97-bp deletion in the CLIC5 gene (87 bp at the 3' end of exon 5 plus 10 bp in the adjacent intron) that leads to skipping of exon 5 and a translational frame shift producing a premature stop codon [183]. For the current study, the CLIC5^{*jbjbg*} mutation in CH3/HeJ mice was backcrossed for 10 generations onto the C57BL/6J background. Breeding heterozygous CLIC5^{*-/+*} females with CLIC5^{*-/-*} or CLIC5^{*+/+*} males generated CLIC5^{*-/-*} and CLIC5^{*+/+*} mice. For each mouse, a small portion of the

tail was removed between 2 and 3 weeks of age, DNA was purified as described by Truett et al [253] Briefly the tail samples were heated at 99°C for 45-60min in alkaline solution (NaOH 25mM, Na₂-EDTA 200mM, pH12) followed by cooling at 4°C and adding neutralization solution (Tris-Cl 40mM pH5.0). PCR was carried out Using 1.0 µl of final preparation as template.

For CLIC5 genotyping the primers EX5F 5'-CAATGACGAGAAGCGACTCA-3' and EX5R 5'- GCTGTCCAGATTCCTCATAAACA-3' were used for PCR [254]. The PCR products of wild-type and CLIC5 mutant (jbg) alleles are 326bp and 229kb in length respectively. PCR from wild-type mice yields only the 326bp product, from heterozygous mice we obtain both, 326bp and 229bp products and from homozygous mutant mice we obtain only the 229bp product.

2.2.2 Generation of CLIC4^{-/-}CLIC5^{-/-} mice

Generation of CLIC4 deficient mice on the CD1 background was previously described [236, 241]. The genotype of every mouse was confirmed as previously described [4]. Male CLIC5^{-/-}/CLIC4^{+/+} mice on the C57BL/6J background were crossed with female CLIC5^{+/+}CLIC4^{-/-} on the CD1 background to generate newly outbred CLIC5^{+/-}CLIC4^{+/-} male and female (mixed genetic background) mice. Multiple pairs of newly outbred male and female CLIC5^{+/-}CLIC4^{+/-} mice were mated to generate CLIC5^{+/+}CLIC4^{+/+}, CLIC5^{-/-}CLIC4^{-/-}, CLIC5^{-/-}CLIC4^{+/+} and CLIC5^{+/+}CLIC4^{-/-} mice. Animals to be studied were randomly chosen.

CLIC5 genotyping was performed as mentioned in 2.2.1 and for CLIC4 genotyping PCR was performed with primers 5'-TGACCACGGCAACTCCTAGAAGGACCGG-3' (forward) and 5'-AGGACTCGGGGTGACACTGTAAATCGAC-3' (reverse) [236]. The PCR products of wild-type and CLIC4 mutant alleles are 863bp and 240kb in length respectively. PCR from wild-type mice yields only the 863bp product, from heterozygous mice we obtain both, 863bp and 240bp products and from homozygous mutant mice we obtain only the 240bp product.

2.3 Cell culture, transfection and cell lysis.

2.3.1 COS7 cells

COS7 cells were maintained at 37⁰C in humidified air and 5% CO₂, in DMEM (Dulbecco's modified Eagle's medium) containing 10% fetal bovine serum (FBS) and 1% Penicillin/Streptomycin. One day prior to transfection, cells were detached with trypsin/EDTA and re-plated into 35 mm plates to reach ~ 90% confluency 24 hours later. Transfections were performed using Lipofectamine 2000 (Invitrogen 11668-027) according the manufacturer's protocol. 48 hours later cells were rapidly rinsed with ice-cold phosphate-buffered saline (PBS) and lysed in 2X Laemmli buffer, followed by western blot (WB) analysis.

2.3.2 Conditionally immortalized mouse podocytes

Conditionally immortalized mouse podocytes (a generous gift from Dr. Tomoko Takano, McGill University Canada, originally derived by K. Endlich, University of Heidelberg, Germany) were grown as previously described [249]. Briefly podocytes were grown on Collagen I (Trevigen, MD, USA) at 33°C and 5% CO₂ in RPMI1640 (Sigma) containing 10% FBS (Life Technologies) and 50 µ/ml mouse Interferon-γ (Roche). The podocytes (~80-90% confluent)

were infected with 10, 50 or 100 MOI (Multiplicity Of Infection) of pAdTrack-CLIC5A or pAdTrack adenovirus in 1.0 ml full growth medium containing 5µg/ml polybrene (Fisher). 48 hours after infection, podocytes were rapidly washed with ice-cold PBS and lysed in 100 µl 2 x Laemmli buffer for WB analysis of the target proteins.

2.3.3 Human glomerular endothelial cells (EC)

Primary human glomerular endothelial cells (EC), free of mycoplasma contamination, were purchased from Angio-Proteomie (Boston, MA) and maintained in EGM-2 MV Bulletkit growth media (Lonza, Walkersville, MD). Cells were cultured on Quick Coating Solution cAP-01 from Angio-Proteomie. CLIC5A was expressed from the adenoviral vector pAdTrack-CLIC5A, which expresses CLIC5A and GFP from separate promoters and was previously described [122] For adenoviral infection, glomerular EC were detached with trypsin/EDTA and re-plated in 35 mm plates at a density sufficient to reach ~ 90% confluency 24 hours later. 24 hours after re-plating they were infected with 1, 5, 10 or 20 MOI (Multiplicity Of Infection) of pAdTrack-CLIC5A or the control pAdTrack adenovirus in 1.0 ml full culture medium containing 5µg/ml polybrene (EMD Millipore, Billerica, MA). 24 - 48 hours after infection, the cells were rapidly washed with ice-cold PBS and lysed in 100 µl 2 x Laemmli buffer for WB analysis. To silence endogenous CLIC4 in glomerular EC, the cells were replated 1 day prior to transfection to produce a monolayer that was 60–70% confluent one day later. The cells were then transfected with 30 nM siRNA using Lipofectamine 3000 (Life technologies, Grand Island, NY) according the manufacturers' protocol. The siRNA targeting human CLIC4 (catalogue no. sc-105213), and nonspecific siRNA (catalogue no. sc-37007) were purchased from Santa Cruz Biotechnology (Dallas, TX). To rescue CLIC4 expression, the glomerular EC were transfected

with 2.5 µg human CLIC4 cDNA or vector cDNA using Lipofectamine 3000 according to manufacturer's instructions.

2.3.3.1 CLIC4 and CLIC5A rescue experiments

For CLIC4 rescue experiments, 24 hours after CLIC4 silencing, human glomerular ECs were transfected with 2.5µg human CLIC4 cDNA or vector cDNA using Lipofectamine 3000 according to manufacturer's instructions.

For CLIC5A rescue experiments, at the same time as CLIC4 silencing, human glomerular ECs were transfected with 20MOI of adenovirus expressing human CLIC5A (AdCLIC5A) or GFP (AdGFP) [122] using 5µg polybrene (EMD Millipore, Billerica, MA).

2.4 Plasmid and Adenoviral Constructs:

GFP-CLIC5A and the GFP-Vector control cDNAs were generated as previously described [4]. A cDNA for CLIC5A encoding the complete open reading frame (ORF) (GenBank™ #DQ679794), was PCR-amplified from human kidney cDNA with 5'-CGCACTCGAG**ACCATGGGGCATCATCATCATC**ATACAGACTCGGCGACAGCTAAC-3' (forward) and 5'-CCGGGATCCTCAGGATCGGCTGAGGCGTTTGGC-3' (reverse) primers. In the forward primer one Kozak consensus sequence (bold) was added to enhance expression and 6xHis tag sequence (italic) was integrated for detection. The PCR product was directly cloned into pCDNA3.1/V5-his-TOPO vector (Life Technologies). This construct is designated pCDNA3.1-CLIC5A, or CLIC5A in the figure legends. The GFP-CLIC5A construct was generated by PCR-amplification of human CLIC5A full coding region from pCDNA3.1-

CLIC5A, and cloning into Xho I/BamHI site of pEGFP-C1 vector (Clontech, Mountain View, CA, USA). Restriction enzyme digestion and full insert sequencing verified the DNA sequence orientation and fidelity.

The cDNA encoding the PI[4,5]P2 reporter RFP-PH-PLC was obtained from S. Grinstein (University of Toronto, Canada). Plasmids encoding GFP-Rac1, and dominant negative Rac1-N17, were prepared as previously described [122]. COS7 cells were transfected with 2 µg of the GFP-CLIC5A cDNA with and without 2 µg GFP-Rac1N17 cDNA (Figure 2) or RFP-PH-PLC cDNA (Figure 3). The GFP-Vector cDNA served as control.

To produce the CLIC5A encoding adenovirus (pAdTrack-CLIC5A), the cDNA fragments of human CLIC5A, previously described [5], was PCR-amplified from pcDNA3.1-CLIC5A [4] with the following primers:

Forward: 5'- CGCAGTCGACGCCACCATGACAGACTCGGCGACAGCTAAC-3', Reverse: 5'- CCGAAGCTTTCAGGATCGGCTGAGGCGTTTGGC-3'. Sal I and Hind III endonuclease sites were incorporated upstream of the ATG start codon in the forward primer, and downstream of stop codon in the reverse primer, respectively. The PCR product was sub-cloned into the Sal I /Hind III site of pAdTrack-CMV (Gift from Amy Barr, University of Alberta), which also encodes GFP under a distinct promoter. Sequence fidelity of the final was confirmed by full sequencing. The pAdTrack-CLIC5A construct was linearized by digestion with restriction endonuclease PmeI, and then transformed into E. Coli (BJ5183) containing the adenoviral backbone plasmid pAdEasy-1 for homologous recombination. The recombinant plasmid was confirmed by PacI restriction endonuclease analysis. The linearized recombinant plasmid was

transfected into the adenovirus packaging cell line HEK293A. The adenoviruses were propagated, harvested, purified and the viral titer was established [122].

A cDNA for CLIC4 encoding the complete open reading frame (ORF) (GenBank TM BC012444), was PCR-amplified from human kidney cDNA (Ambion, Texas, USA) with the primers 5'-**CCACCATGGCGTTGTCGATGCCGCTGAAT**-3' (forward) AND 5'-CCGGGATCCTTACTTGGTGAGTCTTTTGGCTAC-3' (reverse).

In the forward primer one Kozak consensus sequence (bold) was integrated to enhance expression. The PCR product was directly cloned into pTARKET TM vector (Promega, WI USA). pTARKET TM vector was used as control. Restriction enzyme digestions and full-insert sequencing verified the hCLIC4 DNA sequence orientation and fidelity.

2.5 RNA interference.

2.5.1 CLIC4 Silencing

Nonspecific siRNA (catalogue no. sc-37007) was used as a control siRNA. To silence endogenous human glomerular EC CLIC4, human CLIC4 specific siRNA (catalogue no. sc-105213) were purchased from Santa Cruz Biotechnology (Dallas, TX). Glomerular EC were cultured 1 day before transfection at 60–70% cell density and transfected with 30 nM nonspecific control or CLIC4 siRNA using Lipofectamine 3000 reagent (Life technologies, Grand Island, NY) according the manufacturers' instruction.

2.6 GTP-Rac1/Cdc42/Rho pull-down and Rac1 Inhibition.

To determine the abundance of GTP-Rac1, COS7 cells were lysed in 2% IGEPAL lysis buffer (Sigma-Aldrich). The total protein concentration was determined with the Precision Red™ Advanced Protein Assay Reagent (Cytoskeleton, Inc. Denver, Co). Lysate equivalent to 500 µg protein was then incubated with 50 µg GST-Rhotekin-RBD beads (Rho binding domain for GST-Rho) or 10 µg of PAK-PBD (Pak protein binding domain for GTP-Cdc42 or GTP-Rac1) immobilized on beads, and precipitated according to the manufacturer's instructions. PAK-PBD-associated Rac1 and Cdc42, RBD-associated Rho, as well as total Rac1, Cdc42 and Rho in the cell lysates were evaluated by WB analysis. To inhibit Rac1 activity, COS7 cells were treated 48 hours after transfection with the Rac1 inhibitor (NSC 23766, 100 µM) or vehicle (water) in fresh DMEM with 0.5% fetal bovine serum for 5 – 20 minutes followed by cell lysis or live cell imaging.

2.7 Western Blot Analysis (WB) and Quantification.

Glomerular EC monolayers, podocytes and COS7 cells, were washed once with ice-cold PBS and harvested immediately in 250 µl 2× Laemmli buffer and heat-denatured for 5 min at 99°C. Glomerular lysates and mouse urine were heat-denatured at 95°C for 5 min in Laemmli buffer containing β-mercaptoethanol. Proteins were separated by SDS-PAGE and transferred to PVDF membranes. Total and phosphorylated proteins were detected by probing the membranes with appropriate primary antibodies, HRP-conjugated secondary antibodies and Enhanced Chemiluminescence (ECL, GE Amersham, Baie d'Urfe, QC, Canada). The membranes were exposed to X-ray film (Fuji Medical X-Ray Film Super Rx, Fujifilm) for several time-points. Band density was evaluated using ImageJ (NIH).

2.8 Live Cell Imaging:

COS7 cells that had been co-transfected with RFP-PH-PLC and GFP-CLIC5A or GFP-vector and grown on glass cover slips were treated with 100 μ M of Rac1 NSC 23766 or vehicle for 20 min, placed into the imaging chamber (37°C, 5% CO₂) of an Olympus spinning-disk fluorescence microscope (Olympus IX-81), and image acquisition was performed with Volocity (Improvision, Perkin-Elmer, Waltham, MA) software.

2.9 Immunofluorescence studies

Kidney cortex (0.5-cm³ cubes) was incubated in 10% trichloroacetic acid (TCA) at 4°C for one hour, frozen in optimal cutting temperature (Sakura Finetek, Torrance, CA), and stored at -80°C. Frozen sections (5 μ m thick) were thaw-mounted on SuperFrost Microscope slides (Microm International, Kalamazoo, MI) and air dried. Tissue sections were permeabilized for 15 minutes in 0.2% TX-100 in G-PBS (0.03 M glycine in PBS) (3 X 5 min) at room temperature and blocked for 1 hour with 10% donkey normal serum in G-PBS, followed by incubation with the primary antibodies in G-PBS overnight at 4°C. Slides were washed (3 X 5 min) in G-PBS and incubated for 1 h in the dark with 1:750 dilutions of the appropriate secondary antibodies (Donkey anti-goat or Rabbit) coupled with Alexa Fluor 594 or 488 (Molecular Probes, Eugene, OR) in G-PBS. Slides were washed five times in G-PBS, mounted with ProLong Gold Antifade (Molecular Probes), and viewed on a Olympus IX-81 motorised microscope and a Yokogawa CSU10 spinning disk confocal scan-head at X60 magnification.

2.10 UNx-DOCA/Salt hypertension in mice:

At ~10 weeks of age, 14 CLIC5^{+/+} and 14 CLIC5^{-/-} mice underwent a left uninephrectomy (UNx) under isoflurane anaesthesia. Two weeks later mice from each genotype were randomly assigned to UNx-DOCA/Salt hypertensive and UNx control groups. Continuous 21-day release pellets containing 50 or 40 mg DOCA (Innovative Research of America, Sarasota FL) were implanted in the right flank to deliver ~ 100 mg/Kg DOCA per day. The drinking water for the UNx-DOCA/Salt groups was replaced with 1.0% NaCl in tap water one day later. Controls received tap water to drink. Blood pressure was measured at week 0, 2 and 3, usually at 12 noon, using a CODA non-invasive blood pressure system (CODA™ Standard 2, Kent Scientific Corporation) under isoflurane anaesthesia. The mean of 5 successive readings was recorded. Urine was collected from conscious mice every 3 days.

2.11 Urine Protein Electrophoresis and Serum Biochemistry:

In DOCA/Salt experiments, for each urine sample, the creatinine was determined with the Creatinine Enzymatic Assay Kit (DZ072B; Diazyme, San Diego, CA), adjusted to 0.1 µg creatinine/µl with distilled water, diluted 3:1 in 4 X Laemmli buffer and heat-denatured. 10 µl of the diluted urine was then subjected to WB analysis. Blood biochemistry was determined with CHEM8+ ABBT-03P91-25 cartridges and the i-STAT® blood analyzer (i-STAT1 Wireless Analyzer, Abbott Laboratories, Chicago, IL, USA).

For experiments in CLIC4 and CLIC4/CLIC5 deficient mice (Chapter 4), the creatinine concentration for each urine sample was determined with the Creatinine Enzymatic Assay Kit (DZ072B; Diazyme, San Diego, CA), adjusted to 0.3 µg creatinine/µl with distilled water, diluted 3:1 in 4 X Laemmli buffer and heat-denatured. 10 µl of the diluted urine was then

subjected to WB analysis for mouse albumin and quantification by densitometry against mouse albumin standards on the same blots, using goat anti-mouse albumin antibodies (Bethyl Laboratories, Montgomery, TX). Blots were also probed with anti-Vitamin D binding protein (Vitamin D BP) antibodies to detect tubular proteinuria.

2.12 Glomerular Isolation:

CLIC4^{+/+} and CLIC4^{-/-} were anaesthetized with isoflurane [122]. The kidneys were removed and weighed, kidney weights were normalized to body weight. To isolate glomeruli renal cortex was finely minced and incubated in RPMI 1640 medium containing 10 nM Calyculin A (Cal-A) and 1 mg/ml Collagenase IV (Worthington, Lakewood NJ) for 1 hour at 37°C. Glomeruli were then isolated with the sieving technique as previously described [4, 122]. Contaminating tubules were removed by differential adhesion to cell culture plastic (2 X 10-min in RPMI 1640 medium with 0.5% FBS and 10 nM Cal-A). The final glomerular preparations were > 99% pure. Glomeruli were then sedimented and lysed in ice-cold buffer (50 mM Tris pH 7.5, 150 mM NaCl, 1% Nonidet P40, 0.5% sodium deoxycholate, 1X Proteinase Inhibitor Mix, 1X PhosStop and 100 nM Cal-A) for 15 min, and homogenized by passing them through a 28-gauge needle three times. Insoluble material was pelleted by centrifugation at 18,000 X G for 10 min. Proteins in the glomerular lysate were heat-denatured in Laemmli buffer and then subjected to SDS-PAGE and WB analysis.

2.13 Cytoskeleton Preparation:

Cytoskeletal fractions of glomerular EC or renal cortex were prepared according to the protocol developed by Berryman (Berryman et al., 2004) and previously described. Kidney cortex was dissected away from renal medulla in ice-cold PBS containing 5.0 nM of the protein

phosphatase 1 inhibitor Calyculin A (Cal-A). Ten mg of renal cortex was then finely minced with a razor blade, and suspended in 500 μ l lysis buffer (50 mM Tris pH 7.5, 150 mM NaCl, 1% Nonidet P40, 0.5% sodium deoxycholate, 1X Proteinase Inhibitor Mix, 1X PhosStop and 100 nM Cal-A) for 30 min. The material was gently homogenized by passing it 3 times through a 28-gauge needle. A 50 μ l portion of this “total” lysate was set aside. The remainder was subjected to centrifugation at 14,000 X G for 30 min at 4°C. The supernatant “soluble fraction” was separated from the pellet. The “insoluble” pellet largely representing cytoskeleton was re-suspended in 100 μ l lysis buffer. All 3 fractions were boiled in 2 X Laemmle buffer for 5 min, and processed for WB analysis.

2.14 Perfusion Fixation and Microscopy:

Mice were anesthetized with isoflurane inhalation (5% for induction; 1-1.5% for maintenance of anaesthesia) in oxygen. The right kidney was perfused with 0.9% saline from a 125 cm high reservoir for 3 minutes followed by perfusion with fixative (2.5% glutaraldehyde and 2% paraformaldehyde in 0.1 M phosphate buffer, pH 7.6) for 5 min. For Transmission electron microscopy (TEM), $\sim 5 \times 5$ mm cubes of perfusion-fixed kidney cortex were post-fixed with 1% osmium tetroxide in Millonig's buffer solution for 1.5 h, dehydrated and embedded in Spurr resin. Ultrathin sections were stained with 4% uranyl acetate for 30 min and lead citrate for 5 min and viewed with a Philips transmission electron microscope (Morgagni 268, operating at 80 kV). Morphometric analysis for 3-5 mice per group was done in a double-blinded fashion as previously described [5]. For each mouse 5-15 TEM images were captured at 11,000 X magnification by a technician fully blinded to the experimental groups. For each image, the number of fenestrae was determined for the total length of GBM containing adjacent podocytes

and glomerular EC. The total length of GBM counted was 7,958, 6,287, 21,670 and 28,346 μm for UNx CLIC5^{+/+}, UNx CLIC5^{-/-}, UNx-DOCA/Salt CLIC5^{+/+} and UNx-DOCA/Salt CLIC5^{-/-} mice respectively.

The total length of GBM evaluated for fenestrae density was 548 μm for 2 month-old CLIC4^{+/+}/CLIC^{+/+} (n=3 mice), 603 μm for 2 month-old CLIC4^{-/-}/CLIC5^{-/-} (n=3 mice), 749 μm for 8 month-old CLIC4^{+/+}/CLIC^{+/+} (n=5 mice) and 734 μm for 8 month-old CLIC4^{-/-}/CLIC5^{-/-} (n=4 mice). For histologic evaluation, formalin-fixed paraffin-embedded 4 μm -thick sections were stained with periodic acid-Schiff (PAS). In DOCA/Salt studies, for each mouse, an observer blinded to the groups evaluated 20-25 random glomeruli. Microaneurysms were defined as markedly expanded glomerular capillary loops, and glomerular sclerosis as the segmental increase in matrix and collapse and/or obliteration of capillary lumina. Immunofluorescence studies were performed as previously described[4, 5].

2.15. Morphometric analysis of PAS stained glomeruli

For morphometric analysis, all glomeruli in a given PAS stained section from three wild-type and four CLIC5-deficient mice, 10 month of age, were photographed at X100 magnification and 21-24 random glomeruli from each mouse were used. Morphometry was performed by point counting in a blinded fashion, using a grid with points at 7 μm intervals on complete glomerular cross-section. The number of capillary loops per each glomerulus was counted. For each image the lumen area was first normalized to total glomerular area in order to compare the capillary areas in two groups. The lumen area in each glomerulus was divided by the number of loops in each glomerulus to acquire “the lumen area per capillary loop”. The total area counted was

1,211,525, 432,327, 477,407, 301,791 μm^2 for total glomeruli, Bowman's space, glomerular cells and capillary lumen, respectively.

2.16 Statistical Analysis:

All experiments were repeated 3 or more times. Data are presented as mean \pm SEM or mean \pm SD, as indicated. For comparison of two groups the two-tailed Student's t-test was used unless otherwise specified. Comparison of more than two groups was done by one-way ANOVA followed by the Tukey's Multiple Comparison test. *P* values <0.05 were considered significant.

Disclosure: Nothing to report

Table 2.1 | Antibodies

Antibody	Host	Catalog No.	Company	WB	IF
AKT	Mouse	sc5298	Santa Cruz Biotechnology Inc (Santa Cruz, CA, USA)	1:500	1:100
Albumin	Goat	A90-134A	(Bethyl Laboratories, Montgomery, TX, USA)	1:10000	N/A
CDC42	Rabbit	sc87	Santa Cruz Biotechnology Inc (Santa Cruz, CA, USA)	1:250	N/A
CLIC1	Rabbit	sc134859	Santa Cruz Biotechnology Inc (Santa Cruz, CA, USA)	1:1000	N/A
CLIC4	Rabbit	sc130723	Santa Cruz Biotechnology Inc (Santa Cruz, CA, USA)	1:1000	1:200
CLIC5A	Rabbit	ARP35263	Aviva System Biology (San Diego, CA, USA)	1:1000	1:500
Ezrin	Goat	sc6409	Santa Cruz Biotechnology Inc (Santa Cruz, CA, USA)	N/A	1:200
Ezrin	Rabbit	3145	Cell Signaling (Danvers, Ma, USA)	1:3000	N/A
Moesin	Goat	sc6410	Santa Cruz Biotechnology Inc (Santa Cruz, CA, USA)	1:1000	1:200
p-AKT	Rabbit	T308	Cell Signaling (Danvers, MA, USA)	1:1000	1:200
p-ERM	Rabbit	2180-1	Epitomics (Burlingame, CA, USA)	1:5000	1:800
p-PAK1,2,3	Rabbit	Ab5247	Abcam (Cambridge, MA, USA)	1:3000	1:50
p-Smad2/3	Rabbit	9514S	Cell Signaling (Danvers, MA, USA)	1:1000	N/A
PAK1	Goat	sc31683	Santa Cruz Biotechnology Inc (Santa Cruz, CA, USA)	1:200	N/A
PAK1,2,3	Rabbit	2604	Cell Signaling (Danvers, MA, USA)	1:750	N/A
PDGF- B(H-55)	Rabbit	sc7878	Santa Cruz Biotechnology Inc (Santa Cruz, CA, USA)	1:200	N/A
PECAM	Goat	sc1506	Santa Cruz Biotechnology Inc (Santa Cruz, CA, USA)	N/A	1:50
Podxl	Goat	AF1556	(R&D Systems, Inc. Minneapolis, USA)	1:1000	1:1000
Podocin	Goat	sc22298	Santa Cruz Biotechnology Inc (Santa Cruz, CA, USA)	1:500	1:200
Rac1 (C11)	Rabbit	sc-95	Santa Cruz Biotechnology Inc (Santa Cruz, CA, USA)	1:500	N/A
Smad2/3	Rabbit	3102	Cell Signaling (Danvers, MA, USA)	1:1000	N/A
TGF β RI	Rabbit	3712	Cell Signaling (Danvers, MA, USA)	1:1000	N/A
TGF β RII	Rabbit	06-318	Upstate (Darmstadt, Germany)	1:1000	N/A

Antibody	Host	Catalog No.	Company	WB	IF
VEGF164	Goat	AF-493-NA	Novus Biologicals (Littleton, CO, USA)	0.1 ug/mL	15 ug/mL
Vit DBP (H300)	Rabbit	sc32899	Santa Cruz Biotechnology Inc (Santa Cruz, CA, USA)	1:500	N/A
β -Actin	Mouse	A2228	Sigma (Oakville, ON, Canada)	1:10000	N/A
β -Tubulin	Mouse	5661	Millipore (Billerica, MA, USA)	0.1-1 μ g/mL	N/A

Chapter 3

CLIC5A Stimulates Rac1-Dependent Pak and ERM Protein Activation, Protecting Against Hypertension-Induced Glomerular Injury

Chapter 3

CLIC5A stimulates Rac1-dependent Pak and ERM protein activation, protecting against hypertension-induced glomerular injury¹

3.1 Introduction

Podocyte abnormalities are responsible for many proteinuric glomerular disorders that progress to end stage kidney disease [255, 256]. Podocytes extend actin-based primary, and secondary projections (foot processes) around the exterior of glomerular capillary loops, providing capillary tensile strength [2, 132]. Filtration slits between the foot processes contribute to the glomerular capillary wall hydraulic conductivity, and filtration slit diaphragms restrict protein filtration [257, 258].

The apical surface of glomerular podocyte foot processes is covered by sialoglycoproteins, among them podocalyxin. Podocalyxin is composed of a heavily glycosylated extracellular domain [71], a single membrane-spanning domain, and a cytoplasmic tail linked to cortical F-actin by ezrin. Podocalyxin and ezrin localize specifically to the apical domain of podocyte foot processes [247]. Ezrin interacts with podocalyxin directly [6], and indirectly through NHERF2 [58, 247].

¹Portions of this chapter has been published in a peer-reviewed journal:

Mahtab Tavasoli, Laiji Li, Lin-Fu Zhu, Abass Al-Momany, Benjamin Alexander Adam, Zhixiang Wang and Barbara J. Ballermann, *The chloride intracellular channel 5A stimulates podocyte Rac1, protecting against hypertension-induced glomerular injury*. *Kidney Int*, 2016. **89**(4): p. 833-47.

In mice lacking podocalyxin, podocyte foot processes do not develop [259] and genetic defects that lead to hyposialylation of podocalyxin are associated with defective foot processes and the nephrotic syndrome [260, 261]. Sialidase infusion [58, 246, 247], puromycin aminonucleotide nephrosis [262, 263], or acute neutralization of anionic sites with protamine sulfate [264, 265] all disrupt the podocyte architecture and the podocalyxin-ezrin-actin interaction [58].

The ERM (ezrin, moesin, radixin) proteins are widely distributed, and dynamically link many transmembrane spanning proteins to the cortical F-actin cytoskeleton, serving to shape the cell cortex and its actin-based structures [176]. Auto-inhibition between the ERM N- and C-termini prevents binding to actin and membrane spanning proteins [266, 267]. ERM protein activation requires, as a first step, docking of the N-terminus on phosphatidylinositol 4,5 biphosphate (PI[4,5]P₂), inducing a conformational change that leads to F-actin binding and ERM protein phosphorylation [267-270]. De-phosphorylation of activated ERM proteins leads to their degradation [271].

PI[4,5]P₂, an abundant plasma membrane phospholipid, is the substrate for phosphatidylinositol 3-kinase (PI3K), and phospholipase C (PLC). PI[4,5]P₂ also serves as the docking site for several proteins involved in endocytosis [272], exocytosis [273], cytokinesis [274], maintenance of epithelial cell polarity [275] and actin cytoskeleton organization [276]. PI[4,5]P₂ does not diffuse freely in the lipid bilayer, but is confined to function-specific microdomains through mechanisms that are incompletely understood [277].

We have reported that the chloride intracellular channel 5A (CLIC5A) functions to generate PI[4,5]P₂ clusters at the dorsal plasma membrane in COS7 cells, leading to ezrin activation and actin polymerization [4]. These observations suggest that CLIC5A, which is

highly enriched in glomerular podocytes [3, 5, 123] and in the actin-based stereocilia of inner ear hair cells [183], provides a mechanism for the formation of PI[4,5]P2 clusters that regulate actin-based cellular projections through the activation of ERM proteins. CLIC5A is a member of a highly conserved family of metamorphic proteins that can exist as soluble and lipid bilayer-associated forms [278]. The first identified family member, p64, was isolated from kidney cortex by affinity-binding to IAA-94, a non-specific Cl⁻ channel inhibitor [279]. This association, and the fact that these proteins can spontaneously insert into lipid bilayers, creating non-selective ion conductance suggested that they function as Cl⁻ channels [278]. However, CLICs contain only a single N-terminal hydrophobic domain and are not inhibited by specific Cl⁻ channel inhibitors like 4,4'-diisothiocyanato-2,2'-stilbenedisulfonic acid (DIDS) or 4-Acetamido-4'-isothiocyanato-2,2'-stilbenedisulfonic acid (SITS), raising doubts that they function as specific Cl⁻ channels *in vivo* [213]. CLIC5A was first isolated from placental microvilli in a complex that binds ezrin [182], and overexpression of CLIC5A leads to microvillus formation [242]. CLIC5A co-localizes with radixin at the base of cochlear and vestibular hair cell stereocilia and its deletion results in vestibular disturbances and progressive deafness [183, 280], a phenocopy of radixin deficiency [178]. Hearing loss, vestibular dysfunction and mild renal insufficiency have also been described in a family with an autosomal recessive CLIC5 mutation [281]. CLIC5A is extraordinarily enriched in human renal glomeruli where it co-localizes with ezrin at apical plasma membrane of podocyte foot processes[4]. Although the kidneys of mice lacking CLIC5 appear histologically normal, the number of podocyte foot processes is reduced, ezrin abundance is reduced [5, 123], and NHERF2 and ezrin are uncoupled from the actin cytoskeleton[4]. These observations, among others, suggest that CLIC proteins function to regulate ERM activation [282]. Nonetheless, CLIC5A deficient mice have only minimal albuminuria at

baseline [5] implying that CLIC5A is not required for slit diaphragm function and that its action could be spatially restricted to the apical podocalyxin/NHERF2/ezrin complex in podocyte foot processes.

Since it was previously shown that Rac1 is required for PI[4]P5 kinase and ERM protein activation [199, 283], and since Rac1 participates in podocyte actin remodeling [155, 162, 284], we determined whether CLIC5A regulates Rac1 activity and its downstream effectors ezrin and p21 activated kinases (Pak). We observe that ectopic CLIC5A expression in COS7 cells results in Rac1, but not Rho or Cdc42 activation and that CLIC5A-induced PI[4,5]P2 generation as well as Pak1 and ERM activation are Rac1-dependent. Hence, Rac1 is a functional component of the CLIC5A-PI[4,5]P2-ezrin axis. In DOCA/Salt hypertensive mice we find increased phosphorylation of the Rac1 effector Pak, but in mice lacking CLIC5A, neither Pak nor ERM proteins can be phosphorylated, and hypertensive CLIC5 deficient mice develop more severe glomerular injury than their wild-type controls.

3.2 Results:

3.2.1 Activation of Rac1 and Pak1 phosphorylation in COS7 cells expressing CLIC5A

We first determined whether CLIC5A alters Rac1 activity in COS7 cells, which are null for CLIC5A at baseline. In COS7 cells expressing GFP-CLIC5A, Rac1-GTP levels were significantly higher than in cells expressing GFP alone (Figure 3.1 a,b), without change in total Rac1 abundance. By contrast, no change in GTP-Cdc42 or GTP-Rho was observed in response to CLIC5A expression (Figure 3.1 c,d).

Consistent with our previous findings [4], GFP-CLIC5A expression in COS-7 cells also enhanced ERM protein phosphorylation (Figure 3.2 a,b). The ERM proteins ezrin (69.4 kDa), radixin (68.5 kDa) and moesin (67.8 kDa) are phosphorylated on a highly conserved C-terminal Thr residue (Thr567 in human ezrin); hence phosphorylation-specific ERM (p-ERM) antibodies do not distinguish between them. Two distinct p-ERM proteins bands were detected in COS7 cells, representing phosphorylated ezrin and moesin, respectively. The abundance of both p-ERMs increased significantly in cells expressing GFP-CLIC5A compared to cells expressing GFP alone, without change in total ezrin abundance (Figure 3.2 b).

The type 1 p21 associated kinases (Pak1,2 and 3) are highly conserved and are activated by the small GTPases Rac1 and Cdc42. On SDS PAGE gels Pak1 (545aa), Pak3 (544aa) and Pak2 (528aa) run as ~68, 65 and 62 kDa proteins, respectively [285]. Phosphorylation-specific antibodies cannot distinguish the Paks, but p-Pak1,3 can be distinguished from p-Pak2 by their distinct electrophoretic mobility. In COS7 cells Pak2 was the predominant Pak isoform observed on western blots (Figure 3.2 a). The abundance of p-Pak1,3 was significantly higher in COS7 cells expressing GFP-CLIC5A than in GFP expressing cells (Figure 3.2 a,c). By contrast, p-

Pak2 did not change significantly when CLIC5A was expressed (Figure 3.2 d). Hence, GFP-CLIC5A expression in COS7 cells increases Pak1,3, but not Pak2 protein phosphorylation.

At baseline, the CLIC5A protein was not detectable by WB analysis in undifferentiated immortalized mouse podocytes [249]. Transduction of the podocytes with an adenoviral vector containing CLIC5A and GFP cDNAs under separate promoters (pAdTrack-CLIC5A) resulted in CLIC5A protein expression that increased as a function of increasing multiplicity of infection (MOI). No CLIC5A expression was observed in cells transduced with the adenoviral vector expressing only GFP (pAdTrack) (Figure 3.3 a). CLIC5A expression in podocytes stimulated ERM and Pak1,3 protein phosphorylation in a concentration-dependent fashion (Figure 3.3 a-c), consistent with the findings in COS7 cells. As in COS7 cells, p-Pak2 was already very abundant at baseline. CLIC5A expression also increased Pak2 phosphorylation in podocytes but the effect was less pronounced than its effect on ERM and Pak1,3 phosphorylation. Hence, CLIC5A also stimulates ERM and Pak phosphorylation in podocytes, in culture.

3.2.2 CLIC5A-dependent ERM and Pak1,3 phosphorylation require Rac1 activity

To determine whether CLIC5A-dependent Pak1,3 and ERM protein phosphorylation requires Rac1 activity, GFP-CLIC5A and GFP-vector transfected COS7 were treated with NSC 23766, a Rac1-specific inhibitor that does not alter Rho or Cdc42 activity [286]. NSC 23766 (100 μ M, 10 min) abolished the GFP-CLIC5A-dependent increase in p-ERM (Figure 3.4 a,b), without changing ezrin abundance. Also, Pak1,3 phosphorylation was strongly inhibited by NSC 23766 in GFP-CLIC5A and GFP-vector transfected COS7 cells (Figure 3.4 a,c), without changing p-Pak2 (Figure 3.4 a,d). When COS7 cells were co-transfected with RFP-CLIC5A or RFP-Vector and the dominant negative GFP-Rac1 N17, or its control vector [287], CLIC5A did

not induce ERM (Figure 3.4 e,f) or Pak1,3 (Figure 3.4 e,g) phosphorylation. Pak2 phosphorylation tended to be slightly lower in the presence of Rac1 N17 compared to control, but this effect did not reach statistical significance. Thus, CLIC5A-dependent ERM, and Pak1,3 phosphorylation all require Rac1 activity in COS7 cells.

3.2.3 Inhibition of Rac1 abolishes CLIC5A-induced clustered PI[4,5]P₂ accumulation.

It is well-established that ERM activation requires, as a first step, docking on PI[4,5]P₂ [267], and CLIC5A-stimulated ERM phosphorylation does not occur when PI[4,5]P₂ generation is blocked [4]. Since activation of PI[4]P5 kinases, which generate PI[4,5]P₂ is Rac1-dependent [283], we determined whether GFP-CLIC5A-stimulated PI[4,5]P₂ accumulation is inhibited by NSC 23766 using the PI[4,5]P₂ reporter RFP-PH-PLC. In GFP-vector transfected control cells, a few dorsal clusters of RFP-PH-PLC were observed (Figure 3.5 a). These increased substantially in COS7 cells expressing GFP-CLIC5A (Figure 3.5 b), consistent with previous results [4]. The effect of GFP-CLIC5A on RFP-PH-PLC cluster formation was abolished by NSC 23766 (Figure 3.5 c). Not shown, NSC 23766 had no discernable effect on RFP-PH-PLC in GFP-transfected COS7 cells. Thus, CLIC5A-stimulated accumulation of PI[4,5]P₂ in apical membrane clusters requires Rac1 activity.

3.2.4 Glomerular Pak phosphorylation in UNx-DOCA/Salt Hypertension requires CLIC5.

Since Rac1 deficiency potentiates glomerular injury in DOCA/Salt hypertensive mice [155], and since Pak is a Rac1 effector, we next determined whether the response to UNx-DOCA/Salt hypertension involves CLIC5A-dependent Pak activation. We utilized mice with a spontaneous deletion involving exon 5 of CLIC5, and their wild-type littermates on the

C57BL/6J background. At baseline, the systolic blood pressure tended to be lower in the CLIC5^{-/-} compared to the CLIC5^{+/+} control mice (Figure 3.6 a) but the difference did not reach statistical significance. Whereas the C57BL/6N mouse strain has been reported to be relatively resistant to the induction of UNx-DOCA/Salt hypertension and hypertension-induced glomerular injury [288], we observed that hypertension developed reliably in response to UNx-DOCA/Salt in both CLIC5^{-/-} and CLIC5^{+/+} mice, on the C57BL/6J background (Figure 3.6 a). The degree of hypertension was similar in CLIC5^{-/-} and CLIC5^{+/+} mice (Figure 3.6 a). Kidney (Figure 3.6 b) and heart (Figure 3.6 c) size and weight (Table 3.1) increased significantly in response to DOCA/Salt treatment, but did not differ between UNx-DOCA/Salt hypertensive CLIC5^{-/-} and CLIC5^{+/+} mice. All UNx-DOCA/Salt treated mice developed a significant hypochloremic metabolic alkalosis, along with a reduction in the serum K⁺ concentration (Table 3.2).

Although there was no difference in K⁺ levels in normotensive CLIC5^{-/-} and CLIC5^{+/+} mice, the K⁺ levels were higher than the reported values for normal mice [289]. Since 98% of body potassium is intracellular, a small release of potassium from the plasma cells (RBC, WBS and platelets) can significantly enhance the concentration of extracellular potassium [290]. Therefore the higher measured K⁺ levels at baseline may be due to minor red blood cell lysis during blood collection.

Western blots of glomerular lysates showed that the total Pak1,3 but not Pak2 abundance increased significantly in UNx-DOCA/Salt treated CLIC5^{-/-} and CLIC5^{+/+} mice (Figure 3.7 a-c). In glomerular lysates from UNx-DOCA/Salt CLIC5^{+/+} mice phosphorylated Pak1,3 and 2 abundance increased significantly relative to normotensive CLIC5^{+/+} mice (Figure 3.7 a). The increase in p-Pak1,3 was fully accounted for by the increase in total Pak1,3 abundance (Figure 3.7 d), while the increase in p-Pak2 reflected increased Pak2 phosphorylation (Figure 3.7 e). By

contrast, in CLIC5^{-/-} mice, Pak1,3 phosphorylation was nearly undetectable at baseline, and did not increase in response to UNx-DOCA/Salt hypertension, even though the total Pak1,3 abundance was greater than in normotensive CLIC5^{-/-} mice. Also, no increase in p-Pak2 was observed in UNx-DOCA/Salt hypertensive CLIC5^{-/-} mice (Figure 3.7 a,c,e). That deletion of CLIC5 in mice results in reduced Pak1-3 phosphorylation is consistent with the findings of CLIC5-induced Pak-1-3 phosphorylation in cultured podocytes (Figure 3.3).

Immunofluorescence microscopy for p-Pak proteins showed low, but detectable p-Pak immunoreactivity in normotensive CLIC5^{+/+} mice, but was nearly undetectable in the CLIC5^{-/-} mice (Figure 3.7 f). There was a striking increase in p-Pak immunoreactivity in UNx-DOCA/Salt CLIC5^{+/+} mice compared to their normotensive CLIC5^{+/+} controls (Figure 3.7 f), consistent with the findings by WB analysis (Figure 3.7 a). A substantial portion of this p-Pak immunofluorescence co-localized with podocin. By contrast, and consistent with WB analysis (Figure 3.7 a), in CLIC5^{-/-} mice, glomerular p-Pak immunofluorescence increased only slightly in response to UNx-DOCA/Salt hypertension, and co-localization of p-Pak with podocin was not observed (Figure 3.7 f).

To determine whether the increase in p-Pak observed in UNx-DOCA/Salt CLIC5^{+/+} hypertensive mice could be due to a mineralocorticoid effect independent of hypertension, CLIC5^{+/+} mice were given DOCA without salt or uninephrectomy. No change in blood pressure was observed with DOCA alone (not shown), consistent with findings in rats [291]. DOCA alone did not change p-Pak immunofluorescence in renal glomeruli of CLIC5^{+/+} mice (Figure 3.8 a-c). WB detected a modest, but significant increase in p-Pak2 in response to DOCA (Figure 3.8 c), but the level of p-Pak1,3 did not change (Figure 3.8 b-c). Thus, the increase in Pak1,3 abundance and phosphorylation in glomeruli of UNx-DOCA/Salt hypertensive mice is not due to

DOCA alone.

3.2.5 Glomerular ERM phosphorylation in DOCA/Salt hypertension requires CLIC5

By WB analysis, total ezrin in glomerular lysates was reduced in UNx-DOCA/Salt hypertensive CLIC5^{+/+} mice relative to their normotensive controls, with an increase in the fraction of phosphorylated ERM protein (Figure 3.9 a,b,c). Total ezrin was lower in normotensive CLIC5^{-/-}, compared to normotensive CLIC5^{+/+} mice as previously described [5], and p-ERM was markedly reduced in the CLIC5^{-/-} mice. Immunofluorescence microscopy showed co-localization of phosphorylated ERM protein with podocin in both normotensive and UNx-DOCA/Salt hypertensive CLIC5^{+/+} mice (Figure 3.9 d). By contrast, in the CLIC5^{-/-} mice, p-ERM immunoreactivity and its co-localization with podocin were markedly reduced relative to the CLIC5^{+/+} mice and the abundance of p-ERM was much less in UNx-DOCA/Salt hypertensive CLIC5^{-/-} than in UNx-DOCA/Salt hypertensive CLIC5^{+/+} mice. Furthermore, in glomeruli of DOCA/Salt hypertensive CLIC5^{-/-}, the p-ERM did not co-localize with podocin. These data indicate that UNx-DOCA/Salt hypertension-induced ERM phosphorylation in glomeruli requires CLIC5.

3.2.6 Both, DOCA/Salt hypertension and CLIC5 deletion lower glomerular podocalyxin levels

Since active, phosphorylated ezrin links podocalyxin to the actin cytoskeleton in podocytes, and both DOCA/Salt hypertension and CLIC5A induce ezrin phosphorylation, we evaluated the abundance of podocalyxin in glomeruli of DOCA/Salt hypertensive mice with and without CLIC5 deletion. By WB analysis, the podocalyxin abundance was significantly lower in

CLIC5 deficient mice compared to wild-type mice (Figure 3.10 a,b). DOCA/Salt hypertension further decreased podocalyxin levels in both, wild-type and CLIC5 deficient mice (Figure 3.10 a,b). DOCA/Salt hypertension did not change the CLIC5A abundance in wild-type mice (Figure 3.0 a,c). Podocalyxin immunofluorescence co-localized with p-ERM in wild-type, but not in CLIC5 deficient mice, consistent with markedly impaired ERM phosphorylation in podocytes of mice lacking CLIC5A.

3.2.7 CLIC5 deficiency potentiates glomerular injury in DOCA/Salt hypertensive mice.

We next determined whether CLIC5 deficiency potentiates glomerular injury in DOCA/Salt hypertensive mice. Glomerular structure was evaluated by transmission electron microscopy (TEM) with morphometry (Figure 3.11) and by periodic acid Schiff (PAS) histology (Figure 3.12). As previously reported [5], the density of glomerular endothelial fenestrae was similar in normotensive CLIC5 deficient and wild-type mice, but it was significantly lower in UNx DOCA/Salt hypertensive CLIC5^{-/-}, compared to normotensive control CLIC5^{-/-} (Figure 3.11 a,b). By contrast, DOCA/Salt hypertension had no discernable effect on glomerular endothelial fenestrae in wild-type mice. The podocyte foot processes were broader in CLIC5^{-/-} mice, compared to their CLIC5^{+/+} littermates, and the number of foot processes per μm GBM was reduced (Figure 3.11 a,c), as previously reported [5], and DOCA/Salt did not alter the podocyte foot process density in either CLIC5^{+/+} or CLIC5^{-/-} mice. Glomerular microaneurysms were observed in both, UNx-DOCA/Salt hypertensive CLIC5^{+/+} and CLIC5^{-/-} mice (Figure 3.11 e, Figure 3.12 a,c). Transmission electron microscopy (TEM) showed disruption of the mesangial-GBM connection in areas of microaneurysm formation (Figure 3.11 e). The fraction of glomeruli with microaneurysms was nearly 2-fold greater in UNx-DOCA/Salt hypertensive

CLIC5^{-/-} compared to CLIC5^{+/+} mice (Figure 3.12 a,c). No microaneurysms were observed in normotensive mice (data not shown). Mesangial matrix expansion (Figure 3.12 a) and occasional glomerular sclerosis were also observed in UNx-DOCA/Salt hypertensive mice, but the frequency of these changes was low (Figure 3.12 b). Three weeks after initiation of DOCA/Salt treatment, proteinaceous casts were observed in dilated tubules of UNx-DOCA/Salt CLIC5^{-/-} mice, but not in UNx-DOCA/Salt CLIC5^{+/+} mice (Figure 3.13 a). In the UNx-DOCA/Salt hypertensive mice, the urine albumin:creatinine ratio (ACR), determined from urine WB (Figure 3.13 b-d) increased as a function of time (Figure 3.13 b). The ACR was 780 ± 235 and $1,720 \pm 960$ $\mu\text{g}/\text{mg}$, in CLIC5^{+/+} and CLIC5^{-/-} mice, respectively (mean \pm SD, $n = 5/\text{group}$, $p < 0.05$) (Figure 3.13 c,d) 21 days after initiation of DOCA/Salt treatment. Thus, in CLIC5 deficient C57BL/6J mice, UNx-DOCA/Salt hypertension reduces the number of glomerular endothelial fenestrae and is associated with greater glomerular microaneurysm formation and albuminuria, compared to CLIC5^{+/+} mice.

3.2.8 CLIC5 deficiency or DOCA/Salt hypertension do not change VEGF protein expression but reduce VEGFR2 activation in renal glomeruli in mice.

Since podocyte-derived VEGF is critical for glomerular EC differentiation and fenestrae formation [23, 292], we determined whether the basal endothelial defects and the decreased in fenestrae frequency by DOCA/Salt hypertension in CLIC5^{-/-} mice is related to reduced VEGF protein expression in podocytes of CLIC5-deficient mice. By immunofluorescence microscopy VEGF protein expression appeared similar in glomeruli from normotensive and hypertensive CLIC5^{+/+} and CLIC5^{-/-} mice (Figure 3.14 a).

VEGF stimulates cellular responses by binding to the transmembrane receptor tyrosine kinase VEGFR2, causing VEGFR2 dimerization and activation via transphosphorylation. We

next evaluated VEGFR2 expression and phosphorylation in isolated glomerular lysates by western blot analysis. In glomerular lysates from normotensive control CLIC5^{-/-} mice, the VEGFR2 protein expression was not different than that in wild type mice. However, the ratio of p-VEGFR2-to-VEGFR2 was significantly lower in normotensive CLIC5^{-/-}, compared to the wild type mice (Figure 3.14 b). Furthermore, DOCA/Salt treatment significantly decreased the ratio of p-VEGFR2: VEGFR2 in glomeruli from CLIC5^{+/+} mice. In glomerular lysates from UNx-DOCA/salt-hypertensive CLIC5^{-/-} mice total VEGFR2 was enhanced relative to that in normotensive controls and the ratio of p-VEGFR2 : VEGFR2 did not change. Hence, CLIC5 deficiency or DOCA/Salt hypertension does not change VEGF protein expression but both seem to reduce VEGFR2 activation in renal glomeruli in mice.

ERK/mitogen-activated protein kinase (MAPK) and PI3K/Akt are downstream signaling pathways that are activated by VEGF [293-295]. We next explored whether ERK or AKT phosphorylation is different in glomeruli from CLIC5^{-/-} mice compared to the wild type. By western blot analysis glomerular AKT or ERK expression or phosphorylation levels were not altered by CLIC5 deficiency (Figure 3.15 a-d).

3.2.9 CLIC5 deficiency results in expansion of glomerular capillary lumen in mice.

Although our lab previously reported the expansion of EC compartment in CLIC5^{jbjg/jgb} mice, in our study we used mice on a different genetic background, and since the first set of studies was not done with perfusion-fixed tissue, we wanted to confirm whether CLIC5 deficiency results in expansion of glomerular capillary lumens in mice. Morphological analysis by point counting in perfused fixed glomeruli from CLIC5^{+/+} and CLIC5^{-/-} mice all in C57BL/6J background confirms that there are fewer capillary loops in glomeruli of CLIC5^{-/-} mice and that the diameter of each capillary loop is increased (Figure 3.16 a-d).

3.3 Discussion:

The CLIC5A protein is highly enriched in renal glomeruli. In podocytes, CLIC5A is a component of the ezrin-NHERF2-podocalyxin complex at the apical domain of foot processes [5]. We showed previously that CLIC5A enhances clustered PI[4,5]P₂ generation at the apical plasma membrane through an interaction with PI[4]P5 kinases, as a first step in ezrin activation[4]. The activated ERM proteins link cortical F-actin to PI[4,5]P₂ and to membrane spanning proteins, thereby helping to shape actin-based cellular projections like microvilli [296-298], actin-based sensory stereocilia [178, 183, 280] and podocyte foot processes [5, 58, 247]. We now show for the first time, that CLIC5A also activates Rac1, but not Cdc 42 or Rho (Figure 3.1), and that the CLIC5A-mediated formation of apical membrane PI[4,5]P₂ clusters as well as ERM activation require active Rac1 (Figure 3.4). Consistent with CLIC5A-mediated Rac1 activation, CLIC5A also stimulates phosphorylation of the Rac1 effectors Pak1,3 (Figures 3.1-3.4). Based on these finding we propose the following Model (Figure 3.17): CLIC5A association with the plasma membrane results in the formation of a signaling complex in which Rac1 is activated, in turn stimulating PI[4]P5 Kinase(s) [299, 300] to produce PI[4,5]P₂ clusters which serve as a docking site for the activation of ezrin. Active ezrin then links podocalyxin, via NHERF2, to cortical F-actin. Since CLIC5A-stimulated Rac1 also activates Pak1,3, known to stimulate cofilin phosphorylation [301], we speculate that CLIC5A-stimulated actin polymerization [4], may be downstream of CLIC5A-Rac1-dependent Pak1,3 activation.

In podocytes ezrin links podocalyxin to cortical F-actin, via direct, and NHERF-2 mediated interactions [58, 73, 247]. Rac1 controls actin dynamics and plays a central role in podocyte motility and integrity [302-304]. Stimuli that activate Rac1 include shear stress [305], mechanical stretch [306], osmotic stress [307, 308], growth factors [309], aldosterone [310, 311]

and angiotensin II [312]. However, podocyte-specific deletion of Rac1 does not change podocyte morphology or function [155, 310], indicating that Rac1 is not essential for glomerular function under physiological conditions, or that its deficiency can be compensated for by other mechanisms (or by other GTPases). This is similar to the findings in CLIC5 deficient mice, where renal histology is normal, even though the podocyte foot process number is reduced, podocyte ezrin activity is profoundly disrupted, and there is microalbuminuria [5]. We now find that UNx-DOCA/Salt hypertension strongly induces glomerular podocyte Pak1 protein expression and Pak1-3 phosphorylation, indirect evidence that Rac1 is activated (Figure 3.7). However, podocyte-associated Pak1,3 and -2 phosphorylation were substantially reduced in CLIC5A deficient mice, consistent with the findings in cultured cells, where CLIC5A-stimulated Rac1 activity is required for Pak1,3 phosphorylation. Since Pak1,3 phosphorylation requires Rac1 activity, and since Blattner et al [155] reported that podocyte-specific Rac1 deletion potentiates glomerular injury in response to DOCA/Salt hypertension, we conclude that the glomerular response to UNx-DOCA/Salt hypertension requires Rac1, and that CLIC5A is essential for podocyte Rac1 as well as Pak1,3 activation.

We also observed that the abundance of podocalyxin is reduced in CLIC5^{-/-} mice, a finding that differs from our previous evaluation in microdissected mouse glomeruli [5], but is consistent with the observations by Pierchala et al [123]. Furthermore, we observe that DOCA/Salt hypertension reduces podocalyxin protein levels in wild-type mice, even though ezrin activation remains intact and CLIC5A levels do not change (Figure 3.10). Podocalyxin abundance is further reduced in UNx-DOCA/Salt hypertensive CLIC5^{-/-} mice. These data imply that DOCA/Salt hypertension stimulates remodeling of the actin-podocalyxin interaction in the apical domain of podocyte foot processes through Rac1/Pak1,3 and CLIC5-dependent processes.

Shibata et al. [310] showed that in podocytes, constitutively active Rac1 facilitates mineralocorticoid receptor nuclear accumulation via Pak1 phosphorylation [164]. Furthermore, Rac1-dependent mineralocorticoid receptor activation in UNx-DOCA/Salt rats contributed to hypertension and kidney injury [166]. Therefore, defective Rac1 activity in CLIC5A deficient podocytes could blunt nuclear mineralocorticoid action, but our work so far has not addressed this possibility.

Paradoxically, inhibition of Rac1/RhoA can protect from hypertension-induced glomerular injury in mice [164], and an association between a hypoactive mutant of Arhgap24, a Rho GTPase Activating Protein that inactivates Rac1 in podocytes, and familial focal segmental glomerulosclerosis has been described [160]. Thus, increased Rac1 activity in podocytes also seems to have deleterious effects, and inhibition of Rho-GTPases has been proposed as a potential treatment in CKD [149, 164]. It turns out that both increased and reduced podocyte-specific RhoA activity lead to foot process effacement [152], suggesting that fine control over the activity of Rho-GTPases (including Rac1) in podocytes maintains their highly specialized architecture and that deviation towards hyper- and hypo-activity can have deleterious effects [155]. Fine control of Rac1 function could also involve spatially restricted regulation of the ezrin/NHERF2/podocalyxin complex producing in a different podocyte remodeling response than that produced by active Rac1 at the slit diaphragm [313] or during remodeling of focal adhesions [314]. In the UNx-DOCA/Salt hypertensive CLIC5^{-/-} mice we also observed a striking decrease in the density of glomerular endothelial fenestrae, which was not observed in UNx-DOCA/Salt hypertensive CLIC5^{+/+} mice (Figure 3.11). We previously reported that CLIC5 is also highly expressed in glomerular endothelial cells, but we had not observed any change in glomerular endothelial cell fenestrae under unchallenged conditions [5]. The findings here could

indicate that ERM and/or Pak activation in glomerular endothelial cells also play a role in fenestrae formation, or alternatively, that podocyte-derived stimuli required for fenestrae formation are reduced in UNx-DOCA/Salt hypertensive CLIC5^{-/-} mice.

Our lab has reported that CLIC5 deficiency at baseline results in EC vacuolization, expansion of capillary lumen and an increase in the endothelial cell number [5]. Since VEGF antagonists in rats result in glomerular EC vacuolization [315, 316] and podocyte-derived VEGF is critical for glomerular EC differentiation and fenestrae formation [23, 292] we explored the possibility that podocytes of CLIC5-deficient mice produce less VEGF than controls. We observed that CLIC5 deficiency or DOCA/Salt hypertension does not change VEGF protein expression, at least as assessed by immunofluorescence, but it reduces VEGFR2 activation in renal glomeruli in mice (Figure 3.14). However, the p-VEGFR2 protein abundance relative to actin did not change. There seems to be a compensatory increase in total VEGFR2 in the DOCA/Salt treated CLIC5 deficient mice, so I cannot ascribe the reduced glomerular endothelial fenestrae density in these hypertensive mice to reduced VEGFR2 activation. The underlying cause for the loss of fenestrae in UNx-DOCA/Salt hypertensive CLIC5^{-/-} mice clearly needs further investigation.

It is of note that we saw an increase in VEGFR2 expression in CLIC5^{-/-} mice compared to the wild type (Figure 3.14). The increased endothelial cell number in CLIC5^{-/-} mice [5] could, in part, be responsible for this increase in glomerular VEGFR2 protein. One other possible mechanism for VEGFR2 up-regulation by CLIC5 deficiency is the increased mechanical forces in stretched capillaries in CLIC5^{-/-} mice (Figure 3.16). Increased expression and activation of vascular endothelial growth receptor-2 (VEGFR2) by mechanical forces has been reported elsewhere [317-320]. Increased VEGFR2 expression by physical stimuli is mediated by p190

RhoGAP. Mechanical forces activate p190 RhoGAP, an upstream inhibitor of Rho that controls capillary network formation and angiogenesis in human ECs. RhoGAP regulate the balance of activities between antagonistic transcription factors, TFII-I and GATA2, which modulates gene expression of the VEGF receptor VEGFR2 [317-319].

Consistent with the earlier observation in CLIC5^{-/-} mice in C3H/HeJ background, morphological analysis shows that there are fewer capillary loops in CLIC5^{-/-} mice compared to the wild type all in the C57BL/6J background but the diameter of each capillary loop is increased. Here, I used perfusion fixation to preserve the morphology of the capillary loops under physiological pressure. Similar to our findings, disruption of a CLIC5A homolog, EXCretery canal abnormal (EXC)-4, which is localized in the plasma membrane of the excretory canal of *C. elegans*, results in cystic enlargement of the excretory canal [321]. Furthermore CLIC4, that shares 76% homology at the amino acid level with CLIC5A, has a role in endothelial tube formation in vitro [237, 238]; Therefore, it is possible that CLIC5A, similar to its homologs EXC-4 and CLIC4 has a role in capillary lumen formation in glomeruli. According to Laplace's law the increase in capillary lumen diameter in CLIC5^{-/-} mice results in a higher capillary wall tension at baseline. Since VEGFR2 expression is increased by mechanical forces acting on endothelial cells, it is possible that the increase in VEGFR2 protein in the CLIC5 deficient mice results from an increase in glomerular capillary wall tension. Also, since podocyte foot processes play an important role in resisting capillary wall tension, the accentuated glomerular injury in DOCA/Salt hypertensive CLIC5^{-/-} mice may at least in part due to the fact that podocytes from CLIC5^{-/-} mice are not able to further resist the increased mechanical strain.

Since the CLIC5^{-/-} mice are deficient in both, the CLIC5A and CLIC5B isoforms, it may be argued that our findings are not due to CLIC5A. However, CLIC5A and CLIC5B, produced

through alternative usage of exon 1A or 1B, differ substantially in size. The larger CLIC5B (410 aa) is readily distinguished from CLIC5 (251 aa) on SDS-PAGE gels and by RT-PCR. We previously reported that CLIC5B mRNA and protein are not detected in renal glomeruli [5], and we observe abundant glomerular CLIC5A in CLIC5^{+/+} but not in CLIC5^{-/-} mice (Figures 3.7-3.10). Furthermore, the same signaling process induced by CLIC5A in COS7 cells is abrogated in glomerular podocytes in vivo when CLIC5 is deleted. It therefore is highly likely that the absence of CLIC5A, not CLIC5B, is responsible for reduced glomerular Pak and ERM phosphorylation in the CLIC5^{-/-} mice.

In summary, I have shown that CLIC5A increases Rac1 activity in COS7 cells, and that CLIC5A-stimulated PI[4,5]P2 generation, ERM phosphorylation and Pak 1,3 activation are all dependent on Rac1 activity in the cultured cells. In cultured glomerular podocytes, CLIC5A also stimulated ezrin and Pak phosphorylation. In CLIC5 deficient mice I found that activation of both ERM and Pak1,3 in podocytes is markedly reduced and podocalyxin abundance declines, changes that are associated with greater microaneurysm formation and proteinuria in the UNx-DOCA/Salt hypertension model. I can therefore conclude that the organization of the actin cytoskeleton at the apical domain of podocyte foot processes is, in part, dependent on CLIC5A and its downstream effectors, and that stabilization of glomerular capillaries exposed to hypertension requires CLIC5A-dependent Rac1, ezrin and Pak activation.

Figure 3.1

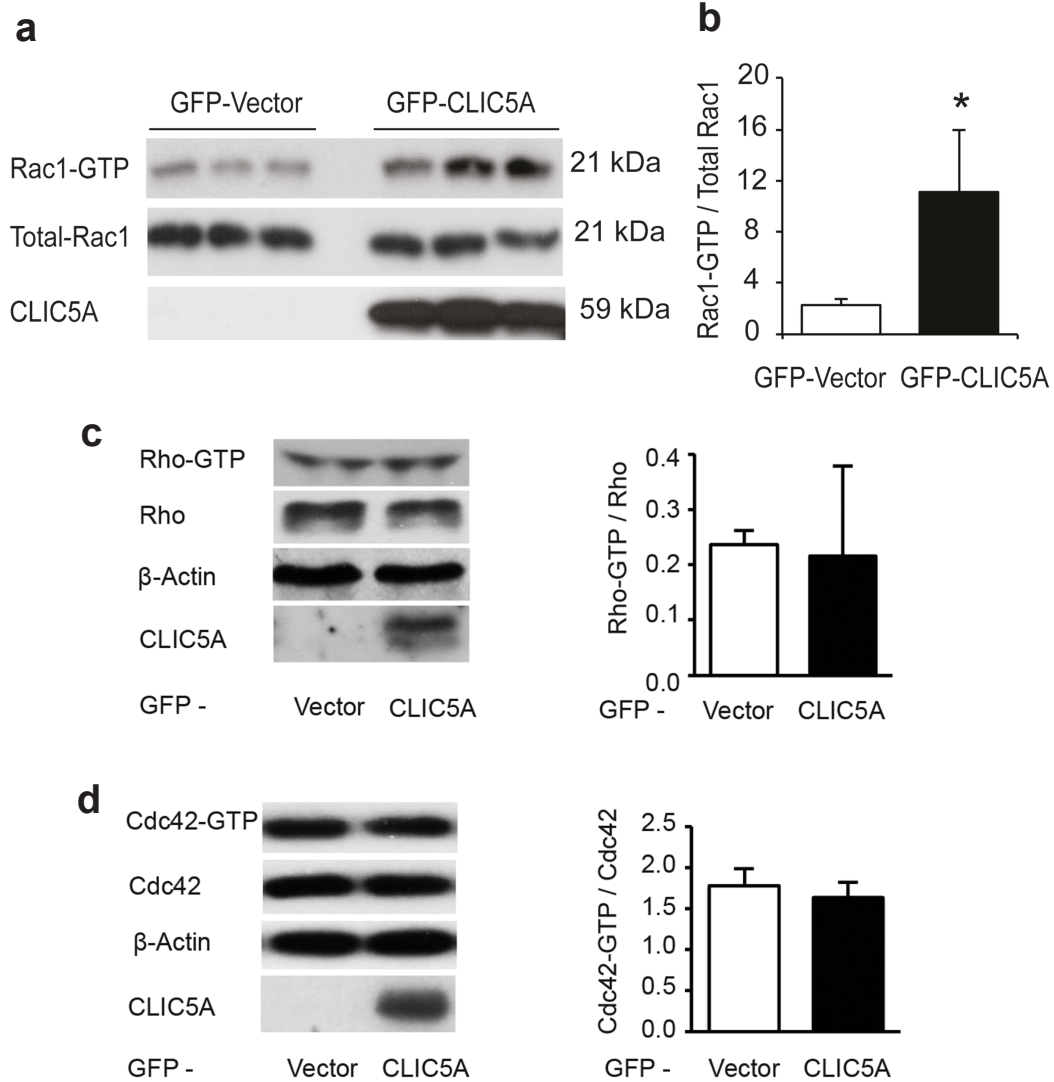


Figure 3.1 | Increased Rac1 activity but not Rho, Cdc42 in COS7 cells expressing CLIC5A. (a) Western blot analysis of COS7 cell lysates probed for Rac1 and CLIC5A. Total Rac1 (middle panel) and CLIC5A (bottom panel) are shown. Triplicates from one experiment are shown. 2 additional experiments, each done in triplicate gave similar results. (b) The ratio of GTP-Rac1: Total Rac1 quantified by densitometry. (mean \pm SEM; n=3 independent experiments, *p < 0.05). (c) Reperasantative Western blot analysis of COS7 cell lysates probed for Rho, β -Actin and CLIC5A. The ratio of GTP-Rho: Total Rho was quantified by densitometry. (mean \pm SD; n=3 independent experiments, *p < 0.05). (d) Reperasantative Western blot analysis of COS7 cell lysates probed for Cdc42, β -Actin and CLIC5A. The ratio of GTP-Cdc42: Total Cdc42 was quantified by densitometry. (mean \pm SD; n=3 independent experiments, *p < 0.05).

Figure 3.2

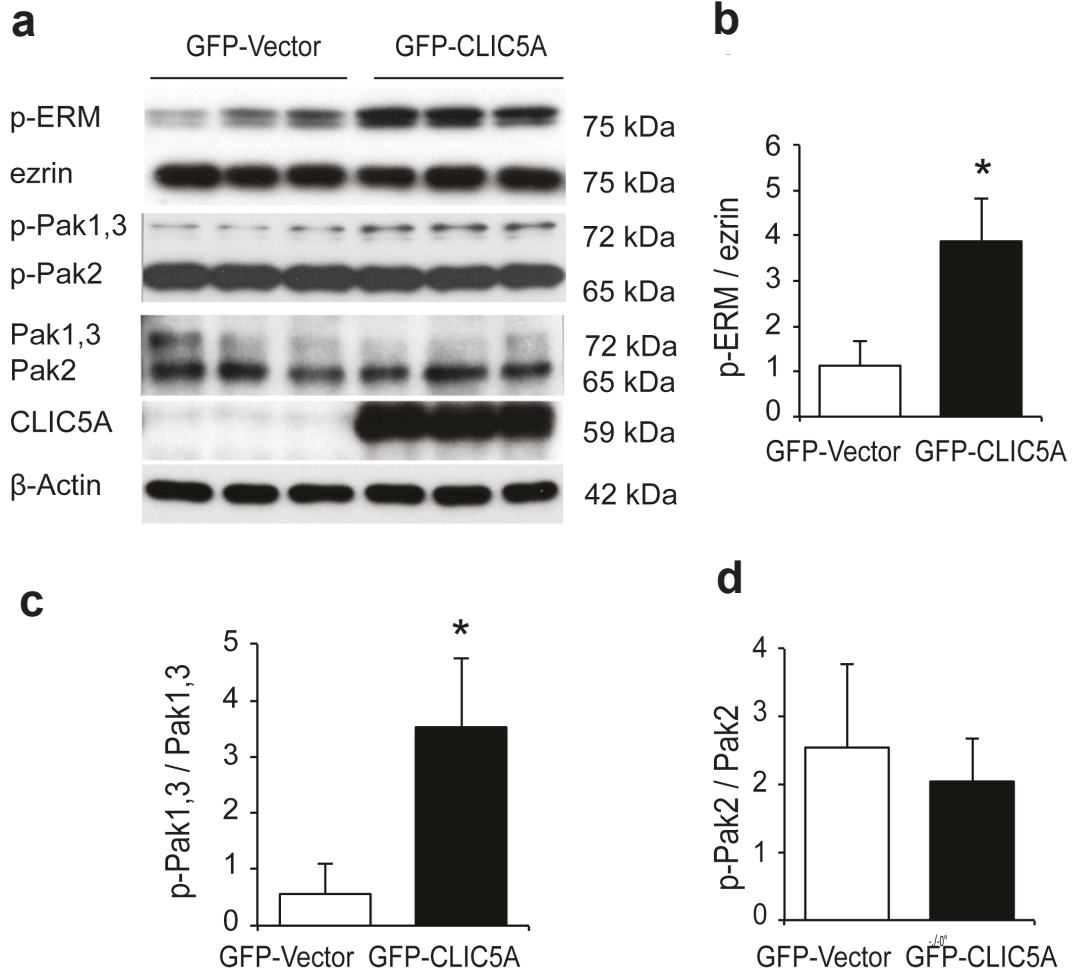


Figure 3.2 | Increased Pak1,3 and ERM protein phosphorylation in COS7 cells expressing CLIC5A. (a) Western blot analysis for phosphorylated ERM proteins (p-ERM), total ezrin, phosphorylated Pak proteins (p-Pak1,3; p-Pak2), total Pak proteins (Pak1,3; Pak2), CLIC5A and β -actin. Each lane represents a distinct experiment. (b-d) Densitometric quantification of WB data; (b) Ratio of p-ERM : total ezrin. (c) Ratio of p-Pak1,3 : total Pak1,3. (d) Ratio of p-Pak2 : total Pak2. (mean \pm SD; n = 3 independent experiments, *p < 0.05).

Figure 3.3

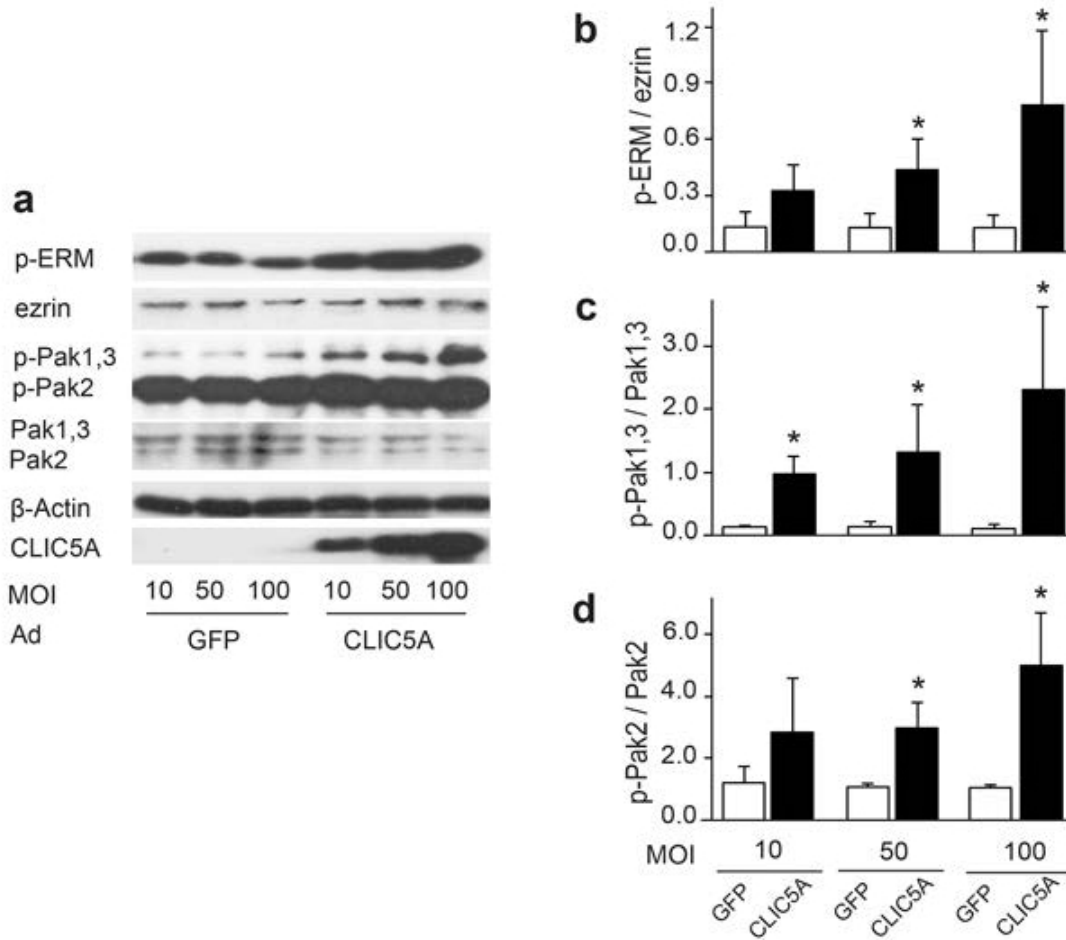


Figure 3.3 | Increased Pak1,2,3 and ERM protein phosphorylation in undifferentiated podocytes expressing CLIC5A. (a) WB analysis of podocytes transfected with 10, 50 or 100 MOI of pAdTrack-GFP (GFP) or pAdTrack-GFP-CLIC5A (CLIC5A) probed for phosphorylated ERM proteins (p-ERM), total ezrin, phosphorylated Pak proteins (p-Pak1,3; p-Pak2), total Pak proteins (Pak1,3; Pak2), CLIC5A and β -actin. A representative experiment is shown. (b-d) Densitometric quantification of WB data: (b) Ratio of p-ERM : total ezrin. (c) Ratio of p-Pak1,3 : total Pak1,3. (d) Ratio of p-Pak2 : total Pak2 (mean \pm SD; n = 3 independent experiments, *p < 0.05 vs the GFP control group; Student t-test).

Figure 3.4

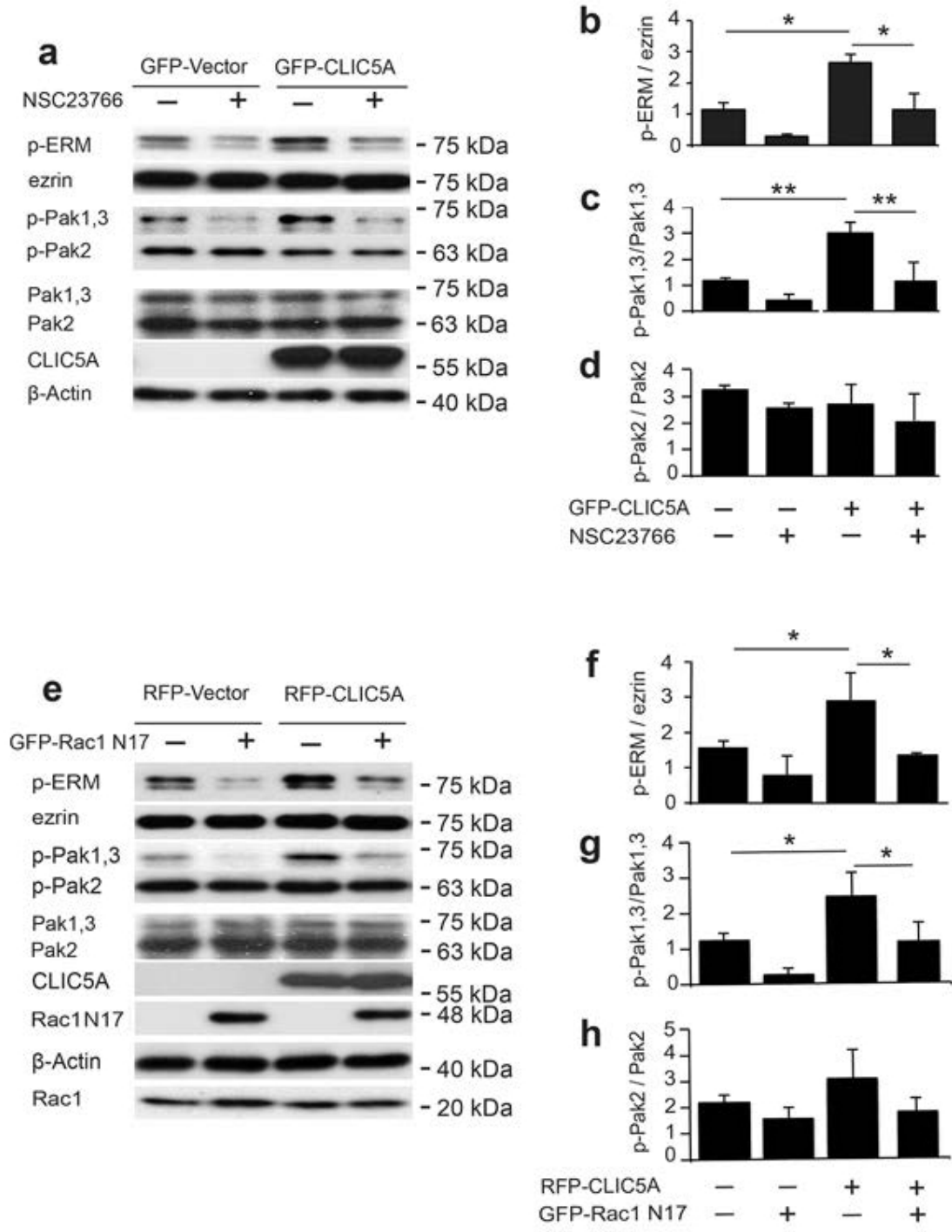


Figure 3.4 | CLIC5A-induced ERM and Pak1,3 protein phosphorylation requires Rac1 activity (Continued on next page)

Figure 3.4 | CLIC5A-induced ERM and Pak1,3 protein phosphorylation requires Rac1 activity (a) WB analysis for ERM and Pak protein abundance and phosphorylation in COS7 cells expressing GFP-CLIC5A or GFP and treated with or without the specific Rac1 inhibitor NSC 23766 (100 μ M) for 10 minutes. A representative experiment is shown.

(b-d) The ratios of phosphorylated : total proteins were determined from densitometric analysis of the WB in (a) and 2 additional independent experiments (mean \pm SD; n=3; *p < 0.05; **p < 0.01). Rac1 inhibition significantly reduced basal and CLIC5A-stimulated ERM protein (b) and Pak1,3 (c), but not Pak2 (d) phosphorylation. (e) Western blot of ERM and Pak protein abundance and phosphorylation in COS7 cells transiently co-transfected with RFP-Vector or RFP-CLIC5A, with or without dominant negative GFP-Rac1 N17. The membranes were also probed with antibodies directed against CLIC5A, β -actin, and Rac1. Note that the molecular mass of GFP-Rac1 N17 is greater than that of endogenous Rac1. (f-h) The ratios of phosphorylated : total proteins determined from densitometric analysis of the WB in (e) and 2 additional, independent experiments (mean \pm SD; n=3; *p < 0.05; **p < 0.01). Expression of the dominant negative GFP-Rac N17 reduced basal and CLIC5A-stimulated ERM protein (f) and Pak1,3 (g), but not Pak2 (h) phosphorylation.

Figure 3.5

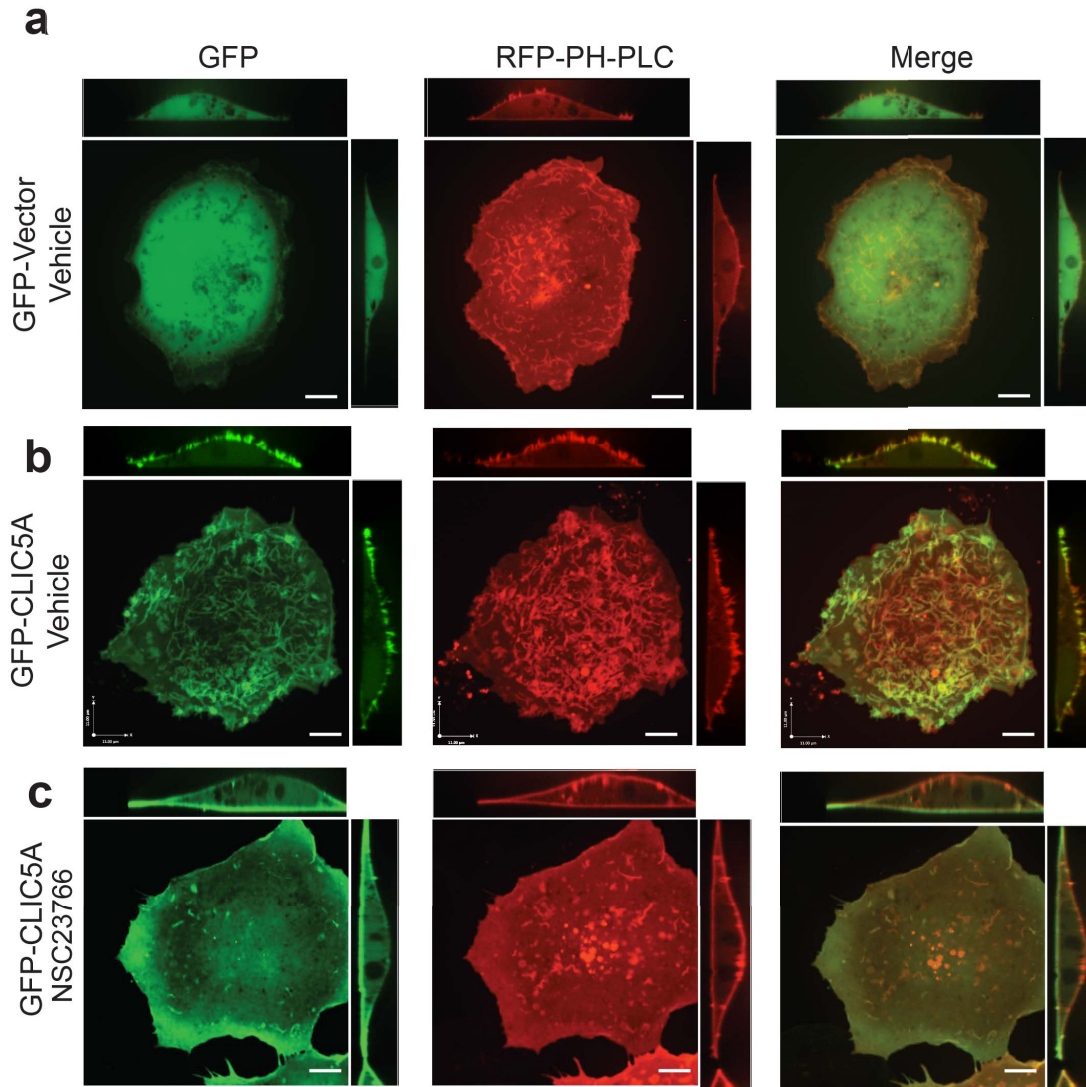


Figure 3.5 | Abrogation of CLIC5A-dependant apical PI[4,5]P2 cluster formation by NSC 23766. COS7 cells were transiently co-transfected with GFP-Vector or GFP-CLIC5A and the PI[4,5]P2 reporter RFP-PH-PLC (3:1, GFP-CLIC5A or GFP-Vector : RFP-PH-PLC cDNA) followed 48 hours later by spinning-disk confocal microscopy in living cells treated with Rac1 inhibitor NSC 23766 (100 μ M) or vehicle for 20 minutes. Relative to GFP-Vector transfected cells (a), GFP-CLIC5A expression (b) resulted in a significant increase of clustered RFP-PH-PLC accumulation at the apical plasma membrane. The RFP-PH-PLC reporter in apical membrane clusters partially co-localized with GFP-CLIC5A (b), but not with GFP (a). Rac1 inhibition (c) resulted in the rapid loss of dorsal membrane RFP-PH-PLC clusters in the COS7 cells expressing GFP-CLIC5A, and redistribution of GFP-CLIC5A away from the apical plasma membrane. Not shown, NSC 23766 was essentially without effect on the density of RFP-PH-PLC clusters in GFP-vector transfected control cells. Scale bar = 10 μ m. One representative experiment is shown. 2 additional independent experiments produced the same results.

Figure 3.6

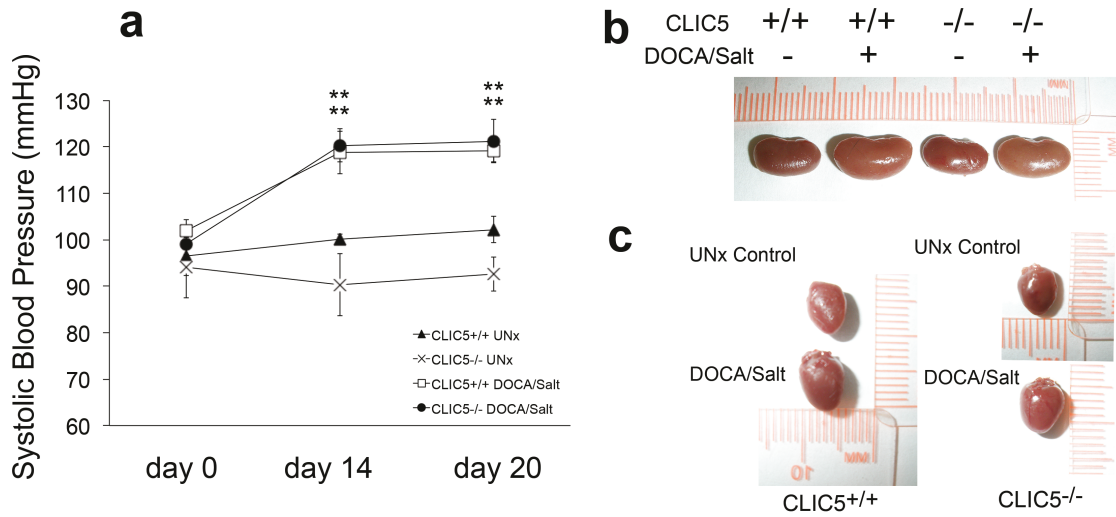


Figure 3.6 | Systemic Hypertension in UNx-DOCA/Salt treated CLIC5+/+ and CLIC5-/- mice. (a) Systolic blood pressure as a function of time in UNx CLIC5+/+ and CLIC5-/- mice, treated with or without DOCA/Salt. Blood pressure was measured with the CODA non-invasive blood pressure monitoring system under anesthesia (mean \pm SEM; n = 7, **p < 0.001 UNx-DOCA/Salt treatment vs. UNx in the same genotype). (b,c) Representative images showing kidney (b) and heart (c) size on day 20 in UNx-DOCA/Salt or UNx-Control CLIC5+/+ and CLIC5-/- mice. Kidney and Heart size was uniformly increased in all mice treated with DOCA/Salt.

Figure 3.7

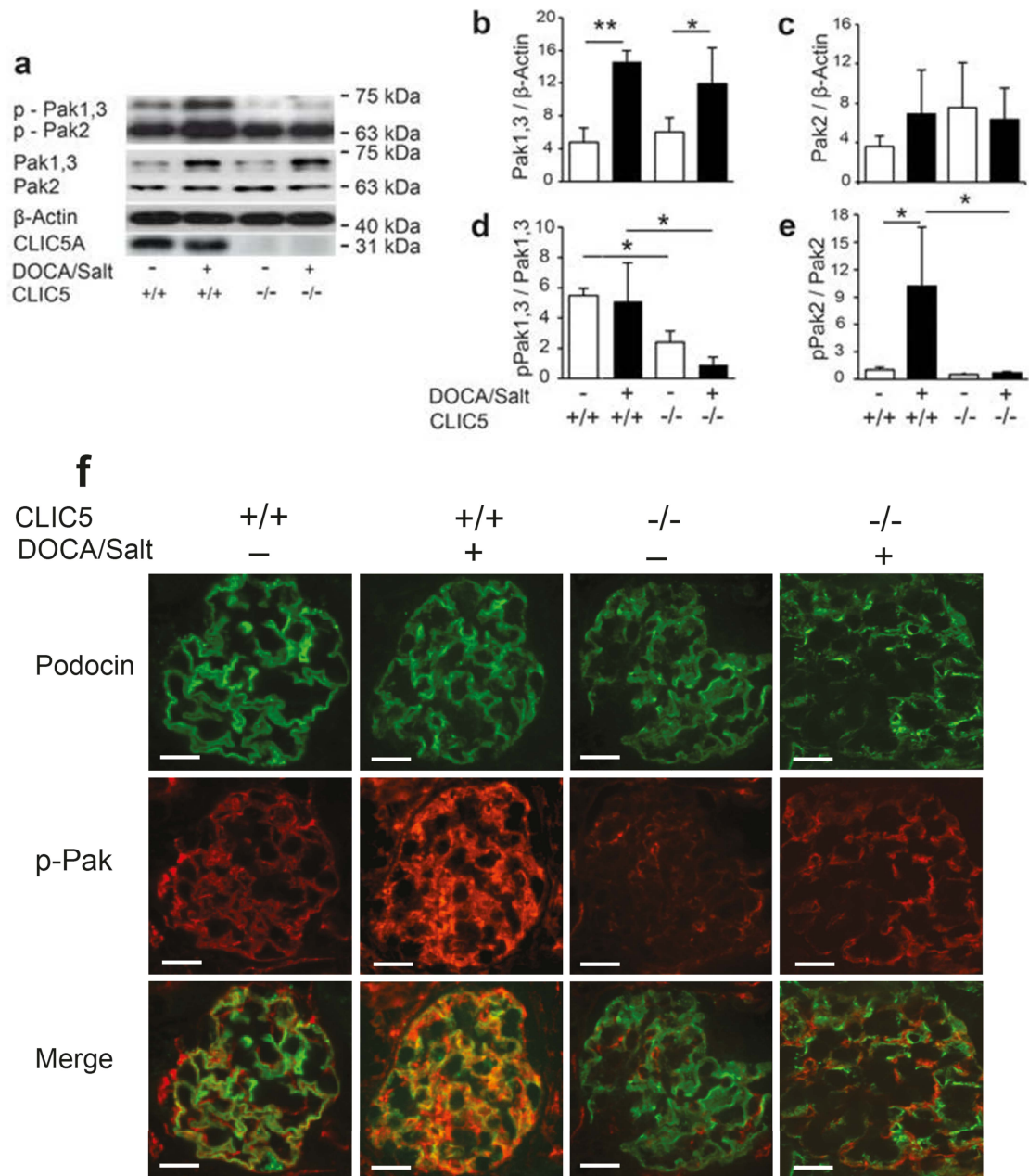


Figure 3.7| Pak Phosphorylation in Glomeruli of UNx-DOCA/Salt and UNx Control CLIC5+/+ and CLIC5-/- mice. (a) WB analysis of lysates from isolated glomeruli. Each lane represents glomeruli from a distinct mouse. In both genotypes, total Pak1 abundance is higher in UNx-DOCA/Salt treated mice than in the UNx controls, and UNx-DOCA/Salt treatment is associated with increased p-Pak1,3 and p-Pak2 in CLIC5+/+, but not in CLIC5-/- mice.

(b-e) Ratios of total Pak: β -actin, and p-Pak:total Pak proteins were determined from densitometry data (Mean \pm SD; n = 3-5 mice per group, *P < 0.05, **P < 0.01). The abundance of total Pak1,3 relative to β -actin (b) increased significantly in UNx-DOCA/Salt treated CLIC5^{+/+} and CLIC5^{-/-} mice, while total Pak2 abundance relative to β -actin (c) remained unchanged. The ratio of p-Pak1,3 : total Pak1,3 (d) was much lower in CLIC5^{-/-} compared to CLIC5^{+/+} mice. UNx-DOCA/Salt increased the fraction of p-Pak2 relative to total Pak2 (e) in CLIC5^{+/+} but not in CLIC5^{-/-} mice. (f) Dual confocal immunofluorescence microscopy of TCA-fixed renal cortex from UNx control and UNx-DOCA/Salt treated CLIC5^{+/+} and CLIC5^{-/-} mice. Affinity-purified goat anti-podocin served as the podocyte marker. In UNx-DOCA/Salt treated CLIC5^{+/+} mice, glomerular p-Pak immunoreactivity was much greater than in control UNx-CLIC5^{+/+} mice, and overlapped with podocin immunofluorescence. By contrast, in CLIC5^{-/-} mice, glomerular p-Pak immunoreactivity did not overlap with podocin and, consistent with the WB analysis (a), was much lower in CLIC5^{-/-} than in CLIC5^{+/+} mice, and increased only slightly in response to DOCA/Salt treatment. (Representative of 3 mice per group. For each mouse 10-15 glomeruli were photographed with similar results, scale bar = 10 μ m).

Figure 3.8

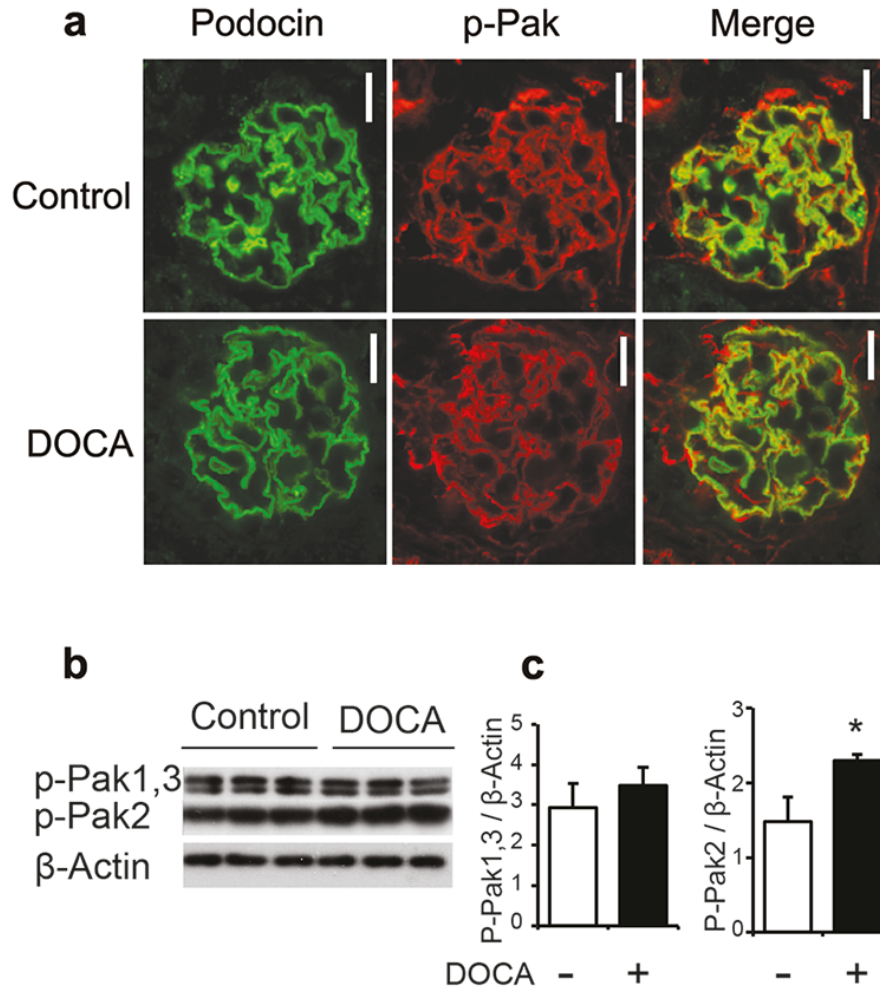


Figure 3.8 | P21-activated kinase (Pak) Phosphorylation in Glomeruli of UNx-DOCA and UNx Control CLIC5^{+/+} mice. (a) Dual confocal immunofluorescence microscopy of trichloroacetic acid (TCA)-fixed renal cortex from UNx control and UNx-DOCA treated CLIC5^{+/+} mice. Affinity purified goat anti-podocin served as the podocyte marker. (b) WB analysis of lysates from isolated glomeruli. (c) Ratios of p-Pak1,3:β-actin, and p-Pak2:β-actin proteins were determined from densitometry data (Mean ± SD; n = 3-5 mice per group, *P < 0.05, **P < 0.01). Each lane represents glomeruli from a distinct mouse. DOCA alone did not change p-Pak immunofluorescence in renal glomeruli of CLIC5^{+/+} mice. WB detected a modest, but significant increase in p-Pak2 in response to DOCA, but the level of p-Pak1,3 did not change.

Figure 3.9

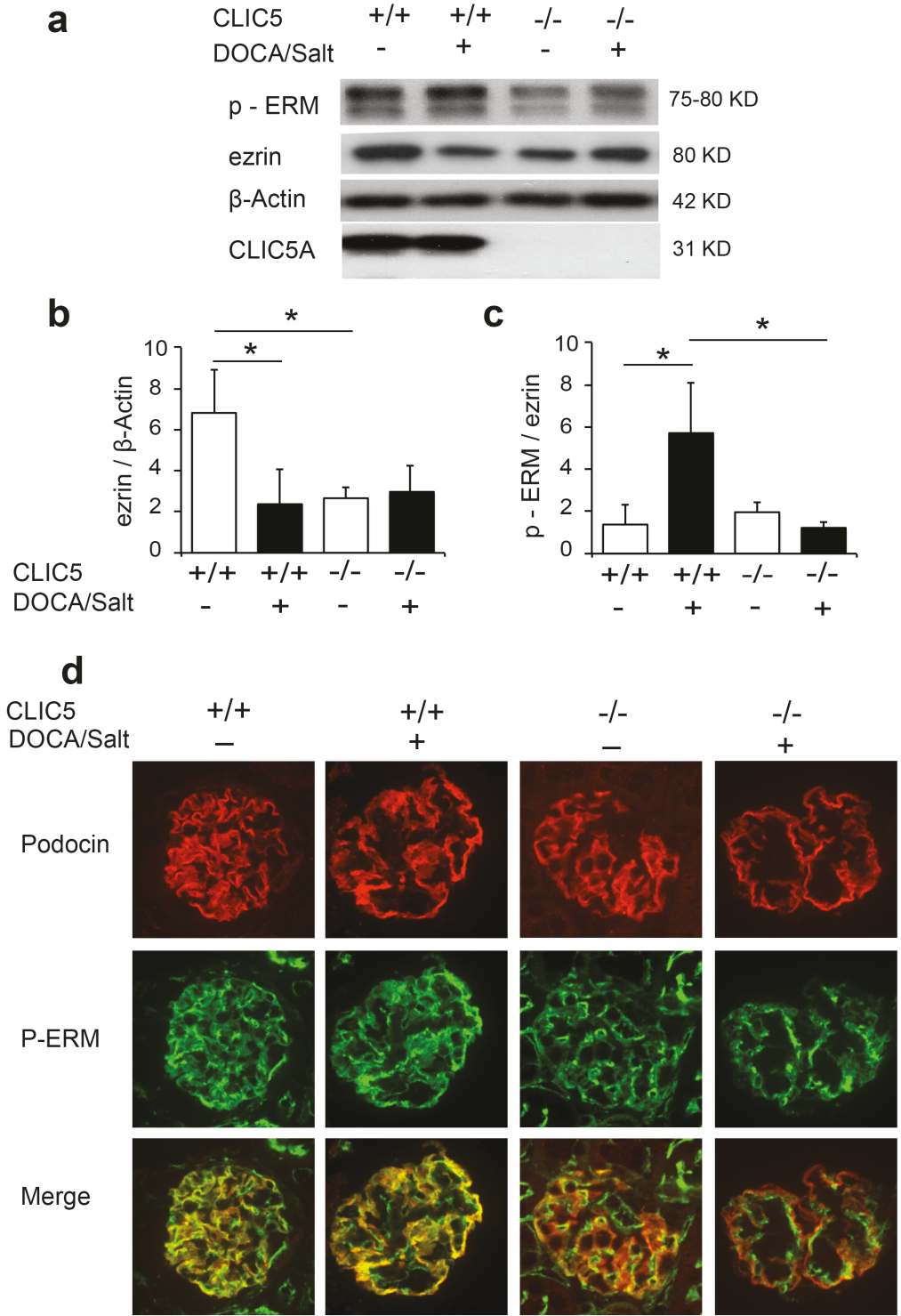


Figure 3.9 | ERM Protein Phosphorylation in Glomeruli of UNx-DOCA/Salt and UNx Control CLIC5^{+/+} and CLIC5^{-/-} mice. (Continued on next page)

Figure 3.9 | ERM Protein Phosphorylation in Glomeruli of UNx-DOCA/Salt and UNx Control CLIC5^{+/+} and CLIC5^{-/-} mice. (a) Representative WB of lysates from isolated glomeruli probed with anti-p-ERM, anti-ezrin, anti- β -actin and anti-CLIC5A antibodies. Each lane represents glomeruli from a distinct mouse. (b,c) Quantification of total ezrin abundance relative to β -actin (b), and p-ERM relative to total ezrin (Mean \pm SD; n = 3-5 mice per group, *P < 0.05, **P < 0.01). In UNx-CLIC5^{+/+} mice, the abundance of total ezrin relative to β -actin (b) decreased in response DOCA/Salt treatment, and the fraction of p-ERM relative to total ezrin (c) increased significantly. In UNx-CLIC5^{-/-} mice, total glomerular ezrin (b) and p-ERM protein (c) abundance were lower than in UNx-CLIC5^{+/+} mice, as previously reported (32-33). In UNx CLIC5^{-/-} mice, ERM protein phosphorylation did not increase in response to DOCA/Salt treatment. (d) Dual confocal immunofluorescence microscopy for p-ERM in TCA-fixed renal cortex from UNx control and UNx-DOCA/Salt treated CLIC5^{+/+} and CLIC5^{-/-} mice. Affinity-purified goat anti-podocin served as the podocyte marker. In UNx-DOCA/Salt CLIC5^{+/+} mice, glomerular p-ERM immunoreactivity was similar as that in control UNx-CLIC5^{+/+} mice, and overlapped partially with podocin immunofluorescence. Consistent with the WB analysis, in UNx-CLIC5^{-/-} mice, glomerular p-ERM immunoreactivity was reduced compared to that in UNx-CLIC5^{+/+} mice and did not co-localize with podocin. P-ERM immunofluorescence was further reduced in UNx- DOCA/Salt CLIC5^{-/-} mice. (Representative of 3 mice per group. For each mouse 10-15 glomeruli were photographed with similar results; scale bar = 10 μ m).

Figure 3.10

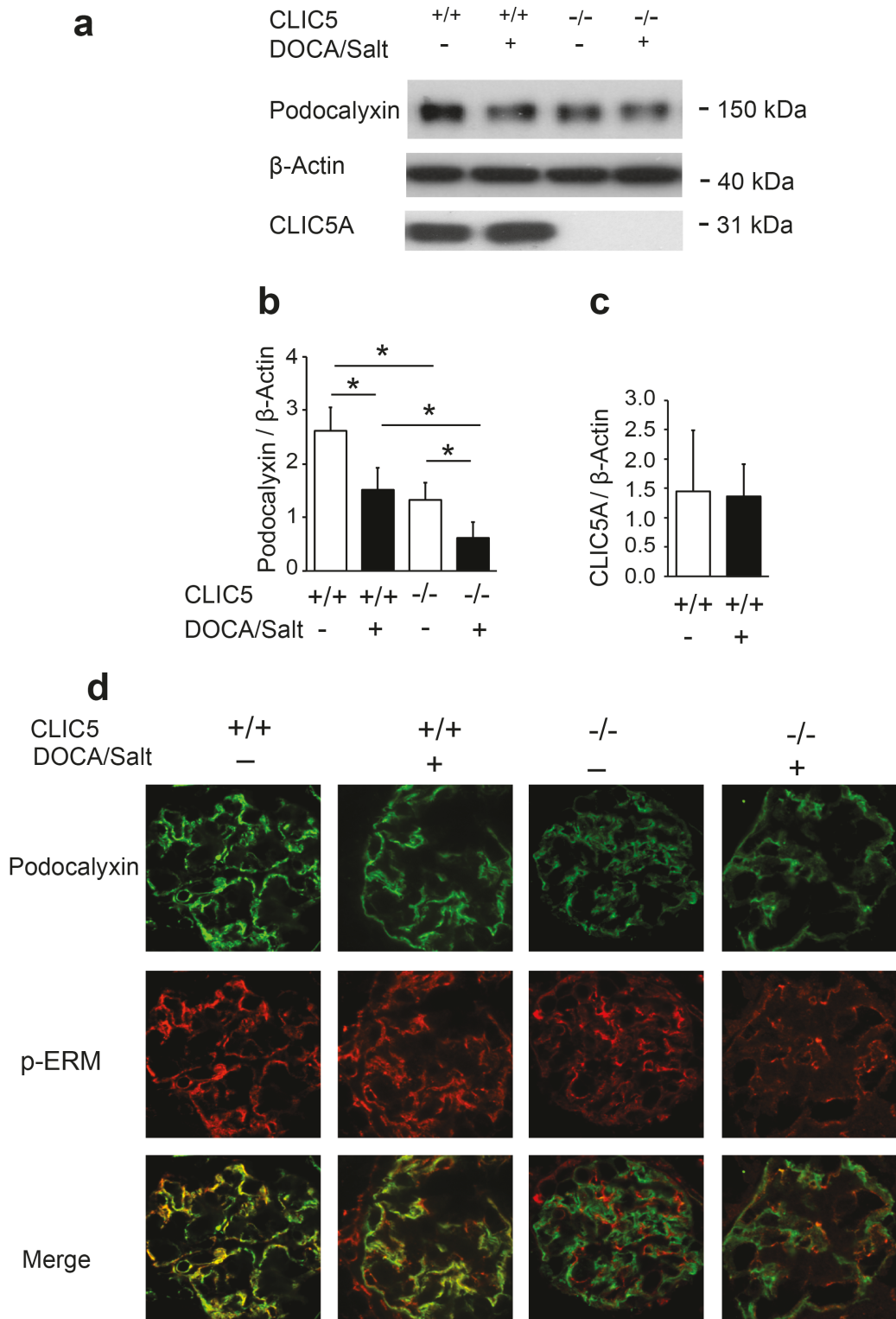


Figure 3.10 | Podocalyxin expression in Glomeruli of UNx-DOCA/Salt and UNx Control CLIC5+/+ and CLIC5-/- mice. (continued on next page)

(a) Representative WB of kidney cortex from UNx-DOCA/Salt and UNx Control CLIC5^{+/+} and CLIC5^{-/-} mice probed with anti-podocalyxin, anti- β -actin and anti-CLIC5A antibodies. Each lane represents kidney cortex from a distinct mouse.

(b,c) Quantification of podocalyxin and CLIC5A abundance relative to β -actin, respectively (Mean \pm SD; n = 3-5 mice per group, *P < 0.05 from the same genotype, #P < 0.05 from the different genotype in the same group, one-way ANOVA followed by Tukey's post-hoc test).

(d) Dual confocal IF microscopy for podocalyxin and p-ERM in TCA-fixed renal cortex from UNx control and UNx-DOCA/Salt treated CLIC5^{+/+} and CLIC5^{-/-} mice. In control UNx-CLIC5^{+/+} mice, podocalyxin immunoreactivity and partially overlapped with p-ERM protein. In UNx-CLIC5^{-/-} mice, glomerular podocalyxin immunoreactivity was reduced compared to that in UNx-CLIC5^{+/+} mice and did not overlap with p-ERM. (Representative of 3 mice per group. For each mouse 10-15 glomeruli were photographed with similar results, scale bar = 10 μ m).

Figure 3.11

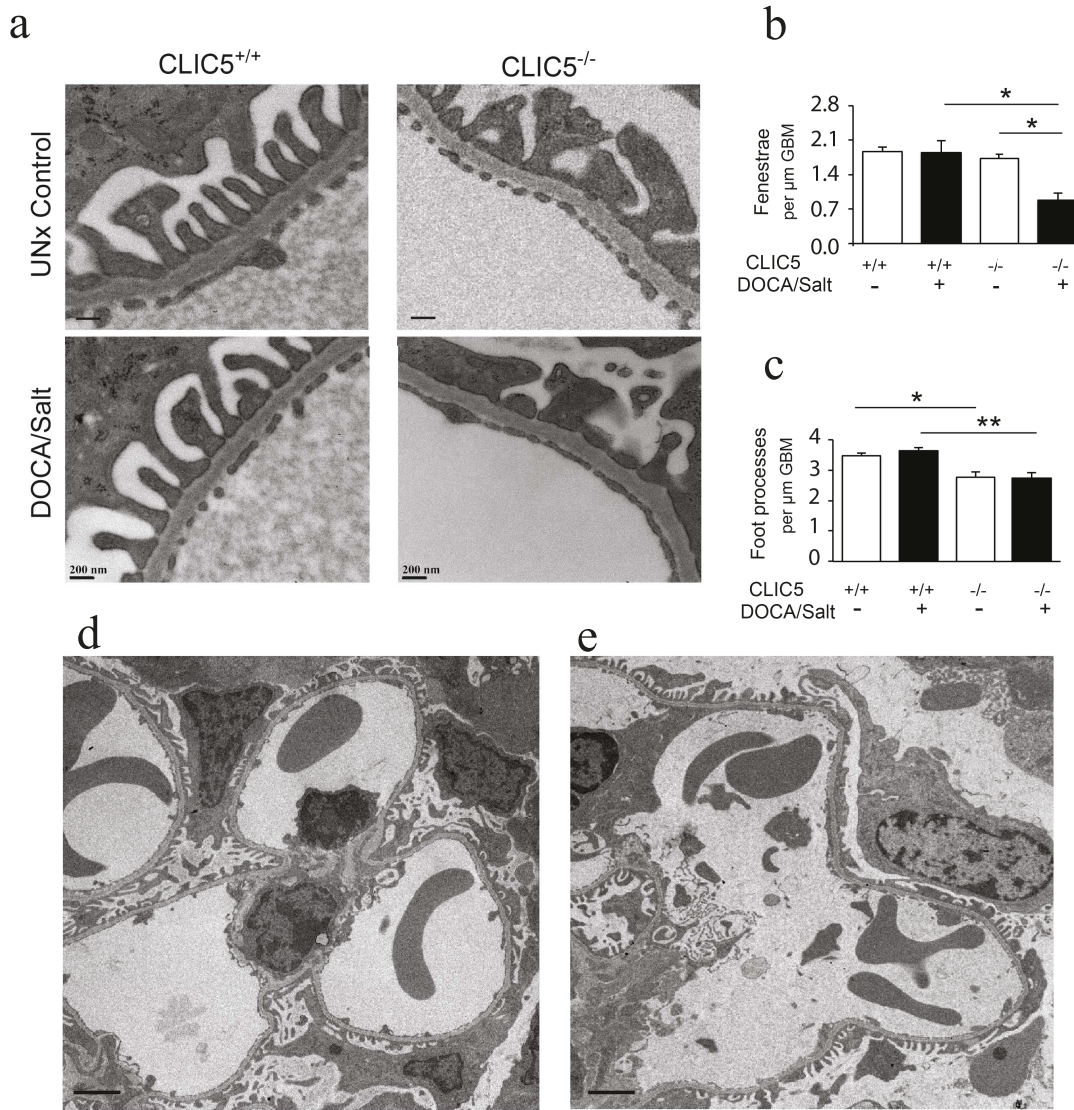


Figure 3.11 | Ultrastructure of glomerular capillaries from UNx-DOCA/Salt and UNx Control CLIC5^{+/+} and CLIC5^{-/-} mice. (a) TEM appearance of glomerular capillary walls from UNx-DOCA/Salt and UNx Control CLIC5^{+/+} and CLIC5^{-/-} mice (representative of 3-5 mice per group). (b,c) Quantifications of endothelial fenestrae and podocyte foot processes in UNx Control and UNx-DOCA/Salt CLIC5^{+/+} and CLIC5^{-/-} mice. (b) The density of glomerular endothelial fenestrae was markedly reduced in DOCA/Salt hypertensive mice CLIC5^{-/-} mice. (c) The density of podocyte foot processes in CLIC5^{-/-} mice is lower than that in CLIC5^{+/+} mice, but DOCA/Salt hypertension was without effect on foot process density (mean \pm SEM; n = 3-5 mice per group, *p < 0.05, **p < 0.001, one-way ANOVA followed by Tukey's post-hoc test, scale bar = 200 nm). (d,e) TEM appearance of intact glomerular capillary loops (d) and a glomerular capillary microaneurysm (e). (d) and (e) represent two different glomeruli from a single UNx-DOCA/Salt treated CLIC5^{-/-} mouse (scale bar = 1 μm).

Figure 3.12

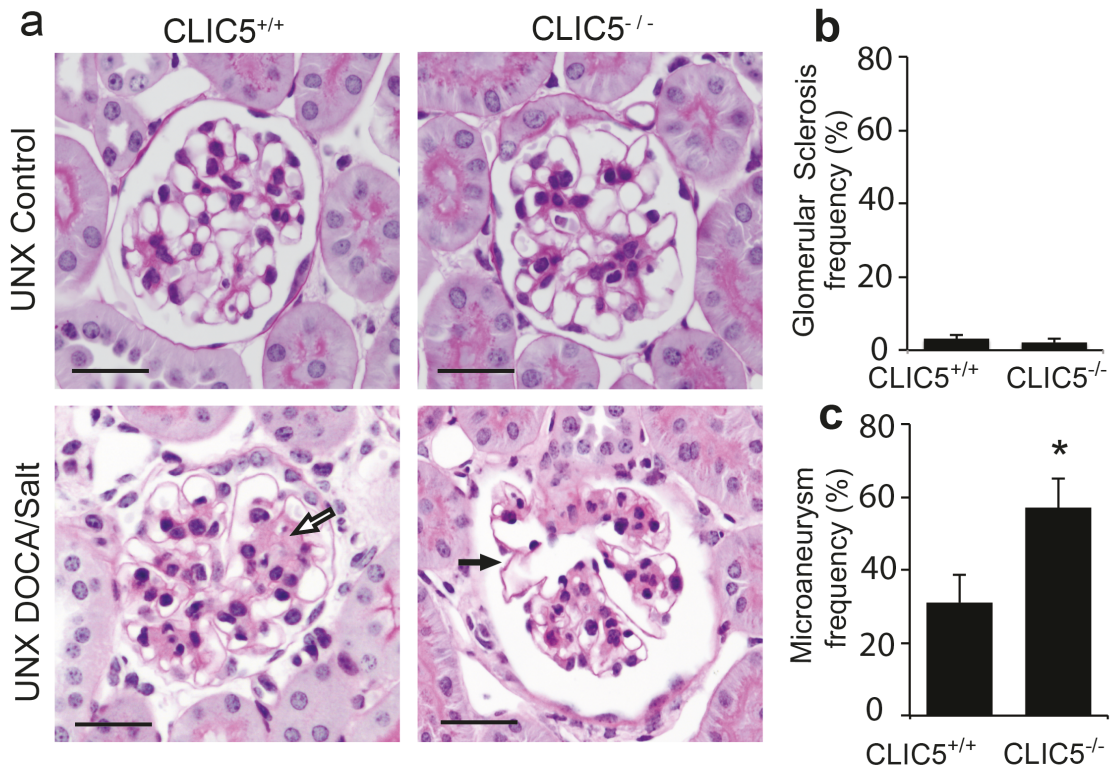


Figure 3.12 | Greater glomerular injury in hypertensive UN_x-DOCA/Salt CLIC5^{-/-} mice. (a) PAS-stained glomeruli from perfusion-fixed UN_x- and UN_x-DOCA/Salt treated CLIC5^{+/+} and CLIC5^{-/-} mice (scale bar = 25 μm). Glomerular microaneurysms (black arrow), mesangial expansion (white arrow) and occasional total glomerulosclerosis (Not shown) were observed in UN_x-DOCA/Salt CLIC5^{+/+} and CLIC5^{-/-} mice, but not in their UN_x controls. (b, c) Quantification (blind to genotype and treatment group), of glomerular sclerosis (b) and microaneurysms (c).

Figure 3.13

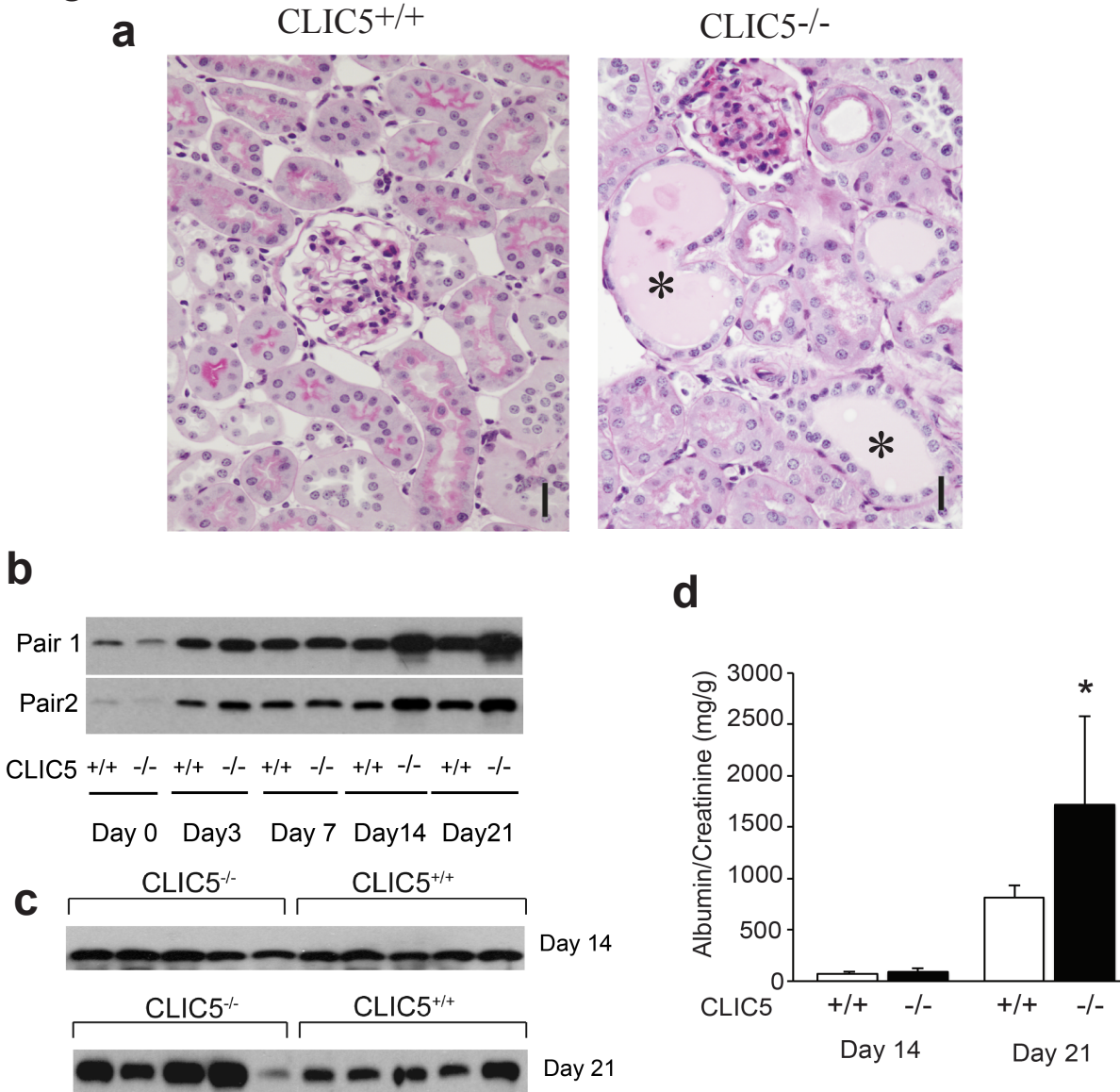


Figure 3.13 | Development of urine albumin-to-creatinine ratio as a function of time in DOCA/Salt. (a) Representative PAS-stained kidney cortex from UNx-DOCA/Salt treated CLIC5^{+/+} and CLIC5^{-/-} mice (scale bar = 20 μ m). Proteinaceous casts in dilated proximal tubules (asterisks) were observed in UNx-DOCA/Salt CLIC5^{-/-}, but not in UNx-DOCA/Salt CLIC5^{+/+} mice. Similar results were obtained in 4 additional mice in each group. (b) Western blot of mice urine from two pairs of CLIC5^{+/+} and CLIC5^{-/-} mice 0, 3, 7, 14 and 21 days after initiation of DOCA/Salt. The equivalent of 0.25 μ l of urine (20 mg/dl creatinine) was loaded per lane. (c) Western blot of mouse urine 2 and 3 weeks after initiation of DOCA/Salt treatment. Each lane represents urine from a separate mouse. The equivalent of 0.25 μ l of urine (20 mg/dl creatinine) was loaded per lane. (d) Albumin:Creatinine ratio (ACR) on days 14 and 21 after initiation of DOCA/Salt treatment. (Mean \pm SD; n=5/group, *p < 0.05 vs. control UNx-DOCA/Salt CLIC5^{+/+} mice).

Figure 3.14

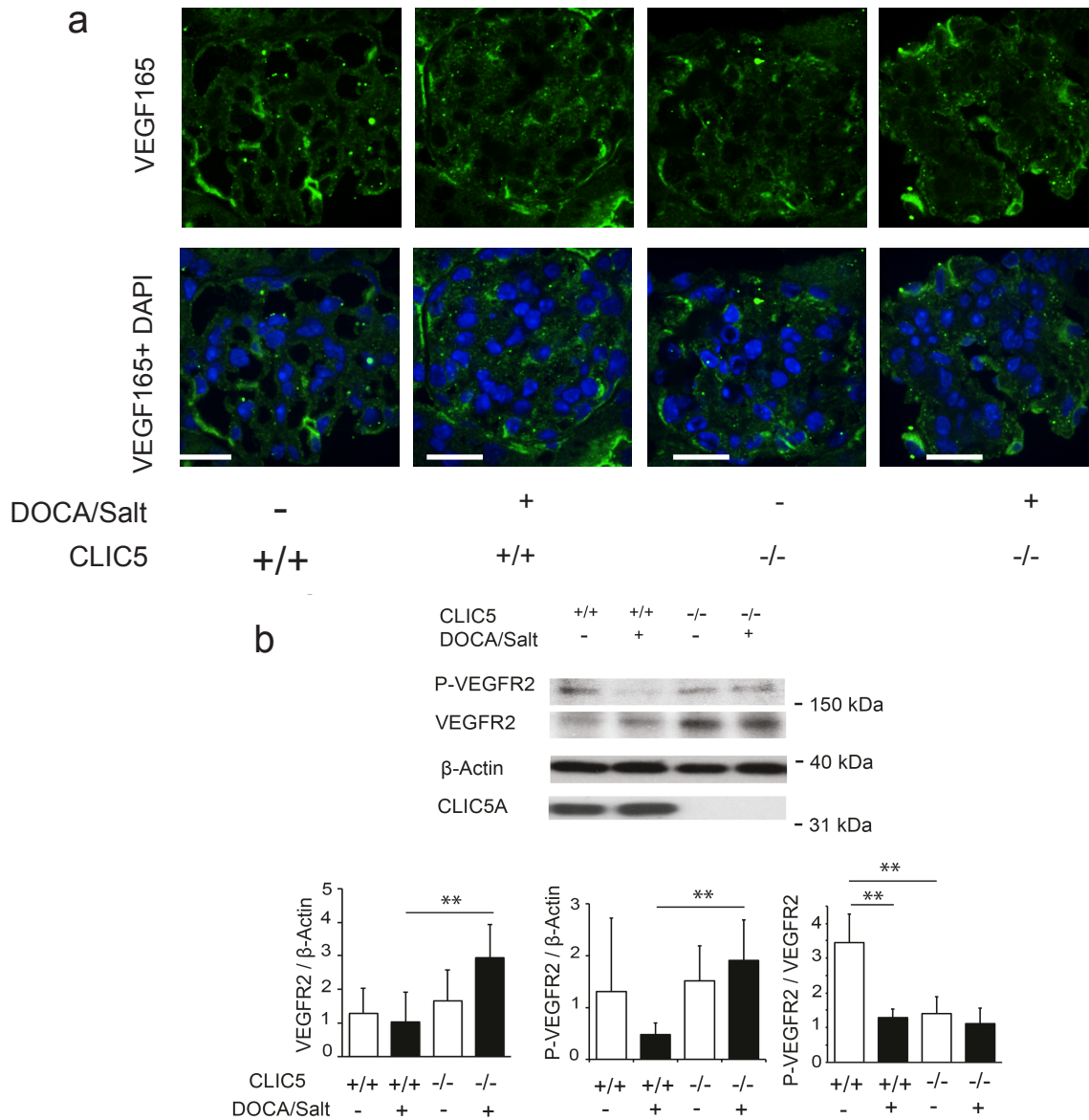


Figure 3.14 | VEGF signaling in glomeruli of uninephrectomized (UNx)-deoxycorticosterone acetate (DOCA)/salt and UNx control chloride intracellular channel 5A (CLIC5)^{+/+} and CLIC5^{-/-} mice. (a) Confocal IF microscopy for VEGF165 in TCA-fixed renal cortex from UNx control and UNx-DOCA/Salt treated CLIC5^{+/+} and CLIC5^{-/-} mice. VEGF protein expression was similar among all the 4 groups. (Representative of 3 mice per group. For each mouse at least 5 glomeruli were photographed with similar results, scale bar = 10 μ m). Representative WB of isolated glomeruli from UNx Control CLIC5^{+/+} and CLIC5^{-/-} mice probed with anti-VEGFR2, anti-P-VEGFR2, CLIC5A anti- β -actin. Each lane represents isolated glomeruli from a distinct mouse. (c) Quantification of P-VEGFR2 abundance relative to β -actin. (d) P-VEGFR2 abundance relative to β -actin and P-VEGFR2 abundance relative to VEGFR2 (Mean \pm SD; n = 3 mice per group, *P < 0.05).

Figure 3.15

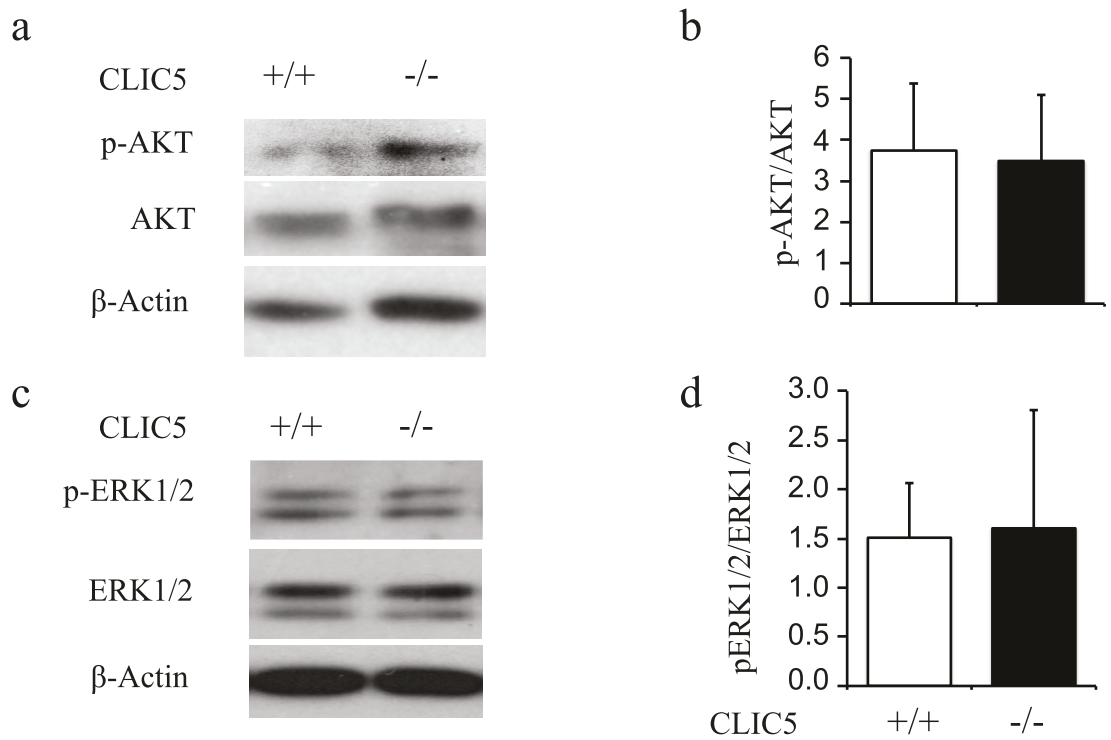


Figure 3.15 | AKT and ERK1/2 phosphorylation in glomeruli of uninephrectomized (UNx)-control chloride intracellular channel 5 (CLIC5)^{+/+} and CLIC5^{-/-} mice. (a). Representative WB of isolated glomeruli from UNx Control CLIC5^{+/+} and CLIC5^{-/-} mice probed with anti-p-AKT, anti-AKT and anti-β-actin. Each lane represents isolated glomeruli from a distinct mouse. (b). Quantification of p-AKT abundance relative to AKT (Mean ± SD; n = 3 mice per group, *P < 0.05). (c). Representative WB of isolated glomeruli from UNx Control CLIC5^{+/+} and CLIC5^{-/-} mice probed with anti-p-ERK1/2, anti-ERK1/2 and anti-β-actin. Each lane represents isolated glomeruli from a distinct mouse. (d). Quantification of p-ERK1/2 abundance relative to ERK1/2 (Mean ± SD; n = 3 mice per group, *P < 0.05).

Figure 3.16

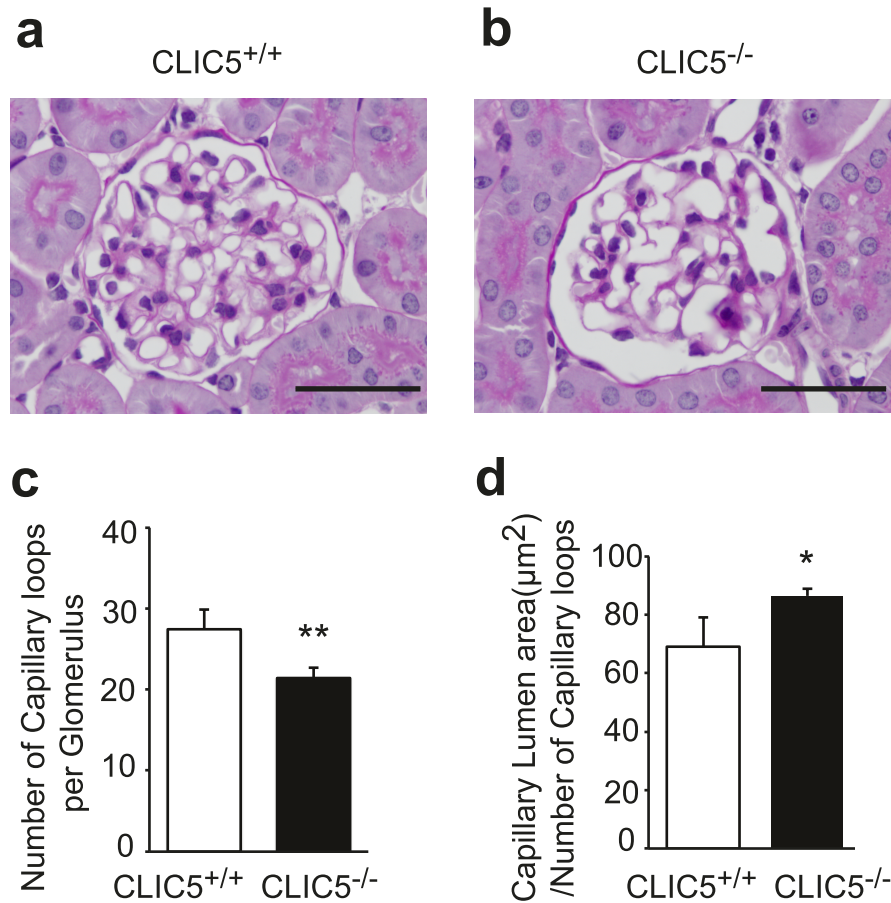


Figure3.16 | CLIC5 deficiency leads to expansion of capillary lumen in mice. (a-b) Representative glomeruli from CLIC5^{+/+} and CLIC5^{-/-} mice by light microscopy (periodic acid-Schiff staining of perfusion fixed kidneys at X100 magnification; scale bar 25 μ m). (c) Quantification of the number of capillary loops in CLIC5^{+/+} and CLIC5^{-/-} mice glomeruli . (d) Quantification of the capillary Lumen area relative to the number of capillary loops. Morphological analysis shows that there are fewer capillary loops in CLIC5^{-/-} mice (c) but the diameter of each capillary loop is increased (d). Statistical analysis was by t-test. . **P<0.01 *P<0.05.

Figure 3.17

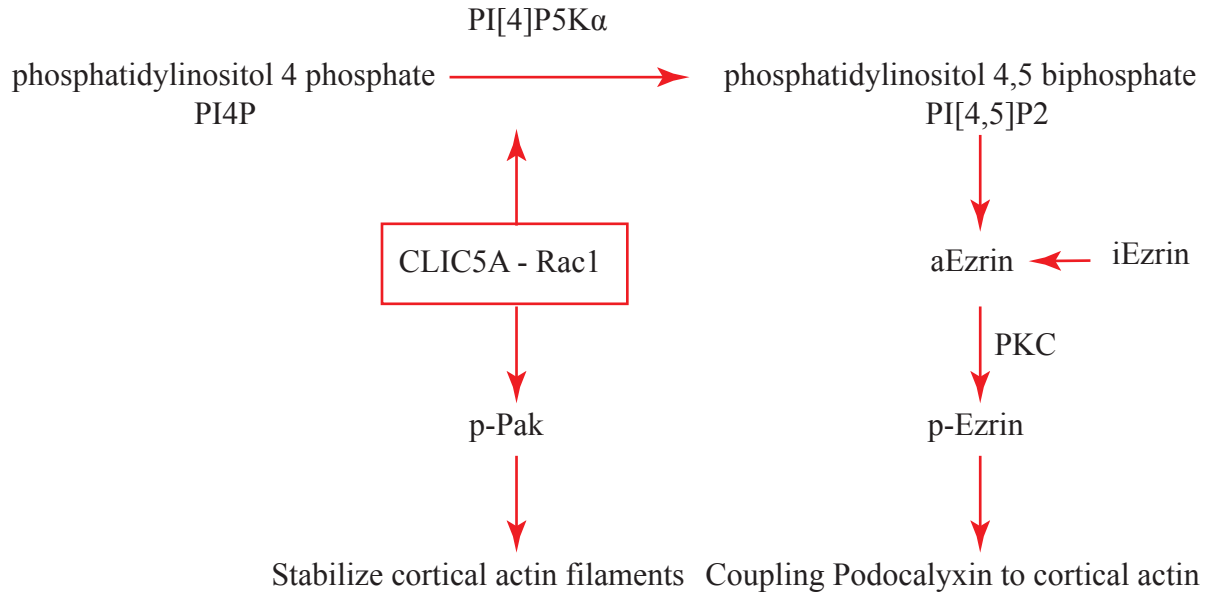


Figure 3.17 | Model of CLIC5A-Rac1 action in podocytes. CLIC5A interacts with Rac1 to stimulate PI[4,5]P2 generation at the plasma membrane which binds the N-terminal domain of ezrin, inducing a conformational change from inactive ezrin (iEzrin) to active ezrin (aEzrin). This allows the ezrin N-terminus to interact with podocalyxin and NHERF-2, and the C-terminus to bind F-actin and to be phosphorylated. CLIC5A/Rac1 furthermore activate Pak1,3 which stabilize F-actin.

Table 3.1 | Bodey, heart, and kidney weights in UNx and UNx-DOCA/salt CLIC5^{+/+} and CLIC5^{-/-} mice.

Treatment group	n	Day 0	Day 20	Day 20	Day 20
		Body weight (g)	Body weight (g)	Kidney weight (g/mm)	Heart weight (g/mm)
UNx CLIC5 ^{+/+}	8	24.2 ± 1.8	24.7 ± 1.8	8.2 ± 0.2	5.5 ± 0.8
UNx-DOCA/salt CLIC5 ^{+/+}	8	24.7 ± 2.2	23.8 ± 1.9	12.7 ± 0.5	7.1 ± 0.9 ^b
UNx CLIC5 ^{-/-}	8	21.1 ± 1.3 ^a	21.7 ± 1.2 ^a	8.3 ± 0.6	5.5 ± 0.3
UNx-DOCA/salt CLIC5 ^{-/-}	7	20.7 ± 1.8 ^a	21.1 ± 1.9 ^a	13.4 ± 1.3 ^b	7.1 ± 1.1 ^b

Kidney and heart weights are expressed in g/mm tibial lengthh.

UNx, uninephrectomized; CLIC5, chloride intracellular channel 5;

DOCA, deoxycorticostrone acetate.

^ap < 0.01 CLIC5^{-/-} versus CLIC5^{+/+} in the same treatment group

^bp < 0.001 UNx versus UNX-DOCA/salt in the same genotype.

Table 3.2 | Serum Electrolytes and Glucose concentrations in CLIC5^{+/+} and CLIC5^{-/-} mice before, and 20 days after initiation of DOCA/Salt treatment

Serum component mmol/L	CLIC5 ^{+/+}		CLIC5 ^{-/-}	
	Baseline	DOCA/salt	Baseline	DOCA/salt
Na ⁺	147.5 ± 1.4	155.9 ± 1.9 ^a	150.5 ± 4.3 ^b	155.5 ± 0.6 ^c
K ⁺	8.4 ± 0.6	5.5 ± 0.9 ^a	8.8 ± 0.6	6.9 ± 2 ^c
Cl ⁻	117.4 ± 3.1	113.1 ± 5.1 ^c	124.9 ± 4.1 ^b	110.2 ± 2.4 ^a
Total CO2	18.4 ± 3.1	28.6 ± 3.2 ^a	17.4 ± 1.3	31 ± 3.4 ^a
Glucose	11.6 ± 1.3	8.9 ± 0.6 ^c	9.2 ± 1.0 ^b	8.9 ± 2.3
Creatinine	20.9 ± 4.5	31.9 ± 8.7 ^a	24.3 ± 7.6	33.5 ± 6.0 ^c

Data are given as mean ± SD

^a P < 0.01 versus baseline in the same genotype.

^b P < 0.01 versus CLIC5^{+/+} at baseline.

^c P<0.05 (1 way analysis of variance with post hoc Tukey test)

Chapter 4

Both CLIC4 and CLIC5A Activate ERM Proteins in Glomerular Endothelium

Chapter4

Both CLIC4 and CLIC5A activate ERM Proteins in Glomerular Endothelium¹

4.1 Introduction

Functional specificity of differentiated cells generally requires an appropriate, and often dynamically regulated cellular architecture. For instance, renal glomerular capillary endothelial cells (EC) are extraordinarily flattened at the periphery of glomerular capillary loops and contain thousands of trans-cellular fenestrae [322], and glomerular podocytes extend primary actin-based projections and secondary foot processes around the exterior of glomerular capillary loops [256]. These characteristic features of glomerular EC and podocytes serve the function of rapid, permselective glomerular filtration. Loss of fenestrae, for example in preeclampsia [323], thrombotic microangiopathies [324] and diabetic nephropathy [38] is associated with a reduction in the glomerular filtration rate [257]. Effacement of foot processes, for instance in minimal change disease [325] and focal segmental glomerulosclerosis [326] markedly reduces the efficacy of glomerular capillary permselectivity [327].

¹Portions of this chapter has been submitted in a peer-reviewed journal:

Mahtab Tavasoli, Abass Al-Momany, Xin Wang, M, Laiji Li, John C. Edwards and Barbara J. Ballermann. *Both CLIC4 and CLIC5A Activate ERM Proteins in Glomerular Endothelium*.

Physiol Am. J. Physiol., Renal Physiology 2016.

Cellular architecture depends, in large part, on the organization of the actin cytoskeleton. Cortical actin is linked to several membrane-spanning proteins and phosphatidylinositol 4,5 bisphosphate (PI[4,5]P₂) by activated ERM (ezrin, radixin, moesin) proteins [328]. In their inactive conformation, ERM proteins are soluble and cannot interact with transmembrane proteins and actin due to intra-molecular interactions between the ERM N- and C-termini. Engagement of their N-terminal FERM (4.1 protein, ezrin, radixin, moesin) domain with PI[4,5]P₂ in the lipid bilayer produces an activating conformational change that then allows binding of the ERM C-terminus to polymerized actin and association with the cytoplasmic domain of membrane-spanning proteins either directly, or indirectly through EBP50 (ezrin binding protein 50) also known as NHERF-1 (sodium-hydrogen exchanger regulatory factor-1) or its homolog E3KARP (Exchanger Type 3 Kinase A Regulatory Protein, NHERF-2). Phosphorylation of a highly conserved C-terminal Thr residue, usually by protein kinase C or ROCK (Rho associated kinase) stabilizes this interaction [328].

In podocytes, ezrin is the predominant ERM protein where it localizes to the apical plasma membrane of foot processes, away from the filtration slit diaphragm [58], and forms a complex with NHERF2 and the cytoplasmic tail of podocalyxin [247]. Podocyte foot process effacement is associated with disruption of the ezrin-NHERF2-podocalyxin complex and ezrin dephosphorylation [58].

In endothelial cells, moesin is the predominant ERM protein [329]. Moesin is required for the formation of blood vessel lumens [330, 331], EC filopodia [332] and the EC docking structure for the transmigration of leukocytes [333].

Evidence is emerging that members of the CLIC family of proteins play a critical role in controlling ERM protein function [282]. Six mammalian CLIC genes (CLIC1-6) produce this family of highly conserved proteins, most with a molecular mass in the 25-32 kDa range, although CLIC5B, one of two CLIC5 isoforms, and CLIC6 are larger with extended N-termini. The first CLIC protein, p64 (CLIC5B), was purified from kidney microsomes using immobilized IAA-94, a nonselective Cl⁻ channel inhibitor, and was found to have Cl⁻ channel activity when reconstituted into phospholipid vesicles [279, 334]. Since then, CLIC1, CLIC4, and CLIC5A have all been shown to impart ion conductances to artificial lipid bilayers [215]. CLIC4 participates in vacuolar acidification and tubulogenesis in EC [236], and CLIC1 plays a role in phagocytosis and phagosomal acidification in macrophages [216]. CLIC4 is associated with mitochondria [335, 336] and can translocate to the nucleus [203, 337]; CLIC1 associates with phagosomes in macrophages [216], CLIC2 associates with ryanodine receptors in the cardiac myocyte endoplasmic reticulum [338, 339], and CLIC5B was found in the Golgi [206]. Because CLIC proteins can associate with various intracellular organelles and Cl⁻ ion conductances in lipid bilayers, they received the name chloride intracellular channel. However, whether they can indeed form true transmembrane channels with selective ion conducting pores has not been shown to date [212].

In vivo, both CLIC4 [229, 340] and CLIC5A [4] interact with cytoskeletal proteins at or near the plasma membrane [4, 182, 183, 229, 316] there also is substantial evidence that CLIC proteins co-localize with, and regulate the ERM-dependent formation of cellular projections. For example, CLIC5A was initially purified from placental microvilli in a complex with ezrin and other cytoskeletal proteins [182], and its overexpression induces the formation of apical projections [4, 242]. In glomerular podocytes in vivo, CLIC5A co-localizes with ezrin at the

apical plasma membrane of foot processes [5], and in inner ear sensory hair cells, it co-localizes with radixin [183, 280]. CLIC4 is found in the proximal tubule brush border [181, 229, 341] and in microvilli of retinal epithelial cells, where it co-localizes with ezrin [231]. In retinal epithelial cells, CLIC4 silencing reduces the formation of apical microvilli, similar to the effect of ezrin deletion [342]. Deletion of CLIC5A leads to deafness and degeneration of actin-based stereocilia in cochlear hair cells [183], abnormalities that are also observed in radixin deficient mice [178]. Similarly, in *C. elegans* the CLIC homolog EXC-4 localizes to the apical plasma membrane of the excretory canal and its deletion leads to abnormal development of this structure [321], a phenotype similar to that observed when ERM-1 is deleted in *C. elegans* [343, 344]. Thus, some CLIC proteins co-localize with, and seem to mimic the function of ERM proteins.

We originally observed that the transcript DKFZp564B076, which is an EST (expressed sequence tag) of CLIC5A is enriched in cultured bovine glomerular EC relative to aortic EC and in glomeruli in vivo [345]. We subsequently showed that the CLIC5 mRNA is enriched ~800 fold in human glomeruli, when compared to other tissues and cells [3]. The glomerular CLIC5 transcript encodes the CLIC5A isoform, co-localizes exquisitely with ezrin, and localizes prominently to the apical domain of podocyte foot processes and the fenestrated region of glomerular EC[5]. In mice lacking CLIC5, glomerular ezrin and podocalyxin abundance is reduced, and podocyte foot processes are fewer in number, broader and shorter than those in wild-type mice [5, 123]. In glomerular EC, we observed a larger number of vacuoles in CLIC deficient, compared to in wild-type mice, but glomerular EC fenestrae were normal. The CLIC5 deficient mice have very mild proteinuria at baseline, but they are more susceptible to glomerular injury induced by Adriamycin [5] and DOCA/Salt hypertension [122]. In regard to the interaction with ERM proteins, we find that CLIC5A activates ezrin and moesin phosphorylation

and their association with the actin cytoskeleton through a Rac1-dependent accumulation of PI[4,5]P₂ clusters at the apical plasma membrane [122]; Hence, CLIC5A acts upstream of ERM protein activation, through enhanced formation of plasma membrane PI4,5P₂ clusters. However, despite the fact the CLIC5A is expressed in glomerular EC in vivo, in CLIC5 deficient mice ERM phosphorylation is reduced in podocytes, but not in glomerular EC [4, 5].

CLIC4 expressed much more ubiquitously than CLIC5A. In vivo, CLIC4 expression is observed in all EC, and in the kidney it is prominently expressed in proximal tubule epithelial cells [341]. CLIC4 expression is induced by TGF-β1 in myofibroblasts [346], and TGF-β1 stimulates CLIC4 relocation to the nucleus [337]. CLIC4 is involved in hollowing of EC during the formation of blood vessel lumens [236]. In CLIC4 deficient mice, capillary density, and the formation of collateral blood vessels in response to ischemia are reduced [240, 241]. Kidneys of CLIC4 deficient mice develop fewer glomeruli and peritubular capillaries than wild-type controls, but the ultrastructure of glomerular EC appears normal [241]. In proximal tubule epithelial cells, CLIC4 appears to be involved in the formation of the tubule lumen and apical microvilli, through an effect on actin-dependent endosome function [229].

Since the formation of EC and epithelial cell lumens requires ERM proteins and CLIC4, this study addressed the question whether CLIC4, like CLIC5A functions upstream of ERM activation in glomerular EC, and whether it can functionally substitute for CLIC5A. In cultured human glomerular EC, we observe that CLIC4 silencing reduces ERM phosphorylation, an effect that is rescued by CLIC4 or CLIC5A overexpression. When CLIC4 or CLIC5A were deleted singly in mice, ERM phosphorylation in glomerular EC persisted but in mice lacking both CLIC4 and CLIC5A, the abundance of phosphorylated ERM protein in glomerular EC was dramatically reduced. While the glomerular EC fenestrae were initially normal in density, there

was a progressive loss of fenestrae, accumulation of sub-endothelial electron-lucent material, mesangial expansion and spontaneous development of proteinuria in dual CLIC4/CLIC5 deficient mice. The observations indicate that both CLIC5A and CLIC4 act on mechanisms upstream of ERM phosphorylation, and suggest that they are important in the long-term maintenance of glomerular EC structure and function.

4.2 Results:

4.2.1 Increased glomerular endothelial cell CLIC4 abundance in CLIC5 deficient mice

We previously reported that CLIC5A is expressed in glomerular EC and podocytes [5], but found that deletion of CLIC5 reduced ezrin activation and function only in podocytes [4, 5, 122]. We therefore asked whether CLIC4, which is highly homologous with CLIC5 [182] and is expressed in EC [238, 240, 341], could compensate for the absence of CLIC5A in glomerular EC of CLIC5 deficient mice. We observed that the abundance of CLIC4 was significantly higher in glomerular lysates from CLIC5 deficient mice, compared to wild-type mice (Figure 4.1 a,b), and that CLIC4 co-localized strongly with PECAM-1, but not with podocin (Figure 4.1 c) in glomeruli of these mice. The data suggest that if CLIC4 can regulate ERM proteins, its expression could potentially compensate for the absence of CLIC5A in glomerular EC, but not in podocytes.

4.2.2 CLIC4 co-localizes with moesin and ezrin in glomeruli, and CLIC4 deletion results in reduced ERM protein abundance in glomerular capillaries.

To probe the relationship between CLIC4 and ERM proteins, we next determined whether CLIC4 co-localizes with moesin, the predominant ERM protein in EC [329], and/or with ezrin in glomerular EC. For dual-label IF studies we used either CLIC5 or CLIC4 deficient mice in order to eliminate potential cross-reactivity of anti-CLIC5A and anti-CLIC4 antibodies with CLIC4 and CLIC5A, respectively. CLIC4 strongly co-localized with moesin and ezrin (Figure 4.2 a) in a capillary loop pattern in glomeruli of CLIC5 deficient mice. The fact that ezrin is observed primarily in a glomerular capillary loop pattern in these mice (Figure 4.2 a) is due to the absence of CLIC5A, required to retain ezrin expression in podocytes [5]. In

glomeruli of CLIC4 deficient mice, ezrin immunoreactivity was more widely distributed and co-localized with CLIC5A (Figure 4.2 b), consistent with CLIC5A and ezrin expression in podocytes and glomerular EC. In the CLIC4 deficient mice, moesin immunoreactivity co-localized with CLIC5A only in a capillary pattern (Figure 4.2 b). These findings indicate that moesin is the predominant ERM protein in glomerular capillary endothelium, where it co-localizes with both, CLIC4 (Figure 4.2 a) and CLIC5A (Figure 4.2 b). By contrast, ezrin and CLIC5A are also observed in moesin-negative glomerular cells (Figure 4.2 b), consistent with previous observations of abundant CLIC5A expression in podocytes [5, 123]. In glomerular lysates from CLIC4 deficient mice, the abundance of total and p-ERM proteins was significantly lower than in wild-type mice (Figure 2 c), similar to previous findings of a reduced glomerular ERM protein abundance in CLIC5 deficient mice [4]. In glomeruli of CLIC4 deficient mice, this reduction in p-ERM was accounted for by reduced total ERM protein.

4.2.3 CLIC4 co-localizes with moesin and ezrin in proximal tubule brush border, and CLIC4 deletion results in reduced ERM protein association with the renal cortical cytoskeletal fraction.

CLIC4 also co-localized with moesin (Figure 4.3 a) and ezrin (Figure 4.3 b) in proximal tubule brush border and was observed in peri-tubular endothelium (Figure 4.3 c) consistent with previous findings [229, 341]. To detect the cytoskeletal association of the ERM proteins, lysates of kidney cortex were separated into Triton X-100 soluble and insoluble fractions (Figure 4.3 d). Association of ezrin and moesin with the insoluble cytoskeletal fraction was markedly reduced in CLIC4 deficient, compared to wild-type mice, while total ezrin and moesin abundance in the soluble fraction and in total kidney cortex lysates did not differ between CLIC4 deficient and wild-type mice (Figure 4.3 d). These findings suggest that CLIC4 is required for actin-

association of ezrin and moesin in the kidney, presumably in both endothelial and proximal tubule epithelial cells. Markedly abnormal proximal tubule microvilli and expansion of proximal tubule vacuoles was observed (Figure 4.4), consistent with previously reported findings by Chou et al. [229].

4.2.4 Reduced ERM protein activation in cultured glomerular EC upon CLIC4 silencing.

We next evaluated whether CLIC4 can regulate ERM protein phosphorylation in cultured glomerular EC. Both moesin and ezrin were observed on WB of glomerular EC lysates. However, moesin was the predominant ERM isoform detected with pan-ERM (ERM) and pan-p-ERM (p-ERM) antibodies (Figure 4.5 a). The CLIC4 protein was expressed in glomerular EC (Figure 4.5 b), and its expression was substantially reduced in cells transfected with CLIC4-specific siRNA, compared to EC cells with control siRNA (Figure 4.5 b). Silencing of CLIC4 resulted in a significant reduction of ERM protein phosphorylation, without change in total ERM protein abundance (Figure 4.5 b). Since the active, phosphorylated form of ERM proteins associates with the actin cytoskeleton [266, 328], we next determined whether CLIC4 silencing would reduce ERM protein in the cytoskeletal fraction of glomerular EC. Compared with cells treated with control siRNA, significantly less ERM protein was associated with the cytoskeletal fraction, after CLIC4 silencing (Figure 4.5 c). Unlike previous observations for CLIC5A [4], very little CLIC4 was observed in the glomerular EC cytoskeletal fraction (Figure 4.5 c). The effect of CLIC4 silencing on ERM phosphorylation in glomerular EC cells was rescued by overexpressed CLIC4 (Figure 4.6 a).

4.2.5 Reduced ERM phosphorylation by CLIC4 silencing is rescued with overexpressed CLIC5A.

Since both CLIC5A and CLIC4 are expressed in glomerular EC in vivo [4] (Figures 4.1,

4.2), we next determined whether CLIC5A also alters ERM protein phosphorylation in cultured glomerular EC and whether CLIC5A rescues the phosphorylation of ERM proteins after CLIC4 silencing. To overexpress CLIC5A, we utilized an adenoviral vector previously described [122] which expresses wild-type CLIC5A and GFP from separate promoters. The control virus expresses only GFP. In glomerular EC, a single experiment showed an MOI-dependent increase in CLIC5A expression (Figure 4.6 c) and an associated increase in ERM phosphorylation. CLIC5A also rescued ERM phosphorylation in glomerular EC in which CLIC4 had been silenced (Figure 4.6 d). Hence, both CLIC4 and CLIC5A induce the phosphorylation of moesin and ezrin in cultured glomerular EC, indicating that they can functionally substitute for one-another in glomerular EC, at least in regard to ERM phosphorylation.

4.2.6 Defective ERM protein phosphorylation in dual CLIC4/CLIC5 deficient mice.

We next determined whether dual knockout of CLIC4 and CLIC5 reduces ERM phosphorylation in glomerular EC in vivo. The dual CLIC4^{-/-}/CLIC5^{-/-} mice were viable and the expected Mendelian ratio of offspring was observed. Dual label immunofluorescence studies for PECAM-1 and p-ERM revealed that glomerular ERM phosphorylation was reduced in mice deficient in CLIC4 or CLIC5 (Figure 4.7 a), but some p-ERM was retained in PECAM-1 positive glomerular EC in CLIC4^{-/-} and in CLIC5^{-/-} mice. By contrast, in mice lacking both CLIC4 and CLIC5, there was a profound reduction in glomerular p-ERM immunoreactivity relative to the wild-type or CLIC4^{+/+}/CLIC5^{-/-} and CLIC4^{-/-}/CLIC5^{+/+} mice (Figure 4.7 a). In total renal cortex lysates, overall ERM protein abundance did not differ between CLIC4^{+/+}/CLIC5^{+/+}, CLIC4^{-/-}/CLIC5^{+/+}, CLIC4^{+/+}/CLIC5^{-/-} or CLIC4^{-/-}/CLIC5^{-/-} mice, however phosphorylation of ERM proteins was markedly reduced in when CLIC4, CLIC5 or both were lacking (Figure 4.8 a-d). These data are interpreted to indicate that both CLIC4 and CLIC5

regulate ERM protein phosphorylation in vivo, and that both CLIC4 and CLIC5 activate ERM phosphorylation in glomerular EC in vivo, whereas only CLIC5 seems to be active in glomerular podocytes.

4.2.7 Ultrastructural abnormalities in glomerular endothelial cells of dual CLIC4/CLIC5 deficient mice.

Previous work had shown that deletion of only CLIC5 [5, 123] or CLIC4 [241] has no apparent effect on glomerular capillary EC fenestrae density, although glomerular EC fenestrae density declines in CLIC5 deficient mice 3 weeks after initiation of DOCA/Salt hypertension, along with the loss of glomerular EC ERM phosphorylation [122]. We therefore determined whether dual CLIC4/CLIC5 deletion alters the density of glomerular EC fenestrae. In young (~2-month old mice), glomerular EC fenestrae density was essentially identical in wild-type and dual CLIC4/CLIC5 deficient mice (Figure 4.9 a,b). However, in older (~8 month-old) mice, there was a marked reduction in glomerular EC fenestrae along with the accumulation of subendothelial electron-lucent material (Figure 4.9 c,d). Glomerular EC fenestrae density was lower in CLIC4^{-/-}/CLIC5^{+/+} and was significantly lower in CLIC4^{-/-}/CLIC5^{-/-} compared to age-matched CLIC4^{+/+}/CLIC5^{+/+} mice at 8 months of age (Figure 4.10 a,b). In addition, we observed the spontaneous development of mesangial hypercellularity (Figure 4.11 a), mesangial matrix deposition and loss of capillary lumens (Figure 4.11 b) in 8-month old mice lacking both CLIC4 and CLIC5, abnormalities that were accompanied by significant proteinuria in CLIC4^{-/-}/CLIC5^{-/-} mice (Figure 4.11 c,d).

4.3 Discussion:

The CLIC5A isoform of CLIC5, which is highly enriched in renal glomeruli relative to most other tissues and cells, activates ERM proteins by increasing the density of apical plasma membrane PI[4,5]P₂ clusters [4], the docking sites for ERM protein activation. In glomeruli, CLIC5A is found in podocytes and in glomerular capillary EC [5], but global deletion of CLIC5 alters only the podocyte ultrastructure, without discernible effect on glomerular capillary EC structure or function. Similarly, the CLIC5A homolog CLIC4 is expressed at high levels in glomerular capillary EC in vivo, as well as proximal tubule epithelial cells, but while global deletion of CLIC4 disrupts the proximal tubule brush border [229] it has no obvious effect on glomerular capillary EC ultrastructure [241]. These findings raise the question whether CLIC4 and CLIC5A have redundant functions in glomerular EC. We therefore sought to resolve whether CLIC4, like CLIC5A, regulates ERM protein activation, and whether CLIC4 and CLIC5A substitute for one-another in glomerular EC. In the present study we found that CLIC4 expression both in vivo and in cultured EC facilitates the activation of ERM proteins, that both CLIC4 and CLIC5A co-localize with ERM proteins in glomerular capillary EC in vivo, and that CLIC4 and CLIC5 can functionally substitute for one another in cultured glomerular EC in vitro and in glomerular capillary EC in vivo, at least in regard to ERM protein activation. Whereas mice lacking CLIC5 or CLIC4 do not develop spontaneous glomerular disease, dual deletion of both CLIC5 and CLIC4 leads to a progressive loss of glomerular EC fenestrae, mesangial proliferation and matrix deposition as well as albuminuria. These findings lead us to conclude that the CLIC proteins CLIC5A and CLIC4 and their downstream effects on ERM proteins are required for the maintenance of the normal glomerular capillary loop structure.

We previously demonstrated that CLIC5A stimulates ERM protein activation. CLIC5A interacts with PI4P5 kinases to facilitate the localized accumulation of PI[4,5]P₂ clusters in the cytosolic leaflet of the apical plasma membrane [4]. Activation of ERM proteins, which are otherwise auto-inhibited due to intra-molecular interactions between the N- and C-termini, requires binding of the ERM N-terminus to PI[4,5]P₂, resulting in a conformational change that then allows the ERM C-terminus to bind actin and to be phosphorylated on a highly conserved C-terminal Thr residue [266]. Activated ERM proteins, in turn, regulate the architecture of the cell cortex by linking sub-plasma membrane actin to integral membrane proteins [328]. At the apical domain of podocyte foot processes ezrin, together with NHERF2, forms a bridge between the cytoplasmic tail of podocalyxin and polymerized cortical actin [58, 247]. We showed that formation of this complex requires CLIC5A expression in podocytes[4]. Although several other CLIC proteins similarly co-localize with ERM proteins, and their deletion can functionally mimic deletion of ERM proteins [282], activation of the ERMs by CLICs other than CLIC5A has not been reported so far. In this study, we now find that silencing of CLIC4 in cultured glomerular EC indeed results in a significant reduction of ERM protein phosphorylation and markedly reduced ERM protein association with the cytoskeletal fraction (Figure 4.5), an effect that is rescued by CLIC4 and CLIC5A overexpression. Similar to our previous findings for CLIC5A, this effect of CLIC4 is abrogated when PI[4,5]P₂ is depleted (data not shown). We observe that CLIC4 co-localizes with ERM proteins in glomerular and peritubular EC and in the proximal tubule epithelial cell brush border (Figures 4.2 & 4.3), and that CLIC4 deletion results in a substantial reduction of cytoskeleton-associated ERM proteins (Figure 4.3). These findings lead us to conclude that CLIC4, like CLIC5A functions upstream of ERM protein activation.

Whereas CLIC4 is widely expressed *in vivo*, CLIC5A expression is much more restricted with very high levels in renal glomeruli [3]. While there is little doubt about CLIC5A protein expression and function in podocytes [4, 5, 122, 123], the findings that CLIC5 deletion altered ERM phosphorylation only in podocytes [5] and not in glomerular EC, raised the question whether CLIC5A immunoreactivity in glomerular capillary EC *in vivo* could actually represent cross-reactivity with the highly homologous CLIC4, given that anti-CLIC4 and anti-CLIC5A antibodies are not completely specific. For this reason, we evaluated the distribution of CLIC5A in CLIC4 deficient mice, and found that CLIC5A is indeed expressed in a capillary pattern in renal glomeruli where it strongly co-localizes with moesin (Figure 4.2 b). This finding is consistent with our previous observation that CLIC5A localizes to glomerular capillary EC in human, bovine and mouse kidney [5], and with the findings that CLIC5A mRNA is enriched approximately 30-fold in glomerular EC relative to aortic EC in culture [345]. In this study, deletion of CLIC4 as well as CLIC5 in mice resulted in a nearly complete loss of phosphorylated ERM proteins in glomerular capillary EC (Figure 6), indicating that both, CLIC5A and CLIC4 stimulate ERM phosphorylation in these cells *in vivo*.

In cultured glomerular EC, we find that CLIC4 and CLIC5A increase the fraction of ERM proteins in the phosphorylated state and their association with the cytoskeletal fraction, without changing total ERM protein abundance (Figure 4.7). Similarly, in renal cortical lysates from CLIC4, CLIC5 or dual CLIC4/CLIC5 deficient mice, the fraction of the total ERM protein pool that is phosphorylated and cytoskeleton-associated is dramatically reduced (Figure 4.8), all consistent with a role for both CLIC4 and CLIC5A in ERM protein activation and association with the cytoskeleton. However, in glomerular lysates, CLIC4 deletion resulted in a reduction of total ERM protein, without changing the ratio of p-ERM: ERM (Figure 4.2 c). This is similar to

our finding of a reduction in total ezrin in lysates prepared from isolated glomeruli of CLIC5 deficient mice [5]. It seems most likely that the reduction in total ERM proteins in glomeruli of mice lacking CLIC4 or CLIC5 is due to enhanced ERM protein degradation, given that dephosphorylated ezrin becomes unstable in cells [271]. Perhaps degradation of inactive ERM proteins occurs in glomeruli during the relatively lengthy isolation procedure, which differs from the collection of lysates from renal cortex and cultured cells. It is also possible that a reduction in total ERM proteins could not be detected in glomerular cortex lysates due to a greater contribution of ERM proteins from cells not expressing CLIC4 or CLIC5A in the tubular fraction. We considered whether ERM gene expression could be suppressed in glomeruli when CLIC5 is deleted, but found that at least in glomeruli of CLIC5 deficient mice, ezrin mRNA expression is, if anything, slightly higher than in wild-type mice (A. Al-Momany, Unpublished data). Nonetheless, the mechanisms that lead to changes in total moesin and ezrin abundance in glomerular EC and podocytes, respectively, will need further investigation.

That some CLICs can functionally substitute for one-another was previously reported. Both CLIC4 and CLIC1 are highly expressed in EC generally, and regulate EC proliferation, network formation and morphogenesis [5] and CLIC4 plays a major role in collateral blood vessel formation [240]. Whereas deletion of CLIC4 or CLIC1 singly [5] produces viable offspring, deletion of CLIC4 as well as CLIC1 results in embryos with angiogenic defects that fail to develop beyond embryonic day 9.5 [347] and attempts to create double knockdown HUVEC cell lines did not result in viable cell [348, 349]. During collateral blood vessel formation in response to hypoxia in CLIC4^{-/-} mice, CLIC1 is upregulated approximately 3-fold, potentially substituting for CLIC4, suggesting that CLIC1 may provide partial compensation for deficient CLIC4 expression [240]. Also, while the absence of CLIC4 at baseline does not result

in compensatory up-regulation of CLIC1 or CLIC5, acute folic acid mediated injury in the kidney leads to up-regulation of CLIC1 and sustained expression of CLIC5 in CLIC4^{+/+} mice but in CLIC4^{-/-} mice, acute folic acid injury causes a significant reduction in CLIC5 protein expression and unlike the wild type CLIC1 protein expression does not change in response to injury [241]. In the current study we also found that the abundance of CLIC4 increases in glomeruli of CLIC5 deficient mice (Figure 4.1). These observations suggest overlapping functions or crosstalk between the members of CLIC family of proteins.

Moesin is the predominant ERM protein in EC, whereas ezrin predominates in epithelial cells, including podocytes and proximal tubule cells. However, so far it seems that CLIC5A and CLIC4 do not display any specificity towards distinct ERM proteins. We previously found that CLIC5A stimulates the phosphorylation of both ezrin and moesin in COS7 cells, HEK293 cells and podocytes, in vitro [4], and in inner ear hair cells radixin is the likely target of CLIC5A [183, 280]. By western blot analysis, which can distinguish p-Ezrin from p-Moesin by size, we find that silencing of CLIC4 in cultured glomerular EC reduces phosphorylation of both, moesin and ezrin (Figure 4.5 b), even though moesin is the predominant ERM protein in these cells (Figure 4.5 a). Since anti-p-ERM antibodies do not distinguish between p-Ezrin and p-Moesin, whether CLIC4 or CLIC5A show specificity towards moesin or ezrin cannot be answered by IF studies. Nonetheless, we find that the phosphorylation of both ezrin and moesin in renal cortex lysates is reduced whether we delete CLIC4 or CLIC5, or both (Figure 4.8). We therefore conclude that CLIC4 and CLIC5A can alter the phosphorylation status of both, moesin and ezrin.

CLIC5A localizes predominantly to the apical plasma membrane where it is associated with actin-based cellular projections like microvilli [182], sensory stereocilia [183] and in

podocytes, with foot processes [5, 123], and deletion of CLIC5 disrupts the ultrastructure of podocyte foot processes and of cochlear hair cell stereocilia. Similarly, CLIC4 associates with the apical brush border of proximal tubule epithelial cells [229, 341] (Figure 4.3), and with apical microvilli of retinal epithelial cells [231]. In both cell types, deletion of CLIC4 disrupts the formation of apical microvilli [229, 231]. In the current study we also observe that CLIC4 deletion disrupts the apical brush border of proximal tubule epithelial cells (Figure 4.4). Since ERM proteins control the formation and maintenance of microvilli and other apical actin-based projections [328], it seems highly likely that the stimulation of ERM protein activation by CLIC4 and CLIC5A is a component of this mechanism. It is also evident from the work in this, and many other studies that distinct CLIC proteins are expressed in distinct cell types, and that they do not universally substitute for one-another. Here, we observe that the CLIC4 abundance increases in glomeruli of CLIC5 deficient mice, but its glomerular expression remains restricted to EC (Figure 4.1), indicating that CLIC4 may compensate for CLIC5 in glomerular EC, but not in podocytes. Also, CLIC5A does not appear to substitute for CLIC4 in proximal tubule epithelial cells (Figure 4.4). Thus, loss of only one CLIC protein, for instance CLIC5A in podocytes and inner ear hair cells, and CLIC4 in proximal tubule and retinal epithelial cells, can have significant consequences on the architecture of their apical actin-based projections, if another CLIC protein does not compensate, as is the case in glomerular capillary EC.

CLIC proteins often co-localize with ERM proteins in tissues and cells [282], but a direct interaction between CLIC and ERM proteins has not been demonstrated. Also, the subcellular location of CLIC proteins is not restricted to the plasma membrane but, as their name implies, they can associate with various intracellular organelles, including endocytic vesicles [229], mitochondria [336], and the nucleus [203]. Moreover, CLIC4 and CLIC1 can translocate from

cytosol to distinct subcellular locations in the cell, depending on specific extracellular stimuli [203, 216, 350]. ERM proteins are not universally found associated with the CLICs in these subcellular locations. Therefore, ERM protein activation probably represents only one of the downstream effects of CLICs. We previously found that CLIC5A stimulates the accumulation of PI[4,5]P₂ clusters in the plasma membrane through an interaction with PI[4,5]P₂-generating kinases, in turn facilitating ERM protein activation and actin-dependent cell surface remodeling [4]. Also, a yeast two-hybrid screen suggests a possible direct interaction between the C-terminal region of PI4P5K β and both CLIC1 and CLIC4 (<http://www.signaling-gateway.org>). Inositol phospholipids including PI[4,5]P₂ play specific functional roles not only in the plasma membrane, but also in subcellular locations, including mitochondria, endosomal vesicles and the nucleus [192]. These observations raise the intriguing possibility that CLIC-mediated activation of PI4P5 kinases could represent a general mechanism of action with downstream effects that include, but are not restricted to ERM protein activation.

CLIC proteins were named based on the initial purification of CLIC5B from kidney cortex by affinity for the Cl⁻ channel inhibitor IAA-94 [279, 334], the findings that CLIC5B and several CLIC proteins confer ion-conducting properties when re-constituted in artificial lipid bilayers [209, 215, 351], and that they are often associated with various intracellular organelles. However, CLIC proteins lack the typical hydrophobic membrane-spanning regions of ion channels and ion-selective pores have not been demonstrated for membrane-associated CLICs [212]. Crystal structures of several CLICs [352-355] show them to be globular proteins that can undergo a conformational change releasing N- from C-terminus, that unmask a very short (~20 aa) hydrophobic region that can reversibly associate with lipid bilayers. At this point, proof that this CLIC N-terminal domain can span lipid bilayers to form an ion-selective pore is lacking.

Even so, it has been suggested that CLIC proteins facilitate organellar acidification by allowing Cl^- movement across lipid bilayers in association with H^+ transport by vacuolar type H^+ -ATPases [216, 236]. Indeed, a role in the acidification of intracellular vacuoles in EC [236], necessary for blood vessel lumen formation has been demonstrated for CLIC4, and acidification of intracellular vesicles that function in osteoclast-dependent bone resorption requires CLIC5B [356]. Similarly, acidification of phagosomes in macrophages requires CLIC1[216]. Could the activation of ERM proteins by CLIC5A and CLIC4 be related to Cl^- channel activity? We are not aware of any reports suggesting that ERM activation requires Cl^- channel activity, and we previously reported that the action of CLIC5A on ERM protein activation is not inhibited by IAA9 [4], the one inhibitor that blocks the lipid bilayer ion conductance induced by CLIC proteins. Therefore, it seems unlikely that CLIC4 and CLIC5A induced ERM protein activation reflect Cl^- channel activity.

Whereas mice in which CLIC5A is deleted develop fewer, broader and shorter podocyte foot processes [5, 123] and CLIC4 deletion reduces the peritubular capillary density and glomerular number [241], we did not observe any overt change in glomerular capillary EC fenestrae in 2-month old CLIC5A, or dual CLIC5A/CLIC4 deficient mice (Figure 4.9 a,b). Also, overexpression of CLIC5A, which results in potent activation of ERM protein phosphorylation in cultured glomerular EC (Figure 4.6c), did not induce the formation of fenestrae in these cells, by scanning electron microscopy (Xin Wang, Unpublished Data). Nonetheless, in dual CLIC5/CLIC4 deficient mice (Figure 4.7) and in hypertensive CLIC5 deficient mice [122] fenestrae density declines significantly as a function of time. In dual CLIC5/CLIC4 deficient mice we also observed glomerular mesangial proliferation, matrix deposition and the spontaneous development of proteinuria, which were not observed when either CLIC4 or CLIC5

were deleted singly. Thus, it seems that CLIC4 and CLIC5A are required for the maintenance of ERM protein activation in glomerular capillary EC, but not for the initial formation of glomerular capillary EC fenestrae. Nonetheless, the long-term maintenance of a normal glomerular structure and open glomerular capillary EC fenestrae requires CLIC4- and CLIC5A-dependent stimuli.

To summarize, both CLIC4 and CLIC5A are expressed in glomerular capillary EC, *in vivo*, and both CLIC4 and CLIC5A stimulate the phosphorylation and cytoskeleton-association of ERM proteins. In glomerular capillary EC, CLIC4 and CLIC5A can substitute for one-another, at least in regard to ERM protein activation. While CLIC4 is required for the development of normal proximal tubule microvilli and CLIC5A is necessary for the formation of normal podocyte foot processes, dual deletion of CLIC4 and CLIC5 does not alter the initial development of glomerular capillary fenestrae. However, maintenance of a normal glomerular capillary EC ultrastructure is disrupted when both CLIC4 and CLIC5 are deleted in mice.

Figure 4.1

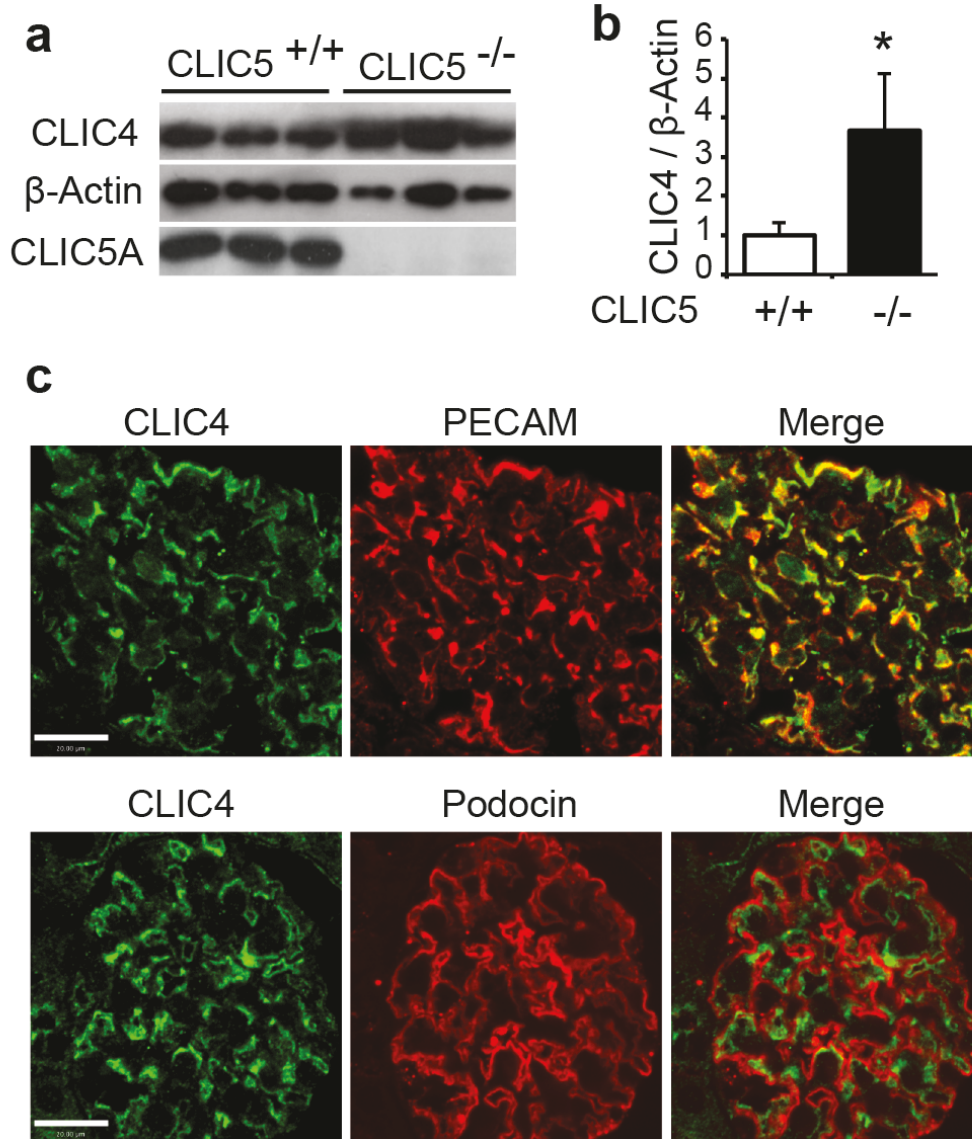


Figure 4.1 | Increased abundance and endothelial localization of CLIC4 in glomeruli of CLIC5 deficient mice. (a) Western blot (WB) of glomerular lysates from CLIC5^{+/+} and CLIC5^{-/-} mice probed with anti-CLIC4, anti- β -actin and anti-CLIC5 antibodies. Each lane represents glomeruli from a distinct mouse. (b) Densitometric analysis of the WB in A. Data are expressed as the ratio of CLIC4 : β -actin (mean \pm SD; n = 3, *P < 0.05). The ratio of CLIC4 : β -actin is significantly higher in CLIC5^{-/-} relative to CLIC5^{+/+} mice. (c) Dual-label confocal immunofluorescence microscopy for CLIC4 (red), PECAM-1 (green) and podocin (green) in glomeruli of CLIC5^{-/-} mice. CLIC4 immunofluorescence overlapped (Yellow, Merge) with PECAM-1, but with not podocin, consistent with an endothelial localization of CLIC4 (representative of 3 mice, scale bar = 20 μ m).

Figure 4.2

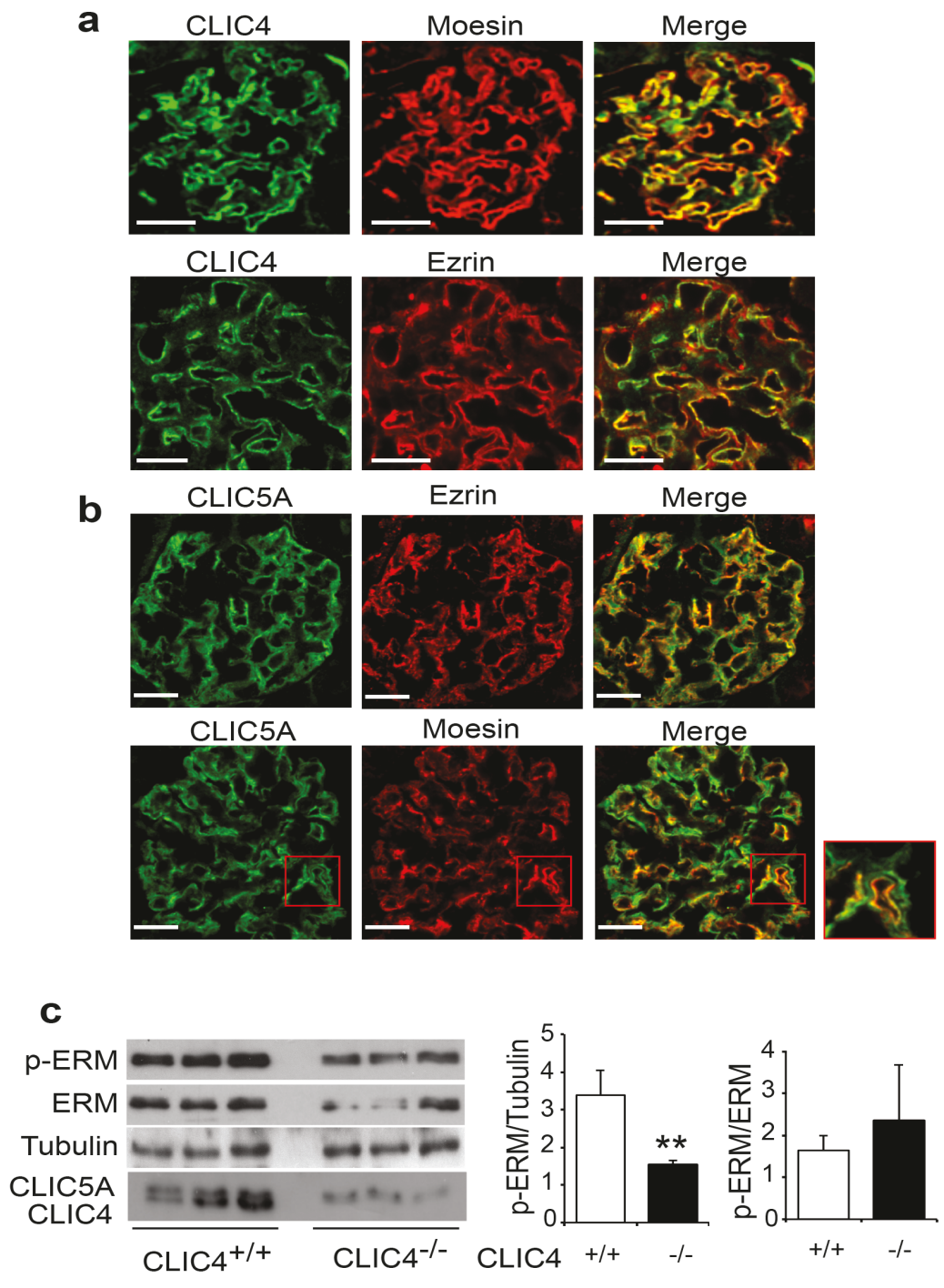


Figure 4.2 | CLIC4 co-localizes with moesin and ezrin in glomeruli, and CLIC4 deletion results in reduced ERM protein abundance in glomerular capillaries.(continued on next page)

(a) Dual-label confocal immunofluorescence microscopy for CLIC4 (green) and moesin (red) or ezrin (red) in glomeruli of CLIC5^{-/-} mice (representative of 3 separate mice, scale bar = 20 μ m). Both, ezrin and moesin immunoreactivity co-localized with CLIC4 in glomeruli of CLIC5^{-/-} mice, in a capillary pattern. (b) Dual-label confocal immunofluorescence microscopy for CLIC5A (green) and ezrin (red) or moesin (red) in glomeruli of CLIC4^{-/-} mice (representative of 3 separate mice, scale bar = 20 μ m). CLIC5A co-localizes with ezrin generally, but with moesin only in glomerular endothelial cells of CLIC4^{-/-} mice. The intensity of moesin immunoreactivity in glomeruli from CLIC4^{-/-} mice is much lower than that in CLIC5^{-/-} mice. A magnified glomerular capillary loop in (b) shows a dual band of CLIC5A immunofluorescence. Only the inner band representing CLIC5A in glomerular endothelial cells, overlaps with moesin immunofluorescence. (c) WB analysis of glomerular lysates from CLIC4^{+/+} and CLIC4^{-/-} mice probed with anti-ERM, anti-p-ERM, anti-tubulin and anti-CLIC4 antibodies. Each lane represents glomeruli from a distinct mouse. CLIC4 antibodies detect two bands in glomerular lysates from CLIC4^{+/+} mice; the upper band represents cross-reactivity with CLIC5A; the lower band represents CLIC4 and is absent from CLIC4^{-/-} glomerular lysates. Densitometry of the WB data shows the ratio of p-ERM:Tubulin and the ratio of p-ERM:total ERM (Mean \pm SD; n = 3 per group, *P < 0.05; Student t-test). Consistent with the moesin immunoreactivity in (b), the abundance of ERM and pERM proteins in glomeruli of CLIC4^{-/-} mice is reduced relative to CLIC4^{+/+} mice, without change in the ratio of phosphorylated : total ERM proteins.

Figure 4.3

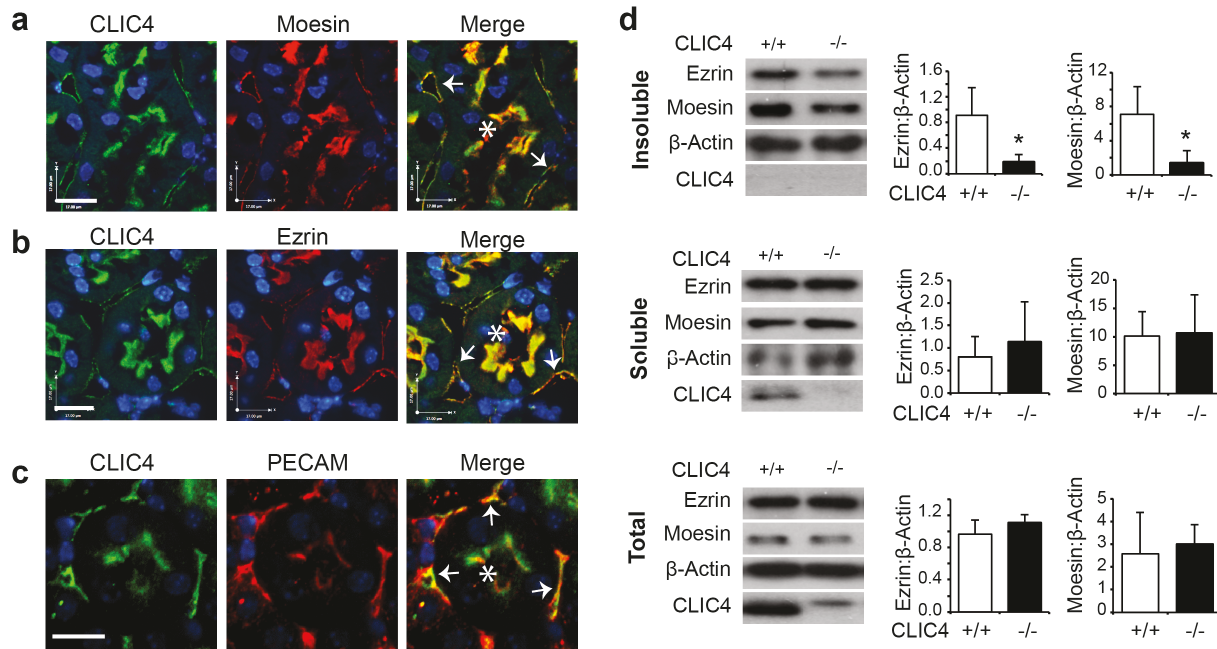


Figure 4.3 | Co-localization of CLIC4 with moesin and ezrin in renal cortex, and reduced ERM protein association with the renal cortical cytoskeletal fraction. (a,b) Dual-label confocal immunofluorescence (IF) microscopy for CLIC4 (green) and moesin (red) (A) or ezrin (red) (b) in renal cortex of CLIC5^{-/-} mice (representative of 3 mice, scale bar = 20 μm). Co-localization of CLIC4 with moesin (A) was observed in the proximal tubule brush border (*) and in a peritubular location (white arrow) in CLIC5 deficient mice. Substantial co-localization of CLIC4 with ezrin (b) was also observed in the proximal tubule brushborder (*) and in the peritubular location (white arrow). (c) Dual-label confocal IF microscopy for CLIC4 (green) and PECAM-1 (red) suggests that peritubular CLIC4 is located in endothelial cells. (d) WB with densitometric analysis of cytoskeletal (top panel) and soluble (middle panel) fractions as well as total lysates (bottom panel) prepared from renal cortex of CLIC4^{+/+} and CLIC5^{-/-} mice. Blots were probed with anti-ezrin, anti-moesin, anti-β-actin and anti-CLIC4 antibodies. The ezrin and moesin abundance is significantly lower in the cytoskeletal fraction of CLIC5^{-/-} compared to CLIC4^{+/+} mice, but the total abundance of moesin and ezrin relative to actin in soluble fractions and in total cortical lysates is similar CLIC5^{-/-} and CLIC4^{+/+} mice (mean ± SD; n = 3 per group, *P < 0.05; Student t-test). CLIC4 was not observed in the cytoskeletal fraction of CLIC4^{+/+} mice.

Figure 4.4

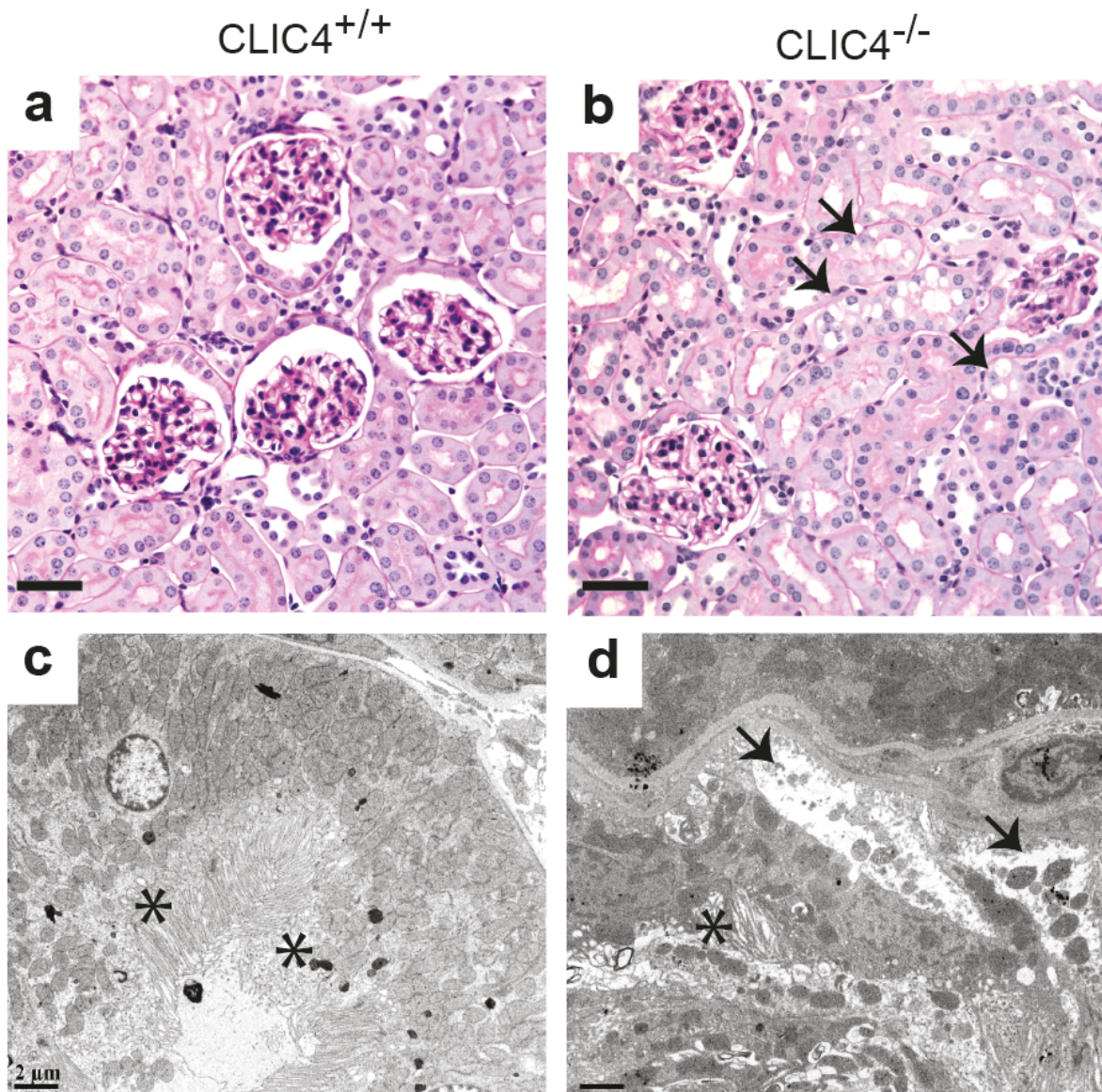


Figure 4.4 | Proximal tubule vacuolization and brush border disorganization in 8-month old $CLIC4^{-/-}$ mice. (a,b) Periodic Acid-Schiff (PAS) stained renal cortex from $CLIC4^{+/+}$ and $CLIC4^{-/-}$ mice. Prominent proximal tubule vacuolization (arrows) was observed in $CLIC4^{-/-}$, but not in $CLIC4^{+/+}$ mice. (c,d) Transmission electron microscopic appearance of the proximal tubule cells in $CLIC4^{+/+}$ and $CLIC4^{-/-}$ mice. Disruption of the proximal tubule brush border (asterisks) and proximal tubule epithelial cell vacuolization (arrows) is shown. (representative of 4 $CLIC4^{-/-}$ and 3 $CLIC^{+/+}$ mice).

Figure 4.5

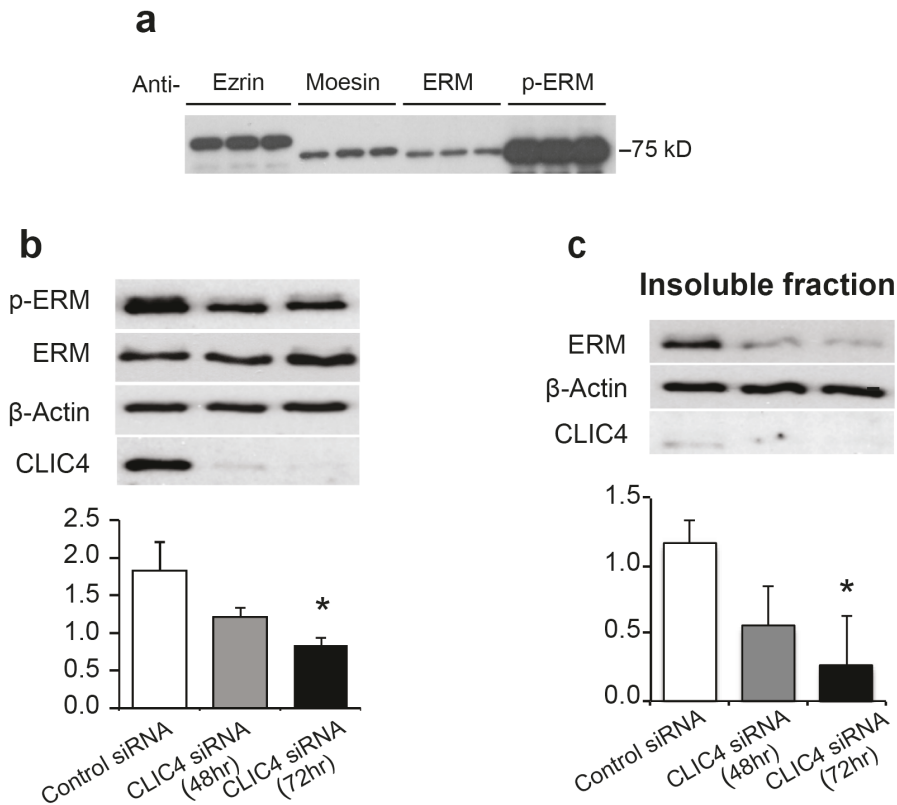


Figure 4.5 | Reduced ERM protein activation in cultured glomerular EC upon CLIC4 silencing. (a) WB for ezrin, moesin, total ERM and phosphorylated ERM proteins in cultured glomerular EC. Lysates from 3 distinct cultures (1,2,3) were separated by SDS-PAGE and transferred to PVDF membranes. The membranes were then cut and incubated with ezrin-, moesin-, pan-ERM and pan-p-ERM antibodies followed by ECL. The membranes were then re-assembled and exposed to film. Though the ezrin antibody recognizes abundant ezrin in the glomerular EC, both the pan-ERM and pan-p-ERM antibodies detect predominantly moesin. (b) WB and densitometric analysis of total cellular lysates prepared from glomerular EC transfected with control (72 hrs post-transfection) or CLIC4-specific (48 and 72 hours post-transfection) siRNA. The blots were probed with anti-ERM, anti-p-ERM, anti- β -actin and anti-CLIC4 antibodies. CLIC4 protein is observed at baseline in the cultured glomerular EC. At 72 hours post transfection, CLIC4-specific siRNA reduced the CLIC4 protein abundance by >90% relative to that observed in cells transfected with control siRNA. The ratio of p-ERM : total ERM protein was reduced in cells transfected with CLIC4 siRNA relative to that observed in cells transfected with control siRNA (mean \pm SD; n = 3 independent experiments, *p<0.05 vs control siRNA; Student's t-test). Not change in total ERM abundance was observed in response to CLIC4 silencing. (c) WB and densitometric analysis of detergent-insoluble fractions of glomerular EC cell lysates treated as in a. Significantly less ERM protein was associated with the cytoskeletal fraction 72 hours after CLIC4 silencing compared compared to cells transfected with control siRNA (mean \pm SD; n = 3 independent experiments, *p<0.05 vs control siRNA; Student's t-test)

Figure 4.6

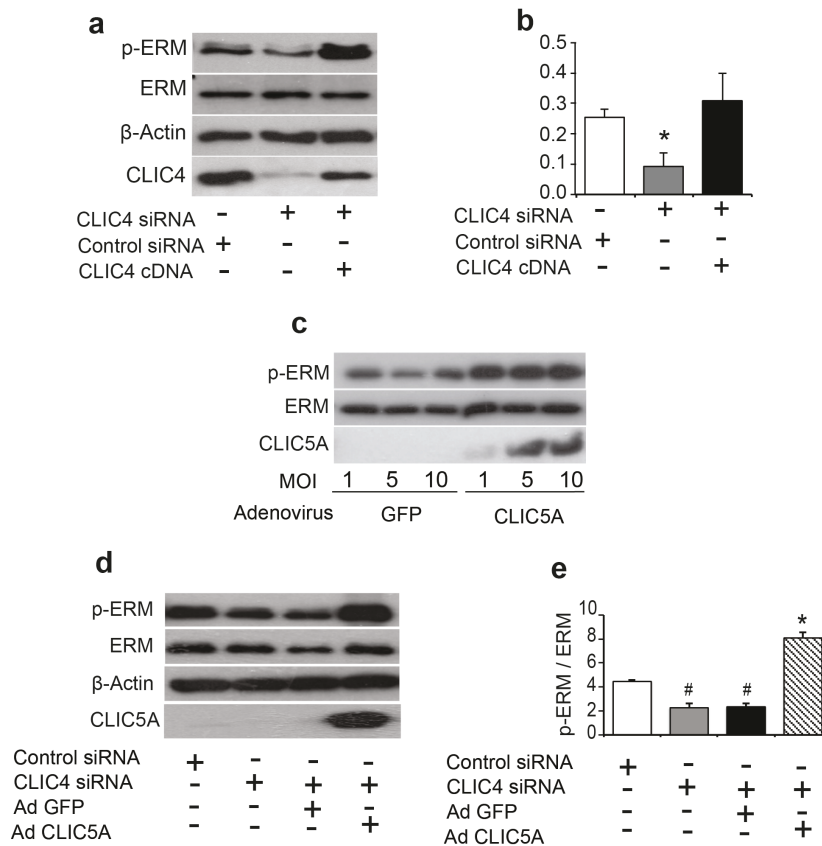


Figure 4.6 | Reduced ERM phosphorylation is rescued with overexpressed CLIC4 or CLIC5A (a,b) WB and densitometric analysis of total cellular lysates prepared from glomerular EC transfected for 48 hours with control siRNA, CLIC4-specific siRNA or both CLIC4-specific siRNA and CLIC4 cDNA. The ratio of p-ERM : total ERM protein was reduced in response to CLIC4 siRNA, and markedly increased in cells transfected with both CLIC4-specific siRNA and CLIC4 cDNA (mean \pm SD; n = 3 independent experiments, *p<0.05 vs the other two groups; one-way ANOVA followed by Tukey's post-hoc test). (c) WB analysis of glomerular EC cells transduced with 1, 5 or 100 MOI of control pAdTrack-GFP (GFP) or pAdTrack-GFP-CLIC5A (CLIC5A) for 24 hours and probed for p-ERM, total ERM, and CLIC5A protein. A representative experiment is shown. CLIC5A expression increased the p-ERM protein abundance. (d,e) WB and densitometric analysis of glomerular EC lysates 48 hours after transfection with control or CLIC4-specific siRNA. Identically treated cultures were transduced for 24 hours with control pAdTrack-GFP (Ad GFP) or pAdTrack-GFP-CLIC5A (Ad CLIC5A). CLIC4 silencing reduced the ratio of p-ERM : ERM protein. This effect was fully reversed in cells forced to express CLIC5A (Ad CLIC5A) but not in cells transduced with Ad GFP (mean \pm SD; n = 3 independent experiments, #p<0.05 vs control siRNA and Ad CLIC5A group. *p<0.05 vs the other groups; one-way ANOVA followed by Tukey's post-hoc test).

Figure 4.7

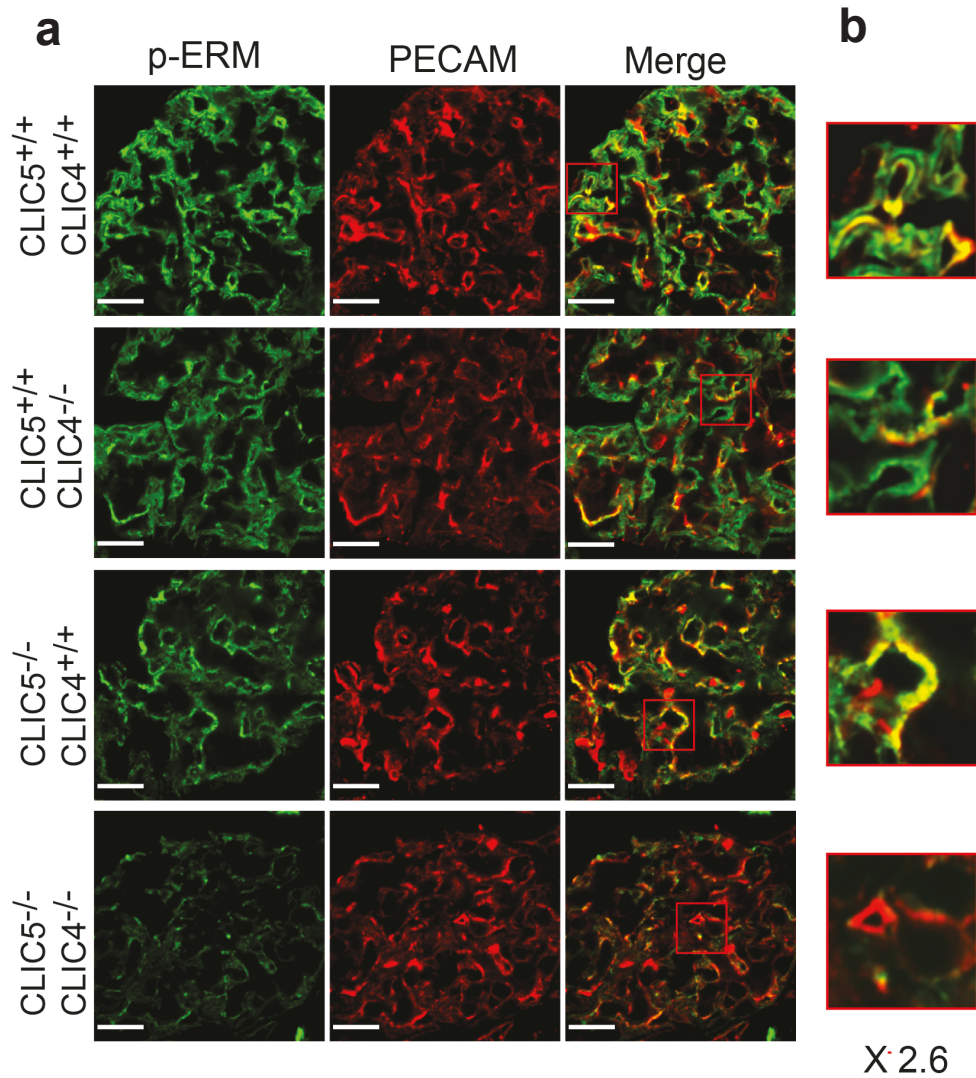


Figure 4.7 | Defective ERM protein phosphorylation in dual CLIC4/CLIC5 deficient mice by immunofluorescence (IF) microscopy. (a,b) Dual confocal immunofluorescence (IF) microscopy of glomeruli from wild type (CLIC4^{+/+}/CLIC5^{+/+}), CLIC4 deficient (CLIC5^{+/+}/CLIC4^{-/-}), CLIC5 deficient (CLIC5^{-/-} CLIC4^{+/+}) as well as dual CLIC4/-CLIC5 deficient (CLIC5^{-/-}/CLIC4^{-/-}) mice. Digitally magnified (2.6 X) portions of capillary loops in the red boxes in (a) are shown in (b). Sections were probed with anti-p-ERM and anti-PECAM-1 antibodies. Partial reduction of p-ERM was observed in glomeruli lacking CLIC4 or CLIC5, but some p-ERM overlapping with PECAM-1 immunoreactivity was still observed whether CLIC4 or CLIC5 were lacking. However, in mice lacking both CLIC4 and CLIC5, p-ERM immuno-reactivity was nearly absent from glomerular capillary loops (scale bar = 20 μ m; representative of 3 separate experiments).

Figure 4.8

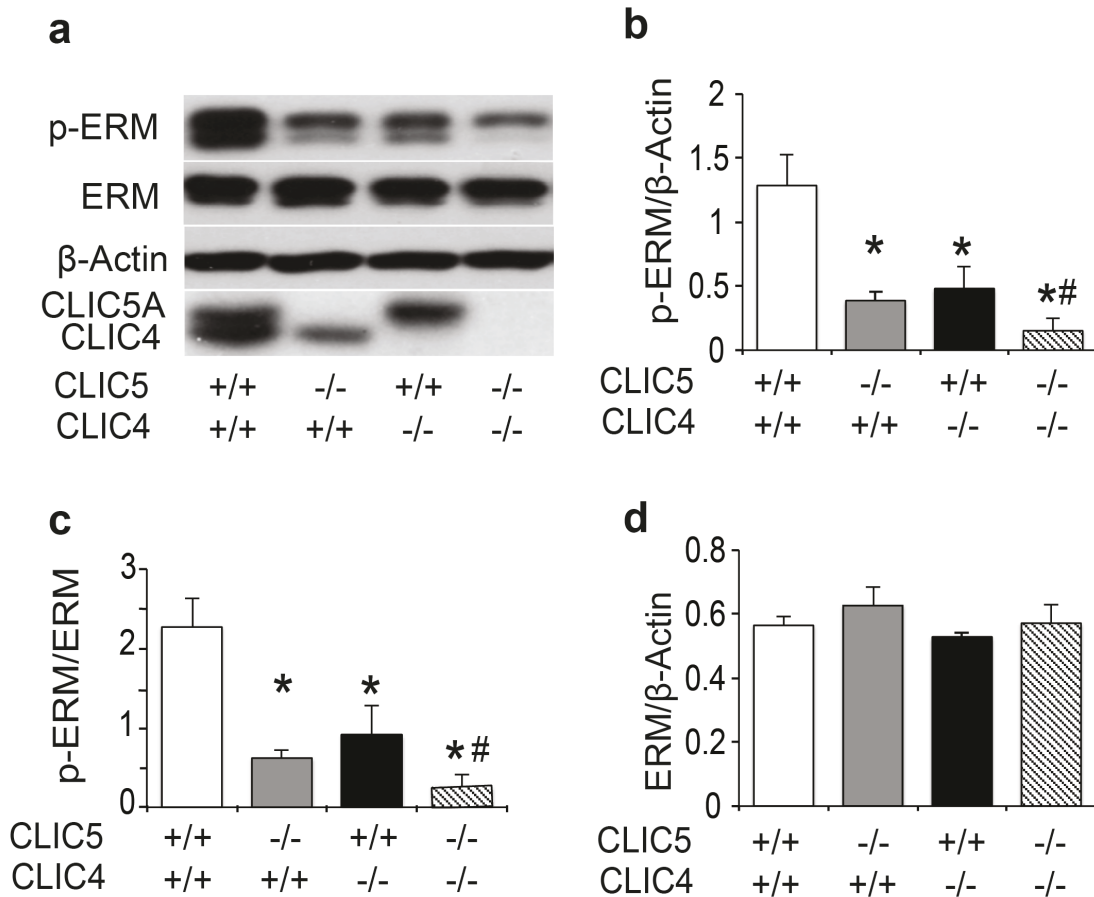


Figure 4.8 | Defective ERM protein phosphorylation in kidney cortex from dual CLIC4/CLIC5 deficient mice. (a-d) WB and densitometric analysis of renal cortical lysates from wild-type (CLIC4^{+/+}/CLIC5^{+/+}), CLIC4 deficient (CLIC5^{+/+}/CLIC4^{-/-}), CLIC5 deficient (CLIC5^{-/-}/CLIC4^{+/+}) and dual CLIC4/CLIC5 deficient (CLIC5^{-/-}/CLIC4^{-/-}) mice. The blots were probed with anti-CLIC4, anti-p-ERM, anti-ERM and anti-β-actin antibodies. The CLIC4 antibody recognizes two bands in lysates from CLIC4^{+/+}/CLIC5^{+/+} mice. The upper band reflecting CLIC5A is absent in CLIC5^{-/-}/CLIC4^{+/+} mice, and the lower band reflecting CLIC4 is absent in lysates from CLIC5^{+/+}/CLIC4^{-/-} mice. Both bands are absent in lysates from CLIC5^{-/-}/CLIC4^{-/-} mice. The ratio of p-ERM : β-actin and p-ERM : total ERM protein were significantly lower in CLIC5^{+/+}/CLIC4^{-/-} and CLIC5^{-/-}/CLIC4^{+/+} when compared to wild-type (CLIC4^{+/+}/CLIC5^{+/+}) mice. In dual CLIC4/CLIC5 deficient mice an even more pronounced reduction in the p-ERM abundance was observed. (Mean ± SD; n=3-5 mice /group, *p < 0.05 vs. wild-type; #p < 0.01 vs. all the other groups; one-way ANOVA followed by Tukey's post-hoc test).

Figure 4.9

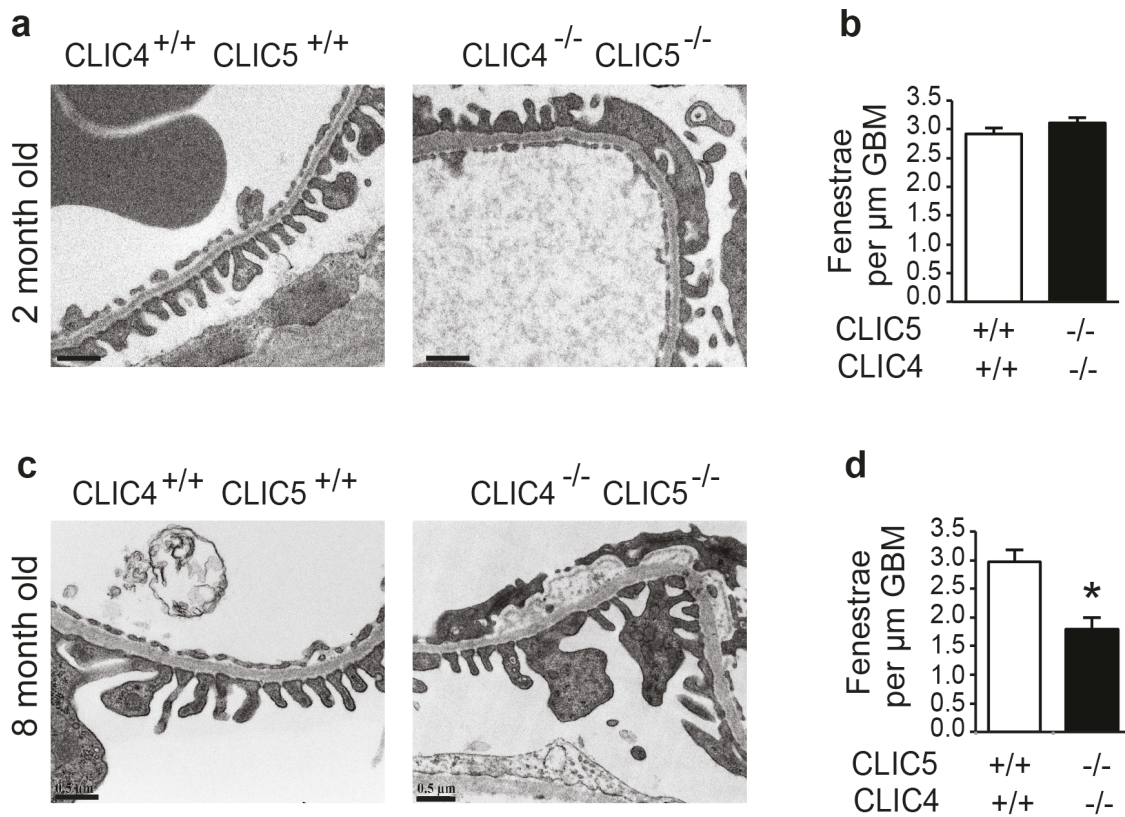


Figure 4.9| Ultrastructural abnormalities in glomerular endothelial cells of dual CLIC4/CLIC5 deficient mice. (a,b) Transmission electron microscopy (TEM) appearance of the glomerular capillary wall of 2-month (a) and 8-month (b) old wild-type (CLIC4^{+/+}/CLIC5^{+/+}) and dual CLIC4/CLIC5 deficient (CLIC4^{-/-}/CLIC5^{-/-}) mice (representative of 3 mice per group, scale bar = 0.5 μm). C,D: Morphometric quantification of endothelial fenestrae in 2-month (c) and 8-month (d) old CLIC4^{+/+}/CLIC5^{+/+} and CLIC4^{-/-}/CLIC5^{-/-} mice. Glomerular EC fenestrae density was similar at 2 months of age, but was markedly lower in CLIC4^{-/-}/CLIC5^{-/-} compared to age-matched CLIC4^{+/+}/CLIC5^{+/+} mice at 8 months of age (mean \pm SEM; n = 3-5 mice per group, *p<0.05; Student t-test).

Figure 4.10

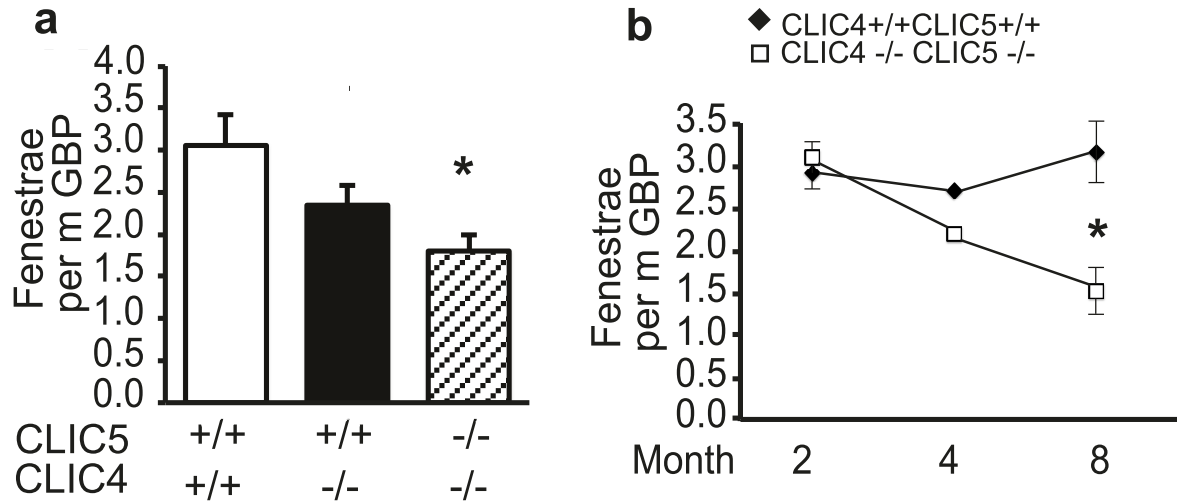


Figure 4.10 | Ultrastructural abnormalities in glomerular endothelial cells of dual CLIC4/CLIC5 deficient mice.

(a) Morphometric quantification of endothelial fenestrae in and 8-month old CLIC4^{+/+}/CLIC5^{+/+}, CLIC4^{+/-}/CLIC5^{+/+} and CLIC4^{-/-}/CLIC5^{-/-} mice. Glomerular EC fenestrae density was lower in CLIC4^{+/-}/CLIC5^{+/+} and was significantly lower in CLIC4^{-/-}/CLIC5^{-/-} compared to age-matched CLIC4^{+/+}/CLIC5^{+/+} mice at 8 months of age. (mean ± SEM; n = 3-5 mice per group, *p<0.05; one-way ANOVA followed by Tukey's post-hoc test). (b) Morphometric quantification of endothelial fenestrae in CLIC4^{+/+}/CLIC5^{+/+} and CLIC4^{-/-}/CLIC5^{-/-} mice as a function of time . (mean ± SEM; n = 3-5 mice per group, *p<0.05; one-way ANOVA followed by Tukey's post-hoc test).

Figure 4.11

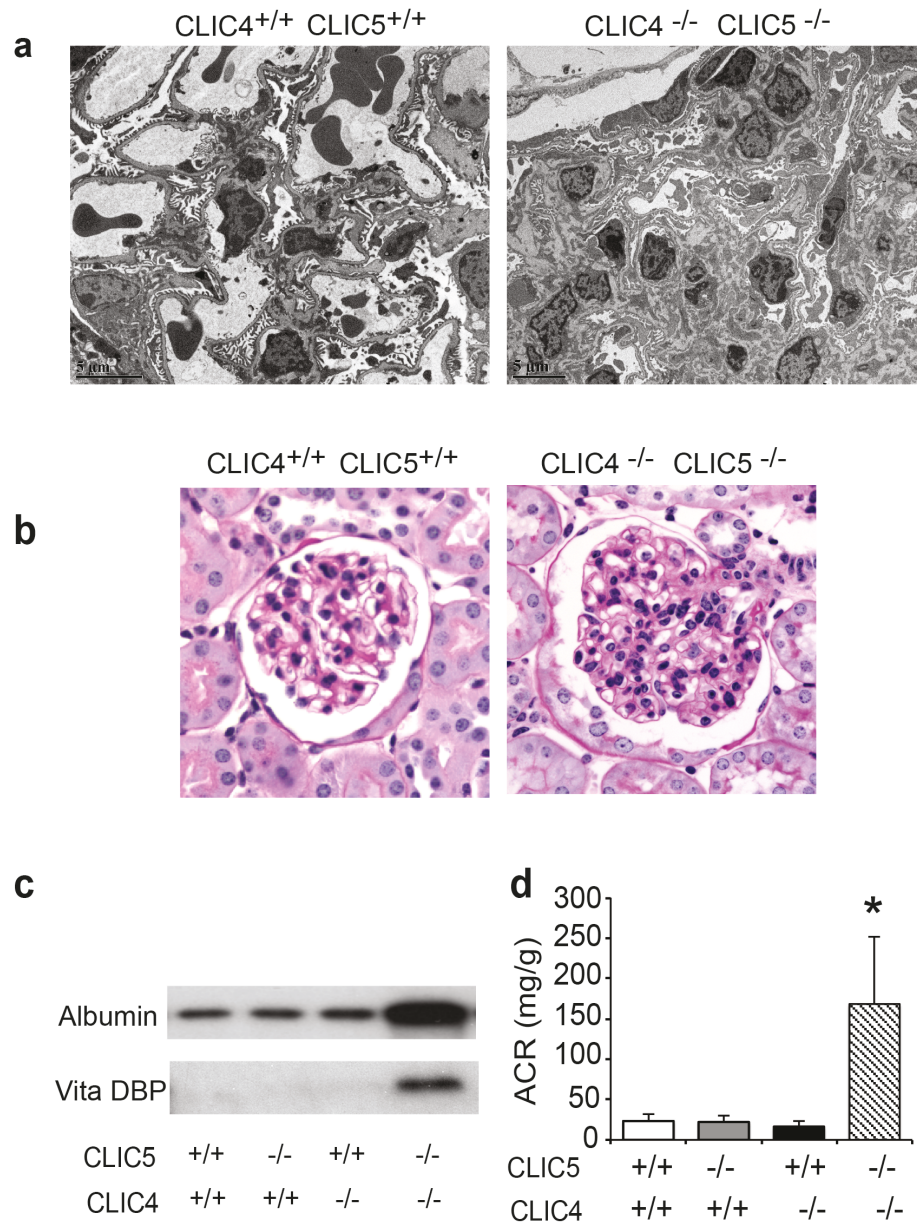


Figure 4.11 | Glomerular hypercellularity, mesangial matrix deposition and albuminuria in 8-month old dual CLIC4/CLIC5 deficient mice. A: Periodic Acid-Schiff stained glomeruli from 8-month-old wild-type (CLIC4^{+/+}/CLIC5^{+/+}) and dual CLIC4/CLIC5 deficient (CLIC4^{-/-}/CLIC5^{-/-}) mice (representative of 3 mice per group, scale bar = 25 μ m).

At 8 months of age, glomerular hypercellularity was observed in CLIC4^{-/-}/CLIC5^{-/-} mice. B: Transmission electron microscopy of glomerular capillary loops from 8-month old wild-type (CLIC4^{+/+}/CLIC5^{+/+}) and dual CLIC4/CLIC5 deficient (CLIC4^{-/-}/CLIC5^{-/-}) mice. Mesangial matrix accumulation is observed in CLIC4^{-/-}/CLIC5^{-/-} mice (representative of 3 mice per group, scale bar = 5 μ m). C. WB of urine from 8-month old wild-type (CLIC4^{+/+}/CLIC5^{+/+}), CLIC4 deficient (CLIC4^{-/-}/CLIC5^{+/+}), CLIC5 deficient (CLIC4^{+/+}/CLIC5^{-/-}) and dual CLIC4/CLIC5 deficient (CLIC4^{-/-}/CLIC5^{-/-}) mice. Loading was based on urine creatinine concentration (1 μ g creatinine/lane). Blots were probed with anti-mouse albumin or anti-vitamin D binding protein (Vitamin D BP) antibodies. Each lane represents urine from a separate mouse. D: The albumin:creatinine ratio (ACR) determined by WB densitometry with mouse albumin standards on the same blots. The urine albumin excretion rate was significantly higher in 8-month old CLIC4^{-/-}/CLIC5^{-/-} mice compared to age-matched mice in all other groups. (Mean \pm SD; n=5/group, *p < 0.05 vs. all the other groups; one-way ANOVA followed by Tukey's post-hoc test).

Chapter 5

Investigating the Interaction Between CLIC5A, CLIC4 and Small Rho-GTPases

Chapter 5

Investigating the interaction between CLIC5A, CLIC4 and small Rho-GTPases

5.1 Introduction

As described in Chapters 1,3 and 4, regulation of the actin cytoskeleton, cell motility, cell adhesion and cell architecture, among many other functions, is regulated by small GTPases, such as Rac1, Cdc42 and RhoA [357, 358]. These small GTPases are also activated under conditions of cell proliferation and during cytokinesis. Rac1 and cdc42, but not RhoA can directly interact with, and activate PI4P5 kinases, in turn stimulating the activation and phosphorylation of ERM proteins and merlin [359]. By contrast, RhoA does not appear to interact with the PI4P5 kinases, but ROCK (Rho associated protein kinase) can directly phosphorylate the ERM proteins [189]. In COS7 cells however, our laboratory found that ERM phosphorylation is not inhibited by the ROCK inhibitor Y27632. By contrast, I observed that Rac1 inhibition with NSC 23766, or expression of the dominant negative Rac1N17 strongly inhibited basal and CLIC5A-stimulated ERM activation, and NSC 23766 also blocked the CLIC5A-stimulated accumulation of PI[4,5]P₂. I also observed that CLIC5A activates Rac1, but not RhoA or Cdc42, at least in COS7 cells. Taken together with the findings that CLIC5A also activates the Rac1/Cdc42 effector Pak1, both in vivo and in vitro, these findings suggest that CLIC5A in some way interacts with, and activates Rac1, and that Rac1, in turn stimulates both PI4P5 kinases and Pak1. However, we also found that NSC 23766 caused the rapid dissociation of CLIC5A from the apical plasma membrane. So, it is also possible that Rac1 is necessary for the CLIC5A association with the plasma membrane, or that it stimulates translocation of CLIC5A to the plasma membrane. Since we also observe that CLIC4 stimulates ERM phosphorylation, it also seems reasonable to

postulate that CLIC4, like CLIC5A stimulates Rac1 or Cdc42, which in turn would then stimulate PI[4,5]P2 generation and downstream ERM phosphorylation.

Questions left unanswered so far include: a) whether CLIC5A actually interacts with Rac1, and if so whether it might act as a Rho GEF or an inhibitor of a Rac1 specific Rho GAP, b) whether amplification of Rac1 activity by CLIC5A is actually upstream or downstream of PI4,5P2 generation, or both, c) whether CLIC4 activates Rac1 and/or Cdc42 and whether the CLICs amplify the activation of ERM protein phosphorylation by growth factors. I have started to make progress towards answering these questions, though this component of the work is as yet incomplete.

It has been proposed that CLICs are involved in the formation of localized multi-protein complexes at the cytoplasmic membrane surface, assembling via multiple weak interactions [202]. Therefore it seems plausible that CLICs directly/indirectly bind to Rho GTPases and are involved in growth factor-initiated signaling events in different cell types.

Many growth factors such as PDGF and EGF initiate signaling events that result in extensive rearrangement of actin cytoskeleton. For example PDGF and EGF dependent dramatic rearrangements of actin cytoskeleton is required for actin-dependent formation of dorsal membrane ruffles and cup formation at early stages of macro-pinocytosis and phagocytosis [358]. EGF treatment promotes Rac1 activation and PI[4,5]P2 production in membrane ruffles [360]. Interestingly, activation of Rac1 by light is sufficient to increase PI[4,5]P2 production and macropinosome formation [360, 361]. Intracellular signaling cascade initiated by growth factors

during phagocytic-cup formation include ERM protein phosphorylation and F-actin coupling which promotes the formation of dendritic membrane protrusions [362]. Moreover EGF treatment results in microvilli formation via ERM proteins activation and translocation from the cytoplasm to microvilli [298]. Since both, CLIC5 and ERM proteins are involved in Rho GTPase-dependent rearrangement of cytoskeletal structures and since EGF trigger signaling cascades to rearrange actin cytoskeleton via ERM activation I determined whether CLICs are involved in EGF -initiated signaling events.

VEGF is a sub-family of the platelet derived growth factor family involved in both vasculogenesis and angiogenesis. In mammals, the VEGF family consists of five members: VEGF-A, VEGF-B, VEGF-C, VEGF-D and placenta growth factor (PGF). In human, Alternative splicing of mRNA from exon 6, 7 and 8 of VEGFA gene results in the formation of multiple isoforms of VEGF-A (VEGF121, VEGF121b, VEGF145, VEGF165, VEGF165b, VEGF189, VEGF206). VEGF family members binding to receptor tyrosine kinases (VEGFRs) on the cell surface, lead to dimerization and activation of VEGF/VEGFR protein complex via transphosphorylation. VEGFR activation mediates endothelial cell survival (via the PI3K/Akt pathway), migration (via the p38MAPK pathway), and proliferation (via the Raf/MEK/Erk pathway). Rho family of small GTPases, among the known effectors of VEGF signaling [363-365]. In endothelial cells, Rac1 mediates VEGF-induced endothelial cell migration, tubulogenesis, adhesion, and permeability by stimulating the formation of lamellipodia and membrane ruffles [364, 365]. VEGF also regulates ERM protein activation. VEGF-C triggers actin cytoskeleton remodeling and cancer cell metastasis in cervical carcinoma cell line (SiHa) by activation of moesin through RhoA/ROCK-2 pathway [366].

In *C. elegans*, excretory tube morphogenesis is critically dependent on ERM-1[344, 367], and on EXC-4, a *C. elegans* CLIC homolog [321]. Hence, CLIC4 and ERM proteins are critical to the development of actin-based cellular structures such as vascular lumens and VEGF is one of the main regulators of lumen formation in part via ERM activation; this raises the question whether CLIC4 is necessary for VEGF-stimulated ERM protein phosphorylation and lumen formation.

I therefore explored the hypothesis that CLICs interact with Rho GTPases and are involved in growth factor-initiated signaling events.

5.2 Results

5.2.1 CLIC5A binds directly/indirectly to Rho GTPase, Rac1

Since it has been shown that both Rac1 and CLIC5A bind to PIP5K and regulate its function and since CLIC5A enhances Rac1 activation we determined whether Rac1 and CLIC5A exist in the same protein complex. To probe whether CLIC5A may interact with Rac1, COS7 cell lysates were incubated with recombinant GST-CLIC5A or GST immobilized on glutathione sepharose beads. Western blot analysis of the eluted proteins showed that Rac1 in cell lysates bound to GST-CLIC5A but not to GST (Figure 5.1 a), consistent with a direct or indirect interaction between CLIC5A and Rac1.

The Pak p21 Binding Domain, (Pak-PBD) beads have been shown to bind specifically to the GTP-bound form of Rac and/or Cdc42 proteins in their native protein complex. The protein complex containing Rac1-GTP and its partners can be pulled down and eluted from pelleted beads in SDS buffer. Specific antibodies on a western blot can detect Rac1 partners. To further determine if CLIC5A and Rac1 exist in the same protein complex cell lysates from CLIC5A transfected COS7 cells were loaded with GTP γ s or GDP and then incubated with PAK PBD beads. GTP γ s and GDP were used as a positive and negative control respectively. The lysates loaded with GTP γ s contained more active Rac1-GTP, which strongly bound to the bead and was pulled down in the assay. The amount of Rac1-bound to the beads was associated with the amount of CLIC5A bound to the beads also consistent with a direct or indirect interaction between Rac1 and CLIC5A (Figure 5.1 b).

5.2.2 Activation of Pak1,3 in human glomerular ECs expressing CLIC5A

Pak1, Pak2 and Pak3 are activated by the small GTPases Rac1 and Cdc42. To determine whether CLIC5A alter Rac1/Cdc42 effector Pak activation, CLIC5A protein expression was induced by infection of human glomerular ECs with the adenoviral pAdTrack-CLIC5A vector, increased with increasing multiplicity of infection (Figure 5.2 a). No CLIC5A expression was observed in cells transduced with the adenoviral vector expressing only GFP (pAdTrack) (Figure 5.2 a). CLIC5A expression in human glomerular EC stimulated Pak1,3 protein phosphorylation in a concentration-dependent fashion (Figure 5.2 a), consistent with the findings in podocytes and COS7 cells. As in podocytes and COS7 cells, p-Pak2 was already very abundant at baseline. CLIC5A expression did not change Pak2 phosphorylation in human glomerular ECs. P-Pak1,3 levels in human glomerular ECs were very low at baseline. On the western blot (Figure 5.2b), it seemed like there was less p-Pak1,3 after CLIC4 silencing than at baseline, but quantification of blots from 3 experiments did not show a significant difference in the ratio of p-Pak : Pak protein (Figure 5.2 b). Since basal levels of p-Pak1,3 were so low, I think it is still possible that CLIC4 alters Pak1,3 phosphorylation, but that this assay is just not sensitive enough to show the effect. Further studies, perhaps in other cells, or in CLIC4 deficient mice will be needed. Pak1,3 phosphorylation was significantly enhanced in glomerular endothelial cells forced to express CLIC5A (Ad CLIC5A) but not in cells transduced with Ad GFP. Hence, CLIC5A regulates Pak1,3 phosphorylation in human glomerular ECs, in culture, similar to its effect in COS7 cells, in cultured podocytes and in glomeruli in vivo.

5.2.3 CLIC4 silencing down-regulates Rac1 and Cdc42 protein expression in human glomerular ECs.

I have shown that CLIC5A regulates Rac1 activation and enhances Rac1-dependant ERM phosphorylation (Chapter 3), and that the CLIC5A homologue, CLIC4 stimulates ERM activation (Chapter 4). I therefore determined whether CLIC4 regulates Rho GTPase activation in cultured human glomerular endothelial cells.

I first tested whether CLIC4 silencing alters Rac1 activity in human glomerular EC. In cultured human glomerular EC CLIC4 silencing reduced Rac1-GTP levels as well as total Rac1 abundance (Figure 5.3 a and b). CLIC4 silencing similarly reduced Cdc42-GTP and total Cdc42 levels (Figure 5.3 c and d). By contrast, no change in GTP-Rho or total Rho was observed in response to CLIC4 silencing (Figure 5.3 e and f). So, in these studies CLIC4 did not seem to alter the level of Rac1 or Cdc42 activation, but rather Rac1 and Cdc42 protein abundance. It is unclear whether this is due to an effect of CLIC4 on expression of Rac1 and Cdc42, or protein stability. I also have to consider the possibility that the CLIC4 siRNA had off-target effects on Rac1 and Cdc42. More work will be needed to define the precise action of CLIC4 on Rac1 and Cdc42 in the cultured glomerular EC.

5.2.4 P21-activated kinase (Pak) phosphorylation and Rac1/Cdc42 protein expression in kidney samples of CLIC4^{+/+} and CLIC4^{-/-} mice.

Since CLIC4 silencing in cultured human glomerular EC resulted in a reduction of Rac1 and Cdc42 protein abundance and we previously reported that Rac/Cdc42 effector, Pak 1,3, phosphorylation is reduced in glomerular lysates from CLIC5 deficient mice, I next determined

whether CLIC4 deficiency in mice results in abrogation of Rac1/Cdc42 protein expression and decreased Pak phosphorylation. Preliminary results from 2 CLIC4^{+/+} mice and 2 CLIC4^{-/-} mice showed that the ratio of p-Pak1,3 : β -Actin in glomerular lysates from CLIC4^{-/-} mice is substantially lower than in CLIC4^{+/+} mice (Figure 5.4 a and b). Unlike the finding in the cultured glomerular EC, CLIC4 deficiency in vivo did not change the total Rac1 or Cdc42 protein levels (Figure 5.4 c and d). The reduction in Pak1,3 phosphorylation in isolated glomeruli from CLIC4^{-/-} mice together with the in vitro finding of decreased active Rac1/Cdc42 protein abundance suggest that CLIC4 similar to CLIC5 may interact and activate Rac1/Cdc42. However, more work will be needed to define whether CLIC4, like CLIC5A stimulates the activation of Rac1 and/or Cdc42.

5.2.5 CLIC4 is required for VEGF mediated ERM activation in cultured human glomerular ECs.

Since VEGF stimulates ERM protein activation via Rho-GTPases in EC, I also determined whether CLIC4 is involved in VEGF-initiated signaling events. CLIC4 silencing reduced the ratio of p-ERM : ERM protein in cultured human glomerular EC. In response to VEGF, pERM levels only slightly increased in the glomerular EC transfected with control siRNA, and less in those transfected with CLIC4 siRNA, and VEGF did not overcome the inhibition of ERM phosphorylation by CLIC4 silencing (Figure 5.5). These experiments raise doubts about the effect of VEGF on ERM phosphorylation, at least in these cultured EC. In any case, VEGF stimulation certainly does not overcome the inhibitory effect of CLIC4 silencing on ERM phosphorylation.

5.2.6 Similar to CLIC5A, EGF dependent ERM protein phosphorylation requires Rac1.

To determine whether CLIC5A is involved in EGF -initiated signaling events and whether CLIC5A effect on ERM phosphorylation is synergistic, redundant or additive with that of EGF, COS7 cells transfected with GFP-vector or GFP-CLIC5A were treated with specific Rac1 inhibitor, NSC 23766 (100 μ M) and EGF (10 ng/ml) alone and in combination for 5 and 25 minutes. EGF treatment and CLIC5A both enhanced ERM phosphorylation without changing total ERM proteins. Rac1 inhibition significantly abolished both, the EGF and the CLIC5A-dependent increase in p-ERM (Figure 5.6), without changing ERM abundance. Moreover EGF could not further increase ERM phosphorylation over that observed by CLIC5A alone (Figure 5.6). The findings in this experiment show that both EGF- and CLIC5A stimulated ERM phosphorylation is Rac1 dependent. Also, the finding that the stimulation of ERM phosphorylation by EGF and CLIC5A were not additive would be consistent with the interpretation that both EGF and CLIC5A act in the same signaling cascade.

5.3 Discussion

CLIC5A regulates PI[4,5]P₂ production in apical plasma membrane patches, promoting Ezrin phosphorylation and actin coupling, which maintains the unique cytoskeletal architecture of podocytes. In chapter 3 I showed that CLIC5A has a role in regulating the specialized architecture of podocytes by increasing Rac1 activity and downstream PAK1,3 and Ezrin phosphorylation. In chapter 4 I observed that CLIC4, similar to CLIC5A induces ERM phosphorylation in endothelial cells. In this chapter I aimed to study the interaction between CLICs and Rho GTPases in more details.

Here I showed for the first time that GST-CLIC5A can pull down Rac1 from cell lysates and that CLIC5A is precipitated with GTP-Rac1. This suggests that CLIC5 directly or indirectly binds to Rac1, at least in COS7 cells. The association between CLIC5A and Rac1 could be indirect via PIP5Ks since our lab previously reported that GST-CLIC5A can pull down several PI[4.5]P₂ generating kinases from cell lysates (possibly via binding to PIP5K C terminal) and a peptide region located at the N-terminus of PIP5K β can directly bind to poly basic region of Rac1 to regulate actin polymerization [299, 300]. All isoforms PI[4.5]P₂ generating kinases contain surface cationic residues conferring a positive charge that allow them to bind negatively charged membrane phospholipids [368]. Similarly polybasic region in Rac1 contact the negatively charged membrane phospholipids [369]. It is also of note that CLIC5 was first isolated from extracts of placental microvilli as a component of a complex consisting of several known cytoskeletal proteins, including actin, ezrin, alpha-actinin, gelsolin, and IQGAP1[182]. IQGAP1 is an effector protein of the small GTPases Rac1 and Cdc42, which regulates actin cytoskeleton dynamics through recruitment of Arp2/3 and/or formin protein complexes [370]. This also suggests that CLIC5 and Rho GTPases are closely related. Finally, the observation that

CLIC5A expression in glomerular EC enhances the phosphorylation of the Rac1/Cdc42 effector Pak1,3 phosphorylation suggests that Rac1 activation by CLIC5A is not podocyte-specific and holds true at least in 3 different cell types (COS7 cells, Podocytes and human glomerular EC).

Future experiments using recombinant wild-type and mutant CLIC5A and Rac1 constructs as well as liposomes containing distinct phospholipids should allow the laboratory to answer the question whether the interaction between CLIC5A and Rac1 is direct or indirect via PIP5K or the membrane phospholipids themselves.

We were surprised to observe that CLIC4 silencing in vitro reduced total Rac1 and Cdc42 levels, without affecting RhoA (Figure 5.3). By contrast, Rac1 and Cdc42 abundance was the same in lysates from kidney cortex of a pair of CLIC4 deficient, and a pair of wild-type mice (Figure 5.4 c,d). Although further studies are required to rule out whether Rac1/Cdc42 down-regulation by CLIC4 silencing in glomerular EC is an off-target effect of siRNAs, it is possible that CLIC4 indeed regulates protein expression, given that CLIC4 can shuttle to the nucleus as part of TGF- β 1 signaling [337, 371] and that the members of Rho GTPases are regulated in part through expression [372]. Rac1 degradation occurs through the proteasomal pathway [373] and ubiquitin/proteasome system (UPS) has been reported and could represent an efficient mechanism for Rho GTPase deactivation [374].

Spiekerkoetter et al [371] reported that loss of CLIC4 in vascular smooth muscle cells resulted in impaired activation and distribution of the small GTPases RhoA and Rac1, necessary for cell retraction and extension of filopodia and lamellipodia during cell migration. Interestingly, they could not detect a significant change in Cdc42 activation but observed that total Cdc42 seemed to be increased with CLIC4 silencing [371]. In another study in MDCK 3D cultures, Cdc42

rescued impaired apical vesicle coalescence and central lumen formation caused by CLIC4 silencing [229]. In our experiment CLIC4 silencing decreased Cdc42 and Rac1 but not Rho protein expression. These observations suggest that the effect of CLIC4 on Rho GTPase activation /expression could be cell-specific and dependent on the kind of stimulus and the conditions in which the stimulations are applied.

Measuring the abundance of Cdc42/Rac1 mRNA will allow us to define whether the decline in Cdc42/Rac1 protein abundance is a result of reduced Cdc42/Rac1 gene transcription. To resolve whether the absence of CLIC4 increases the susceptibility of Cdc42 and Rac1 to degradation, we can inhibit protein synthesis with cyclohexamide (CHX) in cells with or without CLIC4 silencing, and then determine the abundance of Cdc42 and Rac1 as a function of time. If the rate of decline of total Rac1/Cdc42 abundance is more rapid after CLIC4 silencing, this would suggest enhanced degradation. If the degradation rate of these Rho GTPases appears to be enhanced, inhibition of the proteasomal pathway should allow us to determine whether enhanced degradation is via the proteosomal pathway.

Even so, whether the level of GTP-Rac1 and GTP-Cdc42 during CLIC4 silencing is reduced due to an overall reduction in Rac1 and Cdc42 protein abundance, or due to reduced activation, the expected effect would be that the PIP5K activity is reduced, and PI[4.5]P2 cluster formation diminished. This could be the mechanism that explains the decrease in ERM phosphorylation in glomerular EC when CLIC4 is silenced.

At baseline, p-Pak1,3 in cultured glomerular EC was very low and on the WB, and it seemed like the p-Pak1,3 level was slightly decreased by CLIC4 silencing (Figure 5.2 b). However, quantification of the blots did not demonstrate a significant difference. By contrast, in

lysates of kidney cortex prepared from 2 distinct CLIC4 deficient mice, p-Pak1,3 levels were lower than those in wild-type mice (Figure 5.4a,b). It is possible that the assay in cells is not sensitive enough to detect a significant decrease in Pak1,3 phosphorylation when baseline levels are already very low. This would be an example of Type II error or false negative results. Increasing the amount of loaded proteins for WB analysis will increase the signal for p-Pak1,3 which would allow us to detect the possible changes in phosphorylation levels. The other solution would be to stimulate Pak1,3 phosphorylation via a strong Rho GTPase activator. Since CLIC4 protein expression is abundant in basal conditions in cultured glomerular EC, stimulating the cells by growth factors (EGF) or other stimuli to trigger signaling cascades that result in Rho GTPase activation [371] will assist us to further study the role of CLIC4 in Rho GTPase activation.

We also began to test the hypothesis that CLICs play a role in growth factor-initiated signaling events that result in extensive rearrangement of cytoskeletal actin via Rho GTPase-dependent ERM activation. This was of interest because tubulogenesis is stimulated by VEGF, and microvillus formation by EGF. I found that EGF strongly activates ERM phosphorylation in COS7 cells even in the absence of CLIC5A. In the presence of CLIC5A, EGF treatment enhanced ERM phosphorylation only marginally over the CLIC5A-stimulated higher baseline. Both CLIC5A enhanced ERM phosphorylation without changing total ERM protein abundance, and Rac1 inhibition significantly reduced both, the EGF and the CLIC5A-dependent increase in p-ERM. The findings indicate that EGF can stimulate ERM phosphorylation without CLIC5A. We already know the COS7 cells express abundant CLIC4 at baseline. Given our findings in glomerular EC, where both CLIC4 and CLIC5A had to be deleted to abrogate ERM phosphorylation (Chapter 4), it will be of interest to determine whether CLIC4 silencing in the

COS7 cells can inhibit EGF-stimulated ERM protein phosphorylation. The finding that p-ERM increased only slightly above the higher baseline in cells expressing CLIC5A would be in keeping with the idea that EGF and CLIC5A, (or potentially CLIC4) are components of the same signaling cascade. In glomerular EC, we observed that VEGF stimulated ERM protein phosphorylation, but it could not overcome the inhibition of ERM phosphorylation when CLIC4 was silenced. This finding also indicates that VEGF mediated ERM phosphorylation requires CLIC4.

EGF activates the epidermal growth factor receptor (EGFR) at the cell surface. The EGFR is a member of a ErbB family of receptors which is a subfamily of four closely related receptor tyrosine kinases. Activation of tyrosine kinase receptor triggers a sequence of signaling pathways, many of which are mediated by phosphatidylinositol-4,5-bisphosphate 3-kinase (PI(3)K) [375]. PI(3)K phosphorylates the third position on the inositol ring of PI[4,5]P₂ to produce PI[3,4,5]P₃. Similarly, VEGFR2 stimulation by VEGF-A activates PI(3)K to produce PI(3,4,5)P₃ [294, 376], and PI(3,4,5)P₃ serves as a docking site for proteins containing pleckstrin homology (PH) domains recruiting them to the plasma membrane [375]. Since CLIC5A stimulates PI[4,5]P₂ generation at discrete domains of plasma membrane, it would provide abundant substrate for PI(3)K activity, unless distinct PI[4,5]P₂ pools serve as docking sites for ERM proteins, and PI(3)K, respectively. If CLIC5A and CLIC4 (or other CLICs) indeed activate PI[4,5]P₂ substrate generation for PI(3)K, then it is conceivable that EGF- and VEGF-stimulated AKT activation and other downstream effects including EGF- and VEGF-stimulated cell proliferation would be enhanced by CLIC proteins.

CLIC proteins are also able to bind to the cytoplasmic C-terminal tail regions of G-protein coupled receptors (GPCRs) [207, 377] and spatiotemporal regulation of CLIC4 upon

stimulation of Gq13, a RhoA-activating receptor, has been reported [232]. Gq13-coupled receptor-mediated RhoA activation resulted in CLIC4 recruitment to the plasma membrane where CLIC4 made a complex with RhoA and two other proteins, LPA2 and NHERF2. Induction of this signaling complex was strictly dependent on F-actin polymerization [232]. Therefore CLICs appear to be controlled by different members of Rho GTPases and CLICs, in turn, control Rho GTPases, providing feedback stabilization [202].

Clearly, the experiments in this chapter are in progress and more detailed work needs to be done to unravel the mechanism by which CLICs can control the signaling events by growth factors and other stimuli. Experiments that will help us determine whether CLIC4 actually activates Rac1 or Cdc42 in glomerular EC and whether it enhances Pak1,3 phosphorylation or Rac1/Cdc42/RhoA activation will be of great interest as they should tell us whether CLIC5A and CLIC4 use similar, or distinct Rho GTPases. We would also like to determine whether CLIC4 deficiency in mice result in changes in Rac1/Cdc42/RhoA activation and downstream phosphorylation of Paks in kidney glomeruli or whole kidney cortex. Studies in mice should also help us determine whether CLIC4 effects on Rac1/Cdc42 in epithelial cells (for example proximal tubule) and endothelial cells differ. Finally, the mechanism by which CLICs activate the small GTPases needs to be studied. For instance, we would like to determine whether CLIC5A can activate or recruit Rho GEF to confer nucleotide exchange activity toward Rho proteins or in some ways inhibit Rho GAPs or Rho GDI binding to Rho GTPases.

To summarize, the best way to explain the findings in the literature, and our own, is that CLICs are involved in the formation of localized multi-protein signaling complexes at the cytoplasmic face of lipid bilayers containing PIP5K and Rho GTPases. The localization of CLICs to these complexes then triggers signaling cascades that modulates cell cortex

cytoskeletal dynamics. The fact that CLICs form heteromers that associate with lipid bilayers suggest that these proteins may act as scaffolding proteins to bring together active Rho GTPases and PI[4,5]P2 generating kinases and that they therefore are critical for forming areas of the membrane where polymerized actin anchors. In other words, the interaction of CLICs with their partners in signaling complexes may permit timely activation and translocation of PI(4)P5Ks and Rho-GTPases.

Figure 5.1

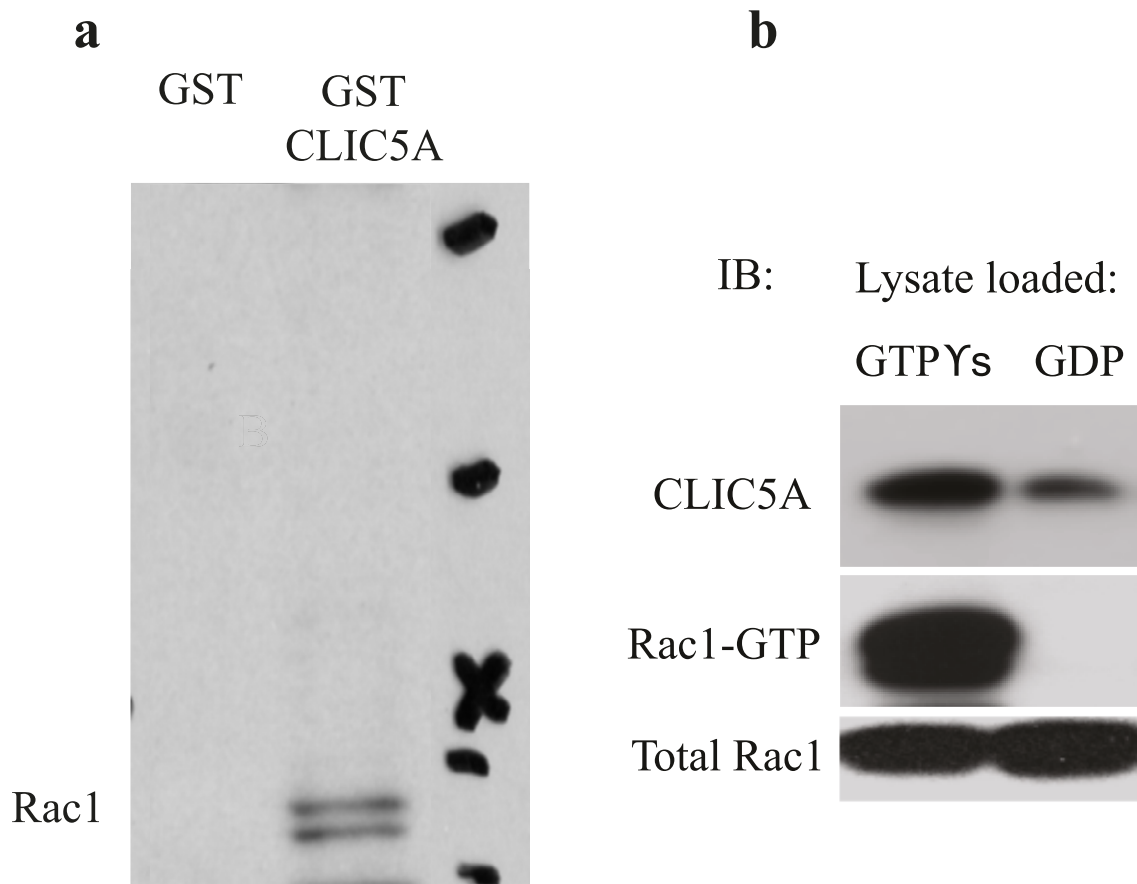


Figure 5.1 | Rac1 binds to GST-CLIC5A in COS7 cells. (a) Cell lysates prepared with Triton X-100 lysis buffer were incubated with recombinant GST or GST-CLIC5A immobilized on glutathione sepharose beads. The beads were precipitated, washed exhaustively, and bound proteins eluted and evaluated by western blot analysis with anti-Rac1 antibody. Rac1 was precipitated with immobilized GST-CLIC5A, but not GST. (b) Cell lysates from CLIC5A transfected COS7 cells were loaded with GTP γ s or GDP and then incubated with PAK PBD beads. The beads were precipitated, washed exhaustively, and bound proteins eluted and evaluated by western blot analysis with anti-Rac1 and CLIC5A antibody. CLIC5A was precipitated with GTP-Rac1 and associated with the amount of GTP-Rac1 bound to the beads.

Figure 5.2

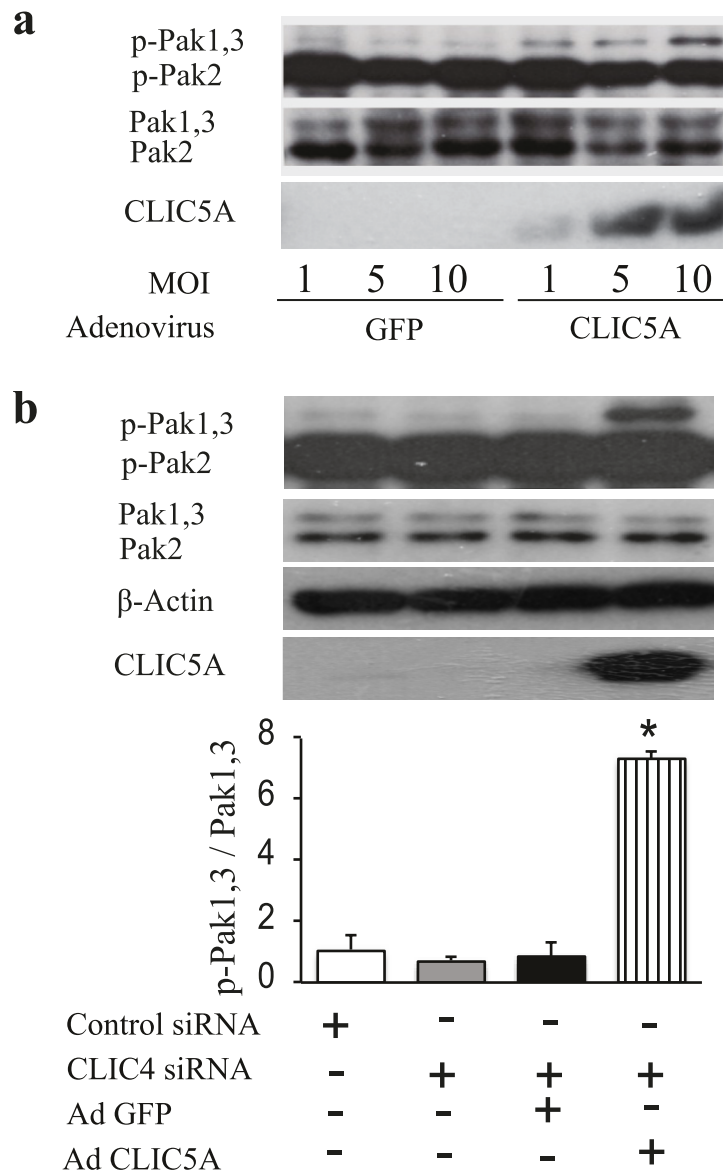


Figure 5.2 | CLIC5A enhances Pak1,3 phosphorylation in hGEN cells. (a) WB analysis of glomerular EC cells transduced with 1, 5 or 10 MOI of control pAdTrack-GFP (GFP) or pAdTrack-GFP-CLIC5A (CLIC5A) for 24 hours and probed for p-Pak, total Pak, and CLIC5A protein. A representative experiment is shown. CLIC5A expression increased the p-Pak1,3 protein abundance. (b) WB and densitometric analysis of glomerular EC lysates 48 hours after transfection with control or CLIC4-specific siRNA. Identically treated cultures were transduced for 24 hours with control pAdTrack-GFP (Ad GFP) or pAdTrack-GFP-CLIC5A (Ad CLIC5A). (mean \pm SD; n = 3 independent experiments, *p<0.05 vs the other groups; one-way ANOVA followed by Tukey's post-hoc test).

Figure 5.3

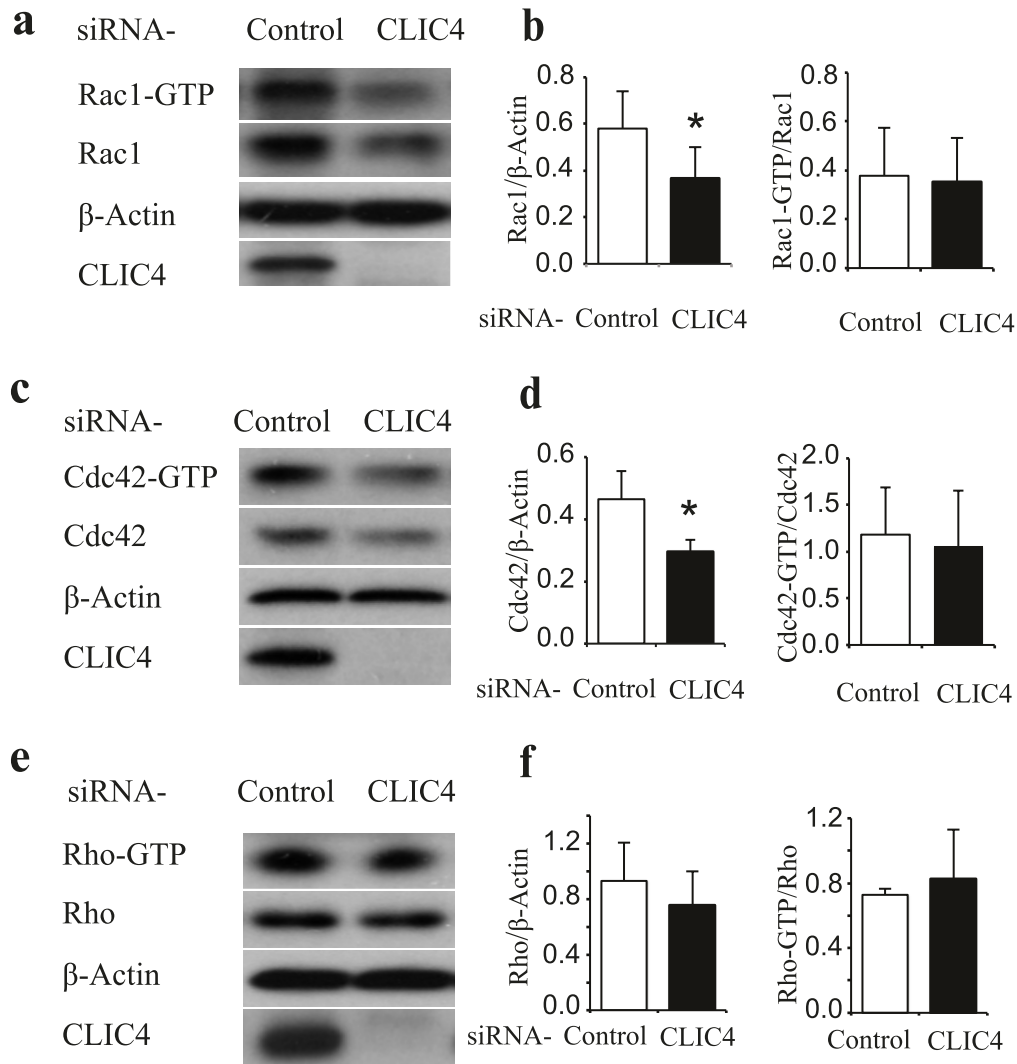


Figure 5.3 | CLIC4 silencing down-regulates Rac1 and Cdc42 protein expression in hGEN cells. (a) Western blot analysis of hGEN cell lysates probed for Rac1, β -Actin and CLIC4. Total Rac1, β -Actin and CLIC4 are shown. (b) The ratio of GTP-Rac1-to- β -Actin and GTP-Rac1-to- Total Rac1 quantified by densitometry. (mean \pm SD; n=3 independent experiments, *p < 0.05). (c) Western blot analysis of hGEN cell lysates probed for Cdc42, β -Actin and CLIC4. Total Cdc42, β -Actin and CLIC4 are shown. (d) The ratio of GTP- Cdc42-to- β -Actin and GTP- Cdc42-to- Total Cdc42 quantified by densitometry. (mean \pm SD; n=3 independent experiments, *p < 0.05). (e) Western blot analysis of hGEN cell lysates probed for Rho, β -Actin and CLIC4. Total Rho, β -Actin and CLIC4 are shown. F. The ratio of GTPRho-to- β -Actin and GTP- Rho-to-Total Rho quantified by densitometry. (mean \pm SD; n=3 independent experiments, *p < 0.05).

Figure 5.4

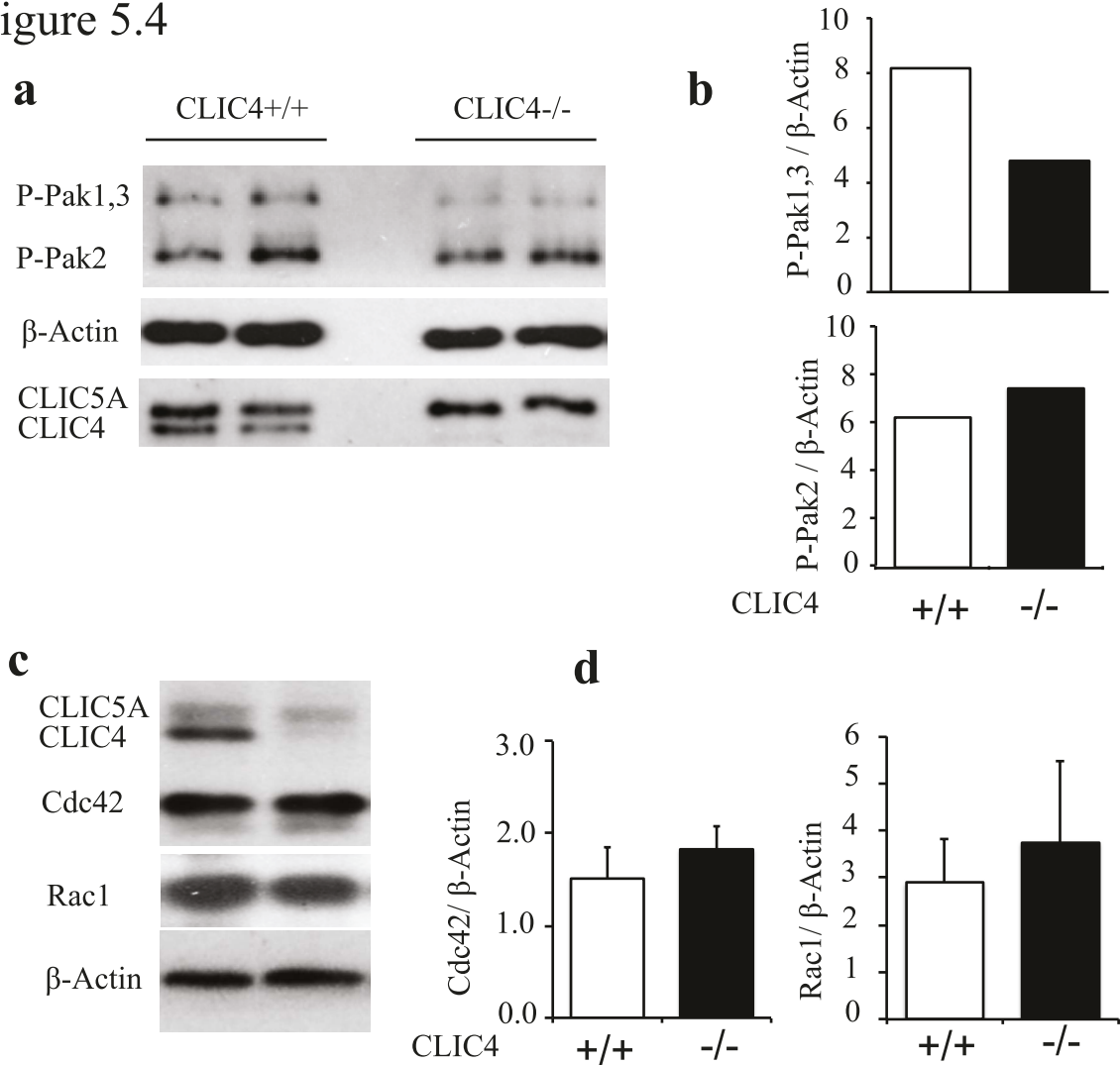


Figure 5.4 | P21-activated kinase (Pak) phosphorylation and Rac1/Cdc42 protein expression in kidney samples of CLIC4^{+/+} and CLIC4^{-/-} mice. A. Western blot (WB) analysis of lysates from isolated glomeruli. Each lane represents glomeruli from a distinct mouse. Primarily data shows that Pak1,3 but not Pak2 phosphorylation is reduced in glomeruli from CLIC4^{-/-} mice compared to the wild type. B. Ratios of p-Pak1,3-to-β-Actin and p-Pak1,3-to-β-Actin proteins were determined from densitometry data. (n=2 mice per group). C. Representative WB of lysates from kidney cortex probed with anti-CLIC4, anti-Cdc42, anti-Rac1 and anti-β-Actin antibodies. Each lane represents kidney cortex from a distinct mouse. D. Quantification of total Cdc42 and Rac1 abundance relative to β-actin. (Mean ± SD; n = 3 mice per group, *P < 0.05).

Figure 5.5

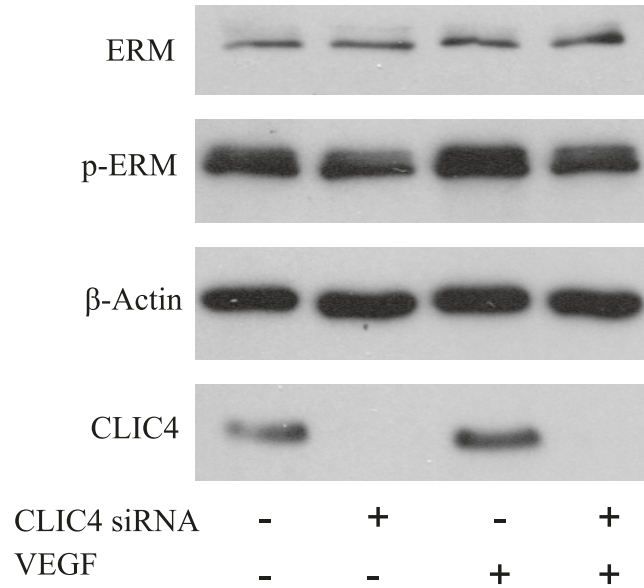


Figure 5.5 | WB and densitometric analysis of glomerular EC lysates 72 hours after transfection with control or CLIC4-specific siRNA with or without treatment with 100ng/ml VEGF for 20 mins. In response to VEGF, pERM levels only slightly increased in hGEN cells transfected with control siRNA not CLIC4 and VEGF cannot overcome the inhibition of ERM phosphorylation by CLIC4 silencing. Hence, VEGF mediated ERM phosphorylation requires CLIC4.

Figure 5.6

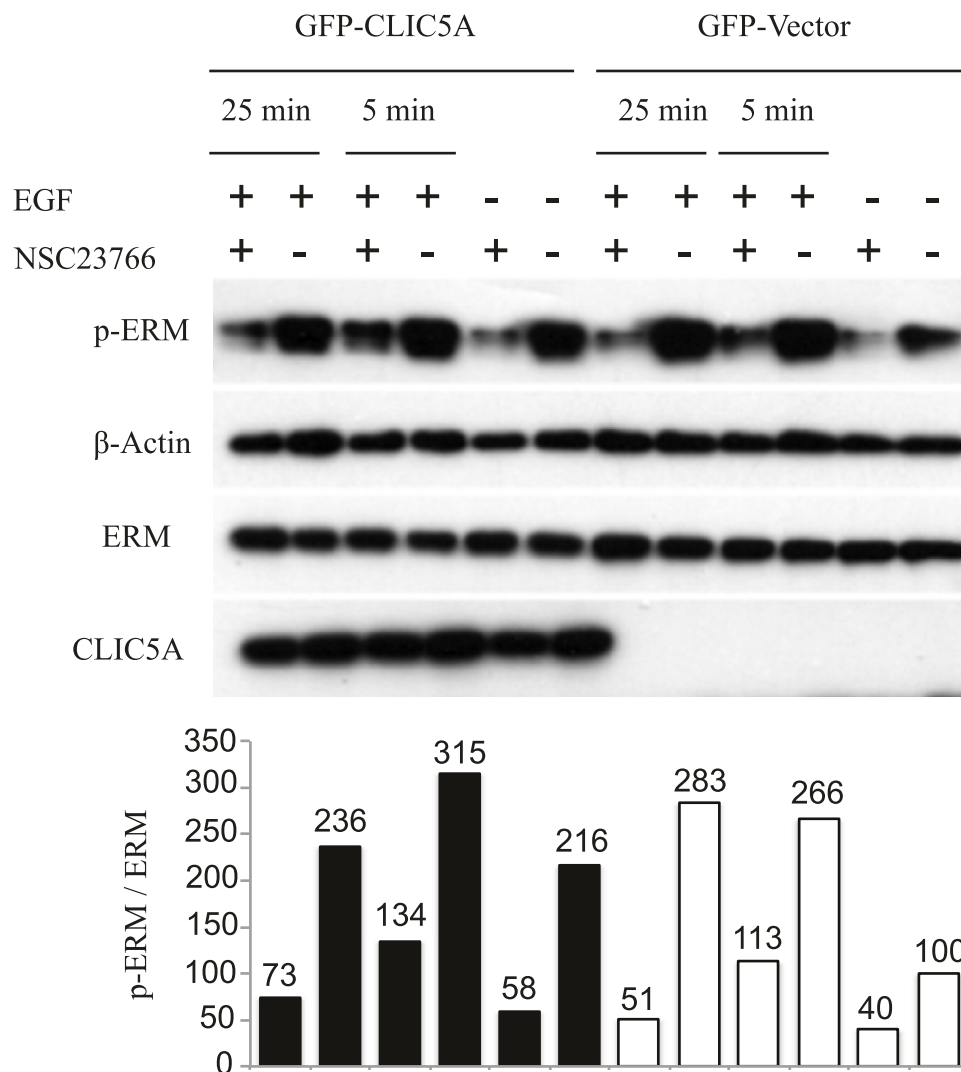


Figure 5.6 | EGF enhances ERM protein phosphorylation via Rac1 in COS7 cells transfected with GFP-Vector and GFP-CLIC5A. (a) Western blot analysis of COS7 cell lysates probed for p-ERM, ERM, β -Actin and CLIC5A. (b) The ratio of p-ERM : ERM in the GFP-Vector transfected control group was considered 100% and calculated for the other groups respectively.

Chapter 6

General Discussion and Future Directions

Chapter 6

General Discussion and Future Directions

6.1 General discussion

This thesis provides experimental evidence for a novel molecular mechanism functionally linking the CLIC, the Rho GTPase and the ERM protein families in maintaining the integrity of the glomerular filtration barrier.

While the founding member of CLIC family (p64) was originally purified with the non-selective Cl^- channel inhibitor IAA-94 [207], and these proteins are often described as chloride channels, evidence that CLICs function as a genuine chloride channels remains unconvincing [211]. The CLIC amino acid sequence does not include the typical hydrophobic domains for ion channels and they do not contain signal peptide, as is the case for most integral membrane proteins. In some studies CLICs displayed poor anion selectivity or could not even differentiate between anions or cations. Moreover, deletion of CLICs has not been shown to abrogate channel activity [211, 212]. Our laboratory also reported that the Cl^- channel inhibitor IAA-94 does not block CLIC5A-stimulated ERM phosphorylation [4]. It is suggested that experimental artifacts during reconstitution of purified CLIC proteins into artificial lipid bilayers or activation of endogenous currents by heterologous overexpression could be the reason behind the observations that resulted in speculation that CLICs have chloride channel activity [212]. Therefore it is highly probable that the terminology CLIC (for Cl^- intracellular channel) was a mistake [201, 212, 213, 378].

Although it is widely accepted that CLICs and ERM proteins are frequently associated in actin-based cellular structures, and CLICs can functionally mimic ERM proteins [228, 229, 237, 238, 240, 379, 380], the details of the functional relationship between CLIC- and Ezrin/Radixin/Moesin (ERM) proteins have not been completely worked out. The work in this thesis shows for the first time that CLIC5A stimulates localized PI[4,5]P₂ generation in COS7 cells by activating Rac1, but not Cdc42 or Rho. CLIC5A also stimulates phosphorylation of the Rac1 effector Pak1,3 in COS7 cells and in cultured mouse podocytes as well as human glomerular endothelial cells. CLIC5A-stimulated PI[4,5]P₂ generation and Pak1 and ERM protein activation all require Rac1 activation.

PI[4]P5K α activation by Rac1 is a major component of Rac1 function. PI4P5 Kinases generate cluster formation of PI[4,5]P₂ at discrete location of plasma membrane. PI[4,5]P₂ binds and activates the ERM proteins, and they, in turn, control coupling of integral membrane proteins to cortical F-actin. Although not part of this thesis, PI[4,5]P₂ also binds other proteins involved in actin remodeling, and it serves as a substrate for PI(3) Kinase leading to PI(3,4,5)P₃ generation. We postulate that CLIC5A activates PI[4]P5K in a manner involving Rac1, (but not cdc42 or RhoA), with consequent ERM and Pak1 activation. Since Paks and ERM protein regulate actin polymerization, we conclude that CLIC5A/ Rac1 organize the apical actin-based architecture of podocyte foot processes and specialized endothelial cell architecture. Still to be evaluated is the question whether the CLIC5A/Rac1 action is restricted to a pool of PI[4,5]P₂ involved in ERM protein activation, or whether they also support the binding of other proteins, and help generate the substrate for PI(3) kinase.

In vivo CLIC5A is expressed at extremely high levels in apical domain of podocytes foot processes away from the basolateral domain and slit diaphragm. Unlike the proteins enriched in

slit diaphragm, CLIC5 deletion in mice only produces mild ultrastructural changes in podocyte foot processes, without a striking defect in glomerular perm-selectivity, suggesting that CLIC5A does not disrupt the podocyte slit diaphragm. However, podocytes not only contribute to the permselective filtration barrier, their actin cytoskeleton also provides capillary wall tensile strength in the face of a high intracapillary hydraulic pressure [249, 255, 381]; Although it is widely accepted that hypertension triggers remodeling of the podocyte actin cytoskeleton [2]; the detailed mechanisms are not clear. Since CLIC5A is highly enriched in apical domain of foot processes, and since it is involved in actin dynamics, we explored the hypothesis that CLIC5A has a role in maintaining the integrity of glomerular filtration barrier in face of high blood pressure.

I observed that hypertension induced Pak phosphorylation levels in podocytes of wild type but not CLIC5^{-/-} mice. Unlike in the wild type glomeruli, p-ERM levels were reduced in glomeruli from CLIC5^{-/-} mice. Although DOCA/Salt increased systemic blood pressure in both genotypes to the same degree, CLIC5^{-/-} mice developed more albuminuria and more glomerular microaneurysms than CLIC5^{+/+} mice. These results suggest that the accentuated hypertension-induced glomerular capillary injury in CLIC5 deficient mice results from alteration of Rac1 dependent Pak1,3 and ezrin activation. I concluded that hypertension-induced CLIC5A/Rac1/Pak1 and CLIC5A/Rac1/ERM protein are required for the appropriate organization of cortical actin, maintaining podocyte tensile strength in the face of high glomerular capillary pressure.

The studies in chapter 4 also provide the first evidence supporting the concept of functional redundancy between CLIC4 and CLIC5A in regulating ERM protein activation in glomerular endothelial cells. Our lab previously reported that CLIC5A is enriched 30 fold in

glomerular EC compared to other ECs and 800 fold in human glomeruli compared to most other tissues [245].

Although CLIC5A is expressed by glomerular ECs in mice and in culture, ERM phosphorylation was diminished only in podocytes and not in glomerular capillary ECs of CLIC5-deficient mice [5, 245]. Since glomerular ECs also express CLIC4, I explored whether ERM proteins can be activated by CLIC4 and if CLIC4 could compensate for the CLIC5A loss in glomerular EC. I observed that CLIC4 protein expression overlaps with CLIC5A in glomerular endothelial cells in mice, *in vivo*, and there is a compensatory increase in CLIC4 protein expression in glomerular endothelial cells of CLIC5 deficient mice, but CLIC4 was not expressed in podocytes even in the absence of CLIC5. In glomerular endothelial cells *in vivo*, CLIC4 and CLIC5A similarly co-localized with moesin and ezrin and CLIC4 or CLIC5 deficiency resulted in a similar reduction in p-ERM abundance in mice kidney cortex. *In vitro*, I observed that silencing CLIC4 expression in cultured human glomerular endothelial cells, strongly reduced ERM phosphorylation and ERM association with the cytoskeleton. The effect of CLIC4 silencing on ERM protein phosphorylation was rescued by CLIC4 or CLIC5A overexpression. These findings suggest that CLIC5A and CLIC4 have overlapping functions, at least in activating ERM proteins. To further assess the possibility of functional redundancy, we generated CLIC4^{-/-} CLIC5^{-/-} double mutant mice. While CLIC5 deficiency alone eliminated podocyte-associated ERM phosphorylation, when CLIC5 or CLIC4 were deleted singly, endothelial ERM phosphorylation persisted. Only the combined CLIC4 and CLIC5 deficiency resulted in a dramatic reduction of p-ERM abundance in both, glomerular podocyte and endothelial cells. These results are interpreted to indicate that in podocytes, which express CLIC5A, but not CLIC4, ERM phosphorylation is dependent on only CLIC5A. By contrast, in

glomerular endothelial cells, which express both CLIC5A and CLIC4, these two CLICs have overlapping functions in stimulating ERM protein activation.

I also determined whether CLICs are involved in fenestrae formation. I did not observe any change in glomerular capillary EC fenestrae in young CLIC5A, or dual CLIC5A/CLIC4 deficient mice, and overexpression of CLIC5A in cultured glomerular EC, did not promote the formation of fenestrae in these cells, by scanning electron microscopy (Xin Wang, Unpublished Data). However, in older dual CLIC5/CLIC4 deficient mice and in hypertensive CLIC5 deficient mice, there is a significant reduction in fenestrae density. The findings suggest that CLIC4/CLIC5A-mediated ERM activation is required for long-term maintenance of glomerular fenestrae.

As mentioned in chapter I, the glycocalyx layer in fenestrae contributes to the overall hydraulic resistance of the glomerular filtration barrier [48, 120] and any changes in glycocalyx within the fenestrae may damage the glomerular filtration barrier and potentially affect GFR [121]. Podocalyxin is the major constituent of the glomerular glycocalyx. Consistent with findings by Pierchala, B.A. et al., I observed a reduction in podocalyxin protein expression in CLIC5^{-/-} mice at baseline [122, 123]. In response to DOCA/Salt hypertension podocalyxin protein expression was further reduced in CLIC5^{-/-} mice compared to the wild type mice along with a reduction in fenestrae frequency [122]. It is of note that in my pilot study perfusion of protamine sulfate in wild type mice that neutralizes anionic charge of mainly podocalyxin resulted in a significant reduction in p-ERM levels as well as defenestration of glomerular endothelial cells (Figure 6.1). Collectively, The reduction in fenestrae frequency in hypertensive CLIC5^{-/-} and normotensive CLIC4^{-/-}CLIC5^{-/-} mice as well as in protamine sulfate infused wild type may be at least in part caused by disruption of endothelial glycocalyx.

6.1.1 Rac1 activation by CLIC5A:

The question that remained to be answered is how Rac1 is activated by CLIC5A.

There are two major cycles regulating Rac1 activation. Rac1 continuously cycles between the GTP-bound active state and GDP-bound inactive state. Activation of small GTPases requires guanine nucleotide exchange factors (GEFs) that facilitate the exchange of GDP for GTP. The inherent GTPase activity, which is enhanced by the GTPase activating Proteins (GAPs), results in inactivation of Rac1 [382]. At basal conditions, most of Rac1 exist in the cytoplasm in complex with Rho GDI, which inhibits its interactions with Rho GEFs or Rho GAPs. The second cycle that controls Rac1 activity is the cytoplasm to membrane translocation cycle. Prenylation of Rac1 GTPase at its C terminus enhances Rac1 binding to plasma membrane [383, 384]. Rac1 localization at the plasma membrane is also regulated positively by the presence of PI[4,5]P₂, PI[3,4,5]P₃ and plasma rafts [384, 385]. Below I summarize some possible mechanisms by which CLIC5A can modulate the activity of Rac1.

6.1.1.1 CLIC5A-induced PI[4,5]P₂ cluster formation results in Rac1 activation:

It is suggested that Rac1 membrane translocation via interaction with phospholipids such as PI[4,5]P₂ and PI[3,4,5]P₃ precedes nucleotide exchange events by Rac-GEFs that result in Rac1 activation [385]. Moreover many members of Rho-GEFs contain PH domains that bind to PI[4,5]P₂ and PI[3,4,5]P₃ which results in their activation [386-388]. Therefore one possible mechanism for CLIC5A-mediated Rac1 activation is that CLIC5A enhances cluster formation of PI[4,5]P₂ in discrete areas of phospholipid bilayers where Rac1 and its activators (Rho GEF) can be recruited and become activated.

6.1.1.2 CLIC5A-induced formation of Podocalyxin/NHERF2/Ezrin complex regulates Rac1/RhoA activation.

In glomeruli CLIC5A is a component of Podocalyxin/NHERF2/Ezrin complex. CLIC5A is expressed at the apical membrane domain of podocyte foot processes, where it co-localizes with podocalyxin, NHERF2 and ezrin and in glomerular lysates podocalyxin co-immunoprecipitates with CLIC5A [5]. In CLIC5 deficient mice, glomerular podocyte ezrin phosphorylation was abrogated, and both ezrin and NHERF2 were found dissociated from the actin cytoskeleton [4, 5]; Therefore CLIC5A promotes the formation of podocalyxin/NHERF2/Ezrin protein complex. Podocalyxin itself has been found to initiate signalling pathways that activate Rac1/RhoA/Cdc42 and regulate cytoskeletal rearrangements [8, 389, 390]. Podocalyxin/NHERF2/Ezrin complex activates small Rho GTPases such as RhoA and Rac1 by sequestering the inhibitory RhoGDI protein by ezrin [389]. As revealed by bioinformatics analysis, 40% of human Rho GEFs contain a putative PDZ-binding motif at their C terminus and NHERF2 functions to recruit Rho GEF through its PDZ domain [8, 391]. Recruiting a putative Rac1 GEF (such as ARHGEF7) through NHERF2 PDZ domain further facilitate the GDP/GTP exchange of Rac1 [8]. Taken together Rac1 activation by CLIC5A may be through the function of Podocalyxin/NHERF2/Ezrin molecular complex.

6.1.2 Model of CLIC5A/Rac1 action in podocytes

Taken together with the findings in Chapters 3, 4 and 5, I therefore propose the following schematic model to explain the mechanism of CLIC5A function in glomerular podocytes (Figure 6.2). In the apical plasma membrane of podocytes from wild type mice (CLIC5^{+/+}) the association of CLIC5A with the inner leaflet of the plasma membrane (along with possible

interaction between CLIC5A and Podocalyxin) results in the formation of a membrane bound protein complex including CLIC5A, Rac1-GTP and PI(4)P5K via multiple weak interactions which serves to promote clustered PI[4,5]P₂ generation. Ezrin binding to PI[4,5]P₂ leads to a conformational change of ezrin, unmasking its N and C terminals, which then promotes binding of one of the lobes in the ezrin N terminal FERM domain to NHERF2 and podocalyxin as well as binding of the ezrin C-terminus to F-actin. The conformational change produced by the PI[4,5]P₂ /ezrin interaction also unmask the C-terminal Thr phosphorylation which is then phosphorylated by PKC.

PI[4,5]P₂ cleavage to inositol trisphosphate (IP₃) and diacylglycerol (DAG) by the enzyme phospholipase C (PLC) initiates intracellular calcium release and PKC activation. Consensus phosphorylation sites for PKC, PKA, and tyrosine kinases on CLIC family members including CLIC5A suggest that post-translational modification contributes to the physiology of CLIC proteins. Hence, I think that PKC not only phosphorylates ERM proteins, but that it may also phosphorylate CLIC5A to stabilize the CLIC5A/Podocalyxin protein complex.

There are multiple potential feedback and amplification loops in this signaling cascade. It has been reported that p-ERM sequesters RhoGDI and results in releasing and activating Rac1 by a putative Rho GEF, recruited by NHERF2, producing a positive feedback effect [38]. Several feedback routes could enhance and stabilize the CLIC5A/Rac1/Pak1,3 effect on actin organization. It is well-accepted that Rac1 activates PI(4)P5K, which generates PI[4,5]P₂, and that PI[4,5]P₂ in turn, binds to several proteins that are activated by Rac1 including Pak1-3, cofilin, profilin and ERM. P-ERM also sequesters RhoGDI and result in releasing and activating Rho GTPases, producing a positive feedback effect [392]. It is of note that a negative feedback loop between Rho GTPases and ERM has also been reported [175]. Pak1 can phosphorylate

RhoGDI, leading to dissociation of RhoGDI from Rac1 and produces another positive feed back route [393].

In my schematic model of the apical plasma membrane of podocytes from CLIC5^{-/-} mice (Figure 6.3), Rac1 is inactive. RhoGDI sequesters Rac1 in the inactive conformation in the cytosol. NHERF2 and ERM protein Ezrin are also in inactive state and the interaction between podocalyxin and subjacent filamentous actin, which requires Ezrin is compromised.

To conclude, I have shown that the action of CLIC5A to stimulate PI[4,5]P2 generation and downstream ERM phosphorylation, as well as its ability to stimulate Pak1,3 phosphorylation both in vivo and in vitro are dependent on the action of CLIC5A on Rac1. I found that this mechanism is induced by DOCA/Salt hypertension in podocytes of wild-type mice but not CLIC5^{-/-} mice. I am postulating that Rac1 is relatively inactive in CLIC5 deficient mice, at least at the apical domain, and that this leads to dissociation of the Podocalyxin/NHERF-2/ERM complex from the actin cytoskeleton. My work in the hypertension model suggests that this complex at the apical domain of podocyte foot processes is critical in allowing podocyte adaptation to the stress of capillary wall tension. Finally, I have also shown that CLIC4 and CLIC5A have similar mechanisms of action, but that CLIC5A is active by itself in podocytes, whereas CLIC4 and CLIC5A operate in glomerular endothelial cells. CLIC4/CLIC5A-mediated ERM activation in endothelial cells is not necessary for fenestrae formation but is required for long-term maintenance of glomerular fenestrae.

This thesis provides a platform for further studies investigating the precise molecular interactions between CLIC family members, the RhoGTPases and the actin cytoskeleton.

6.2 Future Directions

6.2.1 To Explore the nature of molecular and functional interaction between CLIC5A and Rac1.

In COS7 cells, I found that CLIC5A expression, induced the accumulation of the PI[4,5]P2 reporter GFP- or RFP-PH-PLC in discrete dorsal PM patches and enhanced ERM and Pak1,3 phosphorylation. CLIC5A increased Rac1 activity but not Rho or Cdc42 activity. CLIC5A-stimulated PI[4,5]P2 generation, ERM phosphorylation and Pak1,3 activation are all dependent on Rac1. Rac1 inhibition also resulted in redistribution of GFP-CLIC5A from the dorsal membrane to basolateral domain suggesting that Rac1 might be in charge of translocation of CLIC5A to discrete plasma membranes. The questions that are remained to be answered are whether CLIC5A actually interacts with Rac1, and if so whether it might act as a GEF or an inhibitor of a Rac1 specific Rho GAP.

Although CLICs do not contain a known Rho GEF domain (also called Dbl-homologous, a structural domain of guanine nucleotide exchange factor for Rho-Rac-Cdc42 –like GTPases) but variety of unrelated structural domains have been shown to exhibit guanine nucleotide exchange activity; Therefore we will explore the hypothesis that CLIC5A function as a Rho GEF or increase the activity of a putative Rho GEF in cells.

To determine whether CLIC5A can potentially act as a Rho GEF to activate Rac1 or enhances the activity of a putative Rho GEF we would employ the Rho GEF assay kit commercially available by Cytoskeleton Inc. (Denver, CO, U.S.A.). The assay is based on the spectroscopic difference between bound and unbound fluorescent analogs to guanine nucleotides to monitor the states of small GTPases. Once bound to GTPases, the fluorophore emission intensity increases

which reflects the GEF activity. The same company also provides a kit for Rho GAP assay that measures the amount of inorganic phosphate (Pi) that is generated as a result of G-protein dependent hydrolysis of GTP to GDP + Pi. These assays will assist us to determine whether CLIC5A functions as a Rho GEF to enhance the exchange of GDP for GTP or increase the activity of a putative Rho GEF or inhibit the activities of a putative Rho GAP in cells.

6.2.2 Mechanism(s) regulating the CLIC5A-plasma membrane association.

As mentioned in chapter I, CLIC proteins are found in the cytoplasm and at the plasma membrane of the cells and can translocate from cytosolic to membrane compartments [203, 232, 394]. CLICs translocation from cytoplasm to plasma membrane is regulated via the redox state of the molecule as well as pH. Acidic pH and oxidizing conditions enhance the CLICs translocation to plasma membrane. Oxidation produces a dramatic conformational change [395] extending the N-terminal alpha-helical region [396] that promotes partitioning into lipid bilayers [209, 397]. All CLICs can partition into lipid bilayers [215]. This is reminiscent of the association of bacterial porins and Bcl-x family members with lipid bilayers [282, 398].

In my experiments CLIC5A at basal conditions associated with the dorsal plasma membrane of COS7 cells consistent with the distribution of CLIC5A in podocyte foot processes, where CLIC5A is expressed in the apical plasma membrane domain. CLIC5A is a component of Podocalyxin/NHERF2/Ezrin protein complex [5]. In CLIC5^{-/-} mice, the co-localization of p-ERM with podocalyxin in glomeruli is significantly reduced [4]. Furthermore, when I treated the COS7 cells with a Rac1 inhibitor, CLIC5A rapidly dissociated from the plasma membrane. Similarly COS7 treatments with PLC activator that depletes PI[4,5]P2 results in rapid dissociation of CLIC5A from plasma membrane. The CLIC proteins lack signal peptide to direct

them towards the plasma membrane [203]. These results suggest that CLIC5A is targeted to the apical plasma membrane via an unknown mechanism in a reversible fashion. Therefore CLIC5A may either reversibly bind to an integral membrane protein such as podocalyxin or a specialized lipid micro-domains direct CLIC5A binding with discrete locations in plasma membrane. Further studies will assist us in understanding the nature of mechanism(s) regulating the CLIC5A-plasma membrane association.

6.2.3 To explore whether CLIC5A/Rac1-dependent cytoskeletal remodeling is spatially restricted both at baseline and during kidney injury.

In chapter 3 of my thesis I found that CLIC5A/Rac1 protein complex promotes the apical podocalyxin-actin interaction and protects glomerular capillaries from the effects of hypertension. However it is reported that generalized Rac1 activation in podocytes is deleterious, and result in foot process effacement and proteinuria [157, 313, 399]; This suggests that CLIC5A-dependent Rac1 activation maybe tightly restricted to the apical Podocalyxin-NHERF2-Ezrin complex.

In podocytes Rac1 functions at least in 3 domains via its interaction with different protein complexes at different domains of the cell. As mentioned earlier in detail, at the apical domain of podocyte foot processes, signals from Ezrin/NHERF2/podocalyxin, can regulate Rac1 activity [8, 390].

At basal domain Rac1 interacts with the members of focal adhesion complex integrin/talin/FAK/Paxillin and has a major role during the active remodeling of focal adhesion complexes in motile cells [67, 285]. In slit diaphragm Rac1 interacts with

Nephrin/Podocin/CD2AP/Nck protein complex and regulate actin polymerization [66]. In the stable, differentiated podocytes, Rac1 activity at the slit diaphragm and at the basal focal adhesions is low, and aberrant Rac1 activity in focal adhesions and the slit diaphragm complex result in foot process effacement and proteinuria.

My data suggest that CLIC5 deletion may only disrupt the cytoskeletal interaction of the podocalyxin/NHERF2/ezrin complex with detrimental effect during hypertension. I propose that CLIC5A acting on Rac1, produces location- and function-specific PI[4,5]P2 pools at the apical plasma membrane of podocyte foot processes, supporting Ezrin activation and its coupling to Podocalyxin.

To test this hypothesis one would determine whether CLIC5 deficiency at baseline alters the association of slit diaphragm or focal complex proteins from the cytoskeleton or CLIC5A actions are restricted to the apical domain of podocyte foot processes. To study the effect of CLIC5A/Rac1-dependent cytoskeletal remodeling during injury I propose using Protamine Sulfate (PS) model. Podocyte cytoskeletal dysregulation is a central event in albuminuria. In many kidney diseases, podocytes initially undergo simplification and retraction of podocyte FPs (FPs effacement). Protamine sulfate (PS) in an actin dependent process neutralizes anionic charge of mainly podocalyxin and disrupts podocyte-basement membrane interaction within minutes. The injury is reversible, since washout of PS with the polyanion heparin restores podocyte architecture [400]. PS infusion increases Rac1 activation and PodoRac1^{-/-} mice are resistant to protamine sulfate [401]. Rac1 effector PAK1 activates the cofilin phosphorylation through LIM kinase and regulates the cytoskeleton. Mice with podocyte specific deletion of cofilin-1 did not recover normal structure following additional perfusion with heparin sulphate [402]. In my pilot study, PS infusion in a wild type mouse for 15 minutes resulted in extensive

foot process fusion (Figure 6.1). Since my recent data indicates that CLIC5A regulates actin remodeling by Rac1 activation, we test the hypothesis that CLIC5A interaction with podocalyxin is required for podocyte remodeling in protamine sulfate model of acute podocyte injury as well as the restoration of normal podocyte architecture during recovery. Further more by evaluating the association of slit diaphragm or focal complex proteins from the cytoskeleton in podocytes lacking CLIC5A during injury and recovery we can determine whether action of CLIC5A and its downstream effectors are spatially restricted.

6.2.4 To explore the role of CLIC5A-Rac1-Ezrin and CLIC5A-Rac1-Pak1 pathway in diabetic nephropathy.

We have well established that CLIC5A is a major podocyte protein that is essential for the phosphorylation of ezrin via Rac1/PIP5K/PI[4,5]P2 pathway, which in turn serves to organize the apical structure of podocyte foot processes. Phosphorylated ezrin connects podocalyxin to cortical actin with NHERF2 as an intermediate, and loss of this interaction disrupts podocyte function [58]. I showed that in CLIC5^{-/-} mice activation of podocyte ERM and Pak1,3 is reduced and podocalyxin abundance declines. The morphological abnormalities in CLIC5 deficient mice enhance their susceptibility to Adriamycin and DOCA/Salt hypertension kidney injuries. Hence CLIC5A by activating Rac1 enhance the association of apical podocalyxin/Ezrin complex to actin via NHERF2 and defines the apical architecture of podocytes.

It would be of our interest to extend this work to explore the role of CLIC5A-Rac1-Ezrin and CLIC5A-Rac1-Pak axis in human diseases that are associated with kidney injury, specifically diabetic nephropathy. So far majority of studies about podocytes, have focused on the abnormalities in protein complexes of the specialized filtration slit diaphragm [56, 403] and

molecular mechanisms that form the apical domain of podocyte foot processes have attracted much less attention. While it is widely accepted that podocyte damage has a significant role in the development of diabetic nephropathy and it is reported that in diabetic patients podocyte glycocalyx and podocyte architecture are abnormal [404, 405] and podocyte specific deletion of Rac1 results in increased ACR in the type 1 diabetic mouse model [406] the role of the CLIC5A-Rac1-Pak/Ezrin at the apical domain of podocyte, has not been investigated. We postulate that alteration in CLIC5A-dependent regulation of the apical actin-based podocyte architecture may be a potential determinant of human diabetic nephropathy.

Figure 6.1

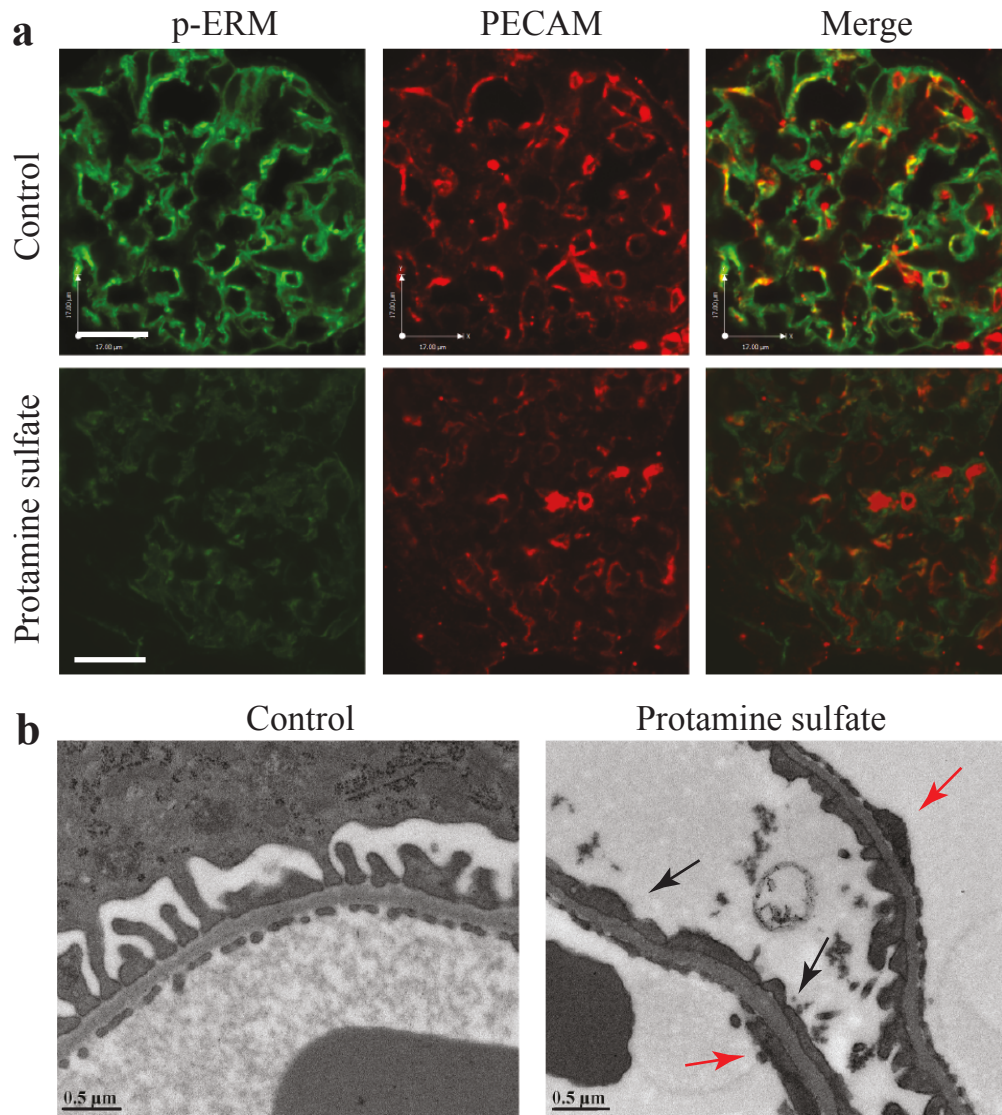


Figure 6.1 | Protamine sulfate infusion results in significant reduction in p-ERM levels in mice glomeruli as well as extensive reduction in EC fenestrae and podocyte foot processes frequency. (new data, pilot experiment). (a) Dual-label confocal immunofluorescence microscopy for p-ERM (green) and PECAM in glomeruli of CLIC5^{+/+} mice;(scale bar = 20 µm). Protamine sulfate treatment significantly reduced p-ERM levels in the wild type mouse . (b) Transmission electron microscopic appearance of glomerular capillary wall. Glomerular EC fenestrae density was markedly reduced after protamine sulphate infusion (red arrows). Protamine sulfate also resulted in extensive fusion of podocyte foot processes (black arrows);(scale bar = 0.5 µm).

Figure 6.2

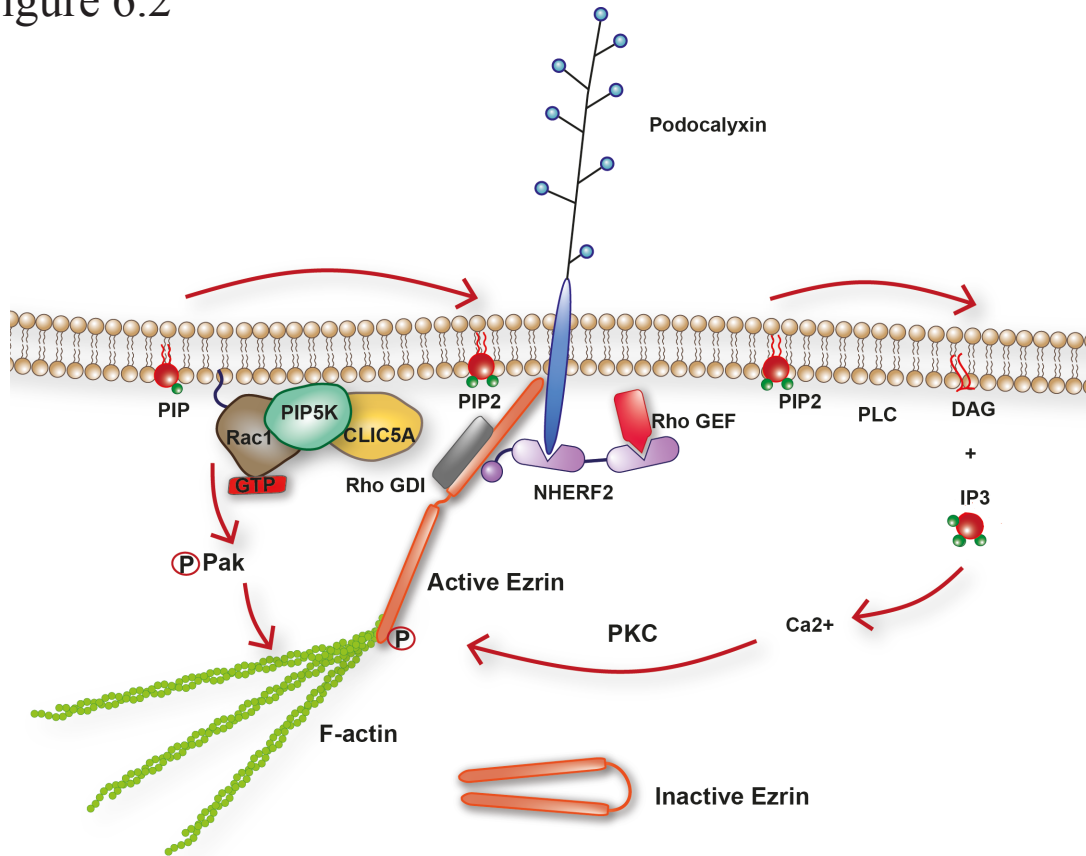


Figure 6.2 | schematic model of CLIC5A function In apical plasma membrane of podocytes. The association of CLIC5A with the inner leaflet of the dorsal plasma membrane of podocyte foot processes (along with possible interaction between CLIC5A and Podocalyxin) results in the formation of a membrane bound protein complex including CLIC5A, Rac1- GTP and PIP5K via multiple weak interactions which serves to promote clustered PI[4,5]P2 generation. Ezrin binding to PI[4,5]P2 leads to a conformational change, unmasking its N and C terminal and promotes binding the ezrin N terminal to NHERF2 and podocalyxin and the ezrin C-terminus to interact with F-actin and to be phosphorylated by PKC. PI[4,5]P2 cleavage to inositol trisphosphate (IP3) and diacylglycerol (DAG) by the enzyme phospholipase C (PLC) initiates intracellular calcium release and PKC activation. P-ERM sequesters RhoGDI and result in releasing and activating Rac1 by a putative Rho GEF which is recruited by NHERF2, producing a positive feedback effect [38]. CLIC5A/Rac1 furthermore activates Pak1,3 which stabilizes F-actin.

CLIC5A:Chloride intracellular channel 5A. Rac1:Ras-related C3 botulinum substrate 1. PIP: Phosphatidylinositol 4 phosphate. PIP2: Phosphatidylinositol 4,5-bisphosphate. PIP5K: Phosphatidylinositol 4 phosphate 5 kinase. Pak1: p21-activated kinase. F-actin: Flamentous actin. NHERF2: Na⁺/H⁺ exchanger regulatory factor 2. PLC: Phospholipase C. DAG: diacylglycerol. IP3: inositol 1,4,5-trisphosphate . PKC: protein kinase C. Rho GDI: Rho protein GDP dissociation inhibitor. Rho GEF: guanine nucleotide exchange factors. GTP: Guanosine triphosphate.

Figure 6.3

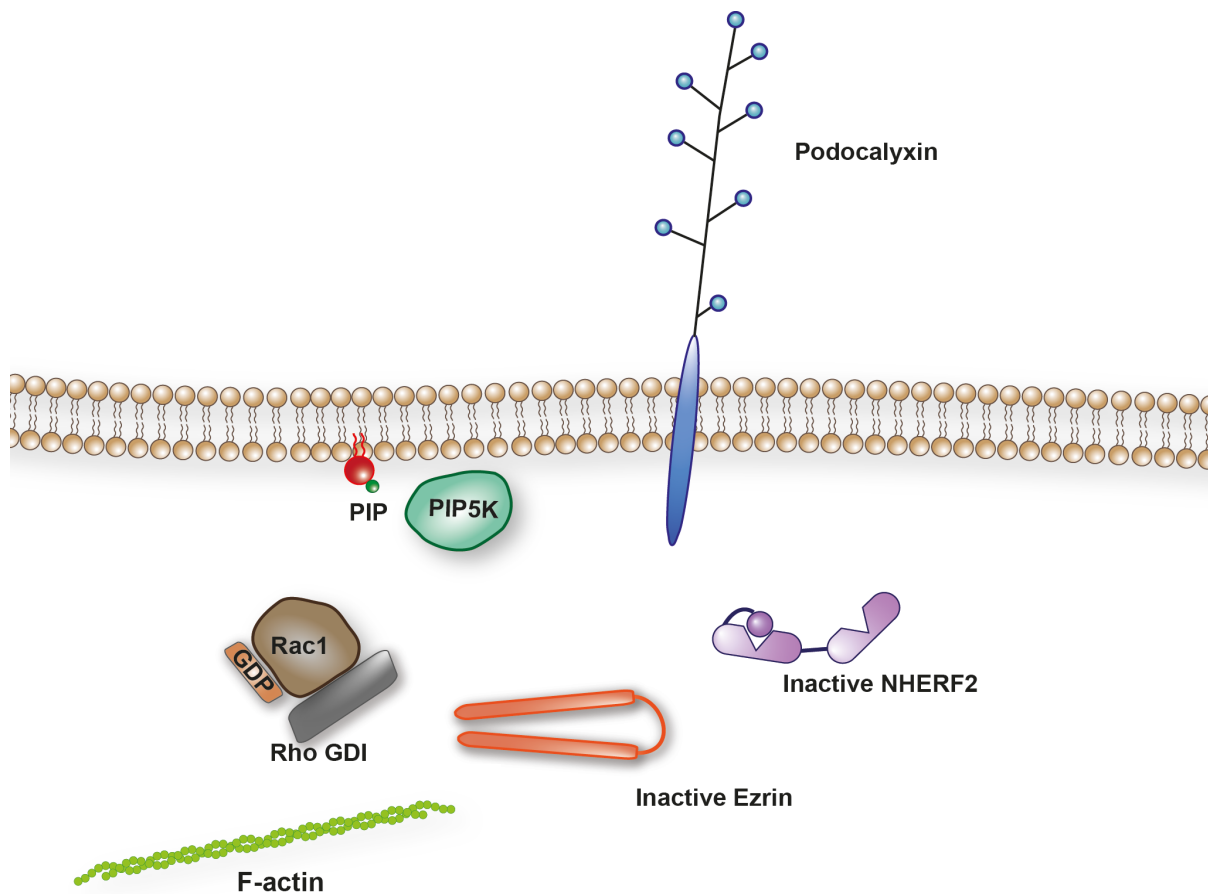


Figure 6.3 | schematic model of apical domain of podocyte foot processes in CLIC5 deficient (CLIC5^{-/-}) mice.

In apical plasma membrane of podocytes from CLIC5^{-/-} mice, Rac1 is bound to GDP (Rac1-GDP) and hence inactive. RhoGDI sequesters Rac1 in the inactive conformation in the cytosol. NHERF2 and ERM protein Ezrin are also in inactive state and the interaction between Podocalyxin and subjacent filamentous actin, which requires Ezrin is compromised.

CLIC5A: Chloride intracellular channel 5A. Rac1: Ras-related C3 botulinum substrate 1. PIP: Phosphatidylinositol 4 phosphate. PIP5K: Phosphatidylinositol 4 phosphate 5 kinase. NHERF2: Na⁺/H⁺ exchanger regulatory factor 2. Rho GDI: Rho protein GDP dissociation inhibitor. GDP: Guanosine diphosphate.

References

1. Haraldsson, B., J. Nystrom, and W.M. Deen, Properties of the glomerular barrier and mechanisms of proteinuria. *Physiol Rev*, 2008. 88(2): p. 451-87.
2. Endlich, N. and K. Endlich, The challenge and response of podocytes to glomerular hypertension. *Semin Nephrol*, 2012. 32(4): p. 327-41.
3. Nystrom, J., et al., A human glomerular SAGE transcriptome database. *BMC Nephrol*, 2009. 10: p. 13.
4. Al-Momany, A., et al., Clustered PI(4,5)P-2 accumulation and ezrin phosphorylation in response to CLIC5A. *J Cell Sci*, 2014. 127(Pt 24): p. 5164-78.
5. Wegner, B., et al., CLIC5A, a component of the ezrin-podocalyxin complex in glomeruli, is a determinant of podocyte integrity. *Am J Physiol Renal Physiol*, 2010. 298(6): p. F1492-503.
6. Fukasawa, H., et al., Phosphorylation of podocalyxin (Ser415) Prevents RhoA and ezrin activation and disrupts its interaction with the actin cytoskeleton. *Am J Pathol*, 2011. 179(5): p. 2254-65.
7. Schmieder, S., et al., Podocalyxin activates RhoA and induces actin reorganization through NHERF1 and Ezrin in MDCK cells. *J Am Soc Nephrol*, 2004. 15(9): p. 2289-98.
8. Hsu, Y.H., et al., Podocalyxin EBP50 ezrin molecular complex enhances the metastatic potential of renal cell carcinoma through recruiting Rac1 guanine nucleotide exchange factor ARHGEF7. *Am J Pathol*, 2010. 176(6): p. 3050-61.
9. Choi, S., et al., PIP kinases define PI4,5P(2)signaling specificity by association with effectors. *Biochim Biophys Acta*, 2015. 1851(6): p. 711-23.

10. Blount, M.A., et al., Expression of transporters involved in urine concentration recovers differently after cessation of lithium treatment. *Am J Physiol Renal Physiol*, 2010. **298**(3): p. F601-8.
11. Kraut, J.A. and N.E. Madias, Metabolic Acidosis of CKD: An Update. *Am J Kidney Dis*, 2016. **67**(2): p. 307-17.
12. Rogerson, F.M., et al., Presence of angiotensin converting enzyme in the adventitia of large blood vessels. *J Hypertens*, 1992. **10**(7): p. 615-20.
13. Li, Y.T. and G.F. Cheng, [New regulator in renin angiotensin system: ACE2]. *Sheng Li Ke Xue Jin Zhan*, 2006. **37**(2): p. 179-81.
14. Burrell, L.M., et al., ACE2, a new regulator of the renin-angiotensin system. *Trends Endocrinol Metab*, 2004. **15**(4): p. 166-9.
15. Johnston, C.I., Franz Volhard Lecture. Renin-angiotensin system: a dual tissue and hormonal system for cardiovascular control. *J Hypertens Suppl*, 1992. **10**(7): p. S13-26.
16. Sarzani, R., et al., Renin-angiotensin system, natriuretic peptides, obesity, metabolic syndrome, and hypertension: an integrated view in humans. *J Hypertens*, 2008. **26**(5): p. 831-43.
17. Schlondorff, D., Roles of the mesangium in glomerular function. *Kidney Int*, 1996. **49**(6): p. 1583-5.
18. Kodner, C., Diagnosis and Management of Nephrotic Syndrome in Adults. *Am Fam Physician*, 2016. **93**(6): p. 479-85.
19. Bierzynska, A., K. Soderquest, and A. Koziell, Genes and podocytes - new insights into mechanisms of podocytopathy. *Front Endocrinol (Lausanne)*, 2014. **5**: p. 226.

20. Ballermann, B.J., Glomerular endothelial cell differentiation. *Kidney Int*, 2005. **67**(5): p. 1668-71.
21. Nagai, T., et al., Actin filaments around endothelial fenestrae in rat hepatic sinusoidal endothelial cells. *Med Electron Microsc*, 2004. **37**(4): p. 252-5.
22. Vasmant, D., M. Maurice, and G. Feldmann, Cytoskeleton ultrastructure of podocytes and glomerular endothelial cells in man and in the rat. *Anat Rec*, 1984. **210**(1): p. 17-24.
23. Eremina, V., H.J. Baelde, and S.E. Quaggin, Role of the VEGF--a signaling pathway in the glomerulus: evidence for crosstalk between components of the glomerular filtration barrier. *Nephron Physiol*, 2007. **106**(2): p. p32-7.
24. Liu, A., A. Dardik, and B.J. Ballermann, Neutralizing TGF-beta1 antibody infusion in neonatal rat delays in vivo glomerular capillary formation 1. *Kidney Int*, 1999. **56**(4): p. 1334-48.
25. Pino, R.M., The cell surface of a restrictive fenestrated endothelium. I. Distribution of lectin-receptor monosaccharides on the choriocapillaris. *Cell Tissue Res*, 1986. **243**(1): p. 145-55.
26. Pino, R.M., The cell surface of a restrictive fenestrated endothelium. II. Dynamics of cationic ferritin binding and the identification of heparin and heparan sulfate domains on the choriocapillaris. *Cell Tissue Res*, 1986. **243**(1): p. 157-64.
27. Cao, R., et al., Comparative evaluation of FGF-2-, VEGF-A-, and VEGF-C-induced angiogenesis, lymphangiogenesis, vascular fenestrations, and permeability. *Circ Res*, 2004. **94**(5): p. 664-70.
28. Ballermann, B.J., Contribution of the endothelium to the glomerular permselectivity barrier in health and disease. *Nephron Physiol*, 2007. **106**(2): p. p19-25.

29. Avasthi, P.S., A.P. Evan, and D. Hay, Glomerular endothelial cells in uranyl nitrate-induced acute renal failure in rats. *J Clin Invest*, 1980. **65**(1): p. 121-7.
30. Lea, P.J., et al., Tridimensional ultrastructure of glomerular capillary endothelium revealed by high-resolution scanning electron microscopy. *Microvasc Res*, 1989. **38**(3): p. 296-308.
31. Jeansson, M. and B. Haraldsson, Morphological and functional evidence for an important role of the endothelial cell glycocalyx in the glomerular barrier. *Am J Physiol Renal Physiol*, 2006. **290**(1): p. F111-6.
32. Jeansson, M., et al., Adriamycin alters glomerular endothelium to induce proteinuria. *J Am Soc Nephrol*, 2009. **20**(1): p. 114-22.
33. Kuwabara, A., et al., Deterioration of glomerular endothelial surface layer induced by oxidative stress is implicated in altered permeability of macromolecules in Zucker fatty rats. *Diabetologia*, 2010. **53**(9): p. 2056-65.
34. Menzel, S. and M.J. Moeller, Role of the podocyte in proteinuria. *Pediatr Nephrol*, 2011. **26**(10): p. 1775-80.
35. Davila-Esqueda, M.E., A.A. Vertiz-Hernandez, and F. Martinez-Morales, Comparative analysis of the renoprotective effects of pentoxifylline and vitamin E on streptozotocin-induced diabetes mellitus. *Ren Fail*, 2005. **27**(1): p. 115-22.
36. Ichimura, K., et al., Glomerular endothelial cells form diaphragms during development and pathologic conditions. *J Am Soc Nephrol*, 2008. **19**(8): p. 1463-71.
37. Kobayashi, M., et al., Glomerular endothelial changes in cyclosporine A-treated rats: scanning and transmission electron microscopic studies. *Jpn J Surg*, 1991. **21**(2): p. 210-15.

38. Toyoda, M., et al., Podocyte detachment and reduced glomerular capillary endothelial fenestration in human type 1 diabetic nephropathy. *Diabetes*, 2007. **56**(8): p. 2155-60.
39. Wavamunno, M.D., et al., Transplant glomerulopathy: ultrastructural abnormalities occur early in longitudinal analysis of protocol biopsies. *Am J Transplant*, 2007. **7**(12): p. 2757-68.
40. Miner, J.H., The glomerular basement membrane. *Exp Cell Res*, 2012. **318**(9): p. 973-8.
41. Jarad, G. and J.H. Miner, Update on the glomerular filtration barrier. *Curr Opin Nephrol Hypertens*, 2009. **18**(3): p. 226-32.
42. Haas, M., Alport syndrome and thin glomerular basement membrane nephropathy: a practical approach to diagnosis. *Arch Pathol Lab Med*, 2009. **133**(2): p. 224-32.
43. Batsford, S.R., R. Rohrbach, and A. Vogt, Size restriction in the glomerular capillary wall: importance of lamina densa. *Kidney Int*, 1987. **31**(3): p. 710-7.
44. Takami, H., et al., Ultrastructure of glomerular basement membrane by quick-freeze and deep-etch methods. *Kidney Int*, 1991. **39**(4): p. 659-64.
45. Bertolatus, J.A. and D. Klinzman, Macromolecular sieving by glomerular basement membrane in vitro: effect of polycation or biochemical modifications. *Microvasc Res*, 1991. **41**(3): p. 311-27.
46. Bolton, G.R., W.M. Deen, and B.S. Daniels, Assessment of the charge selectivity of glomerular basement membrane using Ficoll sulfate. *Am J Physiol*, 1998. **274**(5 Pt 2): p. F889-96.
47. Daniels, B.S., et al., Glomerular basement membrane: in vitro studies of water and protein permeability. *Am J Physiol*, 1992. **262**(6 Pt 2): p. F919-26.

48. Deen, W.M., M.J. Lazzara, and B.D. Myers, Structural determinants of glomerular permeability. *Am J Physiol Renal Physiol*, 2001. **281**(4): p. F579-96.
49. Caulfield, J.P. and M.G. Farquhar, The permeability of glomerular capillaries of aminonucleoside nephrotic rats to graded dextrans. *J Exp Med*, 1975. **142**(1): p. 61-83.
50. Farquhar, M.G. and G.E. Palade, Segregation of ferritin in glomerular protein absorption droplets. *J Biophys Biochem Cytol*, 1960. **7**: p. 297-304.
51. Noakes, P.G., et al., The renal glomerulus of mice lacking α -laminin/laminin beta 2: nephrosis despite molecular compensation by laminin beta 1. *Nat Genet*, 1995. **10**(4): p. 400-6.
52. Zenker, M., et al., Human laminin beta2 deficiency causes congenital nephrosis with mesangial sclerosis and distinct eye abnormalities. *Hum Mol Genet*, 2004. **13**(21): p. 2625-32.
53. Kuhn, K., et al., An ultrastructural study of the mechanisms of proteinuria in rat nephrotoxic nephritis. *Lab Invest*, 1977. **36**(4): p. 375-87.
54. Ryan, G.B. and M.J. Karnovsky, An ultrastructural study of the mechanisms of proteinuria in aminonucleoside nephrosis. *Kidney Int*, 1975. **8**(4): p. 219-32.
55. Venkatachalam, M.A., M.J. Karnovsky, and R.S. Cotran, Glomerular permeability. Ultrastructural studies in experimental nephrosis using horseradish peroxidase as a tracer. *J Exp Med*, 1969. **130**(2): p. 381-99.
56. Welsh, G.I. and M.A. Saleem, The podocyte cytoskeleton--key to a functioning glomerulus in health and disease. *Nat Rev Nephrol*, 2012. **8**(1): p. 14-21.
57. Kerjaschki, D., Caught flat-footed: podocyte damage and the molecular bases of focal glomerulosclerosis. *J Clin Invest*, 2001. **108**(11): p. 1583-7.

58. Takeda, T., et al., Loss of glomerular foot processes is associated with uncoupling of podocalyxin from the actin cytoskeleton. *J Clin Invest*, 2001. **108**(2): p. 289-301.
59. Hattori, M., et al., Increase of integrin-linked kinase activity in cultured podocytes upon stimulation with plasma from patients with recurrent FSGS. *Am J Transplant*, 2008. **8**(7): p. 1550-6.
60. Tryggvason, K., Unraveling the mechanisms of glomerular ultrafiltration: nephrin, a key component of the slit diaphragm. *J Am Soc Nephrol*, 1999. **10**(11): p. 2440-5.
61. Garg, P., et al., Neph1 cooperates with nephrin to transduce a signal that induces actin polymerization. *Mol Cell Biol*, 2007. **27**(24): p. 8698-712.
62. Harita, Y., et al., Phosphorylation of Nephrin Triggers Ca²⁺ Signaling by Recruitment and Activation of Phospholipase C- γ 1. *J Biol Chem*, 2009. **284**(13): p. 8951-62.
63. Zhu, J., et al., Nephrin mediates actin reorganization via phosphoinositide 3-kinase in podocytes. *Kidney Int*, 2008. **73**(5): p. 556-66.
64. George, B., et al., Crk1/2-dependent signaling is necessary for podocyte foot process spreading in mouse models of glomerular disease. *J Clin Invest*, 2012. **122**(2): p. 674-92.
65. Jones, N., et al., Nck adaptor proteins link nephrin to the actin cytoskeleton of kidney podocytes. *Nature*, 2006. **440**(7085): p. 818-23.
66. Zhu, J., et al., p21-activated kinases regulate actin remodeling in glomerular podocytes. *Am J Physiol Renal Physiol*, 2010. **298**(4): p. F951-61.
67. Kraynov, V.S., et al., Localized Rac activation dynamics visualized in living cells. *Science*, 2000. **290**(5490): p. 333-7.

68. Wharram, B.L., et al., Altered podocyte structure in GLEPP1 (Ptpro)-deficient mice associated with hypertension and low glomerular filtration rate. *J Clin Invest*, 2000. **106**(10): p. 1281-90.
69. Kim, Y.H., et al., GLEPP1 receptor tyrosine phosphatase (Ptpro) in rat PAN nephrosis. A marker of acute podocyte injury. *Nephron*, 2002. **90**(4): p. 471-6.
70. Nielsen, J.S. and K.M. McNagny, Novel functions of the CD34 family. *J Cell Sci*, 2008. **121**(Pt 22): p. 3683-92.
71. Kerjaschki, D., D.J. Sharkey, and M.G. Farquhar, Identification and characterization of podocalyxin--the major sialoprotein of the renal glomerular epithelial cell. *J Cell Biol*, 1984. **98**(4): p. 1591-6.
72. Nielsen, J.S., et al., The CD34-related molecule podocalyxin is a potent inducer of microvillus formation. *PLoS One*, 2007. **2**(2): p. e237.
73. Takeda, T., Podocyte cytoskeleton is connected to the integral membrane protein podocalyxin through Na⁺/H⁺-exchanger regulatory factor 2 and ezrin. *Clin Exp Nephrol*, 2003. **7**(4): p. 260-9.
74. Bryant, D.M., et al., A molecular switch for the orientation of epithelial cell polarization. *Dev Cell*, 2014. **31**(2): p. 171-87.
75. Sizemore, S., et al., Podocalyxin increases the aggressive phenotype of breast and prostate cancer cells in vitro through its interaction with ezrin. *Cancer Res*, 2007. **67**(13): p. 6183-91.
76. Tucker, B.J. and R.C. Blantz, An analysis of the determinants of nephron filtration rate. *Am J Physiol*, 1977. **232**(6): p. F477-83.

77. Gilmore, J.P., et al., Direct evidence for myogenic autoregulation of the renal microcirculation in the hamster. *Circ Res*, 1980. **47**(2): p. 226-30.
78. Robertson, C.R., et al., Dynamics of glomerular ultrafiltration in the rat. 3. Hemodynamics and autoregulation. *Am J Physiol*, 1972. **223**(5): p. 1191-200.
79. Navar, L.G., D.W. Ploth, and P.D. Bell, Distal tubular feedback control of renal hemodynamics and autoregulation. *Annu Rev Physiol*, 1980. **42**: p. 557-71.
80. Brenner, B.M., T.W. Meyer, and T.H. Hostetter, Dietary protein intake and the progressive nature of kidney disease: the role of hemodynamically mediated glomerular injury in the pathogenesis of progressive glomerular sclerosis in aging, renal ablation, and intrinsic renal disease. *N Engl J Med*, 1982. **307**(11): p. 652-9.
81. Dworkin, L.D., et al., Hemodynamic basis for glomerular injury in rats with desoxycorticosterone-salt hypertension. *J Clin Invest*, 1984. **73**(5): p. 1448-61.
82. Steiner, R.W., et al., Glomerular hemodynamics in moderate Goldblatt hypertension in the rat. *Hypertension*, 1982. **4**(1): p. 51-7.
83. Hostetter, T.H., H.G. Rennke, and B.M. Brenner, The case for intrarenal hypertension in the initiation and progression of diabetic and other glomerulopathies. *Am J Med*, 1982. **72**(3): p. 375-80.
84. Michels, L.D., M. Davidman, and W.F. Keane, Determinants of glomerular filtration and plasma flow in experimental diabetic rats. *J Lab Clin Med*, 1981. **98**(6): p. 869-85.
85. Blantz, R.C. and C.B. Wilson, Acute effects of antiglomerular basement membrane antibody on the process of glomerular filtration in the rat. *J Clin Invest*, 1976. **58**(4): p. 899-911.

86. Maddox, D.A., et al., Determinants of glomerular filtration in experimental glomerulonephritis in the rat. *J Clin Invest*, 1975. **55**(2): p. 305-18.
87. Anderson, S., et al., Control of glomerular hypertension limits glomerular injury in rats with reduced renal mass. *J Clin Invest*, 1985. **76**(2): p. 612-9.
88. Singh, P., et al., Aberrant tubuloglomerular feedback and HIF-1alpha confer resistance to ischemia after subtotal nephrectomy. *J Am Soc Nephrol*, 2012. **23**(3): p. 483-93.
89. Writing Group, M., et al., Heart disease and stroke statistics--2010 update: a report from the American Heart Association. *Circulation*, 2010. **121**(7): p. e46-e215.
90. Lloyd-Jones, D., et al., Heart disease and stroke statistics--2009 update: a report from the American Heart Association Statistics Committee and Stroke Statistics Subcommittee. *Circulation*, 2009. **119**(3): p. 480-6.
91. Lawes, C.M., et al., Global burden of blood-pressure-related disease, 2001. *Lancet*, 2008. **371**(9623): p. 1513-8.
92. Hill, G.S., Hypertensive nephrosclerosis. *Curr Opin Nephrol Hypertens*, 2008. **17**(3): p. 266-70.
93. Camici, M., et al., Podocyte dysfunction in aging--related glomerulosclerosis. *Front Biosci (Schol Ed)*, 2011. **3**: p. 995-1006.
94. Tracy, R.E., Age trends of renal arteriolar hyalinization explored with the aid of serial sections. *Nephron Clin Pract*, 2007. **105**(4): p. c171-7.
95. Tracy, R.E., et al., Blood pressure and nephrosclerosis in black and white men and women aged 25 to 54. *Mod Pathol*, 1991. **4**(5): p. 602-9.
96. Bidani, A.K., et al., Renal ablation acutely transforms 'benign' hypertension to 'malignant' nephrosclerosis in hypertensive rats. *Hypertension*, 1994. **24**(3): p. 309-16.

97. Hayashi, K., et al., Impaired myogenic responsiveness of the afferent arteriole in streptozotocin-induced diabetic rats: role of eicosanoid derangements. *J Am Soc Nephrol*, 1992. **2**(11): p. 1578-86.
98. Imig, J.D., et al., Chloride alters renal blood flow autoregulation in deoxycorticosterone-treated rats. *J Lab Clin Med*, 1993. **121**(4): p. 608-13.
99. Christensen, P.K., H.P. Hansen, and H.H. Parving, Impaired autoregulation of GFR in hypertensive non-insulin dependent diabetic patients. *Kidney Int*, 1997. **52**(5): p. 1369-74.
100. Hill, G.S., et al., Morphometric evidence for impairment of renal autoregulation in advanced essential hypertension. *Kidney Int*, 2006. **69**(5): p. 823-31.
101. Fine, L.G., C. Orphanides, and J.T. Norman, Progressive renal disease: the chronic hypoxia hypothesis. *Kidney Int Suppl*, 1998. **65**: p. S74-8.
102. Mennuni, S., et al., Hypertension and kidneys: unraveling complex molecular mechanisms underlying hypertensive renal damage. *J Hum Hypertens*, 2014. **28**(2): p. 74-9.
103. Freedman, B.I., et al., Polymorphisms in the nonmuscle myosin heavy chain 9 gene (MYH9) are associated with albuminuria in hypertensive African Americans: the HyperGEN study. *Am J Nephrol*, 2009. **29**(6): p. 626-32.
104. Freedman, B.I. and M. Murea, Target organ damage in African American hypertension: role of APOL1. *Curr Hypertens Rep*, 2012. **14**(1): p. 21-8.
105. Daniels, B.S. and T.H. Hostetter, Adverse effects of growth in the glomerular microcirculation. *Am J Physiol*, 1990. **258**(5 Pt 2): p. F1409-16.

106. Miller, P.L., H.G. Rennke, and T.W. Meyer, Glomerular hypertrophy accelerates hypertensive glomerular injury in rats. *Am J Physiol*, 1991. **261**(3 Pt 2): p. F459-65.
107. Anwar, M.A., et al., The effect of pressure-induced mechanical stretch on vascular wall differential gene expression. *J Vasc Res*, 2012. **49**(6): p. 463-78.
108. Lemarie, C.A., P.L. Tharaux, and S. Lehoux, Extracellular matrix alterations in hypertensive vascular remodeling. *J Mol Cell Cardiol*, 2010. **48**(3): p. 433-9.
109. Lee, Y.U., et al., Effects of Axial Stretch on Cell Proliferation and Intimal Thickness in Arteries in Organ Culture. *Cell Mol Bioeng*, 2010. **3**(3): p. 286-295.
110. Olson, J.L., A.G. de Urdaneta, and R.H. Heptinstall, Glomerular hyalinosis and its relation to hyperfiltration. *Lab Invest*, 1985. **52**(4): p. 387-98.
111. Kobayashi, S., et al., Stretch-induced IL-6 secretion from endothelial cells requires NF-kappaB activation. *Biochem Biophys Res Commun*, 2003. **308**(2): p. 306-12.
112. Ali, M.H., et al., Mitochondrial requirement for endothelial responses to cyclic strain: implications for mechanotransduction. *Am J Physiol Lung Cell Mol Physiol*, 2004. **287**(3): p. L486-96.
113. Lowenstein, C.J., C.N. Morrell, and M. Yamakuchi, Regulation of Weibel-Palade body exocytosis. *Trends Cardiovasc Med*, 2005. **15**(8): p. 302-8.
114. Valentijn, K.M., et al., Multigranular exocytosis of Weibel-Palade bodies in vascular endothelial cells. *Blood*, 2010. **116**(10): p. 1807-16.
115. Xiong, Y., et al., Hypertensive stretch regulates endothelial exocytosis of Weibel-Palade bodies through VEGF receptor 2 signaling pathways. *Cell Res*, 2013. **23**(6): p. 820-34.
116. Hu, Z., et al., Acute mechanical stretch promotes eNOS activation in venous endothelial cells mainly via PKA and Akt pathways. *PLoS One*, 2013. **8**(8): p. e71359.

117. Ribeiro, M.O., et al., Chronic inhibition of nitric oxide synthesis. A new model of arterial hypertension. *Hypertension*, 1992. **20**(3): p. 298-303.
118. Uiker, S. and W. Kriz, Structural analysis of the formation of glomerular microaneurysms in the Habu venom model. *Virchows Arch*, 1995. **426**(3): p. 281-93.
119. Salmon, A.H. and S.C. Satchell, Endothelial glycocalyx dysfunction in disease: albuminuria and increased microvascular permeability. *J Pathol*, 2012. **226**(4): p. 562-74.
120. Drumond, M.C. and W.M. Deen, Structural determinants of glomerular hydraulic permeability. *Am J Physiol*, 1994. **266**(1 Pt 2): p. F1-12.
121. Satchell, S.C. and F. Braet, Glomerular endothelial cell fenestrations: an integral component of the glomerular filtration barrier. *Am J Physiol Renal Physiol*, 2009. **296**(5): p. F947-56.
122. Tavasoli, M., et al., The chloride intracellular channel 5A stimulates podocyte Rac1, protecting against hypertension-induced glomerular injury. *Kidney Int*, 2016.
123. Pierchala, B.A., M.R. Munoz, and C.C. Tsui, Proteomic analysis of the slit diaphragm complex: CLIC5 is a protein critical for podocyte morphology and function. *Kidney Int*, 2010. **78**(9): p. 868-82.
124. Cortes, P., et al., F-actin fiber distribution in glomerular cells: structural and functional implications. *Kidney Int*, 2000. **58**(6): p. 2452-61.
125. Kriz, W., et al., Structure-stabilizing forces in the glomerular tuft. *J Am Soc Nephrol*, 1995. **5**(10): p. 1731-9.
126. Bielek, H., A. Anselmo, and C. Dermardirossian, Morphological and proliferative abnormalities in renal mesangial cells lacking RhoGDI. *Cell Signal*, 2009. **21**(12): p. 1974-83.

127. Akai, Y., et al., Mechanical stretch/relaxation of cultured rat mesangial cells induces protooncogenes and cyclooxygenase. *Am J Physiol*, 1994. **267**(2 Pt 1): p. C482-90.
128. Harris, R.C., M.A. Haralson, and K.F. Badr, Continuous stretch-relaxation in culture alters rat mesangial cell morphology, growth characteristics, and metabolic activity. *Lab Invest*, 1992. **66**(5): p. 548-54.
129. Gruden, G., et al., Mechanical stretch-induced fibronectin and transforming growth factor-beta1 production in human mesangial cells is p38 mitogen-activated protein kinase-dependent. *Diabetes*, 2000. **49**(4): p. 655-61.
130. Krepinsky, J.C., et al., Akt mediates mechanical strain-induced collagen production by mesangial cells. *J Am Soc Nephrol*, 2005. **16**(6): p. 1661-72.
131. Grond, J., et al., Mesangial function and glomerular sclerosis in rats after unilateral nephrectomy. *Kidney Int*, 1982. **22**(4): p. 338-43.
132. Endlich, N. and K. Endlich, Stretch, tension and adhesion - adaptive mechanisms of the actin cytoskeleton in podocytes. *Eur J Cell Biol*, 2006. **85**(3-4): p. 229-34.
133. Faul, C., et al., Actin up: regulation of podocyte structure and function by components of the actin cytoskeleton. *Trends Cell Biol*, 2007. **17**(9): p. 428-37.
134. Morton, M.J., et al., Human podocytes possess a stretch-sensitive, Ca²⁺-activated K⁺ channel: potential implications for the control of glomerular filtration. *J Am Soc Nephrol*, 2004. **15**(12): p. 2981-7.
135. Burford, J.L., et al., Intravital imaging of podocyte calcium in glomerular injury and disease. *J Clin Invest*, 2014. **124**(5): p. 2050-8.

136. Ziembicki, J., et al., Mechanical force-activated phospholipase D is mediated by Galpha12/13-Rho and calmodulin-dependent kinase in renal epithelial cells. *Am J Physiol Renal Physiol*, 2005. **289**(4): p. F826-34.
137. Hall, A., Rho GTPases and the actin cytoskeleton. *Science*, 1998. **279**(5350): p. 509-14.
138. Hall, A. and C.D. Nobes, Rho GTPases: molecular switches that control the organization and dynamics of the actin cytoskeleton. *Philos Trans R Soc Lond B Biol Sci*, 2000. **355**(1399): p. 965-70.
139. Iden, S. and J.G. Collard, Crosstalk between small GTPases and polarity proteins in cell polarization. *Nat Rev Mol Cell Biol*, 2008. **9**(11): p. 846-59.
140. Chi, X., et al., Roles of rho GTPases in intracellular transport and cellular transformation. *Int J Mol Sci*, 2013. **14**(4): p. 7089-108.
141. Su, L.F., R. Knoblauch, and M.J. Garabedian, Rho GTPases as modulators of the estrogen receptor transcriptional response. *J Biol Chem*, 2001. **276**(5): p. 3231-7.
142. Ellenbroek, S.I. and J.G. Collard, Rho GTPases: functions and association with cancer. *Clin Exp Metastasis*, 2007. **24**(8): p. 657-72.
143. Kiss, C., et al., Assignment of the ARHA and GPX1 genes to human chromosome bands 3p21.3 by in situ hybridization and with somatic cell hybrids. *Cytogenet Cell Genet*, 1997. **79**(3-4): p. 228-30.
144. Sun, H., et al., Rho activation of mDia formins is modulated by an interaction with inverted formin 2 (INF2). *Proc Natl Acad Sci U S A*, 2011. **108**(7): p. 2933-8.
145. Brown, E.J., et al., Mutations in the formin gene INF2 cause focal segmental glomerulosclerosis. *Nat Genet*, 2010. **42**(1): p. 72-6.

146. Boyer, O., et al., Mutations in INF2 are a major cause of autosomal dominant focal segmental glomerulosclerosis. *J Am Soc Nephrol*, 2011. **22**(2): p. 239-45.
147. Barua, M., et al., Mutations in the INF2 gene account for a significant proportion of familial but not sporadic focal and segmental glomerulosclerosis. *Kidney Int*, 2013. **83**(2): p. 316-22.
148. Yao, L., et al., The role of RhoA/Rho kinase pathway in endothelial dysfunction. *J Cardiovasc Dis Res*, 2010. **1**(4): p. 165-70.
149. Babelova, A., et al., Activation of Rac-1 and RhoA contributes to podocyte injury in chronic kidney disease. *PLoS One*, 2013. **8**(11): p. e80328.
150. Shibata, S., M. Nagase, and T. Fujita, Fluvastatin ameliorates podocyte injury in proteinuric rats via modulation of excessive Rho signaling. *J Am Soc Nephrol*, 2006. **17**(3): p. 754-64.
151. Komers, R., et al., Rho kinase inhibition protects kidneys from diabetic nephropathy without reducing blood pressure. *Kidney Int*, 2011. **79**(4): p. 432-42.
152. Wang, L., et al., Mechanisms of the proteinuria induced by Rho GTPases. *Kidney Int*, 2012. **81**(11): p. 1075-85.
153. Zhu, L., et al., Activation of RhoA in podocytes induces focal segmental glomerulosclerosis. *J Am Soc Nephrol*, 2011. **22**(9): p. 1621-30.
154. Scott, R.P., et al., Podocyte-specific loss of Cdc42 leads to congenital nephropathy. *J Am Soc Nephrol*, 2012. **23**(7): p. 1149-54.
155. Blattner, S.M., et al., Divergent functions of the Rho GTPases Rac1 and Cdc42 in podocyte injury. *Kidney Int*, 2013. **84**(5): p. 920-30.

156. Yanagida-Asanuma, E., et al., Synaptopodin protects against proteinuria by disrupting Cdc42:IRSp53:Mena signaling complexes in kidney podocytes. *Am J Pathol*, 2007. **171**(2): p. 415-27.
157. Gupta, I.R., et al., ARHGDI1: a novel gene implicated in nephrotic syndrome. *J Med Genet*, 2013. **50**(5): p. 330-8.
158. Gee, H.Y., et al., ARHGDI1 mutations cause nephrotic syndrome via defective RHO GTPase signaling. *J Clin Invest*, 2013. **123**(8): p. 3243-53.
159. Auguste, D., et al., Disease-causing mutations of RhoGDIalpha induce Rac1 hyperactivation in podocytes. *Small GTPases*, 2016: p. 0.
160. Akilesh, S., et al., Arhgap24 inactivates Rac1 in mouse podocytes, and a mutant form is associated with familial focal segmental glomerulosclerosis. *J Clin Invest*, 2011. **121**(10): p. 4127-37.
161. Ishizaka, M., et al., Podocyte-specific deletion of Rac1 leads to aggravation of renal injury in STZ-induced diabetic mice. *Biochem Biophys Res Commun*, 2015. **467**(3): p. 549-55.
162. Attias, O., et al., Rac1 contributes to actin organization in glomerular podocytes. *Nephron Exp Nephrol*, 2010. **114**(3): p. e93-e106.
163. Zhang, H., et al., Role of Rho-GTPases in complement-mediated glomerular epithelial cell injury. *Am J Physiol Renal Physiol*, 2007. **293**(1): p. F148-56.
164. Shibata, S., et al., Modification of mineralocorticoid receptor function by Rac1 GTPase: implication in proteinuric kidney disease. *Nat Med*, 2008. **14**(12): p. 1370-6.
165. Shang, X., et al., Rational design of small molecule inhibitors targeting RhoA subfamily Rho GTPases. *Chem Biol*, 2012. **19**(6): p. 699-710.

166. Kawarazaki, H., et al., Mineralocorticoid receptor--Rac1 activation and oxidative stress play major roles in salt-induced hypertension and kidney injury in prepubertal rats. *J Hypertens*, 2012. **30**(10): p. 1977-85.
167. Eriksson, A., et al., Small GTP-binding protein Rac is an essential mediator of vascular endothelial growth factor-induced endothelial fenestrations and vascular permeability. *Circulation*, 2003. **107**(11): p. 1532-8.
168. Wojciak-Stothard, B., et al., Rho and Rac but not Cdc42 regulate endothelial cell permeability. *J Cell Sci*, 2001. **114**(Pt 7): p. 1343-55.
169. Waschke, J., et al., Requirement of Rac activity for maintenance of capillary endothelial barrier properties. *Am J Physiol Heart Circ Physiol*, 2004. **286**(1): p. H394-401.
170. Hoang, M.V., J.A. Nagy, and D.R. Senger, Active Rac1 improves pathologic VEGF neovessel architecture and reduces vascular leak: mechanistic similarities with angiopoietin-1. *Blood*, 2011. **117**(5): p. 1751-60.
171. Bustelo, X.R., V. Sauzeau, and I.M. Berenjano, GTP-binding proteins of the Rho/Rac family: regulation, effectors and functions in vivo. *Bioessays*, 2007. **29**(4): p. 356-70.
172. Abdel-Magid, A.F., P21-Activated Kinase 4 (PAK4) Inhibitors as Potential Cancer Therapy. *ACS Med Chem Lett*, 2015. **6**(1): p. 17-8.
173. Parrini, M.C., Untangling the complexity of PAK1 dynamics: The future challenge. *Cell Logist*, 2012. **2**(2): p. 78-83.
174. Golovnina, K., et al., Evolution and origin of merlin, the product of the Neurofibromatosis type 2 (NF2) tumor-suppressor gene. *BMC Evol Biol*, 2005. **5**: p. 69.
175. Speck, O., et al., Moesin functions antagonistically to the Rho pathway to maintain epithelial integrity. *Nature*, 2003. **421**(6918): p. 83-7.

176. Fehon, R.G., A.I. McClatchey, and A. Bretscher, Organizing the cell cortex: the role of ERM proteins. *Nat Rev Mol Cell Biol*, 2010. **11**(4): p. 276-87.
177. Doi, Y., et al., Normal development of mice and unimpaired cell adhesion/cell motility/actin-based cytoskeleton without compensatory up-regulation of ezrin or radixin in moesin gene knockout. *J Biol Chem*, 1999. **274**(4): p. 2315-21.
178. Kitajiri, S., et al., Radixin deficiency causes deafness associated with progressive degeneration of cochlear stereocilia. *J Cell Biol*, 2004. **166**(4): p. 559-70.
179. Saotome, I., M. Curto, and A.I. McClatchey, Ezrin is essential for epithelial organization and villus morphogenesis in the developing intestine. *Dev Cell*, 2004. **6**(6): p. 855-64.
180. Bretscher, A., Purification of an 80,000-dalton protein that is a component of the isolated microvillus cytoskeleton, and its localization in nonmuscle cells. *J Cell Biol*, 1983. **97**(2): p. 425-32.
181. Tulk, B.M. and J.C. Edwards, NCC27, a homolog of intracellular Cl⁻ channel p64, is expressed in brush border of renal proximal tubule. *Am J Physiol*, 1998. **274**(6 Pt 2): p. F1140-9.
182. Berryman, M. and A. Bretscher, Identification of a novel member of the chloride intracellular channel gene family (CLIC5) that associates with the actin cytoskeleton of placental microvilli. *Mol Biol Cell*, 2000. **11**(5): p. 1509-21.
183. Gagnon, L.H., et al., The chloride intracellular channel protein CLIC5 is expressed at high levels in hair cell stereocilia and is essential for normal inner ear function. *J Neurosci*, 2006. **26**(40): p. 10188-98.
184. Hatzoglou, A., et al., Gem associates with Ezrin and acts via the Rho-GAP protein Gmip to down-regulate the Rho pathway. *Mol Biol Cell*, 2007. **18**(4): p. 1242-52.

185. D'Angelo, R., et al., Interaction of ezrin with the novel guanine nucleotide exchange factor PLEKHG6 promotes RhoG-dependent apical cytoskeleton rearrangements in epithelial cells. *Mol Biol Cell*, 2007. **18**(12): p. 4780-93.
186. Mackay, D.J., et al., Rho- and rac-dependent assembly of focal adhesion complexes and actin filaments in permeabilized fibroblasts: an essential role for ezrin/radixin/moesin proteins. *J Cell Biol*, 1997. **138**(4): p. 927-38.
187. Hirao, M., et al., Regulation mechanism of ERM (ezrin/radixin/moesin) protein/plasma membrane association: possible involvement of phosphatidylinositol turnover and Rho-dependent signaling pathway. *J Cell Biol*, 1996. **135**(1): p. 37-51.
188. Barret, C., et al., Mutagenesis of the phosphatidylinositol 4,5-bisphosphate (PIP(2)) binding site in the NH(2)-terminal domain of ezrin correlates with its altered cellular distribution. *J Cell Biol*, 2000. **151**(5): p. 1067-80.
189. Matsui, T., et al., Rho-kinase phosphorylates COOH-terminal threonines of ezrin/radixin/moesin (ERM) proteins and regulates their head-to-tail association. *J Cell Biol*, 1998. **140**(3): p. 647-57.
190. Pietromonaco, S.F., et al., Protein kinase C-theta phosphorylation of moesin in the actin-binding sequence. *J Biol Chem*, 1998. **273**(13): p. 7594-603.
191. Ng, T., et al., Ezrin is a downstream effector of trafficking PKC-integrin complexes involved in the control of cell motility. *EMBO J*, 2001. **20**(11): p. 2723-41.
192. Tan, X., et al., Emerging roles of PtdIns(4,5)P₂--beyond the plasma membrane. *J Cell Sci*, 2015. **128**(22): p. 4047-56.

193. Kisseleva, M., et al., The LIM protein Ajuba regulates phosphatidylinositol 4,5-bisphosphate levels in migrating cells through an interaction with and activation of PIPKI alpha. *Mol Cell Biol*, 2005. **25**(10): p. 3956-66.
194. Ling, K., et al., Type I gamma phosphatidylinositol phosphate kinase targets and regulates focal adhesions. *Nature*, 2002. **420**(6911): p. 89-93.
195. Honda, A., et al., Phosphatidylinositol 4-phosphate 5-kinase alpha is a downstream effector of the small G protein ARF6 in membrane ruffle formation. *Cell*, 1999. **99**(5): p. 521-32.
196. Moritz, A., et al., Phosphatidic acid is a specific activator of phosphatidylinositol-4-phosphate kinase. *J Biol Chem*, 1992. **267**(11): p. 7207-10.
197. Brown, F.D., et al., Phosphatidylinositol 4,5-bisphosphate and Arf6-regulated membrane traffic. *J Cell Biol*, 2001. **154**(5): p. 1007-17.
198. Heo, W.D., et al., PI(3,4,5)P3 and PI(4,5)P2 lipids target proteins with polybasic clusters to the plasma membrane. *Science*, 2006. **314**(5804): p. 1458-61.
199. van den Bout, I. and N. Divecha, PIP5K-driven PtdIns(4,5)P2 synthesis: regulation and cellular functions. *J Cell Sci*, 2009. **122**(Pt 21): p. 3837-50.
200. Ashley, R.H., Challenging accepted ion channel biology: p64 and the CLIC family of putative intracellular anion channel proteins (Review). *Mol Membr Biol*, 2003. **20**(1): p. 1-11.
201. Littler, D.R., et al., The enigma of the CLIC proteins: Ion channels, redox proteins, enzymes, scaffolding proteins? *FEBS Lett*, 2010. **584**(10): p. 2093-101.
202. Jiang, L., et al., CLIC proteins, ezrin, radixin, moesin and the coupling of membranes to the actin cytoskeleton: a smoking gun? *Biochim Biophys Acta*, 2014. **1838**(2): p. 643-57.

203. Suh, K.S., et al., The organellular chloride channel protein CLIC4/mtCLIC translocates to the nucleus in response to cellular stress and accelerates apoptosis. *J Biol Chem*, 2004. **279**(6): p. 4632-41.
204. Qian, Z., et al., Molecular cloning and characterization of a mitogen-activated protein kinase-associated intracellular chloride channel. *J Biol Chem*, 1999. **274**(3): p. 1621-7.
205. Valenzuela, S.M., et al., The nuclear chloride ion channel NCC27 is involved in regulation of the cell cycle. *J Physiol*, 2000. **529 Pt 3**: p. 541-52.
206. Shanks, R.A., et al., AKAP350 at the Golgi apparatus. II. Association of AKAP350 with a novel chloride intracellular channel (CLIC) family member. *J Biol Chem*, 2002. **277**(43): p. 40973-80.
207. Chuang, J.Z., et al., A 29 kDa intracellular chloride channel p64H1 is associated with large dense-core vesicles in rat hippocampal neurons. *J Neurosci*, 1999. **19**(8): p. 2919-28.
208. Littler, D.R., et al., The intracellular chloride ion channel protein CLIC1 undergoes a redox-controlled structural transition. *J Biol Chem*, 2004. **279**(10): p. 9298-305.
209. Warton, K., et al., Recombinant CLIC1 (NCC27) assembles in lipid bilayers via a pH-dependent two-state process to form chloride ion channels with identical characteristics to those observed in Chinese hamster ovary cells expressing CLIC1. *J Biol Chem*, 2002. **277**(29): p. 26003-11.
210. Goodchild, S.C., et al., Oxidation promotes insertion of the CLIC1 chloride intracellular channel into the membrane. *Eur Biophys J*, 2009. **39**(1): p. 129-38.
211. Singh, H., Two decades with dimorphic Chloride Intracellular Channels (CLICs). *FEBS Lett*, 2010. **584**(10): p. 2112-21.

212. Stauber, T. and T.J. Jentsch, Chloride in vesicular trafficking and function. *Annu Rev Physiol*, 2013. **75**: p. 453-77.
213. Jentsch, T.J., et al., Molecular structure and physiological function of chloride channels. *Physiol Rev*, 2002. **82**(2): p. 503-68.
214. Berryman, M.A. and J.R. Goldenring, CLIC4 is enriched at cell-cell junctions and colocalizes with AKAP350 at the centrosome and midbody of cultured mammalian cells. *Cell Motil Cytoskeleton*, 2003. **56**(3): p. 159-72.
215. Singh, H., M.A. Cousin, and R.H. Ashley, Functional reconstitution of mammalian 'chloride intracellular channels' CLIC1, CLIC4 and CLIC5 reveals differential regulation by cytoskeletal actin. *FEBS J*, 2007. **274**(24): p. 6306-16.
216. Jiang, L., et al., Intracellular chloride channel protein CLIC1 regulates macrophage function through modulation of phagosomal acidification. *J Cell Sci*, 2012. **125**(Pt 22): p. 5479-88.
217. Vieira, O.V., R.J. Botelho, and S. Grinstein, Phagosome maturation: aging gracefully. *Biochem J*, 2002. **366**(Pt 3): p. 689-704.
218. Russell, D.G., et al., The macrophage marches on its phagosome: dynamic assays of phagosome function. *Nat Rev Immunol*, 2009. **9**(8): p. 594-600.
219. Marion, S., et al., Ezrin promotes actin assembly at the phagosome membrane and regulates phago-lysosomal fusion. *Traffic*, 2011. **12**(4): p. 421-37.
220. Qualmann, B. and H. Mellor, Regulation of endocytic traffic by Rho GTPases. *Biochem J*, 2003. **371**(Pt 2): p. 233-41.
221. Ellis, S. and H. Mellor, Regulation of endocytic traffic by rho family GTPases. *Trends Cell Biol*, 2000. **10**(3): p. 85-8.

222. Okamoto, C.T. and J.G. Forte, Vesicular trafficking machinery, the actin cytoskeleton, and H⁺-K⁺-ATPase recycling in the gastric parietal cell. *J Physiol*, 2001. **532**(Pt 2): p. 287-96.
223. Ramsay, A.G., J.F. Marshall, and I.R. Hart, Integrin trafficking and its role in cancer metastasis. *Cancer Metastasis Rev*, 2007. **26**(3-4): p. 567-78.
224. Dozynkiewicz, M.A., et al., Rab25 and CLIC3 collaborate to promote integrin recycling from late endosomes/lysosomes and drive cancer progression. *Dev Cell*, 2012. **22**(1): p. 131-45.
225. Macpherson, I.R., et al., CLIC3 controls recycling of late endosomal MT1-MMP and dictates invasion and metastasis in breast cancer. *J Cell Sci*, 2014. **127**(Pt 18): p. 3893-901.
226. Knowles, L.M., et al., CLT1 targets angiogenic endothelium through CLIC1 and fibronectin. *Angiogenesis*, 2012. **15**(1): p. 115-29.
227. Tringali, C., et al., The plasma membrane sialidase NEU3 regulates the malignancy of renal carcinoma cells by controlling beta1 integrin internalization and recycling. *J Biol Chem*, 2012. **287**(51): p. 42835-45.
228. Suginta, W., et al., Chloride intracellular channel protein CLIC4 (p64H1) binds directly to brain dynamin I in a complex containing actin, tubulin and 14-3-3 isoforms. *Biochem J*, 2001. **359**(Pt 1): p. 55-64.
229. Chou, S.Y., et al., CLIC4 regulates apical exocytosis and renal tube luminogenesis through retromer- and actin-mediated endocytic trafficking. *Nat Commun*, 2016. **7**: p. 10412.

230. Strauss, O., The retinal pigment epithelium in visual function. *Physiol Rev*, 2005. **85**(3): p. 845-81.
231. Chuang, J.Z., S.Y. Chou, and C.H. Sung, Chloride intracellular channel 4 is critical for the epithelial morphogenesis of RPE cells and retinal attachment. *Mol Biol Cell*, 2010. **21**(17): p. 3017-28.
232. Ponsioen, B., et al., Spatiotemporal regulation of chloride intracellular channel protein CLIC4 by RhoA. *Mol Biol Cell*, 2009. **20**(22): p. 4664-72.
233. Bryant, D.M., et al., A molecular network for de novo generation of the apical surface and lumen. *Nat Cell Biol*, 2010. **12**(11): p. 1035-45.
234. Dong, B., W. Deng, and D. Jiang, Distinct cytoskeleton populations and extensive crosstalk control Ciona notochord tubulogenesis. *Development*, 2011. **138**(8): p. 1631-41.
235. Hogan, B.L. and P.A. Kolodziej, Organogenesis: molecular mechanisms of tubulogenesis. *Nat Rev Genet*, 2002. **3**(7): p. 513-23.
236. Ulmasov, B., et al., Chloride intracellular channel protein-4 functions in angiogenesis by supporting acidification of vacuoles along the intracellular tubulogenic pathway. *Am J Pathol*, 2009. **174**(3): p. 1084-96.
237. Tung, J.J., et al., Chloride intracellular channel 4 is involved in endothelial proliferation and morphogenesis in vitro. *Angiogenesis*, 2009. **12**(3): p. 209-20.
238. Bohman, S., et al., Proteomic analysis of vascular endothelial growth factor-induced endothelial cell differentiation reveals a role for chloride intracellular channel 4 (CLIC4) in tubular morphogenesis. *J Biol Chem*, 2005. **280**(51): p. 42397-404.
239. Logan, M.R. and C.A. Mandato, Regulation of the actin cytoskeleton by PIP2 in cytokinesis. *Biol Cell*, 2006. **98**(6): p. 377-88.

240. Chalothorn, D., et al., Chloride intracellular channel-4 is a determinant of native collateral formation in skeletal muscle and brain. *Circ Res*, 2009. **105**(1): p. 89-98.
241. Edwards, J.C., et al., Absence of chloride intracellular channel 4 (CLIC4) predisposes to acute kidney injury but has minimal impact on recovery. *BMC Nephrol*, 2014. **15**: p. 54.
242. Berryman, M., et al., CLIC-5A functions as a chloride channel in vitro and associates with the cortical actin cytoskeleton in vitro and in vivo. *J Biol Chem*, 2004. **279**(33): p. 34794-801.
243. Lim, R. and A.M. Brichta, Anatomical and physiological development of the human inner ear. *Hear Res*, 2016.
244. Salles, F.T., et al., CLIC5 stabilizes membrane-actin filament linkages at the base of hair cell stereocilia in a molecular complex with radixin, taperin, and myosin VI. *Cytoskeleton (Hoboken)*, 2014. **71**(1): p. 61-78.
245. Sengoelge, G., et al., A SAGE-based comparison between glomerular and aortic endothelial cells. *Am J Physiol Renal Physiol*, 2005. **288**(6): p. F1290-300.
246. Takeda, T., et al., Expression of podocalyxin inhibits cell-cell adhesion and modifies junctional properties in Madin-Darby canine kidney cells. *Mol Biol Cell*, 2000. **11**(9): p. 3219-32.
247. Orlando, R.A., et al., The glomerular epithelial cell anti-adhesin podocalyxin associates with the actin cytoskeleton through interactions with ezrin. *J Am Soc Nephrol*, 2001. **12**(8): p. 1589-98.
248. Friedrich, C., et al., Podocytes are sensitive to fluid shear stress in vitro. *Am J Physiol Renal Physiol*, 2006. **291**(4): p. F856-65.

249. Endlich, N., et al., Podocytes respond to mechanical stress in vitro. *J Am Soc Nephrol*, 2001. **12**(3): p. 413-22.
250. New, L.A., C.E. Martin, and N. Jones, Advances in slit diaphragm signaling. *Curr Opin Nephrol Hypertens*, 2014. **23**(4): p. 420-30.
251. Faul, C., et al., The actin cytoskeleton of kidney podocytes is a direct target of the antiproteinuric effect of cyclosporine A. *Nat Med*, 2008. **14**(9): p. 931-8.
252. Jayasundar, J.J., et al., Open conformation of ezrin bound to phosphatidylinositol 4,5-bisphosphate and to F-actin revealed by neutron scattering. *J Biol Chem*, 2012. **287**(44): p. 37119-33.
253. Truett, G.E., et al., Preparation of PCR-quality mouse genomic DNA with hot sodium hydroxide and tris (HotSHOT). *Biotechniques*, 2000. **29**(1): p. 52, 54.
254. Gabai, G., et al., Endocrine and ovarian responses to prolonged adrenal stimulation at the time of induced corpus luteum regression. *Reprod Domest Anim*, 2006. **41**(6): p. 485-93.
255. Kriz, W., et al., The podocyte's response to stress: the enigma of foot process effacement. *Am J Physiol Renal Physiol*, 2013. **304**(4): p. F333-47.
256. Greka, A. and P. Mundel, Cell biology and pathology of podocytes. *Annu Rev Physiol*, 2012. **74**: p. 299-323.
257. Deen, W.M., Cellular contributions to glomerular size-selectivity. *Kidney Int*, 2006. **69**(8): p. 1295-7.
258. Deen, W.M., M.J. Lazzara, and B.D. Myers, Structural determinants of glomerular permeability. *Am J Physiol Renal Physiol*, 2001. **281**(4): p. F579-96.
259. Doyonnas, R., et al., Anuria, omphalocele, and perinatal lethality in mice lacking the CD34-related protein podocalyxin. *J Exp Med*, 2001. **194**(1): p. 13-27.

260. Weinhold, B., et al., Deficits in sialylation impair podocyte maturation. *J Am Soc Nephrol*, 2012. **23**(8): p. 1319-28.
261. Ito, M., et al., Glycoprotein hyposialylation gives rise to a nephrotic-like syndrome that is prevented by sialic acid administration in GNE V572L point-mutant mice. *PLoS One*, 2012. **7**(1): p. e29873.
262. Kurihara, H., et al., The altered glomerular filtration slits seen in puromycin aminonucleoside nephrosis and protamine sulfate-treated rats contain the tight junction protein ZO-1. *Am J Pathol*, 1992. **141**(4): p. 805-16.
263. Kerjaschki, D., A.T. Vernillo, and M.G. Farquhar, Reduced sialylation of podocalyxin--the major sialoprotein of the rat kidney glomerulus--in aminonucleoside nephrosis. *Am J Pathol*, 1985. **118**(3): p. 343-9.
264. Asanuma, K., et al., Synaptopodin regulates the actin-bundling activity of alpha-actinin in an isoform-specific manner. *J Clin Invest*, 2005. **115**(5): p. 1188-98.
265. Seiler, M.W., M.A. Venkatachalam, and R.S. Cotran, Glomerular epithelium: structural alterations induced by polycations. *Science*, 1975. **189**(4200): p. 390-3.
266. Neisch, A.L. and R.G. Fehon, Ezrin, Radixin and Moesin: key regulators of membrane-cortex interactions and signaling. *Curr Opin Cell Biol*, 2011. **23**(4): p. 377-82.
267. Janke, M., et al., Actin binding of ezrin is activated by specific recognition of PIP2-functionalized lipid bilayers. *Biochemistry*, 2008. **47**(12): p. 3762-9.
268. Fievet, B.T., et al., Phosphoinositide binding and phosphorylation act sequentially in the activation mechanism of ezrin. *J Cell Biol*, 2004. **164**(5): p. 653-9.
269. Matsui, T., et al., Activation of ERM proteins in vivo by Rho involves phosphatidylinositol 4-phosphate 5-kinase and not ROCK kinases. *Curr Biol*, 1999. **9**(21): p. 1259-62.

270. Gary, R. and A. Bretscher, Ezrin self-association involves binding of an N-terminal domain to a normally masked C-terminal domain that includes the F-actin binding site. *Mol Biol Cell*, 1995. **6**(8): p. 1061-75.
271. Grune, T., et al., Ezrin turnover and cell shape changes catalyzed by proteasome in oxidatively stressed cells. *FASEB J*, 2002. **16**(12): p. 1602-10.
272. Posor, Y., M. Eichhorn-Grunig, and V. Haucke, Phosphoinositides in endocytosis. *Biochim Biophys Acta*, 2015. **1851**(6): p. 794-804.
273. Martin, T.F., PI(4,5)P-binding effector proteins for vesicle exocytosis. *Biochim Biophys Acta*, 2015. **1851**(6): p. 785-793.
274. Echard, A., Phosphoinositides and cytokinesis: the "PIP" of the iceberg. *Cytoskeleton* (Hoboken), 2012. **69**(11): p. 893-912.
275. Martin-Belmonte, F. and K. Mostov, Regulation of cell polarity during epithelial morphogenesis. *Curr Opin Cell Biol*, 2008. **20**(2): p. 227-34.
276. Zhang, L., et al., Phosphatidylinositol 4, 5 bisphosphate and the actin cytoskeleton. *Subcell Biochem*, 2012. **59**: p. 177-215.
277. Sun, Y., et al., Phosphatidylinositol 4,5-bisphosphate: targeted production and signaling. *Bioessays*, 2013. **35**(6): p. 513-22.
278. Valenzuela, S.M., et al., Regulation of the membrane insertion and conductance activity of the metamorphic chloride intracellular channel protein CLIC1 by cholesterol. *PLoS One*, 2013. **8**(2): p. e56948.
279. Landry, D., et al., Molecular cloning and characterization of p64, a chloride channel protein from kidney microsomes. *J Biol Chem*, 1993. **268**(20): p. 14948-55.

280. Salles, F.T., et al., CLIC5 stabilizes membrane-actin filament linkages at the base of hair cell stereocilia in a molecular complex with Radixin, Taperin, and Myosin VI. *Cytoskeleton* (Hoboken), 2013.
281. Seco, C.Z., et al., Progressive hearing loss and vestibular dysfunction caused by a homozygous nonsense mutation in CLIC5. *Eur J Hum Genet*, 2015. **23**(2): p. 189-94.
282. Jiang, L., et al., CLIC proteins, ezrin, radixin, moesin and the coupling of membranes to the actin cytoskeleton: A smoking gun? *Biochim Biophys Acta*, 2013.
283. Auvinen, E., N. Kivi, and A. Vaheri, Regulation of ezrin localization by Rac1 and PIPK in human epithelial cells. *Exp Cell Res*, 2007. **313**(4): p. 824-33.
284. Mouawad, F., H. Tsui, and T. Takano, Role of Rho-GTPases and their regulatory proteins in glomerular podocyte function. *Can J Physiol Pharmacol*, 2013. **91**(10): p. 773-82.
285. Bokoch, G.M., Biology of the p21-activated kinases. *Annu Rev Biochem*, 2003. **72**: p. 743-81.
286. Gao, Y., et al., Rational design and characterization of a Rac GTPase-specific small molecule inhibitor. *Proc Natl Acad Sci U S A*, 2004. **101**(20): p. 7618-23.
287. Li, S., et al., PLC-gamma1 and Rac1 coregulate EGF-induced cytoskeleton remodeling and cell migration. *Mol Endocrinol*, 2009. **23**(6): p. 901-13.
288. Kirchhoff, F., et al., Rapid development of severe end-organ damage in C57BL/6 mice by combining DOCA salt and angiotensin II. *Kidney Int*, 2008. **73**(5): p. 643-50.
289. Mazzaccara, C., et al., Age-Related Reference Intervals of the Main Biochemical and Hematological Parameters in C57BL/6J, 129SV/EV and C3H/HeJ Mouse Strains. *PLoS One*, 2008. **3**(11): p. e3772.

290. Asirvatham, J.R., V. Moses, and L. Bjornson, Errors in potassium measurement: a laboratory perspective for the clinician. *N Am J Med Sci*, 2013. **5**(4): p. 255-9.
291. de Champlain, J., L.R. Krakoff, and J. Axelrod, Catecholamine metabolism in experimental hypertension in the rat. *Circ Res*, 1967. **20**(1): p. 136-45.
292. Eremina, V., et al., Glomerular-specific alterations of VEGF-A expression lead to distinct congenital and acquired renal diseases. *J Clin Invest*, 2003. **111**(5): p. 707-16.
293. L'Hote, C.G. and M.A. Knowles, Cell responses to FGFR3 signalling: growth, differentiation and apoptosis. *Exp Cell Res*, 2005. **304**(2): p. 417-31.
294. Gerber, H.P., et al., Vascular endothelial growth factor regulates endothelial cell survival through the phosphatidylinositol 3'-kinase/Akt signal transduction pathway. Requirement for Flk-1/KDR activation. *J Biol Chem*, 1998. **273**(46): p. 30336-43.
295. Shiojima, I. and K. Walsh, Role of Akt signaling in vascular homeostasis and angiogenesis. *Circ Res*, 2002. **90**(12): p. 1243-50.
296. Kondo, T., et al., ERM (ezrin/radixin/moesin)-based molecular mechanism of microvillar breakdown at an early stage of apoptosis. *J Cell Biol*, 1997. **139**(3): p. 749-58.
297. Viswanatha, R., A. Bretscher, and D. Garbett, Dynamics of ezrin and EBP50 in regulating microvilli on the apical aspect of epithelial cells. *Biochem Soc Trans*, 2014. **42**(1): p. 189-94.
298. Yonemura, S., S. Tsukita, and S. Tsukita, Direct involvement of ezrin/radixin/moesin (ERM)-binding membrane proteins in the organization of microvilli in collaboration with activated ERM proteins. *J Cell Biol*, 1999. **145**(7): p. 1497-509.

299. Yang, S.A., C.L. Carpenter, and C.S. Abrams, Rho and Rho-kinase mediate thrombin-induced phosphatidylinositol 4-phosphate 5-kinase trafficking in platelets. *J Biol Chem*, 2004. **279**(40): p. 42331-6.
300. Halstead, J.R., et al., Rac controls PIP5K localisation and PtdIns(4,5)P synthesis, which modulates vinculin localisation and neurite dynamics. *J Cell Sci*, 2010. **123**(Pt 20): p. 3535-46.
301. Ohashi, K., Roles of cofilin in development and its mechanisms of regulation. *Dev Growth Differ*, 2015.
302. Hsu, H.H., et al., Mechanisms of angiotensin II signaling on cytoskeleton of podocytes. *J Mol Med (Berl)*, 2008. **86**(12): p. 1379-94.
303. Wei, C., et al., Modification of kidney barrier function by the urokinase receptor. *Nat Med*, 2008. **14**(1): p. 55-63.
304. Kistler, A.D., M.M. Altintas, and J. Reiser, Podocyte GTPases regulate kidney filter dynamics. *Kidney Int*, 2012. **81**(11): p. 1053-5.
305. Tzima, E., et al., Activation of Rac1 by shear stress in endothelial cells mediates both cytoskeletal reorganization and effects on gene expression. *EMBO J*, 2002. **21**(24): p. 6791-800.
306. Aikawa, R., et al., Reactive oxygen species in mechanical stress-induced cardiac hypertrophy. *Biochem Biophys Res Commun*, 2001. **289**(4): p. 901-7.
307. Uhlik, M.T., et al., Rac-MEKK3-MKK3 scaffolding for p38 MAPK activation during hyperosmotic shock. *Nat Cell Biol*, 2003. **5**(12): p. 1104-10.
308. Friis, M.B., et al., Cell shrinkage as a signal to apoptosis in NIH 3T3 fibroblasts. *J Physiol*, 2005. **567**(Pt 2): p. 427-43.

309. Tong, J., et al., Phosphorylation of Rac1 T108 by extracellular signal-regulated kinase in response to epidermal growth factor: a novel mechanism to regulate Rac1 function. *Mol Cell Biol*, 2013. **33**(22): p. 4538-51.
310. Shibata, S., et al., Podocyte as the target for aldosterone: roles of oxidative stress and Sgk1. *Hypertension*, 2007. **49**(2): p. 355-64.
311. Iwashima, F., et al., Aldosterone induces superoxide generation via Rac1 activation in endothelial cells. *Endocrinology*, 2008. **149**(3): p. 1009-14.
312. Schmitz, U., et al., Angiotensin II-induced stimulation of p21-activated kinase and c-Jun NH2-terminal kinase is mediated by Rac1 and Nck. *J Biol Chem*, 2001. **276**(25): p. 22003-10.
313. Yu, H., et al., Rac1 activation in podocytes induces rapid foot process effacement and proteinuria. *Mol Cell Biol*, 2013. **33**(23): p. 4755-64.
314. Lawson, C.D. and K. Burridge, The on-off relationship of Rho and Rac during integrin-mediated adhesion and cell migration. *Small GTPases*, 2014. **5**: p. e27958.
315. Advani, A., et al., Role of VEGF in maintaining renal structure and function under normotensive and hypertensive conditions. *Proc Natl Acad Sci U S A*, 2007. **104**(36): p. 14448-53.
316. Sugimoto, H., et al., Neutralization of circulating vascular endothelial growth factor (VEGF) by anti-VEGF antibodies and soluble VEGF receptor 1 (sFlt-1) induces proteinuria. *J Biol Chem*, 2003. **278**(15): p. 12605-8.
317. Mammoto, A., et al., A mechanosensitive transcriptional mechanism that controls angiogenesis. *Nature*, 2009. **457**(7233): p. 1103-8.

318. Liu, W.F., et al., Cadherins, RhoA, and Rac1 are differentially required for stretch-mediated proliferation in endothelial versus smooth muscle cells. *Circ Res*, 2007. **101**(5): p. e44-52.
319. Mammoto, A., et al., Role of RhoA, mDia, and ROCK in cell shape-dependent control of the Skp2-p27kip1 pathway and the G1/S transition. *J Biol Chem*, 2004. **279**(25): p. 26323-30.
320. Liu, J. and S. Agarwal, Mechanical signals activate vascular endothelial growth factor receptor-2 to upregulate endothelial cell proliferation during inflammation. *J Immunol*, 2010. **185**(2): p. 1215-21.
321. Berry, K.L., et al., A *C. elegans* CLIC-like protein required for intracellular tube formation and maintenance. *Science*, 2003. **302**(5653): p. 2134-7.
322. Obeidat, M., M. Obeidat, and B.J. Ballermann, Glomerular endothelium: A porous sieve and formidable barrier. *Experimental Cell Research*, 2012. **318**(9): p. 964-972.
323. Lafayette, R.A., et al., Nature of glomerular dysfunction in pre-eclampsia. *Kidney Int*, 1998. **54**(4): p. 1240-9.
324. Eremina, V., et al., VEGF inhibition and renal thrombotic microangiopathy. *N Engl J Med*, 2008. **358**(11): p. 1129-36.
325. Chugh, S.S., L.C. Clement, and C. Mace, New insights into human minimal change disease: lessons from animal models. *Am J Kidney Dis*, 2012. **59**(2): p. 284-92.
326. Chen, Y.M. and H. Liapis, Focal segmental glomerulosclerosis: molecular genetics and targeted therapies. *BMC Nephrol*, 2015. **16**: p. 101.
327. Kawachi, H., et al., Role of podocyte slit diaphragm as a filtration barrier. *Nephrology (Carlton)*, 2006. **11**(4): p. 274-81.

328. Sauvanet, C., et al., Structure, regulation, and functional diversity of microvilli on the apical domain of epithelial cells. *Annu Rev Cell Dev Biol*, 2015. **31**: p. 593-621.
329. Berryman, M., Z. Franck, and A. Bretscher, Ezrin is concentrated in the apical microvilli of a wide variety of epithelial cells whereas moesin is found primarily in endothelial cells. *J Cell Sci*, 1993. **105 (Pt 4)**: p. 1025-43.
330. Wang, Y., et al., Moesin1 and Ve-cadherin are required in endothelial cells during in vivo tubulogenesis. *Development*, 2010. **137(18)**: p. 3119-28.
331. Strilic, B., et al., The molecular basis of vascular lumen formation in the developing mouse aorta. *Dev Cell*, 2009. **17(4)**: p. 505-15.
332. Amieva, M.R. and H. Furthmayr, Subcellular localization of moesin in dynamic filopodia, retraction fibers, and other structures involved in substrate exploration, attachment, and cell-cell contacts. *Exp Cell Res*, 1995. **219(1)**: p. 180-96.
333. Barreiro, O., et al., Dynamic interaction of VCAM-1 and ICAM-1 with moesin and ezrin in a novel endothelial docking structure for adherent leukocytes. *J Cell Biol*, 2002. **157(7)**: p. 1233-45.
334. Redhead, C.R., et al., A ubiquitous 64-kDa protein is a component of a chloride channel of plasma and intracellular membranes. *Proc Natl Acad Sci U S A*, 1992. **89(9)**: p. 3716-20.
335. Fernandez-Salas, E., et al., mtCLIC/CLIC4, an organellar chloride channel protein, is increased by DNA damage and participates in the apoptotic response to p53. *Mol Cell Biol*, 2002. **22(11)**: p. 3610-20.
336. Ponnalagu, D., et al., Molecular identity of cardiac mitochondrial chloride intracellular channel proteins. *Mitochondrion*, 2016. **27**: p. 6-14.

337. Shukla, A., et al., TGF-beta signalling is regulated by Schnurri-2-dependent nuclear translocation of CLIC4 and consequent stabilization of phospho-Smad2 and 3. *Nat Cell Biol*, 2009. **11**(6): p. 777-84.
338. Meng, X., et al., CLIC2-RyR1 interaction and structural characterization by cryo-electron microscopy. *J Mol Biol*, 2009. **387**(2): p. 320-34.
339. Dulhunty, A., et al., The glutathione transferase structural family includes a nuclear chloride channel and a ryanodine receptor calcium release channel modulator. *J Biol Chem*, 2001. **276**(5): p. 3319-23.
340. Ponsioen, B., et al., Spatiotemporal Regulation of Chloride Intracellular Channel protein CLIC4 by RhoA. *Mol Biol Cell*, 2009.
341. Padmakumar, V., et al., Detection of differential fetal and adult expression of chloride intracellular channel 4 (CLIC4) protein by analysis of a green fluorescent protein knock-in mouse line. *BMC Dev Biol*, 2014. **14**: p. 24.
342. Bonilha, V.L., et al., Microvilli defects in retinas of ezrin knockout mice. *Exp Eye Res*, 2006. **82**(4): p. 720-9.
343. Van Furden, D., et al., The *C. elegans* ezrin-radixin-moesin protein ERM-1 is necessary for apical junction remodelling and tubulogenesis in the intestine. *Dev Biol*, 2004. **272**(1): p. 262-76.
344. Gobel, V., et al., Lumen morphogenesis in *C. elegans* requires the membrane-cytoskeleton linker erm-1. *Dev Cell*, 2004. **6**(6): p. 865-73.
345. Sengoelge, G., et al., A SAGE-based comparison between glomerular and aortic endothelial cells. *Am J Physiol Renal Physiol*, 2005. **288**(6): p. F1290-300.

346. Ronnov-Jessen, L., et al., Differential expression of a chloride intracellular channel gene, CLIC4, in transforming growth factor-beta1-mediated conversion of fibroblasts to myofibroblasts. *Am J Pathol*, 2002. **161**(2): p. 471-80.
347. Tung, J.J., Evaluation of Chloride Intracellular Channels 4 and 1 Functions in Developmental and Pathological Angiogenesis. 2012, Columbia University Academic Commons.
348. Tung, J.J., I.W. Tattersall, and J. Kitajewski, Tips, stalks, tubes: notch-mediated cell fate determination and mechanisms of tubulogenesis during angiogenesis. *Cold Spring Harb Perspect Med*, 2012. **2**(2): p. a006601.
349. D'Agati, V.D., F.J. Kaskel, and R.J. Falk, Focal segmental glomerulosclerosis. *N Engl J Med*, 2011. **365**(25): p. 2398-411.
350. Nishizawa, T., et al., Molecular cloning and characterization of a novel chloride intracellular channel-related protein, parghorin, expressed in water-secreting cells. *J Biol Chem*, 2000. **275**(15): p. 11164-73.
351. Tulk, B.M., et al., CLIC-1 functions as a chloride channel when expressed and purified from bacteria. *J Biol Chem*, 2000. **275**(35): p. 26986-93.
352. Mi, W., et al., The crystal structure of human chloride intracellular channel protein 2: a disulfide bond with functional implications. *Proteins*, 2008. **71**(1): p. 509-13.
353. Littler, D.R., et al., Comparison of vertebrate and invertebrate CLIC proteins: the crystal structures of *Caenorhabditis elegans* EXC-4 and *Drosophila melanogaster* DmCLIC. *Proteins*, 2008. **71**(1): p. 364-78.
354. Cromer, B.A., et al., Structure of the Janus protein human CLIC2. *J Mol Biol*, 2007. **374**(3): p. 719-31.

355. Littler, D.R., et al., Crystal structure of the soluble form of the redox-regulated chloride ion channel protein CLIC4. *FEBS J*, 2005. **272**(19): p. 4996-5007.
356. Edwards, J.C., et al., c-Src control of chloride channel support for osteoclast HCl transport and bone resorption. *J Biol Chem*, 2006. **281**(38): p. 28011-22.
357. Maddala, R., et al., Growth factor induced activation of Rho and Rac GTPases and actin cytoskeletal reorganization in human lens epithelial cells. *Mol Vis*, 2003. **9**: p. 329-36.
358. Croise, P., et al., Rho GTPases, phosphoinositides, and actin: a tripartite framework for efficient vesicular trafficking. *Small GTPases*, 2014. **5**: p. e29469.
359. Talias, K.F., L.C. Cantley, and C.L. Carpenter, Rho family GTPases bind to phosphoinositide kinases. *J Biol Chem*, 1995. **270**(30): p. 17656-9.
360. Araki, N., et al., Phosphoinositide metabolism during membrane ruffling and macropinosome formation in EGF-stimulated A431 cells. *Exp Cell Res*, 2007. **313**(7): p. 1496-507.
361. Fujii, M., et al., Dissecting the roles of Rac1 activation and deactivation in macropinocytosis using microscopic photo-manipulation. *Sci Rep*, 2013. **3**: p. 2385.
362. Furutani, Y., et al., Vitronectin induces phosphorylation of ezrin/radixin/moesin actin-binding proteins through binding to its novel neuronal receptor telencephalin. *J Biol Chem*, 2012. **287**(46): p. 39041-9.
363. Ma, J., et al., Role of activated Rac1/Cdc42 in mediating endothelial cell proliferation and tumor angiogenesis in breast cancer. *PLoS One*, 2013. **8**(6): p. e66275.
364. Garrett, T.A., J.D. Van Buul, and K. Burridge, VEGF-induced Rac1 activation in endothelial cells is regulated by the guanine nucleotide exchange factor Vav2. *Exp Cell Res*, 2007. **313**(15): p. 3285-97.

365. Tan, W., et al., An essential role for Rac1 in endothelial cell function and vascular development. *FASEB J*, 2008. **22**(6): p. 1829-38.
366. He, M., et al., Vascular endothelial growth factor C promotes cervical cancer metastasis via up-regulation and activation of RhoA/ROCK-2/moesin cascade. *BMC Cancer*, 2010. **10**: p. 170.
367. Khan, L.A., et al., Intracellular lumen extension requires ERM-1-dependent apical membrane expansion and AQP-8-mediated flux. *Nat Cell Biol*, 2013. **15**(2): p. 143-56.
368. Fairn, G.D., et al., An electrostatic switch displaces phosphatidylinositol phosphate kinases from the membrane during phagocytosis. *J Cell Biol*, 2009. **187**(5): p. 701-14.
369. Wong, K.W., S. Mohammadi, and R.R. Isberg, The polybasic region of Rac1 modulates bacterial uptake independently of self-association and membrane targeting. *J Biol Chem*, 2008. **283**(51): p. 35954-65.
370. Brandt, D.T. and R. Grosse, Get to grips: steering local actin dynamics with IQGAPs. *EMBO Rep*, 2007. **8**(11): p. 1019-23.
371. Spiekerkoetter, E., et al., S100A4 and bone morphogenetic protein-2 codependently induce vascular smooth muscle cell migration via phospho-extracellular signal-regulated kinase and chloride intracellular channel 4. *Circ Res*, 2009. **105**(7): p. 639-47, 13 p following 647.
372. Gomez del Pulgar, T., et al., Rho GTPase expression in tumourigenesis: evidence for a significant link. *Bioessays*, 2005. **27**(6): p. 602-13.
373. Lynch, E.A., et al., Proteasome-mediated degradation of Rac1-GTP during epithelial cell scattering. *Mol Biol Cell*, 2006. **17**(5): p. 2236-42.

374. Nethe, M. and P.L. Hordijk, The role of ubiquitylation and degradation in RhoGTPase signalling. *J Cell Sci*, 2010. **123**(Pt 23): p. 4011-8.
375. Cantley, L.C., The phosphoinositide 3-kinase pathway. *Science*, 2002. **296**(5573): p. 1655-7.
376. Bos, J.L., A target for phosphoinositide 3-kinase: Akt/PKB. *Trends Biochem Sci*, 1995. **20**(11): p. 441-2.
377. Maeda, K., et al., CLIC4 interacts with histamine H3 receptor and enhances the receptor cell surface expression. *Biochem Biophys Res Commun*, 2008. **369**(2): p. 603-8.
378. Edwards, J.C. and C.R. Kahl, Chloride channels of intracellular membranes. *FEBS Lett*, 2010. **584**(10): p. 2102-11.
379. Tung, J.J. and J. Kitajewski, Chloride intracellular channel 1 functions in endothelial cell growth and migration. *J Angiogenes Res*, 2010. **2**: p. 23.
380. McClatchey, A.I., ERM proteins at a glance. *J Cell Sci*, 2014. **127**(Pt 15): p. 3199-204.
381. Kriz, W. and K. Endlich, Hypertrophy of podocytes: a mechanism to cope with increased glomerular capillary pressures? *Kidney Int*, 2005. **67**(1): p. 373-4.
382. Jaffe, A.B. and A. Hall, Rho GTPases: biochemistry and biology. *Annu Rev Cell Dev Biol*, 2005. **21**: p. 247-69.
383. Roberts, P.J., et al., Rho Family GTPase modification and dependence on CAAX motif-signaled posttranslational modification. *J Biol Chem*, 2008. **283**(37): p. 25150-63.
384. Bustelo, X.R., et al., Rac-ing to the plasma membrane: the long and complex work commute of Rac1 during cell signaling. *Small GTPases*, 2012. **3**(1): p. 60-6.

385. Das, S., et al., Single-molecule tracking of small GTPase Rac1 uncovers spatial regulation of membrane translocation and mechanism for polarized signaling. *Proc Natl Acad Sci U S A*, 2015. **112**(3): p. E267-76.
386. Welch, H.C., et al., Phosphoinositide 3-kinase-dependent activation of Rac. *FEBS Lett*, 2003. **546**(1): p. 93-7.
387. Schmidt, A. and A. Hall, Guanine nucleotide exchange factors for Rho GTPases: turning on the switch. *Genes Dev*, 2002. **16**(13): p. 1587-609.
388. Soisson, S.M., et al., Crystal structure of the Dbl and pleckstrin homology domains from the human Son of sevenless protein. *Cell*, 1998. **95**(2): p. 259-68.
389. Takahashi, K., et al., Direct interaction of the Rho GDP dissociation inhibitor with ezrin/radixin/moesin initiates the activation of the Rho small G protein. *J Biol Chem*, 1997. **272**(37): p. 23371-5.
390. Fernandez, D., et al., Control of cell adhesion and migration by podocalyxin. Implication of Rac1 and Cdc42. *Biochem Biophys Res Commun*, 2013. **432**(2): p. 302-7.
391. Garcia-Mata, R. and K. Burridge, Catching a GEF by its tail. *Trends Cell Biol*, 2007. **17**(1): p. 36-43.
392. Louvet-Vallee, S., ERM proteins: from cellular architecture to cell signaling. *Biol Cell*, 2000. **92**(5): p. 305-16.
393. Abramovici, H., et al., Diacylglycerol kinase zeta regulates actin cytoskeleton reorganization through dissociation of Rac1 from RhoGDI. *Mol Biol Cell*, 2009. **20**(7): p. 2049-59.

394. Malik, M., et al., Inducible NOS-induced chloride intracellular channel 4 (CLIC4) nuclear translocation regulates macrophage deactivation. *Proc Natl Acad Sci U S A*, 2012. **109**(16): p. 6130-5.
395. Goodchild, S.C., et al., Oxidation promotes insertion of the CLIC1 chloride intracellular channel into the membrane. *Eur Biophys J*, 2009.
396. Peter, B., et al., Membrane mimetics induce helix formation and oligomerization of the chloride intracellular channel protein 1 transmembrane domain. *Biochemistry*, 2013. **52**(16): p. 2739-49.
397. Tulk, B.M., S. Kapadia, and J.C. Edwards, CLIC1 inserts from the aqueous phase into phospholipid membranes, where it functions as an anion channel. *Am J Physiol Cell Physiol*, 2002. **282**(5): p. C1103-12.
398. Cromer, B.A., et al., From glutathione transferase to pore in a CLIC. *Eur Biophys J*, 2002. **31**(5): p. 356-64.
399. Mundel, P. and J. Reiser, Proteinuria: an enzymatic disease of the podocyte? *Kidney Int*, 2010. **77**(7): p. 571-80.
400. Seiler, M.W., et al., Pathogenesis of polycation-induced alterations ("fusion") of glomerular epithelium. *Lab Invest*, 1977. **36**(1): p. 48-61.
401. Schaldecker, T., et al., Inhibition of the TRPC5 ion channel protects the kidney filter. *J Clin Invest*, 2013. **123**(12): p. 5298-309.
402. Garg, P., et al., Actin-depolymerizing factor cofilin-1 is necessary in maintaining mature podocyte architecture. *J Biol Chem*, 2010. **285**(29): p. 22676-88.
403. Grahammer, F., C. Schell, and T.B. Huber, The podocyte slit diaphragm-from a thin grey line to a complex signalling hub. *Nat Rev Nephrol*, 2013. **9**(10): p. 587-98.

404. Weil, E.J., et al., Podocyte detachment and reduced glomerular capillary endothelial fenestration promote kidney disease in type 2 diabetic nephropathy. *Kidney Int*, 2012. **82**(9): p. 1010-7.
405. Zhu, W.W., et al., Ultrastructural changes in the glomerular filtration barrier and occurrence of proteinuria in Chinese patients with type 2 diabetic nephropathy. *Diabetes Res Clin Pract*, 2009. **86**(3): p. 199-207.
406. Schell, C., et al., Podocyte-Specific Deletion of Murine CXADR Does Not Impair Podocyte Development, Function or Stress Response. *PLoS One*, 2015. **10**(6): p. e0129424.

Appendices:

1. Ethics approval for animal use protocol.

 UNIVERSITY OF ALBERTA	
ETHICS APPROVAL FOR ANIMAL USE PROTOCOL	
RECOMMENDED WORDING TO ACCOMPANY PUBLICATIONS COMPLETED BY PRINCIPAL INVESTIGATORS AT THE UNIVERSITY OF ALBERTA <i>"All animal studies were conducted in accordance with the Canadian Council on Animal Care Guidelines and Policies with approval from the Animal Care and Use Committee: Health Sciences for the University of Alberta."</i>	
ANIMAL CARE AND USE COMMITTEE: HEALTH SCIENCES	
Has reviewed and approved the protocol application entitled:	
<u>GLOMERULAR ENDOTHELIAL CELL DEVELOPMENT & DIFFERENTIATION</u>	
Title	
<u>398/06/12D</u>	<u>September 4, 2012</u>
Protocol Number	Date Issued:
Submitted by:	
<u>Dr. Barbara Ballermann</u>	<u>N/A</u>
Name of Principal Investigator	Co-Investigator(s)
And found the proposed protocol involving animals to meet the standards of the Canadian Council on Animal Care (CCAC), and the proposed facilities in which the animals will be housed and used to comply with the CCAC requirements.	
<u>Mice</u>	<u>450</u>
Species	Number of Animals Approved
<u>Janis R. Rayat</u>	
<u>Signature of ACUC: Health Sciences Chair</u>	<u>July 1, 2012 – June 30, 2013</u>
	Start Date End Date
Animal Care and Use Committee: Health Sciences	
<small>308 Campus Tower, 8625-112 Street, Edmonton, AB T6G 2E1 Canada • Phone: 780-492-5322 • Fax: 780-492-9429</small>	

Notice of Approval for Renewal

Date: November 1, 2014
Study ID: [AUP0000222](#)
Study Title: Glomerular Endothelial cell development and differentiation and Breeding Colony
Principal Investigator: [Barbara Ballermann](#)
Approval Expiry Date: 9/17/2015

	RSO or Project ID	Agency/Sponsor Name
Funding	RES0024007	Division of Nephrology, University of Alberta
Source:	G099001279	General Research
	RES0020991	Kidney Foundation of Canada

Thank you for submitting a renewal to the Animal Care and Use Committee: Health Sciences. Your application for renewal was reviewed and is approved by the Committee.

Approved Animal Numbers: Mouse 202

The Canadian Council on Animal Care (CCAC) requires annual renewal of ethics approval for research projects using animals, and a Full Renewal in the 4th year. These renewals must be approved by the ACUC prior to the anniversary or expiration date of this approval. The University of Alberta's Animal Welfare Assurance Number is #A5070-01.

Any changes to this approved protocol must be submitted as an amendment online.

You will receive electronic reminders to renew your ethics approval 90, 60, 45, and 30 days prior to the expiry date. To allow time for the review process, we recommend you submit your renewal **2 months** prior to the expiry date of this approval. If you do not have a renewal under way before that date, the animal facility and RSO will be notified the study is due to expire, you **will not** be able to order animals, and you may be asked to submit a new animal use application.

All approved animal use protocols are subject to Post-Approval Monitoring (PAM). PAM is a vital part of a robust and effective animal care and use program and it takes many forms including researcher self-assessment, veterinary reports, facility consultation, tracking cage-level care and animal health, lab visits, observation, and education. Post-approval monitoring is a shared responsibility of animal users, ACUCs, veterinarians and animal care staff and the Research Ethics Office. If you have any questions about PAM, please contact Donna Taylor, PAM Coordinator, at 780-492-6828 or donna.taylor@ualberta.ca.

Sincerely,

Nadia Jahroudi, PhD
Chair, ACUC Health Sciences